LBNL-40838
UC-1600

ERNEST ORLANDO LAWRENCE
BERKELEY NATIONAL LABORATORY

A Population-Based Exposure Assessment Methodology for Carbon Monoxide: Development of a Carbon Monoxide Passive Sampler and Occupational Dosimeter

Michael G. Apte

Environmental Energy Technologies Division

September 1997

Ph.D. Thesis

LBNL-40838
UC-1600

A Population-Based Exposure Assessment Methodology for Carbon Monoxide: Development of a Carbon Monoxide Passive Sampler and Occupational Dosimeter

by

Michael Gregory Apte
Ph.D. Thesis

Department of Environmental Health Sciences
School of Public Health
University of California, Berkeley

and

Environmental Energy Technologies Division
Lawrence Berkeley National Laboratory
University of California
Berkeley, CA 94720

September 1997

This work was supported by the Assistant Secretary for Energy Efficiency and Renewable Energy, Office of Building Technology, and the Director, Office of Energy Research, Office of Computational and Technology Research, Laboratory Technology Research Division, of the U.S. Department of Energy under Contract No. DE-AC03-76SF00098.

A Population-Based Exposure Assessment Methodology for Carbon Monoxide: Development of a Carbon Monoxide Passive Sampler and Occupational Dosimeter

by

Michael Gregory Apte

B.S. (University of California, Berkeley) 1978
MPH (University of California, Berkeley) 1994

A dissertation submitted in partial satisfaction of the requirements for the degree of
Doctor of Philosophy
in

Environmental Health Sciences

in the

GRADUATE DIVISION

of the

UNIVERSITY OF CALIFORNIA, BERKELEY

Committee in charge:

Professor S. Katharine Hammond, Chair
Professor Catherine P. Koshland
Professor Robert A. Harley

Fall 1997

A Population-Based Exposure Assessment Methodology for Carbon Monoxide: Development of a Carbon Monoxide Passive Sampler and Occupational Dosimeter

by

Michael Gregory Apte

Abstract

A Population-Based Exposure Assessment Methodology for Carbon Monoxide: Development of a Carbon Monoxide Passive Sampler and Occupational Dosimeter

by

Michael Gregory Apte

Doctor of Philosophy in Environmental Health Sciences

University of California, Berkeley

Professor S. Katharine Hammond, Chair

Two devices, an occupational carbon monoxide (CO) dosimeter (LOCD), and an indoor air quality (IAQ) passive sampler were developed for use in population-based CO exposure assessment studies. CO exposure is a serious public health problem in the U.S., causing both morbidity and mortality (lifetime mortality risk approximately 10^{-4}). Sparse data from population-based CO exposure assessments indicate that approximately 10% of the U.S. population is exposed to CO above the national ambient air quality standard. No CO exposure measurement technology is presently available for affordable population-based CO exposure assessment studies.

The LOCD and IAQ Passive Sampler were tested in the laboratory and field. The palladium-molybdenum based CO sensor was designed into a compact diffusion tube sampler that can be worn. Time-weighted-average (TWA) CO exposure of the device is quantified by a simple spectrophotometric measurement. The LOCD and IAQ Passive Sampler were tested over an exposure range of 40 to 700 ppm-hours and 200 to 4200 ppm-hours, respectively. Both devices were capable of measuring precisely (relative standard deviation <20%), with low bias (<10%). The LOCD was screened for interferences by temperature, humidity, and organic and inorganic gases. Temperature effects were small in the range of 10°C to 30°C. Humidity effects were low between 20% and 90% RH. Ethylene (200 ppm) caused a positive interference and nitric oxide (50 ppm) caused a negative response without the presence of CO but not with CO.

The LOCD was used to monitor personal TWA CO exposures of 154 workshifts in a convention center during heavy use of propane powered forklifts. Performance of the LOCD was compared to an accurate standard method and against the commonly used Dräger CO diffusion tube. Exposure distributions were measured by the LOCD with a precision of about ±1 ppm. The Dräger tube was found to have a negative bias (20% at 8-hour TWA of 10 ppm, 40% below 10 ppm). Only one exposure exceeded the Cal/OSHA PEL of 25 ppm TWA for 8-hours. Workers at the loading docks had the highest 8-hour TWA exposures (50% >12.5 ppm). The LOCD is potentially valuable as a device for measurement of occupational CO exposures.

Table of Contents

Table of Contents iii

List of Tables viii

List of Figures ix

Acknowledgments xi

CHAPTER 1: GENERAL INTRODUCTION 1

References 6

Tables 12

CHAPTER 2: THE IMPORTANCE OF CO EXPOSURE ASSESSMENT IN STUDYING CHRONIC AND SUBACUTE HEALTH EFFECTS 15

Introduction 15

CO Exposure Distribution Relative to Potential Chronic and Sub-acute Health Effects 16
Occupational exposure data from the Washington, DC-Denver study 17

Review of CO Toxic Mechanisms and Health Effects 18
Physiology of CO exposure 18
Toxic mechanisms of CO exposure 18
Endogenous CO Production. 19
Interaction of Diet and CO Exposure. 19
CO Uptake and Distribution 19
Pharmacokinetic Models. 19
Adaptation to CO 20
Lethal and acute CO health effects 20
Physiological Effects of Sub-Acute and Chronic CO Exposure 20
Cardiovascular effects 21
Developmental effects 22
Fetotoxicity and Low Birthweight 22
Neurobehavioral 22
Cardiomegaly 23
Genotoxic effects of CO 23

Discussion 24

Conclusions 26

References 26

Figures 30

CHAPTER 3: REVIEW OF CO SAMPLING AND MEASUREMENT TECHNIQUES SUITABLE FOR POPULATION-BASED EXPOSURE ASSESSMENT 32

Introduction 32

Available Methods for Determination of CO in Air 34
Real-time (Active) Analyzers 34
Real-time electrochemical CO analyzers 35
Real-time infrared CO analyzers 35
Non-specific Active Air Collector 37
Non-Specific Passive Air Collector 37
Actively pumped colorimetric detector tubes 38
CO-Specific Biological Measurement Techniques 38
Existing CO-Specific Passive Samplers 39
CO Passive Samplers Under Development 40
LBNL's CO Passive Samplers 41
Palladium-related compounds investigated for use CO sensors 42
Harvard's CO Passive Sampler 43

References 44

Tables 48

CHAPTER 4: DEVELOPMENT OF A CO PASSIVE SAMPLER AND OCCUPATIONAL CARBON MONOXIDE DOSIMETER 49

Introduction 49

Occupational Dosimeter Development Approach 50

Apparatus 50

Sensor Technology Development 51
The CO Sensor 51
Methods 52
Theory of quantification of sensor reaction kinetics 52
Spectrophotometric measurement of sensor response 52
A forward reaction kinetic model 53
A note on copper contamination as a competitive reaction 54
A reverse reaction kinetic model 54
Experimental 56
Direct exposure method 56
Analysis of the direct method data 57
Quantification of reverse sensor reaction kinetics 58
History of the sensor technology development 58
Early sensor regeneration research 59
Identification of copper contamination in the sensor substrate 60
A sensor with low reversibility was developed 61
Discussion of sensor history 62
Investigation of performance of non-reversible sensors for use in CO passive samplers 62
Improved sensor materials (Goal 3) 62
Batch homogeneity characterization 63

Inter- and intra-batch sensor variability in response slope and linearity 63
CO capacity limits 64
Sensor conditioning prior to use 64
Direct Test sensor regeneration (sensor batches AP-AU) 64
Sensors used in final laboratory and field validation experiments (sensor batch AW) 65
Direct test calibration data for AW sensors 65
Reversibility of Direct Test exposed AW sensors 65
Aging and variability of AW sensors 66

Development of Diffusion Sampler Technology 66
Passive sampler concept 66
Methods 67
Diffusion sampler laboratory test method 67
Analysis of the diffusion sampler laboratory test method data 69
Calculating a diffusion scaling factor for comparing diffusion samplers to direct test forward response data. 69
Empirically derived diffusion sampler response used to calibrate passive samplers 70
Definition and calculation of precision, bias, and accuracy 70
Sensor storage and silica gel preparation for use in passive samplers 71
Results: PS1 and PS2 laboratory tests 71
Summary of PS1 results 71
PS1 design 71
PS1 laboratory exposure tests 72
Discussion of PS1 design 72
Goal 1 - Prototype dosimeter development (passive sampler 2, PS2) 72
Design of critical components and enhancements 72
Evaluation of sampler materials for use in PS2 73
Goal 2 - Evaluation of PS2 74
PS2 response characteristics 74
Humidity effects 75
PS2 Sensor reversibility after exposure 75
Response of unexposed PS2 controls 76
Initial Occupational Dosimeter Configuration (PS3/D1) 76
Goal 4 - Occupational dosimeter configuration (PS4/D2) 76
Results: D2 response, precision, bias, accuracy, and humidity control verification 77
Precision, bias, and accuracy of occupational dosimeter D2 78
Discussion of D2 development results 79
Goal 5 - Diffusion Sampler D2/D3 Validation 79
Dosimeter performance at lowered and elevated temperatures 80
Analysis of sensor behavior at 10°C 80
Discussion: implications of temperature effects 81

Interferent Screening Tests 81
Dosimeter interferent screening test method 81
Results: Dosimeter performance in the presence of potential interferents 83
Ethylene in the environment 84

Preliminary Field Testing 84
Field test methods and protocol 84
Preliminary Field test results for PS1 and PS2 85
Preliminary Field test results for LOCD in residential environments 85

Sampling Rate Validation 86
Method for measurement of QGI sensor's mass conversion rate and calculation of volumetric sampling rate. 86

Results: Measurement of QGI sensor's mass conversion rate, calculation of dosimeter (LOCD) sampling rate, and comparison of empirical and sampling rates 87

References 89

Tables 91

Figures 101

CHAPTER 5: A STUDY OF OCCUPATIONAL CARBON MONOXIDE EXPOSURES 132

Introduction 135

Methods 136
Study Design 136
Moscone Convention Center Physical Characteristics 136
Protection of Human Subjects 137
Moscone Convention Center Employer, Union, and Worker Classifications 137
MCC Employers and Unions 138
MCC Workforce 138
Participant Selection 139
Measurement Methods 139
Methods Used by LBNL 139
The LBNL/QGI Occupational Carbon Monoxide Dosimeter (LOCD) 139
LOCD analysis 140
The Bag Sampler 140
Methods Used by Crawford 141
Dräger Diffusion Tubes 141
Real-time Datalogging Personal Monitors 141
Extended Workshifts 141
Carboxyhemoglobin Simulation 142

Results 143
Area Measurements Using Bag Sampler and LOCD 143
Personal Monitoring of Workers Using the LOCD 144
Personal dosimetry by date 145
Personal dosimetry by job category 145
Personal dosimetry by location 146
Personal dosimetry by union affiliation 146
Personal dosimetry by employer 147
Real-time Personal Monitoring of Workers 147
Comparison of parallel LOCD and Dräger diffusion tube exposure measurements. 148
Simulation of Worker Carboxyhemoglobin Concentrations 149

Discussion 150
Personal Monitoring 150
Methods comparison: Dräger vs. LOCD 150
Simulated Carboxyhemoglobin Concentrations 151

Conclusions 151

References 152

Tables 154

Figures 161

CHAPTER 6: SUMMARY, CONCLUSIONS, AND RECOMMENDATIONS FOR FUTURE RESEARCH 193

Summary 193
Development of new passive CO monitoring technologies 193
An industrial hygiene CO exposure assessment study using the LBNL/QGI Occupational Carbon Monoxide Dosimeter 196

Conclusions 198

Future Research Needs 199
NIOSH validation for the LOCD 199
Develop a portable reader for dosimeter 199

References 200

List of Tables

Table 1-1. Carbon monoxide air quality standards for ambient and occupational environments.

Table 1-2. Key Health effects of exposure to Carbon Monoxide.

Table 1-3. Observed occupational CO exposures.

Table 3-1. Techniques available for measurement of carbon monoxide.

Table 4-1. Instrumentation used for laboratory testing of the QGI CO sensors and the LBNL/QGI Passive Sampler and Occupational Dosimeter prototypes.

Table 4-3. Early sensor performance investigations.

Table 4-4. Early CO sensor development summary, MD15 sensors

Table 4-5. QGI CO sensors used for dosimeter development. and validation

Table 4-6. MD15 sensor response characteristics. Inter- and intra-batch differences.

Table 4-7. Sensor regeneration after exposure to 40 ppm CO in direct exposure tests.

Table 4-8. Materials compatibility tests for LBNL/QGI carbon monoxide passive samplers.

Table 4-9. LBNL/QGI occupational dosimeter (D2) humidity effects tests.

Table 4-10. Effect of temperature during 25 ppm CO exposure.

Table 4-11. Preparation of target gas species from liquids at 20 °C: interference tests.

Table 4-12 Target gas concentrations to be used in test atmospheres for interference tests.

Table 5-1. Job Categories for which workers were monitored at the Moscone Convention Center

Table 5-2. LOCD and bag sampler fixed-site monitoring carbon monoxide data from the Moscone Convention Center.

Table 5-3. Moscone Center CO exposure survey summary statistics by date of measurement.

Table 5-4. Moscone Center CO exposure survey summary statistics by Job category.

Table 5-5. Moscone Center CO exposure survey summary statistics by work location.

Table 5-6. Moscone Center CO exposure survey summary statistics by union.

Table 5-7. Moscone Center CO exposure survey summary statistics by Employer.

Table 5-8. Time-weighted average CO exposures measured at the Moscone Convention Center

List of Figures

Figure 2-1. Estimated probability distribution of carboxyhemoglobin (COHb) levels in blood samples from non -smokers in the U.S.
Figure 2-2. The relationship between CO inhalation exposure and carboxyhemoglobin levels.
Figure 4-1. Diagram of laboratory exposure system for testing CO diffusion samplers.
Figure 4-2. Key elements of the QGI carbon monoxide sensor chemistry.
Figure 4-3. Diagram of a flow-through sensor holder for use in the Direct Method tests.
Figure 4-4. Diagram depicting three different systems for measuring the absorbance spectra of the QGI CO sensor.
Figure 4-5. A typical "direct method" experiment response profile.
Figure 4-6. Typical sensor response spectrum from 400 to 1100 nm.
Figure 4-7a. Observed average change in 700nm absorbance of four MD15 sensors.
Figure 4-7b. First order kinetics in Mo_{blue}
Figure 4-7c. Second order kinetics in Mo_{blue}.
Figure 4-7d. Third order kinetics in Mo_{blue}.
Figure 4-7e. Fourth order kinetics in Mo_{blue}.
Figure 4-7f. 3.3 order kinetics in Mo_{blue}.
Figure 4-8. Third order oxidation kinetics in Mo_{blue}, batch K.
Figure 4-9. Third order oxidation kinetics in Mo_{blue}, batch J.
Figure 4-10. Forward sensor response to CO and curve fit for MD-15 sensors using the Direct Method.
Figure 4-11. Individual sensor response curves at 700 nm from three QGI sensors from a single batch.
Figure 4-12. Average sensor response curves at 700 nm for 8 batches of MD15 sensors.
Figure 4-13. A comparison of Direct Method response curves for conditioned (desiccated) and unconditioned (wet) AP sensors exposed to 40 ppm
Figure 4-14. Direct Test response curves for seven batches of QGI MD15 sensors.
Figure 4-15. Diagram of the first prototype LBNL/QGI passive sampler (PS1).
Figure 4-16. NIOSH nomogram for calculating accuracy from precision and bias.
Figure 4-17. Schematic of the LBNL/QGI Passive Sampler #2 (PS2)
Figure 4-18. LBNL/QGI PS2 passive sampler laboratory test results.
Figure 4-19. LBNL/QGI PS2 laboratory test results. High humidity.
Figure 4-20. Percent regeneration of five QGI sensors in LBNL/QGI PS2 samplers.
Figure 4-21. Average increase in background absorbance of six capped PS2 samplers.
Figure 4-22. Laboratory test results for the occupational dosimeter configuration of PS3/D1 passive samplers.
Figure 4-23. Exploded view of LBNL/QGI occupational dosimeter (D2 and D3).
Figure 4-24. Humidity test results from LBNL/QGI CO Occupational Dosimeter D2.
Figure 4-25. Arrhenius plot of D2 CO dosimeter response as a function of temperature.
Figure 4-26. Interference screening test results.
Figure 4-27. Combined preliminary field test results from PS1 and PS2.
Figure 4-28. Comparison of LBNL/QGI Occupational Dosimeter measurements and bag sampler measurements made in three residences
Figure 5-1. Diagram of the LBNL/QGI Carbon Monoxide Occupational Dosimeter.
Figure 5-2. Conceptual design for use of the LBNL/QGI Carbon Monoxide Occupational Dosimeter (LOCD.

Figure 5-3. Fixed-site locations for bag sampler/LOCD monitoring.
Figure 5-4. LBNL/QGI CO Occupational Dosimeter (LOCD) vs. Bag Sampler Data collected at fixed-sites throughout the Moscone convention Center
Figure 5-5. Carbon monoxide exposure distribution at the Moscone Convention Center. All job titles, all three days of the CO exposure study.
Figure 5-6. The probability distribution of measured time-weighted average CO exposures at the Moscone Convention Center.
Figure 5-7. The probability distribution of the natural logarithm of measured time-weighted average CO exposures at the Moscone Convention Center.
Figure 5-8. Carbon monoxide exposure distribution. All job categories on January 3, 1997.
Figure 5-9. Carbon monoxide exposure distributjon. All job categories on January 5, 1997.
Figure 5-10. Carbon monoxide exposure distribution. All job categories on January 6, 1997.
Figure 5-11. Carbon monoxide exposure distribution. By job Category - Attendant
Figure 5-12. Carbon monoxide exposure distribution. By job category - Forklift Operator.
Figure 5-13. Carbon monoxide exposure distribution. By job category - Installer/Decorator..
Figure 5-14. Carbon monoxide exposure distribution. By job category - Supervisor.
Figure 5-15. Carbon monoxide exposure distribution. By job location - Red Dock.
Figure 5-16. Carbon monoxide exposure distribution. By job location - Green Dock.
Figure 5-17. Carbon monoxide exposure distribution. By job location - Blue Dock.
Figure 5-18. Carbon monoxide exposure distribution. By job location - North Hall.
Figure 5-19. Carbon monoxide exposure distribution. By job location - South Hall.
Figure 5-20. Carbon monoxide exposure distribution. By union, Teamsters Local 85.
Figure 5-21. Carbon monoxide exposure distribution. By union, Management.
Figure 5-22. Carbon monoxide exposure distribution. By union, SDAC Local 510.
Figure 5-23. Carbon monoxide exposure distribution. By union, SEI Local 14.
Figure 5-24. Carbon monoxide exposure distribution. By employer, Sullivan Transfer Co.
Figure 5-26. Carbon monoxide exposure distribution. By employer, Freeman Decorating Co.
Figure 5-27. Real-time Carbon Monoxide Exposure Profile.
Figure 5-28. Comparison between parallel 8-hour TWA LOCD and Dräger diffusion tube CO measurements
Figure 5-29. Simulated carboxyhemoglobin concentrations derived from real-time data.
Figure 5-30. Simulated carboxyhemoglobin concentrations., 10 ppm CO/8-hr workshift.
Figure 5-31. Simulated carboxyhemoglobin concentrations, 16.4 ppm CO/8-hr workshift..
Figure 5-32. Simulated carboxyhemoglobin concentrations. 25 ppm CO/8-hr workshift.

Acknowledgments

I would like to thank all of the people in the Indoor Environment Program at Lawrence Berkeley National Laboratory for their positive support through the years that I have worked with them. Special thanks go to Greg Traynor with whom I started this project almost 18 years ago and with whom the thinking behind this project evolved. Thanks also go to Joan Daisey for her strong support and encouragement, and to Lara Gundel for the thoughtful and steady scientific mentoring.

Equal thanks go to my dissertation Chair and a wonderful person, Kathie Hammond. Her faith and support throughout this project, including a period as a helpful hand during the field sampling phase of the project. (Lara was there too!)

Thanks to Catherine Koshland and Robert Harley, the other part of my dissertation committee, for reading this and trying to make sense of it.

I have had several very important partners in the laboratory over the years that I worked on this project: Alicia Woods, Gee-Min Chang, and Agnes Bodnar. Without your help I could not have done this. Thanks.

Then there is Quantum Group, Inc. Thanks go to Mark Goldstein who is responsible for developing the original QGI sensor and was willing to jump into this project with me. Bill Helfman spent many hours developing and improving the CO sensor technology to its current level. Thanks to you too. Michelle Oum, thanks to you too. You worked with me on the project early on.

Thanks to Dan Cox of Crawford Risk Control Services, and to all the willing and helpful participants of the field study at the Moscone Convention Center.

Last, but really always first are my family: Ursula, Joshua, Zac, and Oliver; and my parents: Robert and Evelyn, who have put up with all this for far too long. Thanks for waiting, thanks for the support and just for being with me.

This work was supported in part by the Office of Building Technology and the Office of Energy Research, Laboratory Technology Research Program, of the U.S. Department of Energy under contract No. DE-AC03-76SF0098.

Chapter 1: General Introduction

The history of human exposure to carbon monoxide (CO) must date back at least 500,000 to 1,000,000 years to the period when cave-dwelling man first learned to use fire. CO is a product of combustion that is emitted whenever burning hydrocarbons are not fully oxidized. Despite other major physiological changes in man over this time span, human physiological evolution has not included a successful development of resistance to the effects of CO inhalation. CO exposure can critically compromise the oxygen carrying capacity of hemoglobin and other body pigments causing serious health effects including death.

The purpose of this chapter is to describe the issues surrounding CO exposure in the U.S. from a public health perspective. This chapter should be considered an overview of the issues. Many of the details of these issues are presented in the following chapters. The second chapter presents information on CO exposure assessment and chronic and subacute health effects. Chapter three presents the current state of CO monitoring technology suitable for population-based total CO exposure and occupational CO exposure assessment studies. Together the first three chapters represent a detailed literature review of the field of CO exposure assessment. Chapter four presents a new CO monitoring technology for occupational and indoor air quality CO exposure assessment. Chapter five reports on an industrial hygiene CO exposure assessment study conducted using the new occupational CO monitoring technology. Chapter six is a summary of this work.

Chronic exposures to CO at levels close to the current ambient and occupational exposure standards may be responsible for considerable morbidity, but current exposure assessment methods have not been adequate to accurately quantify the population's exposure distribution. The body of work presented here has been aimed at improving CO measurement methods suitable for conducting CO exposure assessment, in order to better understand the statistical distribution of CO exposures at the scale of communities or populations. The last two chapters of this dissertation are new research - the results of the development of a new technology for CO exposure assessment. The work includes the theoretical basis and laboratory and field testing of the technology. Results from the development and testing of an occupational exposure measurement device, the LBNL/QGI CO Occupational Dosimeter (LOCD), in the laboratory and in a real exposure assessment study are presented. Additionally results from a similar device, intended for residential CO monitoring, the LBNL/QGI CO Passive Sampler are presented. Conceptually, this device is well suited for use in large-scale population-based exposure assessment studies where statistically valid random samples can be used to provide information on the distribution of CO exposures within a community or population.

As with our biological adaptation to CO, methods suitable for population-based CO exposure assessment also have, on a different time scale, had a long time to evolve with little progress. Although CO was identified as a substance when it was produced by gasification from coal by Reverend John Clayton in 1688, and first used as fuel to illuminate a factory in 1798, the first crude quantitative measurement methods were not developed until the early 1940s (Shephard, 1983). In the intervening half century, methods for accurate stationary CO real-time analyzers have been perfected (USEPA, 1991; Woebkenberg, 1995).

Miniature, accurate real-time CO monitors, using electrochemical sensors and integrated datalogging systems, which can measure personal exposures over periods of hours to days (dosimeters) are also available now (Mage, 1993; Ott, 1986; Ott, 1995; Smith, 1994; Stetter, 1980; Woebkenberg, 1995). Instantaneous and time averaging direct reading CO detector tubes using small sampling pumps are available to measure personal CO exposures (Shepherd, 1947; Leichnitz, 1993; Saltzman, 1995). Time-averaging, direct reading diffusion tubes and badges are available for personal CO monitoring (Hossain, 1989; Leichnitz, 1993; McConnaughey, 1985; Saltzman, 1995). Finally a number of methods are available for measuring or estimating CO biologically via blood carboxyhemoglobin (COHb) concentrations either directly from blood samples or calculated from expired alveolar breath samples of CO exposed individuals (USEPA, 1991; Shephard, 1983; Wallace, 1988; Lawler, 1984; Radford, 1984). Although these methods can be used to provide CO exposure measurements, due to many factors such as unit price and labor costs, size and weight, and poor sensitivity or accuracy, they have been inadequate for use in large-scale population-based exposure assessment projects.

The health effects of acute and subacute CO exposure are well documented. Upon inhalation, CO enters the blood, binds with hemoglobin and dissolves into the plasma. As it is circulated throughout the body it also binds with myoglobin and interacts with cytochrome P-450 within cellular mitochondria (Shephard, 1983). Acute exposure can lead to coma and death within minutes. Survivors of acute CO poisoning are often left with serious disabilities caused by hypoxia leading to damage to the heart, brain, and other organs. Subacute exposures can cause flu-like symptoms, which can easily be misdiagnosed, so that individuals often return to additional CO exposure. Chronic exposures to lower concentrations have been implicated in the development of coronary artery disease and other cardiovascular diseases, developmental effects including low birthweight, enlarged heart size, and neurological decrements. Sensitive populations include the pregnant mother and fetus, children, and the elderly. Individuals with cardiovascular disease suffer from angina pectoris when exercising during exposure to low concentrations, and are at risk for heart attack (Kirkpatrick, 1987; Heckerling, 1988; Dolan, 1987; USEPA, 1991).

The United States carbon monoxide mortality data (USDHHS, 1986-1992) indicate that acute CO poisoning is a serious public health problem. Although there is considerable public concern about CO safety, very little is known about the actual extent and distribution CO exposures in the U.S. (USEPA, 1991). One view of the CO toxic exposure currently available to us is through analyses of death certificates collected by the U.S. Centers for Disease Control (Cobb, 1991; Girman, 1993). An analysis of the CO mortality data indicates that the current lifetime risk of unintentional fatal CO poisoning is about 10^{-4}, a factor of 100 times greater risk than the U.S. Environmental Protection Agency uses to regulate toxic substances such as benzene. This is based on 500-1000 unintentional CO poisoning fatalities reported in death certificates annually (USDHHS, 1986-1992). Although this risk level is high, it is certainly an underestimate and can be considered the absolute lower bound for lifetime mortality risk from CO poisoning in the U.S. since many CO-related deaths are not counted in death certificates as the effects of CO poisoning are easily overlooked or misdiagnosed.

In 1995 some 19,000 CO poisonings, rising from 13,000 in 1993, were reported to the American Association of Poison Control Centers (AAPCC) (Litovitz, 1994; Litovitz, 1996). The Poison Control Centers receive reports of only a portion of the actual number of CO

poisoning events (Soslow, 1992). These statistics place CO exposure among the most frequent causes of poisonings in the U.S.

The toxic effects of CO are a function of dose, body mass, metabolic level, and individual sensitivity factors. Dose, the quantity of inhaled CO absorbed into the bloodstream, is primarily a function of total exposure. CO exposure is defined as the product of the integrated CO concentration (C) inhaled in an environment and time (t) for which it is inhaled, or $E = Ct$. Total exposure is the sum of exposures received in all environments encountered within a given time frame, or

$$E_T = \sum_i C_i t_i,$$

where E_T is total exposure, and C_i and t_i are the concentration and time in the ith micro-environment. Each micro-environment, such as the outdoors, residential-indoors, inside an automobile or bus, in an industrial or office environment, etc., could be a contributor to the total exposure. The sources of CO within each micro-environment are likely to be different. For example the source of CO concentrations indoors in a residence could be both infiltrating outdoor air, and emissions from a malfunctioning combustion appliance. Sources in an industrial setting might be emissions from a blast furnace and exhaust from internal combustion engine powered equipment. CO sources in outdoor air may be emissions from automobiles and factories.

CO is a ubiquitous pollutant present in outdoor air. Indoor combustion sources can cause indoor CO levels to be significantly higher than those outdoors. The U.S. Environmental Protection Agency (USEPA) has deemed CO a *Criteria Pollutant* and has set a National Ambient Air Quality Standard (NAAQS) of 9 ppm time-weighted-average (TWA) for 8-hours or 35 ppm TWA for 1 hour, not to be exceeded more than once a year (USEPA, 1991). This standard was based on epidemiological data and clinical studies of human physiological responses to CO exposures. It was designed to protect the population by ensuring that even its most sensitive individuals; those with anemia or impaired cardiovascular or cardiopulmonary systems, the fetus, infants or the elderly, are not exposed to deleterious concentrations in ambient air (USEPA, 1991). The NAAQS for airborne CO is intended to keep blood COHb levels below 2.1% (USEPA, 1991).

The NAAQS for CO is frequently reached or exceeded in the outdoor air of major urban centers (USEPA, 1991). Selected ambient CO air quality standards (AAQS) are listed in Table 1-1. Note that both the European (WHO, 1994) and the State of California (CARB, 1989) have more stringent AAQS in order to provide a larger margin of safety than the NAAQS.

Standards for occupational CO exposure (see Table 1-1) have been developed using the same information as the NAAQS, but assume because workers are healthier than the general population, that members of the workforce will be less vulnerable to CO effects than the general population (OSHA, 1993; NIOSH, 1994b; NIOSH, 1972; ACGIH, 1991). The U.S. Occupational Safety and Health Administration (OSHA) currently has set the occupational CO standard to keep worker COHb levels from exceeding 5% COHb (OSHA, 1993), while the National Institute of Occupational Safety and Health (NIOSH) and the American Conference of Governmental Industrial Hygienists have used 3.5% COHb as the safety threshold (NIOSH, 1972, ACGIH, 1991). For perspective, Table 1-2 summarizes the key

health effects which have been used for setting of AAQS. Symptoms are documented as low as 2.3% COHb (e.g., reduced maximal exercise performance), and at 3% COHb individuals with ischemic heart disease display reduced exercise duration to onset of angina (chest pain).

Regulation of ambient (outdoor) CO concentrations does little to ensure that individuals are not exposed indoors to levels which cause health effects. Since people spend approximately 65-70% of their time in their residences, and including their occupational and other environments, 90% of their time indoors (Szalai, 1972; Chapin, 1974; Quackenboss, 1982; Spengler, 1983), their total exposure is dominated by the indoor component. Thus, ambient air quality monitoring for outdoor CO does not reflect the actual total exposure of the population (Wallace, 1985). Outdoor CO levels are not the main determinant of high indoor CO levels. Elevated indoor CO levels are caused by indoor CO sources.

Few true population-based CO exposure assessment studies have been conducted. The criterion for identification of such a study is that it would be able to produce statistically valid estimates of the distribution of CO exposures within the measured population. Only one study, NHANES II conducted 20 years ago, has provided such data reflecting the CO exposures of the U.S. population at a national level (Radford, 1982; Wallace, 1985). In addition, the USEPA conducted statistically-valid random studies of winter CO exposures in Washington DC and Denver, Colorado (Ackland, 1985; Johnson, 1984; Wallace, 1988). The NHANES II study used blood COHb measurements of smokers and non smokers to assess the distribution of CO blood levels in the representative samples of Americans, while the USEPA used electrochemical personal exposure monitors and exhaled alveolar breath CO measurements of nonsmokers to assess exposures in the randomly selected residents of the two cities. Both studies were in good agreement, with an estimate that 8-10% of the measured populations having exposures in excess of the NAAQS (Wallace, 1988).

Non-random, CO exposure assessments of populations conducted in Germany and in Mexico were used to estimate population exposure distributions (Fernandez-Bremauntz, 1993; Roscovanu, 1985). The distributional data from both countries showed that significant percentages of the populations were exposed above their countries' and international CO AAQS's. In Germany, COHb levels of people aged 10, 50, and 60 years were measured in a non-random survey of 13,000 inhabitants in several communities in the region of North Rhine-Westphalia. The percentage of the populations of measured individuals with levels above 2.5% COHb ranged from 0% to 28% depending upon the community and time of year (Roscovanu, 1985). Personal CO exposures of commuters in Mexico City were monitored, finding that about 8 percent of the commuter population was exposed to CO in excess of Mexico's AAQS of 13 ppm TWA for 8-hr, and a full 90 percent of the population was exposed above the WHO guideline of 9 ppm TWA for 8 hours (Fernandez-Bremauntz, 1993).

No systematic population-based studies of occupational CO exposures have been reported, however numerous reports have presented results from occupational CO exposure assessments. Table 1-3 summarizes the observations of these studies. The NIOSH National Occupational Exposure Survey indicated that more than 3.5 million workers in the private sector are occupationally exposed to CO, primarily via motor exhaust (NIOSH, 1990; Steenland, 1996). Referencing Hosey and NIOSH, the USEPA Criteria Document for the CO NAAQS states that the number of persons potentially exposed to CO in the work

environment is greater than that for any other physical or chemical agent, estimating that about a million workers are occupationally exposed at high levels (USEPA, 1991; Hosey, 1970; NIOSH, 1972). A recent Alert was posted by federal and state agencies including NIOSH, OSHA, the U.S. Consumer Product Safety Commission, and USEPA, warning of the poisoning dangers of small gasoline-powered engines and tools. These devices are capable of producing life-threatening CO concentrations in excess of 1200 ppm in a matter of a few minutes (USDHHS, 1996).

Occupational groups exposed to CO that have had exposure assessment efforts reported in the literature include (see Table 1-3) forklift operators (McCammon, 1996; Ely, 1995; Fawcett, 1992a; Fawcett, 1992b; Fleming, 1992; USEPA, 1991), workers in foundries and other heavy industry (Virtamo, 1976; Gardiner, 1992; USEPA, 1991; Shepherd, 1983), bus drivers (Limasset, 1993), traffic workers and on the roadway (Jabara, 1980; Gourdeau, 1995; Kamei, 1997; Colwill, 1980; Ott, 1994; Flachsbart, 1995; USEPA, 1991; Raaschou-Nielsen, 1995), airport workers (McCammon, 1981; Bellin, 1980), firefighters (Brotherhood, 1990; Lees, 1995; Jankovic, 1991; Materna, 1992; USEPA, 1991; Shephard, 1983), chainsaw and other small gasoline-powered tool operators (Nillsen, 1987; Hagberg, 1985; van Netten, 1987; USDHHS, 1996), and office workers (Wallace, 1983). Additionally, indoor sporting events have been monitored for CO levels which could effect participants, workers, and audience (Levesque, 1997; Levesque, 1991; MMWR, 1994; MMWR, 1996; Johnson, 1975).

Ecological epidemiological studies have found that coronary heart failure (CHF) hospitalizations of the elderly in major urban centers are statistically associated with centrally measured ambient CO concentrations (average levels well below the NAAQS), providing strong evidence that CO may cause adverse health effects at concentrations previously considered safe (Morris, 1995; Schwartz, 1995a). These studies suggest that annually, many thousands of cases of CHF are associated with ambient CO exposures. The ecological nature of these studies raise questions regarding the true total CO exposures of the CHF victims, since total CO exposure including the indoor component, causes health effects.

Retrospective occupational epidemiology studies have shown similar, often statistically significant, cardiovascular disease mortality where chronic worker CO exposure was postulated to be the causative factor. The effects were seen in cohorts of tunnel workers, motor vehicle examiners, foundry workers, bus drivers and firefighters (Melus, 1995; Stern, 1981; Stern, 1988; Koskela, 1994; Michaels, 1991). These studies are discussed in more detail in Chapter 2. The CO influence on cardiovascular disease mortality that is inferred by these studies would lead to much higher estimates of the mortality risk from CO exposure than those given above.

From the perspective of morbidity and mortality, CO is clearly a serious public health issue. CO exposures are not limited to residential or occupational environments, but can occur in almost every conceivable microenvironment inhabited by people. One common theme throughout the epidemiological literature is that actual CO exposure measurements are scant. In the case of the ambient air pollution studies, Schwartz stated that a better understanding of the relationship between ambient CO levels and CHF could be reached by studying the distributions of both residential and occupational indoor and outdoor CO concentrations (Schwartz, 1995b). Traditionally epidemiological research has been interested in health effects with a neglect of the exposure part of the "dose-response"

equation (Peters, 1984). Historically, a major hurdle in conducting population-based CO exposure assessments has been the CO exposure measurement technology. The new technology which is presented in the following chapters should assist in providing the data needed to better understand the role of CO exposure in human morbidity and mortality.

References

Ackland, G. G., Hartwell, T. D., Johnson, T. R., and Whitmore, R. W. (1985). "Measuring Human Exposure to Carbon Monoxide in Washington, DC, and Denver, Colorado, During the Winter of 1982-1983." *Environmental Science and Technology*, 19(10), 911-918.

ACGIH. (1991). *Documentation of the Threshold Limit Values and Biological Exposure Indicies*, American Conference of Governmental Industrial Hygienists, Cincinnati, OH.

Bellin, P., and Spengler, J. D. (1980). "Indoor and Outdoor Carbon Monoxide Measurements at an Airport." *Journal of the Air Pollution Control Association*, 30(4), 392-394.

Brotherhood, J. R., Budd, G. M., Jeffery, S. E., Hendrie, A. L., Beasley, F. A., Costin, B. P., and Wu Zhien. (1990). "Fire Fighters' Exposure to Carbon Monoxide During Australian Bushfires." *American Industrial Hygiene Journal*, 51(4), 234-240.

Cal/OSHA. (1997). "Title 8 - General Industry Safety Orders, Section 5155 - Airborne Contaminants." *California Code of Regulations*, Register 97 No. 22; 5-30-97, Sacramento, CA.

CARB. (1989). *Adequacy of the Statewide Carbon Monoxide Ambient Air Quality Standard: The Impact of Recent Health Effects Studies.* Staff Report of the California Air Resources Board, Sacramento, CA, December 1989.

Chapin, F. S. (1974). *Human Activity Patterns in the City*, Wiley-Interscience, New York, NY.

Colwill, D. M., and Hickman, A. J. (1980). "Exposure of Drivers to Carbon Monoxide." *Journal of the Air Pollution Control Association*, 30(12), 1316-1319.

Dolan, M. C., Haltom, T. L., Barrows, G. H., Short, C., and Ferriell, K. M. (1987). "Carboxyhemoglobin Levels in Patients with Flu-Like Symptoms." *Annals of Emergency Medicine*, **16**, 782-786.

Ely, E. W., Moorehead, B., and Haponik, E. F. (1995). "Warehouse Workers' Headache: Emergency Evaluation and Management of 30 Patients with Carbon Monoxide Poisoning." *American Journal of Medicine*, 98(2), 145-155.

Fawcett, T. A., Moon, R. E., Francia, P. J., Mebane, G. Y., Theil, D. R., and Piantadosi, C. A. (1992a). "Warehouse Workers Headache. Carbon Monoxide Poisoning from Propane-Fueled Forklifts." *Journal of Occupational Medicine*, 34(1), 12-15.

Fawcett, T. A., Moon, R. E., Francia, P. J., Mebane, G. Y., Theil, D. R., and Piantadosi, C. A. (1992b). "Letters to the Editor: Warehouse Workers' Headache - The Author Replies." *Journal of Occupational Medicine*, 34(9), 871-872.

Fernandez-Bremauntz, A. (1993). Doctoral Thesis: "Commuters' Exposure to Carbon Monoxide in the Metropolitan Area of Mexico City," University of London, London, UK.

Flachsbart, P. G. (1995). "Human Exposure to Exhaust and Evaporative Emissions From Motor Vehicles." Accepted in: *Motor Vehicle Air Pollution: Public Health and Control Measures*, Second Edition, World Health Organization, Geneva, Switzerland.

Fleming, J. L., and Opheim, G. S. (1992). "Letters to the Editor: Warehouse Workers' Headache." *Journal of Occupational Medicine*, 34(9), 872.

Gardiner, K., Trethowan, W. N., Harrington, J. M., Calvert, I. A., and Glass, D. C. (1992). "Occupational Exposure to Carbon Monoxide and Sulfur Dioxide During the Manufacture of Carbon Black." *Annals of Occupational Hygiene*, 36(4), 363-372.

Girman, J.R., Chang, Y.L., Hayward, S.B. and Liu, K.S. (1993) Causes of Unintentional Deaths from Carbon Monoxide Poisoning in California. Department of Health Services, Berkeley, CA, 94704.

Gourdeau, P., Parent, M., and Soulard, A. (1995). "Exposition à l'oxyde de carbone dans les garages d'automobiles: évaluation chez les mécaniciens." *Canadian Journal of Public Health*, 86(6), 414-417.

Hagberg, M., Kolmodin-Hedman, B., Lindhal, R., Nilsson, C.-A., and Nordstrom, Å. (1985). "Irritative Complaints, Carboxyhemoglobin Increase and Minor Ventilatory Function Changes Due to Exposure to Chain-saw Exhaust." *European Journal of Respiratory Disease*, 66, 240-247.

Heckerling, P. S., Leikin, J. B., and Maturen, A. (1988). "Occult Carbon Monoxide Poisoning: Validation of a Prediction Model." *The American Journal of Medicine*, **84**, 251-256.

Hosey, A. D. (1970). "Priorities in Developing Criteria for "Breathing Air" Standards." *Journal of Occupational Medicine*, 12, 43-46.

Hossain, M. A., and Saltzman, B. E. (1989). "Laboratory Evaluation of Passive Colorimetric Dosimeter Tubes for Carbon Monoxide." *Applied Industrial Hygiene*, 4, 119-125.

Jabara, J. W., Keefe, T. J., Beaulieu, H. J., and Buchan, R. M. (1980). "Carbon Monoxide: Dosimetry in Occupational Exposures in Denver, Colorado." *Archives of Environmental Health*, 35(4), 198-204.

Jankovic, J., Jones, W., Burkhard, J., and Noonan, G. (1991). "Environmental Study of Firefighters." *Annals of Occupational Hygiene*, 35(6), 581-602.

Johnson, C. J., Moran, J. C., Paine, S. C., and Anderson, H. W. (1975). "Abatement of Toxic Levels of Carbon Monoxide in Seattle Ice Skating Rinks." *American Journal of Public Health*, 65(10), 1087-1090.

Johnson, T. (1984). *A Study of Personal Exposure to Carbon Monoxide in Denver, Colorado.* U.S. Environmental Protection Agency, Environmental Monitoring Systems Laboratory, Research Triangle Park, NC. Report No. EPA-600/4-84-014

Kamei, M., and Yanagisawa, Y. (1997). "Estimation of CO Exposure of Road Construction Workers in Tunnel." *Industrial Health*, 34, 119-125.

Kirkpatrick, J. N. (1987). "Occult Carbon Monoxide Poisoning." *The Western Journal of Medicine*, **146**, 52-56.

Lawler, P. J. (1984). "Current Use of Ambient and Biological Monitoring: Reference Workplace Hazards. Inorganic Toxic Agents - Carbon Monoxide II." In: *Assessment of Toxic Agents in the Workplace Roles of Ambient and Biological Monitoring*, A. Berlin, R. E. Yodaiken, and B. A. Henman, eds., Kluwer Academic Publishers Group, Boston, MA.

Lees, P. S. J. (1995). "Combustion Products and Other Firefighter Exposures." Occupational Medicine: State of the Art Reviews, Hanley and Belfus, Inc., Philadelphia, PA, 691-706.

Leichnitz. (1993). "Determination of the Time-Weighted Average Concentration of Carbon Monoxide in Air Using a Long-Term Detector Tube." *IARC Scientific Publications*, 109, 346-352.

Levesque, B., Lavoie, R., Dewailly, E., Prud'Homme, D., and Allaire, S. (1991). "An Experiment to Evaluate Carbon Monoxide Absorption by Hockey Players in Ice Skating Rinks." *Veterinary and Human Toxicology*, 33(1), 5-8.

Levesque, B., Allaire, S., Prud'Homme, D., Rhainds, M., Lebel, G., Bellemarre, D., and Dupuis, K. (1997). "Indoor Motocross Competitions: Air Quality Evaluation." *American Industrial Hygiene Journal*, 58, 286-290.

Limasset, J., Diebold, F., and Hubert, G. (1993). "Assessment of Bus Drivers' Exposure to the Pollutants of Urban Traffic." *The Science of the Total Environment*, 134, 39-49.

Litovitz, T. L., Clark, L. R., and Soloway, R. A. (1994). "1993 annual report of the American Association of Poison Control Centers Toxic Exposure Surveillance System." *American Journal of Emergency Medicine*, 12(5), 546-84.

Litovitz, T. L., Felberg, L., White, S., and Klein-Schwartz, W. (1996). "1995 annual report of the American Association of Poison Control Centers Toxic Exposure Surveillance System." *American Journal of Emergency Medicine*, 14(5), 587-537.

Materna, B. L., Jones, J. R., Sutton, P. M., Rothman, N., and Harrison, R. J. (1992). "Occupational Exposures on California Wildland Fire Fighting." *American Industrial Hygiene Journal*, 53(1), 69-76.

McCammon, C. S., Halperin, W. F., and Lemin, R. A. (1981). "Carbon Monoxide Exposure from Aircraft Fueling Vehicles." *Archives of Environmental Health*, 36(3), 136-138.

McCammon, J. B., McKenzie, L. E., and Heinzman, M. (1996). "Carbon Monoxide Poisoning Related to the Indoor Use of Propane-Fueled Forklifts in Colorado Workplaces." *Applied Occupational and Environmental Hygiene*, 11(3), 192-198.

McConnaughey, P. W., McKee, E. S., and Pritts, I. M. (1985). "Passive Colorimetric Dosimeter Tubes for Ammonia, Carbon Monoxide, Carbon Dioxide, Hydrogen Sulfide, Nitrogen Dioxide, and Sulfur Dioxide." *American Industrial Hygiene Journal*, 45, 357-362.

Michaels, D., and Zoloth, S. R. (1991). "Mortality Among Urban Bus Drivers." *International Journal of Epidemiology*, 20(2), 399-404.

MMWR. (1994). "CO Levels During Indoor Sporting Events - Cincinnati, 1992-1993." *Journal of the American Medical Association*, 271(6), 419.

MMWR. (1996). "CO Poisoning on an Indoor Ice Arena and Bingo Hall - Seattle, 1996." *Morbidity and Mortality Weekly Report*, 45(13), 265-267.

Morris, R. D., Naumova, E. N., and Munasinghe, R. L. (1995). "Ambient Air Pollution and Hospitalization for Congestive Heart Failure among Elderly People in Seven Large US Cities." *American Journal of Public Health*, 85, 1361-1365.

Nillsen, C.-A., Lindahl, R., and Norstrom, Å. (1987). "Occupational Exposure to Chain Saw Exhausts in Logging Operations." *American Industrial Hygiene Association*, 48(2), 99-105.

NIOSH. (1972). *Criteria for a recommended standard Occupational Exposure to Carbon Monoxide.* NIOSH Publication Number 73-11000, *NTIS Publication Number PB-212-629*, U.S. Department of Health, Education, National Institute for Occupational Safety and Health, National Technical Information Service, Springfield, VA.

NIOSH. (1990). *National Occupational Exposure Survey.* NIOSH Pub. No. 89-103, U.S. Department of Health and Human Services, Centers for Disease Control and Prevention, National Institute for Occupational Safety and Health, Cincinnati, OH.

NIOSH. (1994). *Documentation for Immediately Dangerous to Life or Health (IDLHs).* NTIS Pub. No. PB-94-195-047, U.S. Department of Health and Human Services, Centers for Disease Control and Prevention, National Institute for Occupational Safety and Health, Springfield, VA.

OSHA. (1993). 29 CFR Part 1910.1000 Air Contaminants, Table Z-1; Amended by *Federal Register* 58:35308, 35340 (June 30, 1993); corrected by *Federal Register* 58:40191 (July 27, 1993)., U.S. Department of Labor, Occupational Safety and Health Administration.

Ott, W. R., Rodes, C. E., Drago, R. J., Williams, C., and Burmann, F. J. (1986). "Automated Data-Logging Personal Exposure Monitors for Carbon Monoxide." *Journal of the Air Pollution Control Association*, 36(8), 883-887.

Ott, W., Switzer, P., and Willits, N. (1994). "Carbon Monoxide Exposures Inside an Automobile Traveling on an Urban Arterial Highway." *Journal of the Air and Waste Management Association*, 44(8), 1010-18.

Ott, W. R., Vreman, H. J., Switzer, P., and Stevenson, D. K. (1995) "Evaluation of Electrochemical Monitors for Measuring Carbon Monoxide Concentrations in Indoor, In-Transit, and Outdoor Microenvironments." *Proceedings of the Air and Waste Management Conference on Measurement of Toxics and Related Air Pollutants*, Research Triangle Park, NC, May 1995.

Peters, J. M. (1984). "Multidisciplinary Approach to Prevention and Health Protection by Monitoring: Role of Individual Disciplines. The Epidemiologist: Value of Monitoring." In: *Assessment of Toxic Agents in the Workplace Roles of Ambient and Biological Monitoring*, A. Berlin, R. E. Yodaiken, and B. A. Henman, eds., Kluwer Academic Publishers Group, Boston, MA.

Quackenboss, J. J., Kanarek, M. S., Spengler, J. D., and Letz, R. (1982). "Personal monitoring for nitrogen dioxide exposure: methodology considerations for a community study." *Environment. International*, 8, 249-258.

Raaschou-Nielsen, O., Nielsen, M. L., and Gehl, J. (1995). "Traffic-Related Air Pollution: Exposure and Health Effects in Copenhagen Street Cleaners and Cemetery Workers." *Archives of Environmental Health*, 50(3), 207-213.

Radford, E. P. (1984). "Current Use of Ambient and Biological Monitoring: Reference Workplace Hazards. Inorganic Toxic Agents - Carbon Monoxide I." In: *Assessment of Toxic Agents in the Workplace Roles of Ambient and Biological Monitoring*, A. Berlin, R. E. Yodaiken, and B. A. Henman, eds., Kluwer Academic Publishers Group, Boston, MA.

Roscovanu, A., Krämer, U., Baginski, B., and Dolgner, R. (1985). "Carboxyhemoglobin Levels of Selected Population Segments Living in Urban and Rural Environments of North Rhine-Westphalia." *Zbl. Bakt. Hyg., I. Abt. Orig. B*, 180, 359-380.

Saltzman, B. E., and Caplan, P. E. (1995). "Chapter 18. Detector Tubes, Direct-Reading Passive Badges, and Dosimeter Tubes." In: *Air Sampling Instruments for Evaluation of Atmospheric Contaminants, 8th Edition*, B. S. Cohen and S. V. Hering, eds., American Conference of Certified Industrial Hygienists, Cincinnati, Oh, 401-437.

Schwartz, J., and Morris, R. (1995a). "Air Pollution and Hospital Admissions for Cardiovascular Disease in Detroit, Michigan." *American Journal of Epidemiology*, 142, 23-35.

Schwartz, J. (1995b). "Editorial: Is Carbon Monoxide a Risk Factor for Hospital Admission for Heart Failure?" *American Journal of Public Health*, 85, 1343-1345.

Shephard, R. J. (1983). *Carbon Monoxide, The Silent Killer*, Charles C. Thomas, Springfield, Il.

Shepherd, M. (1947). "Rapid Determination of Small Amounts of Carbon Monoxide. Preliminary Report on the NBS Colorimetric Indicating Gel." *Analytical Chemistry*, 19(2), 77-81.

Smith, J. P., and Shulman, S. A. (1994). "Evaluation of a Personal Data Logging Monitor for Carbon Monoxide." *Appl. Occup. Environ Hyg.*, 9(6), 418-417.

Soslow, A. R., and Woolf, A. D. (1992). "Reliability of Data Sources for Poisoning Deaths in Massachusetts." *American Journal of Emergency Medicine*, 10(2), 124-127.

Spengler, J. D., Duffy, C. P., Letz, R., Tibbitts, T. W., and Ferris, B. G. J. (1983). "Nitrogen dioxide inside and outside 137 homes and implications for ambient air quality standards and health effects research." *Environmental Science and Technology*, 17, 164-168.

Steenland, K. (1996). "Epidemiology of Occupation and Coronary Heart Disease: Research Agenda." *American Journal of Industrial Medicine*, 30, 495-499.

Szalai, A., ed. (1972). *The Use of Time: Daily Activities of Urban and Suburban Populations in Twelve Countries*, Morton Publishers, The Hague, Netherlands.

USDHHS. (1986-1992). In Annually Published Reports: *Vital Statistics of the United States, 1984 - 1992: Volume II - Mortality, Part A.*, U.S. Department of Health and Human Services, Public Health Service, National Center for Health Statistics, Hyattsville, MD.

USDHHS. (1996). *Preventing Carbon Monoxide Poisoning from Small Gasoline-Powered Engines and Tools.* DHHS (NIOSH) Pub. No. 96-118, U.S. Department of Health and Human Services,

Centers for Disease Control and Prevention, National Institute for Occupational Safety and Health, Cincinnati, OH.

USEPA. (1991). *Air Quality Criteria for Carbon Monoxide.* EPA-600/8-90/045F, U.S. Environmental Protection Agency, Research Triangle Park, NC.

van Netten, C., Brubaker, R. L., Mackenzie, C. J. G., and Godolphin, W. J. (1987). "Blood Lead and Carboxyhemoglobin Levels in Chainsaw Operators." *Environmental Research*, 43, 244-250.

Virtamo, M., and Tossavainen, A. (1976). "Carbon Monoxide in Foundry Air." *Scandinavian Journal of Work and Environmental Health*, 2,Suppl. 1, 37-41.

Wallace, L. A. (1983). "Carbon Monoxide in Air and Breath of Employees in an Underground Office." *Journal of the Air Pollution Control Association*, 33(7), 678-682.

Wallace, L. A., and Ziegenfus, R. C. (1985). "Comparison of Carboxyhemoglobin Concentrations in Adult Nonsmokers with Ambient Carbon Monoxide Levels." *Journal of the Air Pollution Control Association*, 35(9), 944-949.

Wallace, L., Thomas, J., Mage, D., and Ott, W. (1988). "Comparison of Breath CO, CO Exposure, and Coburn Model Predictions in the U.S. EPA Washington-Denver (CO) Study." *Atmospheric Environment*, 22(10), 2183-2193.

WHO (1994). "Update and Revision of the Air Quality Guidelines for Europe." *Meeting of the Working Group "Classical" Air Pollutants*, Bilthoven, The Netherlands, EUR/ICP/EHAZ 94 05/BP01.

Woebkenberg, M. L., and McCammon, C. S. (1995). "Chapter 19. Direct-Reading Gas and Vapor Instruments." In: *Air Sampling Instruments for Evaluation of Atmospheric Contaminants, 8th Edition*, B. S. Cohen and S. V. Hering, eds., American Conference of Certified Industrial Hygienists, Cincinnati, Oh, 439-510.

Tables

Table 1-1. Carbon Monoxide Air Quality Standards for Ambient and Occupational Environments.

Standard/Environment	Date of Standard	Concentration	Time
Ambient Air			
National Ambient Air Quality Standard[1]	1985	9 ppm[a]	8 hr
		35 ppm[a]	1hr
California Air Resources Board[2]	1982	9 ppm	8 hr
		20 ppm	1 hr
World Health Organization Europe[3]	1987	90 ppm	15 min
		50 ppm	30 min
		25 ppm	1 hr
		9 ppm	8hr
Occupational			
OSHA (PEL)[4]	1992	50 ppm	8 hr
NIOSH (REL)[5]		35 ppm	8 hr
		200 ppm	Ceiling
		1200 ppm	IDLH[b]
ACGIH (TLV)[6]	1992	25 ppm	8 hr
		1200 ppm	IDLH[b]
CAL/OSHA[7]	1995	25 ppm	8 hr

[a]Not to be exceeded more than once a year

[b]Immediately Dangerous to Life or Health (not actually a standard, but a guideline for respirator selection).

[1]USEPA, 1991

[2]CARB, 1989

[3]WHO, 1994

[4]OSHA, 1993

[5]NIOSH, 1972, NIOSH, 1994

[6]ACGIH, 1991

[7]Cal/OSHA, 1997

Table 1-2. Key Health effects of exposure to Carbon Monoxide which have been used to set ambient air quality standards. Note that fetuses, infants, pregnant women, elderly people, and people with anemia or a history of cardiac, respiratory, respiratory or vascular disease may be more sensitive to CO than the general population. (adapted from USEPA, 1991).

Target Organ	Health Effect	Sensitive Population
Heart	Angina pectoris (chest pain) causing reduced exercise duration with peak ambient exposure (3-6% COHb)	Individuals with ischemic heart disease
Heart/Lung	Maximal exercise performance reduced with 1-hr peak CO exposures (≥ 2.3% COHb)	Healthy individuals
Brain	Effects observed (equivocal) on neuro-behavioral performance such as visual perception, hearing, vigilance, motor and sensor-motor coordination, etc. (≥ 5% COHb). Neurological symptoms: Headache, dizziness, weakness, nausea, confusion, disorientation, and visual disturbances (≥ 10% COHb). With increasing exposure to high levels leading to unconsciousness and death	Healthy individuals

Table 1-3. Observed occupational CO exposures, carboxyhemoglobin (COHb) levels, or environmental CO measurements for various categories of jobs or work environments.

Occupational Category	Measured CO Exposures	References
Forklift Operators and workers in facilities with forklifts	8 - 48 ppm 8hr TWA 21.1± 0.7%COHb 4.2-28.2% COHb < 50 ppm 8 hr TWA	McCammon, 1996 Ely, 1995 Fawcett, 1992a USEPA, 1991
Foundries/Heavy Industry	>6% COHb in 26% NS 0-83 ppm 4h TWA 2% COHb increase 2.3-14.9% COHb NS 50-250 ppm ENV	Virtamo, 1976 Gardiner, 1992 USEPA, 1991 Shepherd, 1983 Shepherd, 1983
Bus Drivers	8 - 13 ppm TWA 1-23 ppm TWA	Limasset, 1993 USEPA, 1991
Traffic/Roadway Workers	>5% COHb in 45% NS 5 - 42 ppm in tunnel 12-60 ppm INT >9ppm 8hr in 30% 10-40 ppm TWA 1-4.3 ppm ENV	Gourdeau, 1995 Kamei, 1997 Colwill, 1980 Flachsbart, 1995 USEPA, 1991 Raaschou-Nielsen, 1995
Airport Workers	5-300 ppm INT 5-11 ppm ENV	McCammon, 1981 Bellin, 1980
Firefighters	3-7% COHb NS 11-1100 ppm ENV 100 - 5000 ppm ENV 1.4 -38 ppm TWA 10-14% COHb	Brotherhood, 1990 Lees, 1995 Jankovic, 1991 Materna, 1992 Shephard, 1983
Chainsaw/gas tool operators	4 - 70 ppm TWA 4 - 75 ppm TWA 15 - 55 ppm TWA >200 ppm in < 120 sec	Nillsen, 1987 Hagberg, 1985 van Netten, 1987 USDHHS, 1996
Office Workers	8-26 ppm 8 hr TWA	Wallace, 1983
Sporting Events	19 -56 ppm 4 hr TWA 0-5% COHb 80-140 ppm ENV 3-14% COHb 100-300 ppm ENV	Levesque, 1997 Levesque, 1991 MMWR, 1994 MMWR, 1996 Johnson, 1975

NS = Non-smokers; ENV = short-term environmental measurements;
INT = Interior of vehicle
Percent of population exposed presented using expression "in %" (e.g., >9ppm 8hr in 30% means 30% of population exposed > 9 ppm)

Chapter 2: The Importance of CO Exposure Assessment in Studying Chronic and Subacute Health Effects

Introduction

Health effects from exposure to CO as an air pollutant can be categorized roughly into four categories; lethal, acute, sub-acute, and chronic. Most of the statistics compiled on CO poisoning are for the first two categories – lethality and acute effects. Although these statistics point to a serious public health problem, it is possible that a much larger number of people experience sub-acute and possibly chronic health effects from recurrent or continual exposure to CO. The CO health effects literature suggests that CO exposures much lower than those causing acute effects may have profound consequences to exposed populations, especially sub-populations of sensitive individuals.

As discussed in the previous chapter, the U.S. Environmental Protection Agency (USEPA) has set the National ambient Air Quality Standard (NAAQS) for CO at 35 ppm for 1-hour and 9 ppm for 8-hours (neither to be exceeded more than once per year). This standard is designed to protect sensitive individuals in the population from carboxyhemoglobin levels rising above 2.1% (USEPA, 1991). This NAAQS is based upon CO induced angina pectoris experienced at COHb levels of about 2-3% during exercise in otherwise healthy, young individuals with ischemic heart disease. Although the NAAQS for CO is already quite stringent, it is questionable whether this threshold-based standard is set low enough to be health-protective for other large sensitive populations in the U.S. Furthermore, because the NAAQS is applicable to the quality of outdoor air only, it does not protect against exposures due to indoor CO sources.

The state of knowledge of the distribution of CO exposures in the U.S. has been limited by the cost of accurate population-based CO exposure surveys. The current approach to population-based CO monitoring involves the use of a network of fixed-site outdoor monitoring stations where at best a few monitoring instrument are used to infer the exposure of tens of thousands to millions of individuals (USEPA, 1991). Although the instrumentation used in this network is very sensitive and accurate, the approach lacks the ability to represent personal exposures since outdoor CO monitoring is known to correlate poorly with total CO exposures of the inhabitants of the communities where the monitors are placed (Wallace, 1985; Akland, 1985).

The poor specificity of the current population-based exposure monitoring network precludes the ability to infer whether sub-acute and chronic CO exposure in our populations carries a significant health burden. With the development of more sensitive and accurate means of assessing individuals' exposures, previously indiscernible relationships between chronic CO exposure and health effects may be resolved. For example, the role, if any, that chronic CO exposure plays in the etiology of heart disease or developmental defects in the human fetus may be discernible through improvements in CO exposure assessment techniques.

It is possible that the human fetus and the developing neonate are a more sensitive group than individuals with pre-existing cardiovascular disease. In the course of setting the standards for CO, USEPA conducted a thorough literature review of CO toxicology including animal studies, and where available, human epidemiological data. The review includes a body of literature on the developmental toxicity of CO, an alternative to the cardiovascular toxicity endpoints upon which the standard is based. This chapter provides a brief review of CO toxicology literature in the context of the broader issues of the health effects of CO exposure, including developmental toxicology.

CO Exposure Distribution Relative to Potential Chronic and Sub-acute Health Effects

Although CO has been monitored in the urban outdoors since the 1960s, very little is known about the distribution of the concentrations of CO in various indoor environments (USEPA, 1991). This is unfortunate, because enclosed spaces are where CO is likely to be present in higher concentrations. The reasons for this are (1) indoor environments limit available dilution air, and (2) combustion sources including automobiles and other internal combustion devices, space heating, water heating, and cooking devices have the potential to emit CO into these enclosed spaces. Furthermore, studies have shown that on average people spend approximately 90% of their time indoors and 65 to 70% of their time in their residences (Chapin *et al.*, 1974; Quackenboss *et al.*, 1982; Spengler *et al.*, 1983; Szalai, 1972). It is likely that the distribution of indoor CO in the U.S. population is continuous. The concentrations which cause acute poisonings are at the tail of this distribution. It is also likely that there is a huge population, the body of the exposure distribution curve, which is exposed to CO at levels which are not high enough to cause acute symptoms but are elevated to the extent that they pose a health risk.

As discussed in Chapter 1, two main studies have provided evidence that a significant sub-population with CO chronic or sub-acute CO exposures does indeed exist. These were the NHANES II (Radford, 1982) and the Washington DC and Denver (Akland, 1985; Johnson, 1984; Wallace, 1988) studies.

The NHANES II study measured COHb levels in blood of a randomly selected sample of about 8400 smoking and non-smoking persons 3-74 years of age living throughout the U.S. (Radford, 1982). The COHb data of never-smokers aged 12-74 years (N = 3141) from this study were approximately lognormal with a geometric mean (GM) of about 0.725 and a geometric standard deviation (GSD) of about 2.15. Figure 1 shows a hypothetical lognormal probability distribution with these parameters. The shaded area under the curve represents the population at risk due to COHb levels in excess of the NAAQS. From the study it was found that 6.4% of the never-smoking population had levels above 2.1% COHb, a level at which adverse health effects can occur in sensitive populations. COHb levels in smokers were much higher.

The Denver-Washington, DC study is the only large-scale population-based CO exposure field study that has been undertaken to date (USEPA, 1991). Three approaches were used to assess the CO exposures of the inhabitants of these cities. Electrochemical personal exposure monitors (PEMs) were used to collect randomly selected 24-hour CO exposure profiles on 450 participants in Denver and 800 participants in Washington, DC (Akland,

1985). The personal exposure measurements were compared to ambient CO concentrations monitored using the nearest fixed-site CO monitors (Akland, 1985). Finally, personal end-expired breath samples were taken from the participants that carried the PEMs. The random probability samples from these cities represented 1.2 million non-smoking adult inhabitants in Washington, DC and 500,000 in Denver.

The PEM data in the Denver-Washington, DC study showed that over 10% of the Denver residents had 8-hr exposures in excess of the 9 ppm NAAQS. This was not reflected in the simultaneous fixed-site monitoring where CO measurements exceeded 9 ppm only 3% of the time (Akland, 1985). An end-expired breath CO concentration of 10 ppm is equivalent to about 2% COHb (USEPA, 1991). About 12.5% of the Denver participants had end-expired breath CO levels in excess of 10 ppm (Wallace, 1988).

Similarly, the PEM results for Washington, DC showed that 4% of the residents had 8-hr exposures in excess of the 9 ppm NAAQS. The outdoor fixed-site monitors never detected levels as high as 9 ppm (Akland, 1985). About 6% of the Washington, DC participants had had end-expired breath CO levels in excess of 10 ppm (Wallace, 1988). Some corrections were necessary for the Washington, DC data because of instrumental measurement drift in the electrochemical PEMs. After correction, 10% of the participants in Washington, DC were found to have 8-hr average CO exposures above the NAAQS of 9 ppm.

The implication of these population based exposure studies is that about 10% of the population of the US may be exposed to CO levels which are known to adversely affect the health of sensitive individuals. Assuming a U.S. population of 250 million, and the 6.4% figure from the NHANES II study, some 16 million individuals may have COHb levels above 2%. From the representative probability samples of non-smoking adults in Washington, DC and Denver, an estimate of about 120,000 and 60,000, respectively, of these individuals may be exposed above the NAAQS. Of this long-tailed right-skewed distribution, only the very extreme right end represents exposures causing the documented acute health effects.

Occupational exposure data from the Washington, DC-Denver study

An analysis of the distribution of CO exposures by occupational status was included in the Washington, DC study. The exposure distributions of persons not working outside of home were compared to those for persons in low and in high CO exposure occupational categories (determined *a priori* by job type not by measurement). The high occupational exposure category included jobs as truck drivers, taxi drivers, bus drivers, automobile mechanics, garage workers, and policemen (Hartwell, 1984).

The maximum 8-hour CO concentration distribution indicated that about 30% of the workers in the high exposure category were exposed above 9 ppm for 8 hours. In contrast, about 4% of the low exposure occupational group and 2% the non-occupational group had exposures exceeding 9 ppm for 8-hours. About 3% of the high exposure category had 8-hour average exposures above 25 ppm (Hartwell, 1984).

Review of CO Toxic Mechanisms and Health Effects

Physiology of CO exposure

Toxic mechanisms of CO exposure

The toxic effects of exposure to CO are primarily due to hypoxia caused by the reduced oxygen carrying capacity of blood, and interference of the intracellular biochemical usage of oxygen (O_2). The toxic mechanism, competitive binding of CO to hemoglobin molecules in the red blood cells, displaces oxygen uptake. At higher CO concentrations CO also competes for sites in the myoglobin in muscle tissue. Additionally, CO is thought to have a role in poisoning of cytochrome a_3 and cytochrome P-450 within mitochondria at high CO exposures (USEPA, 1984; Shephard, 1983). The formation of carboxyhemoglobin (COHb) occurs through chemical binding of CO to hemoglobin, analogous to the normal formation of oxyhemoglobin. Due to the chemistry of these formations, CO has an affinity to hemoglobin 220 to 250 times that of O_2 (USEPA, 1991). An air concentration of CO 0.4% of that of oxygen will therefore cause a 50% saturation of the blood's oxygen carrying capacity with COHb. The transport of O_2 is further compromised by its reduced ability to disassociate from a hemoglobin molecule which has CO bound to one if its four heme units. This loss of "facilitation" causes a left-ward shift in the oxygen-disassociation curve as compared to common anemia (USEPA, 1984). Additional important factors influencing the accumulation of COHb are blood pH, carbon dioxide concentration, temperature, and 2,3-diphosphoglycerate (2,3-DPG) the availability of which in red blood cells strongly affects the affinity of O_2 for hemoglobin (Jain, 1990).

Myoglobin reacts with CO to form carboxymyoglobin (COMb). The myoglobin molecule contains only one heme group as compared to four in hemoglobin. Myoglobin normally serves as an intracellular oxygen store and facilitates O_2 diffusion in muscle tissue, and is critical in periods of physical exertion where brief bursts of oxygen are needed (Shephard, 1983). Disruption of this function by displacement of oxygenated myoglobin with COMb is likely to be important in the toxicology of CO exposure, especially with regard to creation of hypoxic conditions in cardiac tissue.

Some effects of CO poisoning are not explained simply by COHb induced tissue hypoxia. It is possible that intracellular CO may inhibit mitochondrial electron transport affecting cellular respiration and energy metabolism mechanisms. The active center of the cytochromes are iron containing heme groups just as in hemoglobin and myoglobin (Huheey, 1978). Due to the similarity of cytochrome chemistry to that of hemoglobin, it is no surprise that CO would be implicated in disrupting cellular respiration. CO can bind with mitochondrial cytochrome a_3 oxidase and cytochrome P-450 blocking oxidation. There seems to be much question as to the exact mechanisms of mitochondrial response to CO, and on the ultimate burden on metabolism that is causes. However, there is some indication that the CO-cytochrome reactions occur at levels below 30% COHb (Jain, 1990).

Endogenous CO Production.

The natural decay of hemoglobin in red blood cells is the primary source of endogenous CO production. One mole of CO and one mole of bilirubin are produced for each mole of heme catabolized in the liver as the body eliminates the spent corpuscles. Other sources of CO are the degradation of other heme containing compounds in the liver, and lipid peroxidation. Diseased bone marrow is another site of CO generation (Jain, 1990). The turnover of myoglobin is quite slow, and therefore has little contribution as an endogenous source. An urban non-smoker who is not chronically exposed to other major CO sources has a baseline blood COHb concentration of about 1%. About ½ of this is due to endogenous sources (Shephard, 1983). Females in the progesterone period of their menstrual cycle have about twice the endogenous CO production rate as during the estrogen phase and of that of men (Jain, 1990). The newborn infant has about an order of magnitude higher endogenous CO production. Thus, the pregnant woman has the additional burden of the fetal endogenous CO production which is exchanged across the placenta, and accounts for about 3% of her COHb (Shephard, 1983).

Interaction of Diet and CO Exposure.

Recent research suggests that protein deficiency in the maternal diets of mice causes a statistically significant exacerbation of placental COHb at levels in CO as low as 65 ppm (Singh *et al.*, 1992). It is possible that a synergy in the effects of poor diet and CO exposures may adversely affect human fetal development disproportionately.

CO Uptake and Distribution.

Once inhaled, CO and O_2 diffuse across the alveolar capillary membrane in much the same way. Physiological uptake is affected by many factors including the following: (1) the atmospheric concentration and density of CO, and the relative concentrations of O_2, CO_2, and nitrogen; (2) the temperature and relative humidity of the atmosphere of exposure; (3) the alveolar ventilation rate and the gradient of CO partial pressures across the alveolar membranes to the pulmonary capillary blood; (4) the cardiac output; (5) the diffusing capacity of the lungs for CO; (6) the CO-hemoglobin rate kinetics; (7) the quantity and flowrate of lung capillary blood; (8) the hemoglobin concentration and hematocrit values; (9) the rate of endogenous CO production; and (10) the rates of metabolic CO consumption and CO elimination. Once within the body, at least 80% of the CO binds with hemoglobin, 10-15% binds with myoglobin, and about 5% may react with heme-containing molecules in the liver and other organs (USDHHS, 1986).

Pharmacokinetic Models.

Several pharmacokinetic models have been developed for mammalian exposure to CO (Shephard, 1983). The model currently thought to be the most accurate for the range of possible CO exposures is the Coburn-Foster-Kane equation (Coburn *et al.*, 1985). Figure 2-2 was calculated using this model applied to a normally healthy adult under light physical activity with various exposures to CO. Included are an overlay of acute and sub-acute responses to these exposures. This model incorporates most of the factors discussed above, considering the pulmonary CO uptake and elimination as well as endogenous CO production and dilution of the CO stored in the body. Mathematical details of this model

are not included here; however, it forms an important part of risk-assessment and standards development for CO exposure (USEPA, 1991; WHO, 1979).

CO readily diffuses across the placenta into fetal blood. Fetal uptake and elimination of CO is 2 to 3 times slower than that of the mother's. Deleterious effects are thought to be from impairment of the fetal metabolism as well as from hypoxia (Jain, 1990).

Adaptation to CO

Short-term physical adjustment to CO poisoning may be mediated by increased coronary blood flow, cerebral blood flow or peripheral oxygen extraction. This may be possible when activity is low, but in the case of exercise, little excess flow capacity is available. Long-term acclimatization has been shown to occur through development of polycythemia (increased red cell count), much as with acclimatization to altitude. Moderate increases in COHb may lead to increases in 2,3 DPG which facilitates the unloading of O_2 into active tissues (Shephard, 1983).

Lethal and acute CO health effects

It is likely that the U.S. mortality and poisoning statistics grossly underestimate the true values since CO poisoning often goes undetected unless it is specifically tested for. Death can occur with prolonged exposure to about 500 ppm, and at 20,000 ppm, CO exposure is rapidly fatal. Acute CO poisoning symptoms include unconsciousness, temperature rise, increased pulse and breathing rate, impaired hearing and vision, and general weakness. Death is the likely outcome of acute CO poisoning if no intervention occurs. A long list of outcomes of survival from acute CO poisoning exists. The mechanism of toxicity basically stems from the asphyxiation of perfused tissues at the cellular level. In particular, those tissues most requiring oxygen are the most likely damaged, i.e., the heart and the brain. Long-term consequences are due to central nervous system damage, often with some delay after the actual poisoning, causing reduction or loss of hearing and eyesight, neuropsychiatric sequelae, and necrotic damage throughout the organ systems of the body (USEPA;, 1991; Jain, 1990). There is no debate with regard to the extreme effects of acute poisoning.

Physiological Effects of Sub-Acute and Chronic CO Exposure

Whereas acute CO poisoning has rather violent clinical features, sub-acute and chronic poisoning can often be disregarded for long periods of time. As outlined above, a very large sub-population may be exposed to these lower concentrations. The medical evidence of adverse effects from low level exposures to carbon monoxide is based on (1) epidemiology studies, (2) animal toxicology studies, and (3) human clinical studies. Many of the features of chronic CO poisoning are well documented and form the basis of the USEPA standards for CO which are set low enough to protect sensitive individuals (USEPA, 1991). For otherwise healthy persons, COHb concentrations less than 10% are unlikely to have acute symptoms. Exposure at this level has been termed "occult" poisoning, with vague and often misdiagnosed symptoms such as headache, fatigue, dizziness, paresthesias, chest pains, palpitation and visual disturbances (Kirkpatrick, 1987).

Tobacco smoking is a common long-term source of CO exposure and can be significant for the smoker. CO concentrations in mainstream cigarette smoke are about 400 ppm, and corresponding COHb levels can exceed 10%. The U.S. mean COHb concentrations for cigarette smokers is above 4% (Radford and Drizd, 1982). This population falls into the chronic exposure category without additional exposure, and is subject to much epidemiological and clinical study. Mortality due to heart disease and cancers in smokers is 70% higher than in similar non-smoking populations, but the effects of CO are confounded by those of nicotine and thousands of other compounds present in tobacco smoke. Animal toxicology studies have been conducted in an effort to resolve some of these confounding issues.

Physiological effects of long-term exposure to CO at chronic and sub-acute levels have been investigated with the results being controversial. For healthy young adults, decreased oxygen uptake capacity and resultant decreased work capacity under maximal exercise conditions have been shown to occur starting at 5% carboxyhemoglobin, and several studies observed small decreases in work capacity at carboxyhemoglobin levels as low as 2.3 to 4.3% (USEPA, 1991).

Cardiovascular effects

People with obstructive coronary artery disease are likely to display a decreased threshold for angina and claudication with even mild exercise at COHb levels of 3 to 4%, an increase of about 2% COHb over baseline (Jain, 1990; Allred *et al.*, 1989). It is precisely this sensitive group of individuals which the USEPA has designed the CO standard to protect (USEPA, 1991).

Individuals with coronary artery disease (CAD) are potentially at risk of developing ventricular arrhythmias when exposed to CO. In a clinical setting CAD patients with no baseline ectopy exposed to CO to reach COHb levels of 4% showed no increase in ventricular arrhythmias during exercise when compared with controls (Hinderliter *et al.*, 1989). However, individuals with CAD and higher levels of ventricular ectopy displayed ventricular arrhythmias at 5.3% COHb during exercise (Sheps *et al.*, 1990, 1991).

A study of 36 patients in Southern California with ischemic heart disease (IHD), a form of CAD, was conducted in their natural urban setting (Colome, 1992). The study was conducted to validate the clinical findings of the relationship between CO exposure, activity level, and ST-segment depression (an electrocardiograpically observable precursor to angina pectoris symptoms). The main hypothesis of the study was that: IHD subjects are at risk of developing levels of carboxyhemoglobin reported in clinical studies to cause ischemia and shorten the time to onset of angina. The subjects were monitored for CO exposure and electrocardiographic events and data were recorded every minute. They maintained a diary of activities, locations, and symptoms as they went about their daily routines. Monitoring sessions lasted for 24 hours. The researchers found, using a multiple logistic regression model, that the probability of an episode of ST-segment depression was significantly associated with level of metabolic activity (odds ratio =3.22, $p < 0.001$) and COHb estimated from CO exposure profile (odds ratio = 1.34, $p < 0.001$). The model predicted that 15% of the incident ST-segment episodes were attributable to ambient CO exposures (Colome, 1992). Thus, the authors suggested that their main finding was that urban CO exposures contribute to the total burden of myocardial ischemia experienced by men with IHD.

Epidemiological studies have indicated excess arteriosclerotic heart disease mortality for workers chronically exposed to CO in their occupation (Stern *et al.*, 1988, Stern *et al.*, 1989); however, USEPA postulates that the increased mortality may be the due the arrhythmogenic effects of acute CO exposure discussed above (USEPA, 1991). Animal studies are equivocal on this affect, showing CO induced atherosclerosis at high (>10%) COHb levels and hypercholesterolemic dietary conditions, with the exception of rabbits which developed aortic atherosclerosis on normal diets (Penney and Howley, 1991). This may be due to CO damage caused to the arterial endothelium and increased permeability to lipids (Doyle, 1979).

A human epidemiological study (not discussed by USEPA) strongly suggests that humans are susceptible to cardiac hypertrophy from CO (Goldsmith, 1970). The residents of Kinasa, a small village in Japan, at an elevation of about 1000 meters, were engaged in the manufacture of tatami mats indoors in the winter. Charcoal fires were used to heat the indoor spaces. COHb levels were found to reach 20 to 30%. The inhabitants of the village showed a 35.3% prevalence of abnormal heart conditions, with the frequency of angina pectoris attacks 3-5 times the average for the country. Cardiac enlargement was frequently found, among other physiological abnormalities.

Developmental effects

Acute CO poisoning of humans is known to cause major birth defects and fetal death, but the precise effects of chronic exposure on the developing organism are still controversial. Recent animal studies on fetal development have shown strong indications that CO induced fetotoxicity causes increased fetal mortality, decreased birthweight, impaired neurological and cardiac development, and possibly a genotoxic effect.

Fetotoxicity and Low Birthweight

Most developmental toxicology studies where pregnant animals were exposed to CO found that the CO exposure negatively affects birthweight. A CO dose-response function was measured for fetotoxicity in rats, with an effective lowest observed adverse effect level (LOAEL) of 125 ppm (this corresponds to an estimated COHb level of approximately 15%) when pregnant rats were exposed mid-gestation, suggesting fetal sensitivity to chronic CO exposure (Singh and Scott, 1984). Offspring of rabbits exposed in utero to 90 ppm (8-9% COHb) or 180 ppm (16-18% COHb) were found to have up to 20% reduction in birthweight and an increase of 34% in neonatal mortality. Offspring of human mothers who smoked during pregnancy have been shown to have a statistically significant reduction in birthweight compared to those of non-smoking mothers, although the presence of other constituents of tobacco smoke confound a clear analysis of the affects of CO (Astrup *et al.*, 1972).

Neurobehavioral

Cerebellar weight of rats exposed to 75 ppm up to 300 ppm CO of (11.5% to 26.8% COHb) were decreased compared to that of rats exposed to 0 ppm (baseline 2.5% COHb). Total cerebellar content of γ–aminobutric acid (GABA), a neurochemical indicator of cerebellar cortical neurons, was also lowered with maternal exposure to CO. These effects were statistically significant at 300 ppm. These results identified developmental processes in the cerebellum of the rat as vulnerable to early CO exposure (Storm *et al.*, 1986). A similar

study found that the developing neostriatum of the basal ganglia of the rat brain is altered by mild CO-induced hypoxia during the period of neuronal proliferation and synaptogenesis. The neurochemical changes included significant elevations of DNA and dopamine 11 days after CO exposures were discontinued for concentrations as low as 150 ppm (19% COHb). Additionally, the CO-exposed offspring had statistically significantly lower birthweights. The neurological changes are thought to reflect glial cell proliferation in response to neuronal injury. These changes are correlated with significant negative neuro-behavioral developmental consequences including deficits in performance in homing and negative geotaxis tests and possibly permanent memory deficits (Fechter *et al.*, 1987). Earlier research by the same researchers (Storm and Fechter, 1985) found that altered patterns of postnatal neurochemical development and postnatal development of the cerebellum are evident with chronic prenatal exposure of rats to CO in the range of 75 to 300 ppm (11.5% to 18.5% COHb). These cerebellar alterations continued to be evident 42 days after cessation of CO exposure, and the authors suggest that they may represent a permanent consequence for the CO-exposed fetus.

The lowest measured developmental exposure to CO to cause neurobehavioral effects are in the range of 6 to 11% COHb for mice perinatally exposed throughout gestation. The results of this work are controversial because of a lack of detail on exposure and measurement; however the CO-exposed mice were found to have an increased number of errors in maze tests at 6 weeks of age (Abbatiello and Mohrmann, 1979).

Cardiomegaly

Offspring of rats exposed to 200 ppm CO after the 7th day post-conception until birth were observed to develop cardiomegaly, while those neonates in the air-exposed control-group did not. Although COHb levels are not reported they are likely to be around 27-33% based on other similar exposure studies in rats (USEPA, 1991). The observed heart enlargement is due to a delayed binucleation of the myocytes which increases the duration of hyperplastic growth (cell number increase). When CO exposure is only prior to birth, the size of the right ventricle increases. CO exposure continued post-partum leads to myocyte hyperplasia of the left ventricle. This effect is thought to be due to the increased hemodynamic load caused by carboxyhemoglobinemia (Clubb *et al.*, 1986). Other researchers found a statistically significant increase in fetal rat heart weights at birth after a continuous exposure during pregnancy of 60 ppm CO (Prigge and Hochrainer, 1977). This appears to be a LOAEL for this effect. Cardiomegaly or cardiac hypertrophy due to CO exposure observed in rats is discussed thoroughly by USEPA. Experiments have found a threshold for cardiac hypertrophy near 200 ppm (12% COHb) for adult rats (USEPA, 1991). According to USEPA, no dose-response experiments have been published which present a no observed adverse effect level (NOAEL) for this endpoint.

Genotoxic effects of CO

In a recent experiment, pregnant mice were chronically exposed to 500 ppm CO for 60 minutes a day during pregnancy during different 1-week gestational periods (Kwak *et al.*, 1986). Other pregnant mice were administered single acute exposures to CO during different gestational periods. Both the chronically exposed and the acutely exposed mice were found to have a statistically significant increase in fetal blood and maternal bone marrow micronuclei and sister chromatid exchanges (SCE) for all gestational exposure

periods, when compared to controls which were exposed to zero ppm CO. Additionally, the acutely exposed mice showed a dose-dependent response to CO for both micronuclei and SCE, but the differences between exposed and control values for maternal bone marrow and fetal blood measurements were not statistically significant. These results indicate the possibility of a very different type of toxic endpoint than those observed above. The elevated levels of micronuclei and SCE may indicate a genotoxic mechanism; however, such a mechanism has not been established for CO exposure. Nonetheless the study appears to be conducted properly from a technical standpoint (Smith, 1993). This work is unique in the literature and may be questionable, however it would be interesting to know if it is reproducible. That this finding was not discussed in the current USEPA criteria document adds to its obscurity.

Discussion

The NAAQS for CO was developed to protect all individuals in the U.S. against adverse health effects from ambient CO exposures. The NAAQS was based on cardiovascular effects directly observed in humans with ischemic heart disease, at exposure levels only slightly above those set by the standard. Thus, the standard was designed assuming that individuals with ischemic heart disease form the most sensitive population. In reviewing the relevant literature it is clear that there are many other CO-related health endpoints, usually without direct human evidence, which are of equal importance to public health. In particular the potential for chronic CO exposure to cause significant developmental problems is of great concern.

The USEPA's choice of the cardiovascular effects endpoint to base the NAAQS for CO is quite defensible since the strongest conclusions can be drawn from these data. There is a large body of human health effects data which have been extensively confirmed for this endpoint, and there is a large population of sensitive individuals with heart disease at risk at rather low exposure levels. The NAAQS is designed to keep human COHb below 2.1%. Effects have been observed in healthy adult males at 2.3% COHb while undergoing maximal exercise, and patients with ischemic heart disease (IHD) have been found to experience angina pectoris at levels as low as 3.0% COHb. This implies that the NAAQS provides at best about 1% COHb or a factor of about two (i.e., 3% COHb IHD effect LOAEL minus baseline endogenous 1% COHb = 2% COHb margin between baseline and IHD effects), as a margin of safety for individuals with IHD. A factor of two may be a sufficient safety margin for this health endpoint given the fact that the standard is based on a measured human physiological response, and because the major sources of variability have already been accounted for, including the use of sensitive individuals to determine the LOAEL. The factor of two only has to account for the range of sensitivity within the sensitive population.

Nonetheless, compelling arguments can be made to suggest that an analysis of what safe CO exposure levels should be to protect against other CO-related adverse health effects. Developmental endpoints are of special concern.

Over 4.1 million children were born in 1990 (USDHHS, 1992). A recent review of developmental toxicology (Schardein and Keller, 1989) discusses four classes of human developmental toxicity. These are (1) intrauterine growth retardation (IUGR), primarily manifested by low birth weights; (2) embryolethality, manifested by miscarriage or

spontaneous abortion; (3) malformation, usually structural malformations but also functional, metabolic and behavioral disorders; and (4) functional disorder as a result of dysfunction, impairment, or deficit of any biological system. Selected estimated frequencies in humans for these classes are as follows. IUGR 7%, embryolethality (miscarriage) 11-25%, congenital malformation (at 1 year) 6-7%, and functional changes (neurologically abnormal at 1 year) 16-17%. Thus, the human fetus and developing infant are a very large population and from 100,000 to a million conceptions a year result in some sort of abnormal developmental endpoint each year. Schardein and Keller (1989) suggest that developmental toxicants may play a significant role in contributing to this problem.

The above review of developmental toxicology indicates the large number of documented developmental endpoints which can potentially be affected by chronic CO exposure, and which fall within the structure of classes of discussed by Schardein and Keller. These include increased fetal mortality, low birthweight, impaired neurological and cardiac development, and possibly genotoxicity. However, merely because there is evidence that CO is a developmental toxicant does not necessarily mean that exposure to CO is the cause of the large incidence of human developmental problems, but only that the potential may exist.

Chronic levels of CO seen in animals to cause developmental problems, range from a LOAEL of 125 ppm during the gestation period for rat fetotoxicity, to a 60 to 200 ppm LOAEL for cardiac hypertrophy (cardiomegaly) in fetal rats. Possible permanent memory deficits were seen in rats exposed prenatally to levels as low as 150 ppm.

As stated earlier, there is very little published evidence for the genotoxicity of CO. Spontaneous abortions, stillbirths and heritable diseases have been shown to be related to of alterations of DNA and of chromosomal aberrations, and many illnesses are the result of dominant gene mutations (Lu, 1991). Thus, genetic toxicity can lead to important health endpoints. The genotoxic response data in mice observed by Kwak *et al.* do raise the question of a possible genotoxic effect and what the developmental outcome(s) of such an effect would be.

The lack of documented human evidence for these alternative endpoints adds a large uncertainty to what exposure levels would be necessary to minimize risk. Standard chemical risk assessment practice would be to convert animal exposures to human equivalents, and then apply protective uncertainty factors to account for LOAEL to NOAEL scaling, inter-species variability, and intra-species variability (Calabrese and Kenyon, 1991). This is necessary to ensure, in the absence of human data, that they have accounted for the possibly large differences between lower animals and humans. It is likely that such calculations would yield recommended standards at or lower than those of the NAAQS.

Regardless of the exact level necessary to protect sensitive individuals from CO-induced morbidity the fact remains that we do not know much about the distribution of CO exposures. The little that we do know shows that a significant population is exposed to CO levels which could lead to chronic or sub-acute health effects. Without additional, more sensitive study of exposures and health endpoints we will not be able to detect this potentially major causes of disease.

Conclusions

The broad variety of documented developmental effects in animals discussed here is fairly strong evidence that chronic CO exposure may play a role in morbidity and mortality of the fetus and neonate, and may therefore, pose an important threat to human health. The NAAQS may be inadequate to protect pregnant women and the fetus against CO. The current USEPA standard, which is designed to protect the population from ambient (outdoor air) CO exposures leading to COHb levels above 2.1% is marginally adequate for most non-pregnant individuals if CO were to be controlled in all environments. However, there are no existing health protective standards designed to prevent people from being exposed to excessive CO indoors, and in many parts of the U.S., the standard is not attained outdoors either. It is probable that large numbers of people are exposed to indoor and occupational environmental levels many times higher than the standard on a regular basis. If this is the case, then the general population is experiencing excess morbidity from CO in spite of the USEPA's protective standards. The current exposure assessment paradigm, where exposure is inferred from fixed outdoor CO monitors, is inappropriate for tracking the relationship between CO exposure and morbidity. More specificity in assessing personal exposures, in the direction of the population-based NHANES II and Washington, DC - Denver studies, is needed to provide the data necessary for sensitive epidemiological analysis of the chronic and sub-acute health effects from CO exposure.

References

Abbatiello, E.R., and Mohrmann, K. (1979) Effects on the offspring of chronic low exposure to carbon monoxide during mice pregnancy. *Clin toxicol.* 14:401-406.

Akland, G. G., Hartwell, T. D., Johnson, T. R., and Whitmore, R. W. (1985). "Measuring Human Exposure to Carbon Monoxide in Washington, D.C., and Denver, Colorado, During the Winter of 1982-1983." *Environmental Science and Technology*, 19(10), 911-918.

Allred, E.N. *et al.* (1989) Short-Term Effects of Carbon Monoxide Exposure on the Exercise Performance of Subjects with Coronary Artery Disease. *The New England Journal of Medicine*, 311(21):1426-1432.

Astrup, P., Olsen, H.M., Trolle, D., and Kjeldsen, K. (1972) Effect of moderate Carbon-Monoxide Exposure on Fetal Development. *The Lancet* (ii):1220-1222.

Calabrese, E.J. and Kenyon, E.M. (1991) *Air Toxics and Risk Assessment.* Lewis Publishers, Chelsea MI.

Chapin, F.S. (1974) *Human Activity Patterns in the City.* Wiley-Interscience, New York, NY.

Clubb, F.J., *et al.* (1986) Cardiomegaly due to Myocyte Hyperplasia in Perinatal Rats Exposed to 200 ppm Carbon Monoxide. *Journal of Molecular Cell Cardiology* 18:477-486.

Cobb N. and Etzel R.A. (1991) Unintentional Carbon Monoxide-Related Deaths in the United States, 1979 Through 1988. *Journal of the American Medical Association* 166, 659-663.

Coburn, R.F., Foster, R.E., Kane, P.B. (1965) Considerations of the physiological variables that determine blood carboxyhemoglobin concentration in man. *J Clin Invest* 44:1899-1910.

Colome, S. D., Davidson, D. M., Lambert, W. E., Kleinman, M. T., and Wojciechowski, S. (1992). *Cardiac Response to Carbon Monoxide in the Natural Environment.* Contract No. A3-138-33, California Air Resources Board, Sacramento, CA.

Dean, B.J. (1985) Recent findings on the genetic toxicology of benzene, toluene, xylenes, and phenols. *Mutation Research.* 154:153-181.

Doyle, J.T. (1979) Risk Factors in Arteriosclerosis and Cardiovascular Disease with Special Emphasis on Cigarette Smoking. *Preventative Medicine* 8:264-270.

Fechter, L.D., *et al.* (1987) Disruption of Neostriatal Development in Rats Following Perinatal Exposure to Mild, But chronic Carbon Monoxide. *Neurotoxicology and Teratology* 9:277-281.

Goldsmith, J.R. (1970) Carbon Monoxide Research - Recent and Remote. *Arch Environ Health.* 11:118-119.

Hartwell, T. D., Clayton, C. A., Ritchie, R. M., Whitmore, R. W., Zelon, H. S., Jones, S. M., and Whitehurst, D. A. (1984). *Study of Carbon Monoxide Exposure of Residents of Washington, DC and Denver, Colorado.* EPA-600/4-84-031, U.S. Environmental Protection Agency, Research Triangle Park.

Hinderliter, A.L., *et al.* (1989) Effects of low-level carbon monoxide exposure on resting and exercise-induced ventricular arrhythmias in patients with coronary artery disease and no baseline ectopy. *Arch. Environ. Health* 44:89-93.

Huheey, J. E. (1978). *Inorganic chemistry; principles of structure and reactivity*, Second Edition, Harper & Row, New York.

Jain, K.K. (1990) *Carbon Monoxide Poisoning*, Warren H. Green, Inc. St. Louis, MO.

Johnson, T. (1984). *A Study of Personal Exposure to Carbon Monoxide in Denver, Colorado.* U.S. Environmental Protection Agency, Environmental Monitoring Systems Laboratory, Research Triangle Park, NC. Report No. EPA-600/4-84-014.

Kirkpatrick J.N. (1987) Occult Carbon Monoxide Poisoning. *The Western Journal of Medicine* 146, 52-56.

Kwak, H.M., Yang, Y.H., and Lee, S.L. (1986) Cytogenic Effects on Mouse Fetus of Acute and Chronic Transplacental In Vivo Exposure to Carbon Monoxide: Induction of Micronuclei and Sister Chromatid Exchanges. *Yonsei Medical Journal* 17(3):205-211.

Lu, F. C. (1991) *Basic Toxicology: Fundamentals, Target Organs and Risk Assessment.* Second edition. Hemisphere Publishing Co.

Marsh B.T. (1982) Housing and Health The Role of the Environmental Health Practitioner. *Journal of Environmental Health* 45, 123-128.

Novick R.E. (1972) Urban Anthropology: The Emerging Science of Modern Man. *The Science Teacher* 39, 21-22.

Penney, D.G. and Howley, J.W. (1991) Is There a Connection between Carbon Monoxide Exposure and Hypertension? *Environmental Health Perspectives* 95:191-198.

Prigge, E. and Hochrainer, D. (1977) Effects of Carbon Monoxide Inhalation on Erythropoiesis and Cardiac Hypertrophy in Fetal Rats. *Toxicology and Applied Pharmacology.* 41, 225-228.

Quackenboss, J.J., Kanarek, M.S., Spengler, J.D. and Letz, R. (1982) Personal monitoring for nitrogen dioxide exposure: methodology considerations for a community study. *Environ. Intern.* 8, 249-258.

Radford, E.P., and Drizd, T.A.(1982) Blood Carbon Monoxide Levels in Persons 3-74 Years of Age. United States, 1976-80, *Advance data from Vital and Health Statistics*, No. 76. DHHS Pub. No. (PHS) 82-1250. Public Health Service, Hyattsville, MD.

Schardein, J.L., and Keller, K.A. (1989) Potential Human Developmental Toxicants and the Role of Animal Testing in their Identification and Characterization. *CRC Critical Reviews in Toxicology.* 19(3):251-328.

Shephard, R.J. (1983) *Carbon Monoxide: The Silent Killer.* Thomas Books: Springfield, IL.

Sheps, D.S., *et al.* (1991) *Effects of 4 percent and 6 percent carboxyhemoglobin on arrhythmia production in patients with coronary artery disease.* Cambridge, MA: Health Effects Institute. Research Report No. 41.

Sheps, D.S., *et al.* (1990) Production of arrhythmias by elevated carboxyhemoglobin in patents with coronary artery disease. *Ann. Intern. Med.* 113: 343-351.

Singh, J., Smith, C., and Moore-Cheatum, L. (1992) Additivity of protein deficiency and carbon monoxide on placental carboxyhemoglobin in mice. *Am J Obstet Gynecol* 167:843-846.

Singh, J. and Scott, L. (1984) Threshold for Carbon Monoxide Induced Fetotoxicity. *Teratology* 30: 253-257.

Smith, M (1993) Private communication.

Spengler, J.D., Duffy, C.P., Letz, R., Tibbitts, T.W., and Ferris, B.G., Jr. (1983) Nitrogen dioxide inside and outside 137 homes and implications for ambient air quality standards and health effects research. *Environ. Sci. Technol.* 17, 164-168.

Stern, F.B., Halpern, W.E., Hormung, R.W., Ringenburg, V.L., and McCammon, C.S. (1988) Heart disease mortality among bridge and tunnel officers exposed to carbon monoxide. *American Journal of Epidemiology.* 118(6):1276-88.

Stern, F.B, Lemen, R.A., and Curtis, R.A. (1981) Exposure of Motor vehicle Examiners to Carbon Monoxide: A Historical Prospective Mortality study. *Archives of Environmental Health.* 36(2):59-65.

Storm, J.E., Valdes, J.J., and Fechter, L.D. (1986) Postnatal Alterations in Cerebellar GABA Content, GABA Uptake and Morphology following exposure to Carbon Monoxide early in Development. *Dev. Neurosci* 8:251-261.

Storm, J.E., and Fechter, L.D. (1985) Prenatal Carbon Monoxide Exposure Differentially Affects Postnatal Weight and Monoamine Concentration of Rat Brain Regions. *Toxicology and Applied Pharmacology* 81:139-146.

Szalai, A., ed. (1972) *The Use of Time: Daily Activities of Urban and Suburban Populations in Twelve Countries.* Morton Publishers, The Hague, Netherlands.

USDHHS (1992) In *The World Almanac and Book of Facts.* Pharos Books, New York, N.Y.

USEPA (1984) *Revised Evaluation of Health Effects Associated with Carbon Monoxide Exposure; An Addendum to the 1979 EPA Air Quality Criteria Document for Carbon Monoxide.* EPA-600/8-83-033F. USEPA, Research Triangle Park, NC.

USEPA (1991) *Air Quality Criteria for Carbon Monoxide.* EPA-600/8-90/045F. USEPA, Research Triangle Park, NC.

USDHHS (1986) *Vital Statistics of the United States, 1984: Volume II - Mortality, Part A.* U.S. Department of Health and Human Services, Public Health Service, National Center for Health Statistics. Hyattsville, MD.

USDHHS (1982) Carbon Monoxide Intoxication - A Preventable Environmental Health Hazard. U.S. Department of Health and Human Services, Center for Disease Control, *Morbidity and Mortality Weekly Report* 31 529-530.

Wallace, L. A., and Ziegenfus, R. C. (1985). "Comparison of Carboxyhemoglobin Concentrations in Adult Nonsmokers with Ambient Carbon Monoxide Levels." *Journal of the Air Pollution Control Association*, 35(9), 944-949.

Wallace, L., Thomas, J., Mage, D., and Ott, W. (1988). "Comparison of Breath CO, CO Exposure, and Coburn Model Predictions in the U.S. EPA Washington-Denver (CO) Study." *Atmospheric Environment*, 22(10), 2183-2193.

WHO (1979) *Carbon Monoxide. Environmental Health Criteria, 13.* World Health Organization. Geneva, Switzerland.

Figures

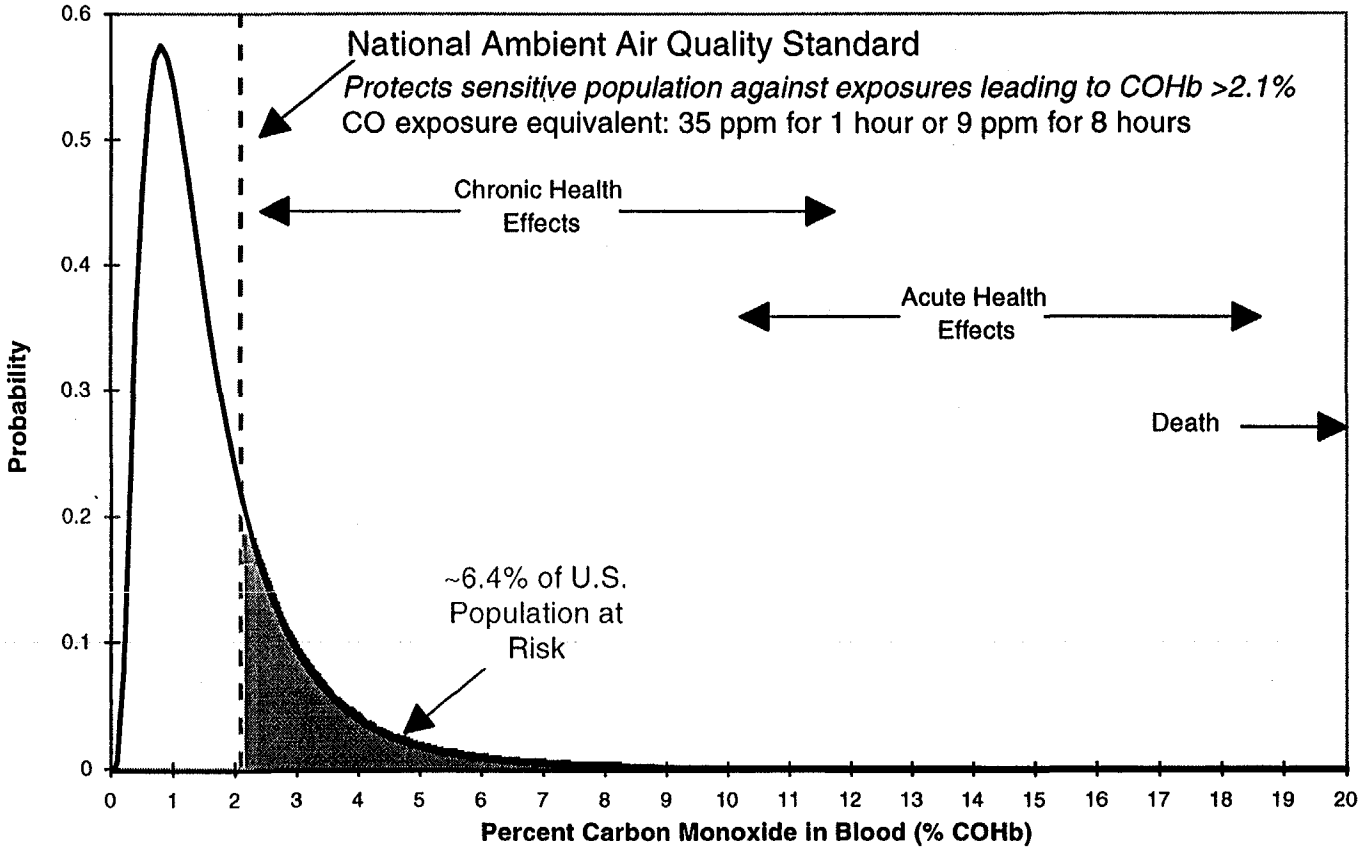

Sources: Data adapted from Radford and Drizd (1982)
USEPA (1991)

Figure 2-1. Estimated probability distribution of carboxyhemoglobin (COHb) levels in blood samples from non - smokers in the U.S. The curve is based on approximately lognormally distributed measurements (GM = 0.725, GSD = 2.15) from a random selection of 3141 subjects throughout the U.S. collected in the NHANES II study.

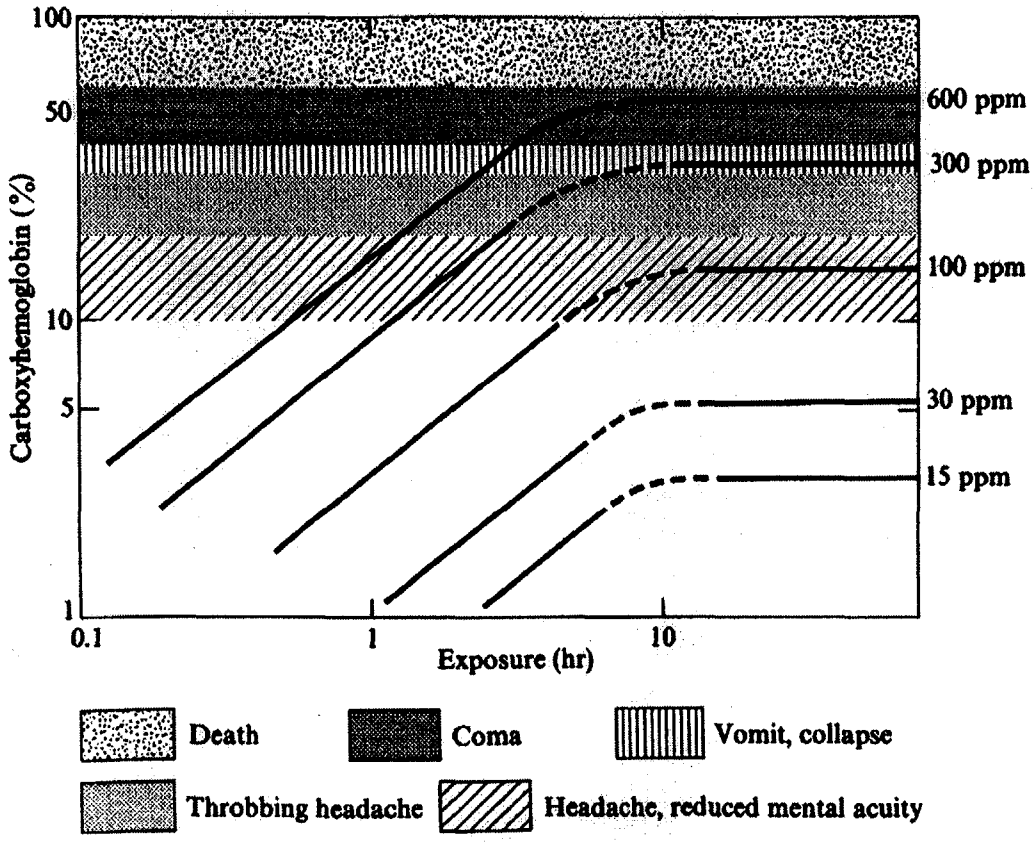

Physiological response of normally healthy adults at light activity to various carbon monoxide exposures. (W. Agnew, *Proc. Roy. Soc.*, A307, 153, 1968; courtesy of General Motors Corporation.)

XBL 771-7183

Figure 2-2. The relationship between CO inhalation exposure and carboxyhemoglobin levels. Health effects at the different exposure levels are included to place them in perspective.

Chapter 3: Review Of CO Sampling and Measurement Techniques Suitable for Population-Based Exposure Assessment

Introduction

Given both the clear public health issues evident from the CO mortality and poisoning statistics, and the potentially enormous populations affected by chronic and sub-acute CO exposure, it is surprising that our knowledge of the actual CO exposure distribution in our population is so poor. Although sensitive and accurate CO measurement methods exist (Woebkenberg, 1995), the cost of using them for large-scale exposure studies is prohibitive. The less expensive and more widely used devices are too inaccurate, insensitive or cumbersome to be used effectively in population-based studies. The studies which have been conducted to date have been extremely costly and are rapidly becoming dated since emissions from CO sources are changing with technological and regulatory improvements (e.g., automobile tailpipe emissions have been reduced while on the other hand residential unvented gas-fired space heaters have been legalized in most states). It is unlikely, given the trend towards less public money for environmental health research, that such large expenditures on exposure assessment will be duplicated unless the resulting data can be used to characterize the U.S. population's CO exposure distribution as a whole.

Similarly, in the occupational exposure arena, CO exposures are a major industrial hygiene issue, with many work environments having significant CO sources. Violations of regulated occupational exposure limits are common, and CO poisoning incidents in the workplace are frequently documented (MMWR, 1995; McCammon, 1996; Ely, 1995; Fawcett, 1992a; Fawcett, 1992b; USDHHS, 1996; USEPA, 1991). Although occupational CO personal monitoring instrumentation exists, it is either expensive to own and operate, or relatively inexpensive but inaccurate and insensitive. Thus, a need exists for a device that is inexpensive enough to be used by a small business but accurate enough to provide reliable data on workers' CO exposures.

Any approach to compiling accurate data on the probability distribution of pollutant exposures in a population must in some way infer the *total exposure* of individuals to the species of interest. This can be achieved by (1) measurement and apportionment of the concentration of the species within each of the (micro)environments where the individuals spend time (area or fixed-site monitoring); (2) by measurement of the concentration of the species at the breathing zone of the individuals throughout their daily routine (personal sampling); or (3) by use of a biological markers of the dose of pollutants which the individuals received during the exposure period (biomarker measurement). All of these approaches have been used by researchers to measure CO exposures (e.g., fixed site: Ott, 1988; Law, 1997; personal sampling: Johnson, 1984; biomarker: Radford, 1982; Wallace; 1988).

Measurement techniques must be refined for a particular use so that they are appropriate for the lifestyle, activities, and regulatory exposure limits set for the individuals that they are

monitoring. For example a device suitable for occupational exposure measurements should be designed around the typical workshift duration of 8-hours, while a device suitable for monitoring indoor or outdoor pollutant concentrations in residential and other non-occupational settings should be designed to operate over 24-hour or 168-hour (one week) period representative of a full cycle of the activities of the monitored individuals. Thus a device which is designed for an occupational setting may not be appropriate for a non-occupational setting depending upon its range and flexibility. A total exposure assessment must include representative measurements from both the occupational and personal periods of the individuals' daily lifestyles. Personal exposure measurements spanning full daily or weekly cycles including occupational, transit, school, shopping, residential, etc., periods are necessary to fully assess individuals' exposures

Air pollutant sampling techniques suitable for population-based exposure assessment studies can be divided into two rough categories, *active* or *passive*, based upon their principles of operation. Requirements of both active and passive samplers are (1) that they yield quantitative data on the pollutant of interest with accuracy and precision suitable for their application, (2) that their responses are stable (i.e., insignificant drift or loss of analyte of interest) in the environment in which they are to be used, and (3) that they are not significantly affected by interferences from other chemical species present. Additionally, to be suitable for exposure assessment studies they must be easily transportable. To be useful in all microenvironments for *total exposure* measurements they must be small, light, and quiet, yet rugged enough to withstand the rigors of daily use in an active occupational or personal environment.

Active systems mechanically sample the environment using pumps, and may use electronic detectors to monitor concentrations. These systems usually require training to operate as well as frequent calibration. They also tend to be large and sometimes quite noisy. Real-time infrared CO analyzers and electrochemical CO analyzers are examples of fully-contained active CO monitors. There are other active systems available, such as integrating bag collectors (bag samplers), which are not as cumbersome as these fully-contained active systems. An integrating bag collector operates by slowly filling an empty bag with the air to be sampled. Bags are usually filled by a peristaltic pump. The gas sample collected in the bag is subsequently analyzed using a real-time monitor.

Passive samplers do not require a power source during sampling. They can rely solely on molecular diffusion for sample collection (e.g., diffusion samplers), or can sample using pressure driven flow (e.g., evacuated canisters) -- provided no external power supply is required during sampling. As outlined earlier, effective passive samplers, ones that can be used in large indoor air pollution field surveys, need to be reliable, cost-effective, small and unobtrusive, and capable of being deployed with simple instructions. A diffusion tube sampler such as the Palmes tube for NO_2 (Palmes *et al.*, 1976) is an example of such a passive sampler. Another example of a passive sampler is a pre-evacuated canister, which operates by slowly filling the canister with the air to be sampled. The canister is filled using its own vacuum, coupled with an orifice flow control system. The gas sample collected by the canister is subsequently analyzed using a real-time monitor. Compared to a diffusion tube sampler, the canister sampler is large, obtrusive, and more complicated to deploy.

Two different types of gas monitoring methods are used with the air pollutant sampling techniques mentioned above, real-time methods or integrating methods. A real-time method

continuously measures the concentration of the gas species of interest. An integrating method cannot provide a profile of the gas species concentration over time, but instead continuously collects/samples the air to provide a time-weighted-average measurement of the gas concentration. There are two general integrating methods. The first method (e.g., diffusion tube sampler, badge detector) uses a gas-specific detector placed in an environment. When exposed to the environment, the detector's response to the gas is proportional to the time the detector is exposed and to the gas concentration level. The other method (e.g., integrating bag collector, evacuated canister) uses a collector to sample the air.

The main advantage of real-time CO instrumentation, compared with integrating monitors, is that the former supplies a continuous concentration profile that allows for the identification of short-term peak concentrations. This profile can be obtained over the entire sampling period. Some real-time analyzers also measure concentrations over a very wide range of values with a high degree of accuracy and precision. However, for many exposure field surveys, the additional information from the concentration profiles provided by these analyzers is not needed and the measurements given by integrating monitors are often adequate. Many times researchers average the real-time profiles in their survey data for use in their analyses. Only rarely are short-term data (i.e., less than 1 hour or even 8 hour averages) used in interpretation of exposure.

As is further discussed below, each CO-sampling technique has potential advantages and disadvantages associated with it, depending on the data collection requirements of a particular study. Research design and selection of instrumentation to be used in field surveys must be based on such data collection requirements with specific requirements determined by the goal of the study.

Available Methods for Determination of CO in Air

The currently available measurement techniques for CO are discussed below. Some information in this section has been obtained from Beatty, 1955; Slusher, 1966; LBL, 1976; and Girman, Traynor, and Hollowell, 1982. Although real-time CO monitors, active integrating bag/canister collectors and detector tubes, and crude diffusion samplers are available for use in field surveys, none are fully suited for affordable population-based CO exposure assessment studies. Table 3-1 compares the different CO measurement technologies available for use in such surveys.

Real-time (Active) Analyzers.

The most widely-used methods for real-time monitoring of CO concentrations are (1) the electrochemical method and (2) non-dispersive infrared (NDIR) methods. The U.S. Environmental Protection Agency has adopted two specific NDIR methods (the double-beam method and the gas-filter-correlation method) as its reference methods for monitoring outdoor CO concentrations (USFR, 1971; USFR, 1975). NDIR methods are more popular than the electrochemical method because of their designation as EPA reference methods; however, the electrochemical method is less expensive. Most real-time methods for monitoring CO use active pumps to bring the sampled air to the detection system.

Real-time electrochemical CO analyzers

CO analyzers using the electrochemical technique consist of a cell that measures the current induced by the electrochemical oxidation of CO at a sensing electrode. Electrochemical cell analyzers, introduced commercially about 1970, avoid the wet chemistry (e.g., reagent handling, etc.) of the traditional colorimetric and amperometric analyzers by using a sealed module, the electrochemical cell, inside which all chemical reactions occur. CO diffuses through a semi- permeable membrane into the cell with the rate of diffusion being proportional to the CO concentration. At the sensing electrode, the CO undergoes electrochemical oxidation which produces electrons. This oxidation creates a lower potential in the sensing electrode compared with the counter-electrode, causing an electron current to flow. This current is proportional to the sample CO concentration. Sampling can be either active (i.e., using a pump) or diffusive depending on the design of the instrument. There are several combustion-generated pollutants that interfere (positively) with the electrochemical cell and thus a pre-filter (supplied by the manufacturer) is often needed to eliminate this effect. Specifications for electrochemical CO monitors vary among models and manufacturers. Typical specifications for electrochemical analyzers are, ranges of 0-2000 ppm down to 0-50 ppm, accuracy and precision of ±1-3% of full scale, minimum sensitivity of 0.5 ppm, response time of 60 seconds to 90% of concentration, and weight ranging from 0.25 kg to 4 kg.

A miniaturized electrochemical personal exposure monitor was used by the USEPA in the Washington, DC -Denver CO exposure study (Ott, 1986; Akland, 1985). This device was equipped with a datalogger and an activity button which allowed the user to record the beginning and end of activities or changes in microenvironments. Although this monitoring system was revolutionary for population-based exposure assessment, it was very expensive to use. The electrochemical cells required continual calibration because of drift. Even so, Wallace *et al.* found that the data collected in Washington DC were seriously biased, and reported that the cause of this bias was due to "battery discharge effects", and "improper calibration techniques" (Wallace, 1988).

Newer models of datalogging CO monitors are available which are much more compact and have dealt with issues of interferences (Ott, 1995; Smith, 1994, Woebkenberg, 1995). Recent advances notwithstanding, studies using electrochemical detectors are still very vulnerable to errors due to miscalibration and drift. This problem was experienced in the CO exposure field study presented in the final chapter of this work.

Real-time infrared CO analyzers

NDIR methods utilize the infrared-absorbing capabilities of CO. CO absorbs infrared radiation in the wavelength range of 4.67 μm to 4.72 μm (Pierson, 1956). In this analyzer, infrared radiation from energy radiating filaments is directed onto two cells. One cell is a

reference cell filled with a non-infrared absorbing gas, such as nitrogen or argon. The other is a sample cell through which the sampled air containing the gas of interest is continuously drawn. The detector consists of two gas-impermeable chambers with a flexible metal diaphragm as a partition between the chambers. Both detector chambers are filled with the gas of interest, in this case, CO. The infrared radiation which passes through the reference cell enters one chamber of the detector, while the radiation passing through the sample cell enters the other chamber. The gas in each chamber is heated by the incoming energy, thus causing a pressure increase in the two chambers. The rise in pressure is greater in the chamber receiving radiation from the reference cell, since a portion of the radiation transmitted through the sample cell has been absorbed by the gas of interest before entering the chamber on the sample cell side. This difference in pressure causes a diaphragm displacement, which is electronically measured as a capacitance change. The infrared radiation is chopped by an optical chopper to cause a periodic capacitance change, which modulates a radio-frequency signal from an oscillator. This signal is subsequently demodulated, amplified, and the output signal is continuously fed to a meter or a data recording device. The amplitude of the output signal is proportional to the concentration of CO. Typical specifications for double-beam NDIR analyzers are: ranges of 0-1000 ppm down to 0-50 ppm, accuracy and precision of less than ±1% full scale, minimum sensitivity of 0.5 ppm, linearity of ±0.5% full scale, variable response times of 1-16 seconds to 90% of concentration, and weight of approximately 30 kg.

A second NDIR analyzer uses the gas-filter-correlation method and is generally considered more suitable for air monitoring than the double-beam NDIR method because of its overall improved performance and reliability. This method uses infrared radiation is passed through a rotating chopper and through a continuously rotating gas filter which alternates between CO and N_2. The infrared beam then passes through a narrow bandpass filter and into a sample-cell, where it makes multiple passes before exiting onto to a solid-state infrared detector. As the CO side of the gas filter wheel rotates across the infrared beam, it produces a reference pulse which is not affected by the CO in the sample chamber. Since N_2 is transparent to infrared radiation, the N_2 side of the filter wheel produces a measure pulse which can be absorbed by CO. This pulse is then attenuated by absorption by the CO in the sample cell. The chopped signal, which is modulated by the difference in pulses due to the two gas sensors, is sensed by the detector. The amplitude of the difference is proportional to the concentration of the CO in the sample cell. The specificity of this method to CO is very high since other gases present in the sample cell are equally absorbed by the reference and the measure pulses. In currently available models, the signal is demodulated and amplified using digital circuitry, then processed and linearized using microprocessors. Typical specifications for gas-filter-correlation NDIR analyzers are: ranges of 0-1000 ppm down to 0-1 ppm, accuracy and precision of ±0.1 ppm, minimum sensitivity of 0.1 ppm, linearity of ±1% of full scale, response time of 60 seconds to 95% of concentration using a 30-second averaging time, and a weight of about 20 kg.

Current costs for both types of NDIR analyzers are in the range of $6,000 to $10,000 per unit. Electrochemical analyzers cost in the range of $800 to $3,000 per unit. In addition, extra costs must be allowed for, since these analyzers usually need separate data logging and calibration systems.

As mentioned earlier, the primary advantage to real-time techniques is that short-term peak concentrations can be obtained. The disadvantages are all associated with the high cost of accurately using real-time monitors. They have a high initial cost (analyzer, data logger, calibration system), require daily calibration, and require extensive set-up and removal costs. In addition, a computer is usually needed for reduction of the data to usable concentrations averaged over a specified time-period(s). The infrared analyzers are the method of choice for accurate analysis of CO samples collected by integrating bag samplers which are discussed below.

Non-specific Active Air Collector

Currently, the most inexpensive technique for sampling indoor and outdoor CO concentrations over an extended period of time (e.g., one week) is the bag collector (Brown, 1995). Bag collection is an integrating technique. Air is collected into an evacuated sampling bag using an active pump. Low-flow peristaltic pumps are often used to collect one-week air samples. Higher flow rate pumps are used for shorter sampling periods. Most bag-collector units fit into a suitcase-sized container. Once the air sample is collected, it is analyzed in the laboratory using one of the real-time monitors previously discussed. These collectors have been successfully deployed in numerous studies (e.g., Traynor *et. al.*, 1989).

Bag collectors are usually custom-built and cost approximately $1,500 per unit. This technique is advantageous because (1) real-time, labor-intensive CO analyzers can stay in the laboratory and can analyze the CO concentration in hundreds of bags per week, thus saving considerable amounts of money; (2) bag-collection systems are easily reusable and (3) other stable, non-reactive pollutants, such as air-exchange rate tracer gases or CO_2, can also be measured using the same bag samples. The disadvantage, as discussed earlier, is that short-term CO concentration data are not directly measured.

In order for bag samplers to operate properly it is necessary for the system to be leak free, non-reactive, and maintain a constant and continuous flow-rate during sampling. Tedlar sampling bags have been found to work reliably without leaking for many samples. The bags are evacuated and purged twice with pure air and evacuated again to ensure that no contaminants remain in them. Gases that react readily with surfaces such as nitrogen dioxide would not be stable in a bag sample, however, CO is very non-reactive and so is quite stable under these storage conditions.

Non-Specific Passive Air Collector

A passive integrating technique which has just recently become commercially available is the evacuated canister sampler (Brown, 1995). This technique uses an evacuated stainless steel canister to sample air and uses a flow control system to provide a constant air flow to the canister. A 6-liter evacuated canister with the flow control system costs between $1,000 and $1,500. Automated canister sampling, purging, and re-evacuation systems (including pumps) can cost as much as $6,500. The main advantage of evacuated canisters, compared with bag collectors, is that some volatile organic compounds (VOCs) could also be measured using the canister, since certain VOCs that might react in a bag do not react in a properly treated stainless steel canister. One disadvantage of canisters, again compared with bag collectors, is the initial expense associated with purchasing a reevacuation system.

Actively pumped colorimetric detector tubes

A number of manufactures produce short and long-duration pumped direct-reading detector tubes for CO (National Dräger, Pittsburgh, PA; Sensidyne/Gastec, Clearwater, FL; Mine Safety Appliances, CO, Pittsburgh, PA; Mathesson/Kitagawa, Secaucus, NJ). The short-duration tubes are intended for grab sample measurements using a manual bellows pump or a battery-powered sampling pump to draw a sample of approximately 0.5 to 1 liter within 1-5 minutes, depending on the tube model. The long-duration tubes are designed to assess time-weighted average concentrations for periods up to 8-hours sampling at rates of about 1 liter-hr^{-1}. The long-duration detector tubes use a continuous low-flow pump system to draw a sample at a constant rate throughout the exposure period.

Both types of detectors are configured within glass tubes, sealed at each end, containing a packing of a substrate material such as silica gel with an impregnated chemical indicator system. This system reacts with CO by changing color along a front - the length of colored stain extending in proportion to concentration or exposure (exposure = concentration time product). A calibrated scale is provided on (or within) the tube for direct visual determination of the exposure. The tubes are activated by breaking the glass ends off and connecting them to the sampling system.

The long-duration sampling systems are often miniature and can be worn on the belt of an individual for personal sampling. The detector tube can be clipped to the lapel so personal sampling can be conducted at the breathing zone. However, the performance of the CO detector tubes has never been found to be particularly good for accurate exposure determinations (Saltzman, 1995). Problems include poor resolution of the stain length, poor inherent accuracy of the method, and susceptibility to bias from a wide range of interferents. Furthermore, although the tubes are reasonably inexpensive, the active sampling systems are costly and require a trained operator to conduct regular flow-rate calibrations.

Three common colorimetric reactions are commonly used in CO gas detector tubes. These are presented in Saltzman, 1995. All three methods have been in use for many years and there do not appear to be any appreciable improvements in the technologies. These reactions are (1) the reduction of iodine pentoxide plus fuming sulfuric acid to iodine; (2) the reduction for ammonium molybdate plus palladium sulfate to molybdenum blue; and (3) the reaction with potassium paladiosulfite.

The reactions using palladium containing compounds are discussed again later in this chapter. The iodine reaction is a variant on a method discussed by Haldane as early as 1920 where $5CO + I_2O_5 = I_2 + 5CO_2$ (Haldane, 1920). This method has poor specificity as evidenced by the number compounds that it reacts with: benzene, carbon disulfide, ethyl benzene, hydrocarbons (non-specific), methylene chloride, methane, petroleum hydrocarbons, toluene, acetylene, vinyl chloride, xylene, chlorobenzene, and monobromobenzene (Saltzman, 1995). The Dräger long-duration CO detector tube was found to be equally sensitive to acetylene (Leichnitz, 1993).

CO-Specific Biological Measurement Techniques

One way of monitoring CO in an environment is to measure CO concentration in the blood of humans exposed to such an environment. CO combines with the blood's hemoglobin and forms carboxyhemoglobin (COHb). There are a wide variety of methods for measuring

CO in blood. The most popular methods discussed in the literature are (1) spectrophotometric methods, (2) gas chromatographic methods, (3) NDIR methods and (4) the Conway Diffusion Cell Method. However, none of these methods is suitable for analyzing indoor CO for two general reasons. First, CO blood levels are a weighted average (sometimes with unknown weighting factors) of the dose of CO the subject received in the various environments previously occupied; thus, the effect of exposure to CO in any given environment cannot be isolated. Second, these methods are costly. For more information on such CO-specific biological measurement techniques, see Commins (1975), Shephard (1983), and WHO (1976).

Measurement of the CO concentration in breath is another biological technique used to estimate CO exposure and is less intrusive than blood measurements. This technique has been successfully used for many years (Shephard, 1983; WHO, 1976; Wallace *et al.*, 1988). The basic concept is to measure alveolar CO at equilibrium with the COHb. Wallace *et al.* (1988) discuss the physiological modeling of this technique with solutions. The model is based on the Coburn differential equation (Coburn, *et al.*, 1965) which is solved analytically. The relationship is dependent on many parameters including lung diffusivity, barometric pressure, water vapor pressure, alveolar ventilation rate, inspired CO pressure, endogenous CO production rate, capillary O_2 pressure, and oxyhemoglobin levels. In order to predict the COHb level, an expired breath sample is collected in a bag after a period of breath holding. The sample is subsequently conditioned to filter out interferences, and then analyzed with an electrochemical or NDIR analyzer. Recent smoking or other transient exposures to CO can skew the results if the subject's COHb is not yet equilibrated. This method can be used in exposure assessment studies although it is quite labor-intensive, requires a trained technician to make the measurements, and gives results that are sometimes difficult to interpret.

Existing CO-Specific Passive Samplers

Passive samplers use diffusion of gases to "collect" the pollutant of interest. The gas diffusion is driven by the concentration gradient between the air being sampled and the zero (or near zero) concentration at the surface of the collection material. There exist several CO passive samplers under this general definition.

The two main categories of existing CO passive samplers are (1) badge detectors such as the "Dead Stop" CO detector (Kemi Aps, St. Louis, MO), "Air-Zone" detector (Enzone USA, Inc., Davie, FL) and the "Quantum Eye" detector (Quantum Group, Inc., San Diego, CA) and (2) passive colorimetric dosimeter tubes such as those manufactured by Sensidyne (Clearwater, FL), National Dräger (Pittsburgh, PA), and Mine Safety Appliances (Pittsburgh, PA).

Badge detectors change color when exposed to high levels of CO (e.g., >100 ppm). Badge detectors can reverse this color change and recover when exposed to subsequently lower levels of CO (e.g., 1-5 ppm). Such detectors appear to have the ability to protect building occupants from fatal levels of CO if the badge is checked regularly and is noticed when it turns color. However, these detectors cannot quantify average CO concentration because color change is a qualitative measure (at least when the human eye is used as the color-change indicator), and because the color change in each monitor is designed to be reversible,

thereby being more indicative of recent CO concentrations rather than to the average CO concentration during exposure.

Passive colorimetric dosimeter tubes are a variant of the pumped color detector tubes used for occupational safety measurements. These tubes have become a favorite method for measurement of industrial hygienists to measure occupational workshift CO exposures. A sealed glass tube is packed with silica gel beads impregnated with a CO sensitive color-indicator. To deploy, one end of the tube is broken off. CO diffuses down the tube and the length of the indicator stain is measured at the end of the sampling period. Recent research indicates that these tubes are not fully satisfactory for quantitative determination of CO (Hossain and Saltzman, 1989). Problems include poor accuracy and statistically significant humidity effects. At best, these devices are designed to have an accuracy of ±25% at high concentrations and are not suitable for CO passive sampling in residential settings.

The ACT Monitoring Card System is an interesting new passive CO measurement technology that has recently come on the market, (Envirometrics Inc., Charleston, SC). The device is a diffusion membrane type passive sampler, using a proprietary sensing substrate. An electronic reflectometer is available from the manufacturer to measure the response of the device. No peer-reviewed data on the device have been found to date, but the manufacturer specifications state the device has an exposure range of 0-50 ppm CO for 8-hours with a limit of detection of 1 ppm. It has an environmental operational range of 15°C - 32°C and 20 -80% relative humidity. Its stated accuracy is ±25% at the 95% confidence level. Stated interferences include hydrogen sulfide, nitrogen dioxide, and sulfur dioxide. Close inspection of the manufacturer's literature indicates that the response of the sensor is extremely non-linear with a strong dependence on exposure time.

CO Passive Samplers Under Development

Because existing CO passive samplers have had their shortcomings, as mentioned above, both Lawrence Berkeley National Laboratory (LBNL) and Harvard have sought to develop "ideal" passive samplers, ones that fit the needs of a residential field survey. LBNL has worked on two different methods: the reflective CO passive sampler and a near-infrared-absorbing passive sampler (the topic of this work). Harvard had some success with a Zn-Y-zeolite CO passive sampler (Hishinuma and Yanagisawa, 1989). An "ideal" passive sampler is one that can be used to accurately measure the integrated concentration of the gas of interest and one that has an appropriate capacity, accuracy, precision, and sensitivity for residential as well as occupational settings. Ideal passive samplers are also small so that deployment through the mail is possible. Some existing passive samplers (which sample gases other than CO) that pass these requirements are the Palmes NO_2 passive sampler (Palmes *et al.*, 1976); the LBNL formaldehyde passive sampler (Geisling *et al.*, 1982), and a water vapor passive sampler (Palmes *et al.*, 1976; Girman *et al.*, 1986); the nicotine passive sampler (Hammond and Leaderer, 1987); and the radon Track-Etch Detector (Teradex, Pleasanton, CO). All of these passive samplers consist of a closed tube which can be uncapped at one end and which contains a chemical sampling analyte at the end which remains closed. To deploy, the cap is removed allowing the sampling compound to be exposed. The sampled gas is transported to the closed end by diffusion; the transport rate is given by Fick's Laws of Diffusion and is confirmed by experimental data. A CO passive sampler should also have these ideal characteristics and might have similar design features.

The rough design criteria for a CO passive sampler for residential indoor air quality (IAQ) CO exposure assessment studies are that the sampler be capable of measuring CO exposure in the range of 1-100 ppm-week with precision of ±1 ppm-week. Likewise the criterion for a CO occupational passive sampler, or *dosimeter*, is a range of 10 - 800 ppm-hr with a precision of ±10 ppm-hr. Both devices should have an accuracy of ±20% at their respective regulatory levels; i.e., 9 ppm (USEPA, 1991) for the residential IAQ device and 35 ppm (NIOSH, 1972) for the occupational dosimeter. The criterion for a minimum sensitivity is based on the need for the device to be capable of measuring outdoor CO levels which often range from 1 to 5 ppm. The nominal sampling time for the residential sampler is one week, which would measure the average concentration over a complete work-week/weekend life-style cycle. The criterion for the accuracy and precision of the device is based on the need to distinguish between indoor and outdoor levels where very small indoor sources are present (e.g., when the average indoor CO concentration is 2 ppm greater than the outdoor concentration).

Discussed here for completeness are the basics of diffusion dosimetry, a key mechanism in the operation of passive samplers. The mass of CO that diffuses to the sampling compound in a given time can be calculated using Fick's first law. If one assumes 100% collection efficiency, this mass can be described by the following equation.

$$M = \frac{D_{co} C A t}{L}$$

where:

M = mass diffused to end of diffusion tube (g);
D_{co} = diffusion coefficient for CO in air (cm^2/sec);
C = bulk air to sensing surface CO concentration gradient (g/cm^3);
A = cross-sectional area of tube (cm^2);
t = sampling time (sec);
L = length of tube (cm).

No measured diffusion coefficient for CO in air was found in the literature; however, it can be estimated for a given temperature and pressure using the Wilke and Lee method (Lyman *et al.*, 1982). Using this method D_{CO} is calculated to be 0.245 cm^2/sec at standard temperature (20°C) and pressure (1 atmosphere) conditions.

LBNL's CO Passive Samplers

Starting in the early 1980s LBNL undertook the task of developing an improved passive CO measurement technology. A CO passive sampler, utilizing a diffusion tube sampling design, and analyzed by measuring the reflectivity of its sensing surface was tested (Traynor, 1991). After funding was cut in about 1982 the project was abandoned until about 1989. At that juncture a search for a more suitable chemistry led to the development of the *near-infrared-absorbing* CO passive sampler which is presented in the following two chapters. The initial development of LBNL's reflective CO passive sampler concentrated on exploring the use of

palladium-related compounds (PRC) as the CO sensing media. The three palladium based CO reactions follow.

Palladium-related compounds investigated for use CO sensors

In both of its CO passive samplers, LBL uses palladium-related compounds (PRC's) as the sensing media. Although a large number of chemical methods for measuring CO have been explored and are described in the literature (Shephard, 1983, WHO, 1979), very few are appropriate for use in a diffusion tube configuration. Reasons include instability, insensitivity, and toxicity of the reagents involved. There are three techniques using PRC's in methods for determining CO in air described in the literature which have shown promise for application in a passive sampler. These compounds include potassium pallado sulfite (Silverman and Gardner, 1965; Main-Smith and Earwicker, 1946), a palladous silicomolybdate (Shepherd, 1947; Shuler and Schrauzer, 1977; Palmer *et al.*, 1982), and palladium sulphite (Earwicker, 1960).

Potassium pallado sulfite is a yellow crystalline chemical. On reaction with CO, it forms a carbonyl compound which, at ambient temperatures, decomposes to form CO_2, SO_2, and palladium. As the concentration of palladium metal increases, the system darkens. The reactions which are thought to occur follow.

$$K_2Pd(SO_3)_2 + CO \xrightarrow{H_2O} K_2(SO_3)_2PdCO$$

$$K_2(SO_3)_2PdCO \xrightarrow{H_2O} SO_2 + Pd + K_2(SO_3) + CO_2$$

yellow *brown*

This method has been used in CO indicator tubes where the compound has been impregnated on highly purified silica gel. The method is sensitive to moisture, which affects the sensitivity and color of the stain and, in the case of high moisture levels, causes a spontaneous deterioration and color change of the impregnated silica gel. The compound has been shown to be insensitive to oxygen, nitrogen and carbon dioxide, but can react with hydrogen sulfide, acetylene, arsine, phosphine and stibene in a manner similar to CO. Temperature effects are small.

The use of palladium sulphite was discussed by Earwicker (1960). It is very sensitive to CO, and its color changes predictably upon exposure to CO. It reacts with CO in nearly dry or humid conditions, which could simplify sampler configuration. The reaction with CO follows.

$$Pd(SO_3)(H_2O)_3 + CO \xrightarrow{H_2O} Pd + CO_2 + 3H_2O + SO_2$$

The palladous silicomolybdate method was developed originally in 1941 for detection of CO on aircraft (Main-Smith, 1941). In this method, silica gel is impregnated with ammonium

molybdate, sulfuric acid and palladium chloride, forming a yellow silicomolybdate complex. The palladium acts as a catalyst for the reduction of the complex by CO. The silica gel provides the water required for the reactions. The resulting products of the reduction are a mixture of oxides of molybdenum and are blue in color. The method was later improved by the National Bureau of Standards by substituting palladium sulfate for palladium chloride, yielding a gel four times as sensitive (Shepherd, 1947). Further innovations to the complex were developed in the 1970's and 1980's by the addition of copper salts to the complex to make the reaction reversible, thereby making detectors reusable (Shuler and Schrauzer, 1977; Palmer *et al.*, 1982). The reversibility is of limited value in the case of CO passive samplers where quantitative results are required. This chemistry was the basis for the CO sensing system developed by Quantum Group, Inc. which is discussed in the next chapter.

Harvard's CO Passive Sampler

Early results of a third CO passive sampler under development at Harvard have been reported in the literature (Lee, 1992; Hishinuma and Yanagisawa, 1989). In this sampler the collecting sorbent is a conditioned Zn-Y-zeolite molecular sieve. The sampler has an exposure range of up to 1600 ppm-hours in dry conditions and an assumed sensitivity of 30 ppm-hours. Analysis is conducted by thermal desorption of the Zn-Y-zeolite molecular sieve and quantitative conversion of the collected CO to methane. The resultant methane is then measured by gas chromatography with a flame ionization detector. The device was found to operate independent of temperature over the range of -5°C to 40°C. Due to a low sampling rate (small inside diameter and long length of the diffusion tube - 0.32 mm X 50 mm) the device was also found to be unaffected by wind at speeds up to 1 $m\text{-}sec^{-1}$. The authors indicate that the capacity of the sorbent is decreased under humid conditions; however, they also propose a method for increasing the range of the device under such conditions. No information on testing of the device for interferents was published. The current status of the Harvard CO passive sampler is unknown. It does not appear to have been used in any work published over the last several years.

References

Akland, G. G., Hartwell, T. D., Johnson, T. R., and Whitmore, R. W. (1985). "Measuring Human Exposure to Carbon Monoxide in Washington, D.C., and Denver, Colorado, During the Winter of 1982-1983." *Environmental Science and Technology*, 19(10), 911-918.

Beatty L. (1955) *Methods for Detecting and Determining Carbon Monoxide.* Bulletin 557. Bureau of Mines. U.S. Government Printing Office. Washington, D.C.

Coburn R. F., Forster R. E. and Kane P. B. (1965) Considerations of the Physiological Variables that Determine the Blood Carboxyhemoglobin Concentration in Man. *Journal of Clinical Investigation* 44, 1899-1910.

Commins (1975) Measurement of Carbon Monoxide in the Blood: Review of Available Methods. *Annals of Occupational Hygiene* 18, 67-77.

Earwicker C. A. (1960) The Sulphito-Compounds of Palladium(II). *Journal of the Chemical Society* 2, 2620.

Ely, E. W., Moorehead, B., and Haponik, E. F. (1995). "Warehouse Workers' Headache: Emergency Evaluation and Management of 30 Patients with Carbon Monoxide Poisoning." *American Journal of Medicine*, 98(2), 145-155.

Fawcett, T. A., Moon, R. E., Francia, P. J., Mebane, G. Y., Theil, D. R., and Piantadosi, C. A. (1992a). "Warehouse Workers Headache. Carbon Monoxide Poisoning from Propane-Fueled Forklifts." *Journal of Occupational Medicine*, 34(1), 12-15.

Fawcett, T. A., Moon, R. E., Francia, P. J., Mebane, G. Y., Theil, D. R., and Piantadosi, C. A. (1992b). "Letters to the Editor: Warehouse Workers' Headache - The Author Replies." *Journal of Occupational Medicine*, 34(9), 871-872.

Geisling K.L., Tashima M.K., Girman J.R., Miksch R.R. and Rappaport S.M. (1982) A Passive Sampling Device for Determining Formaldehyde in Indoor Air. *Environment International* 8, 153-158.

Girman, J.R., Traynor, G.W. and Hollowell, C.D. (1982) *A Carbon Monoxide Passive Monitor: A Research Need.* Lawrence Berkeley National Laboratory, Report No. LBID-501, Berkeley, CA.

Girman J.R., Allen J.R. and Lee A.Y. (1986) A Passive Sampler for Water Vapor. *Environment International* 12, 461-465.

Haldane, J. S. (1920). *Methods of Air Analysis, Third Edition,* Charles Griffin & Company, Ltd., London, England.

Hammond, S. K., and Leaderer, B. P. (1987). "A diffusion monitor to measure exposure to passive smoking." *Environmental Science and Technology*, 21, 494-497.

Hishinuma M. and Yanagisawa Y. (1989) Passive Sampler for Carbon Monoxide Using a Solid Adsorbent. Paper No. 89-82.4. *Proceedings of the 82nd Annual Meeting of the Air and Waste Management Association*, Anaheim, CA, June 25-30, 1989.

Hossain M.A. and Saltzman B.E. (1989) Laboratory Evaluation of Passive Colorimetric Dosimeter Tubes for Carbon Monoxide. *Applied Industrial Hygiene* ,4, 119-125.

Johnson, T. (1984). A *Study of Personal Exposure to Carbon Monoxide in Denver, Colorado.* EPA-600/4-84-014, U.S. Environmental Protection Agency, Environmental Monitoring Systems Laboratory, Research Triangle Park, NC.

Law, P. L., Lioy, P. J., Zelenka, M. P., Huber, A. H., and McCurdy, T. R. (1997). "Evaluation of a Probabilistic Exposure Model Applied to Carbon Monoxide (pNEM/CO) Using Denver Personal Exposure Monitoring Data." *Journal of the Air and Waste Management Association*, 47, 491-500.

LBL (1976) *Instrumentation for Environmental Monitoring: Air Gases, Part 1A.* Lawrence Berkeley Laboratory, Berkeley, CA.

Lee, K., Yanigasawa, Y., Hishinuma, M., Spengler, J. D., and Billick, I. H. (1992). "A Passive Sampler for Measurement of Carbon Monoxide Using a Solid Adsorbent." *Environmental Science and Technology*, 26(4), 697-702.

Leichnitz. (1993). "Determination of the Time-Weighted Average Concentration of Carbon Monoxide in Air Using a Long-Term Detector Tube." *IARC Scientific Publications*, 109, 346-352.

Lyman W. J., Reehl W. F. and Rosenblatt D.H. (1982) *Handbook of Chemical Property Estimation Methods: Environmental Behavior of Organic Compounds,* McGraw-Hill Book Co., New York, New York.

Main-Smith J.D. (1941) Royal Aircraft Establishment Report CH 324.

Main-Smith J.D. and Earwicker G. (1946) Improvements in or Relating to the Detection and Quantitative Determination of Carbon Monoxide in Air or Other Gases at Such Temperatures as Occur in the Atmosphere and Reagents Therefore. Patent Specification 582,184, The Patent Office, London, England.

McCammon, J. B., McKenzie, L. E., and Heinzman, M. (1996). "Carbon Monoxide Poisoning Related to the Indoor Use of Propane-Fueled Forklifts in Colorado Workplaces." *Applied Occupational and Environmental Hygiene*, 11(3), 192-198.

MMWR. (1995). "Carbon Monoxide Poisoning from the Use of Gasoline-Fueled Power Washers in an Underground Parking Garage." *Morbidity and Mortality Weekly Report*, 44(18), 356-364.

Ott, W. R., Rodes, C. E., Drago, R. J., Williams, C., and Burmann, F. J. (1986). "Automated Data-Logging Personal Exposure Monitors for Carbon Monoxide." *Journal of the Air Pollution Control Association*, 36(8), 883-887.

Ott, W., Thomas, J., Mage, D., and Wallace, L. (1988). "Validation of the Simulation of Human Activity and Pollutant Exposure (Shape) Model Using Paired Days from the Denver, CO, Carbon Monoxide Study." *Atmospheric Environment*, 22(10), 2101-2113.

Ott, W. R., Vreman, H. J., Switzer, P., and Stevenson, D. K. "Evaluation of Electrochemical Monitors for Measuring Carbon Monoxide Concentrations in Indoor, In-Transit, and

Outdoor Microenvironments." *Proceedings of the Air and Waste Management Conference on Measurement of Toxics and Related Air Pollutants*, Research Triangle Park, NC.

Palmer J. G., Cecil M., Schrauzer G. N. and Shuler K. E. (1982) *Preparation and Evaluation of Self-Regenerative Carbon Monoxide Detection Gels.* A Minerals Research Contract Report, Bureau of Mines, U.S. Department of the Interior, Report No. OFR 92-83.

Palmes E.D., Gunnison A.F., DiMattio J. and Tomczyk C. (1976) Personal Sampler for Nitrogen Dioxide. *American Industrial Hygiene Association Journal* **37**, 570-577.

Pierson R.H., Aaron N.F., and St. Clair Cantz E. (1956) Catalog of Infrared Spectra for Qualitative Analysis of Gases. *Analytical Chemistry* 28, 1218.

Radford, E. P., and Drizd, T. A. (1982). "Blood Carbon Monoxide Levels in Persons 3-74 Years of Age: United States, 1976-1980." *PHS 82-1250. Advance Data from Vital and Health Statistics No. 76*, U.S. Department of Health and Human Services, Public Health Service, National Center for Health Statistics, Hyattsville, MD.

Saltzman, B. E., and Caplan, P. E. (1995). "Chapter 18. Detector Tubes, Direct-Reading Passive Badges, and Dosimeter Tubes." Air Sampling Instruments for Evaluation of Atmospheric Contaminants, 8th Edition, B. S. Cohen and S. V. Hering, eds., American Conference of Certified Industrial Hygienists, Cincinnati, Oh, 401-437.

Shephard R.J. (1983) *Carbon Monoxide: The Silent Killer.* Thomas Books: Springfield, IL.

Shepherd M. (1947) Rapid Determination of Small Amounts of Carbon Monoxide. Preliminary Report on the NBS Colorimetric Indicating Gel. *Analytical Chemistry* **19,** 77-81.

Shuler K. E. and Schrauzer G. N. (1977) Catalyst and Method for Oxidizing Reducing Gases. U.S. Patent 4,043,934.

Silverman L. and Gardner G. (1965) Potassium Pallado Sulfate Method for Carbon Monoxide Detection. *Industrial Hygiene Journal* March-April, 97-105.

Slusher G.R. (1966) *An Evaluation of Low-Cost Carbon Monoxide Indicators.* Report No. ADS-80. Federal Aviation Agency. Aircraft Development Service. Washington, D.C.

Smith, J. P., and Shulman, S. A. (1994). "Evaluation of a Personal Data Logging Monitor for Carbon Monoxide." *Appl. Occup. Environ Hyg.*, 9(6), 418-417.

Traynor, G. W., Apte, M. G., Diamond, R. C., and Woods, A. L. (1991). "A Carbon Monoxide Passive Sampler: Research and Development Needs." *LBL-26880*, Lawrence Berkeley National Laboratory, Berkeley, CA.

Traynor G.W. *et al.* (1989) Macromodel for Assessing Residential Concentration of Combustion-Generated Pollutants: Model Development and Preliminary Predictions for CO, NO_2 and Respirable Suspended Particles. Lawrence Berkeley Laboratory, Report No. LBL-25211, Berkeley, CA.

USDHHS. (1996). "Preventing Carbon Monoxide Poisoning from Small Gasoline-Powered Engines and Tools." *DHHS (NIOSH) Pub. No. 96-118*, U.S. Department of Health and Human Services, Centers for Disease Control and Prevention, National Institute for Occupational Safety and Health, Cincinnati, OH.

USEPA. (1991). "Air Quality Criteria for Carbon Monoxide." *EPA-600/8-90/045F*, U.S. Environmental Protection Agency, Research Triangle Park, NC.

USFR (1971) U.S. Federal Register 36(228), 22384.

USFR (1975) U.S. Federal Register, 40(33), Part II, February 18.

Wallace, L., Thomas, J., Mage, D., and Ott, W. (1988). "Comparison of Breath CO, CO Exposure, and Coburn Model Predictions in the U.S. EPA Washington-Denver (CO) Study." *Atmospheric Environment*, 22(10), 2183-2193.

WHO (1976) *Selected Methods of Measuring Air Pollutants.* World Health Organization. Geneva, Switzerland.

WHO (1979) *Carbon Monoxide: Environmental Health Criteria 13.* World Health Organization. Geneva, Switzerland.

Woebkenberg, M. L., and McCammon, C. S. (1995). "Chapter 19. Direct-Reading Gas and Vapor Instruments." *Air Sampling Instruments for Evaluation of Atmospheric Contaminants, 8th Edition*, B. S. Cohen and S. V. Hering, eds., American Conference of Certified Industrial Hygienists, Cincinnati, Oh, 439-510.

Tables

Table 3-1. Techniques available for measurement of carbon monoxide.

Method	Resolution	Sampling technique	Method of analysis	Minimum sensitivity	Range	Accuracy ± Precision	Cost per unit	Cost per field measurement	Training required	Comments
Double-beam NDIR	Real-time	Mechanical pump	Absorption in Infrared	0.5 ppm	0 - 50 ppm to 0 - 1000 ppm	1% ± 1% of full scale	>$5000	>$100	A	D
Gas filter correlation NDIR	Real-time	Mechanical pump	Absorption in Infrared	0.1 ppm	0 - 1 ppm to 0 - 1000 ppm	0.1% ± 0.1% of full scale	>$5000	>$100	A	D
Electrochemical	Real-time	Mechanical pump or diffusion	Electrochemical cell	1 ppm	0 - 1000 ppm	1% ± 2% of full scale	$800 to $3000	>$100	A	E
Bag samplers	Integrated over sample period	Peristaltic pump into sample bag	Infrared or electrochemical analysis of collected sample	<1 ppm (average)	0 - 1000 ppm	See infrared or electrochemical analysis	$1000 to $2000	>$50	B	
Evacuated canisters	Integrated over sample period	Flow control across vacuum	Same as bag samplers	<1 ppm (average)	0 - 1000 ppm	See infrared or electrochemical analysis	$1000 to $1500	>$50	B	
Qualitative badge detectors	Integrated over sample period	Sensor in direct contact with air	Visual color change with exposure	One type turns gray at aprox. 50 ppm for 24 h	NA	NA	$10	<$25	C	F
Passive colorimetric dosimeter tubes	Integrated over sample period	Color indicating gel in diffusion tube	Visual inspection of stain length	6.3 ppm	50 to 600 ppm-h	>25%	$6.5	<$25	C	G
Quantitative Badge Detector	Integrated over sample period	Controlled diffusion through membrane	Measure change in reflectance of sensor surface using reflectometer	1 ppm	0 to 400 ppm-h	±25%	$30 - reader costs $2000	$40-100	B or possibly C	G
LBL reflective passive sampler	Integrated over sample period	Treated disk at end of diffusion tube.	Measure change in reflectance of disk using reflectometer	<30 ppm-h	<30 to >500 ppm-h	Unknown	$10 (estimate)	<$25 to $50	C	H
Zn-Y-Zeolyte passive sampler	Integrated over sample period	Diffusion of sample onto solid adsorbent	Thermal desorption of sample into G.C.	30 ppm-h	30 to 1600 ppm-h	Unknown	Unknown	Unknown	C	H

A. Trained technician, field visit required; B. Field visit required; C. Mail -out with instructions. D. Does not include data acquisition costs; E. Some models include data acquisition costs; F. Qualitative only. Primarily used as a warning device. Reversible; G. Maximum sampling time is 8 h; H. Method under development. Temperature and humidity effects unknown

Chapter 4: Development of a CO Passive Sampler and Occupational Carbon Monoxide Dosimeter

Introduction

The need for a passive sampler for population-based exposure assessment is outlined in the previous chapter. The work presented here is the result of a focused effort to develop a dosimeter for the measurement of workplace exposures to carbon monoxide. The approach was to modify and improve on an earlier prototype CO passive sampler developed at LBNL. This work was the result of collaborations between researchers in the Indoor Environment Program at LBNL and Quantum Group, Inc. (QGI, San Diego, CA), a company that has developed a unique CO sensing technology. While QGI has worked to perfect their CO sensing technology, LBNL's efforts focused on developing the diffusion sampler technology, testing sensor performance, and integrating the QGI sensor technology into the passive sampler and occupational dosimeter designs. Highlights of the history of the passive sampler development are presented here to show how the dosimeter technology developed from concept to a reality. Prototype dosimeter designs and related performance assessment studies are also summarized. Additionally, results from the final design's validation studies are presented. The results of a field study conducted using the occupational dosimeter are presented in the following chapter.

Although this project was specifically aimed at the development of an occupational dosimeter, a secondary interest in a similar passive sampler design intended to be used to measure one-week average indoor CO concentrations in residences was also pursued. It was hoped that this project would result in the development of an inexpensive quantitative method to assess time-weighted-average workplace exposures to CO and provide researchers and industrial hygienists with a means to conduct cost effective surveys of occupational CO exposures and residential indoor air quality studies.

The overall goal was to develop and validate an occupational dosimeter capable of measuring time weighted average (TWA) CO concentrations ranging from 10 to 800 parts-per-million-hours (ppm-h), i.e., 8-hour workshift TWA CO concentrations of 1 to 100 ppm. It was desired that the device should have an accuracy of ±20% and a precision of ±10 ppm-h at exposures above 40 ppm-h. These sampling ranges are appropriate for CO exposure assessment based upon the permissible levels set by regulatory bodies. The current Personal Exposure Limit (PEL) set by the U.S. Occupational Safety and Health Administration (OSHA, 1993) is 50 parts per million measured as a time-weighed-average (TWA) over 8-hours. The National Institute for Occupational Safety and Health (NIOSH) recommends an exposure limit of 35 ppm TWA for 8-hours (NIOSH, 1972), and the American Conference of Governmental Industrial Hygienists recommends a Threshold Limit Value (TLV) of 25 ppm TWA for 8-hours (ACGIH, 1991].

Conceptually, the passive sampler and the occupational dosimeter both operate on the principle of gas diffusion sampling (Rose, 1982; Palmes, 1976). They require no pump. CO reacts on the surface of the sensor so that the surface CO concentration is close to zero. In the LBNL/QGI diffusion sampler design the sensor is encased in a small vessel, with a tube that communicates from the inside, at the sensor surface, to the outside air. A removable cap at the opening of the tube is used to control CO diffusion to the sensor. Since the CO concentration ([CO]) at the sensor surface is zero, a CO partial pressure gradient exists along the tube, from CO laden environmental air to the sensor. When the cap is removed, this partial pressure gradient drives a diffusive flow of CO along the tube to react at the surface of the sensor. As the sensor reacts with CO, it changes color in a manner that can be used to assess CO exposure quantitatively. The sampling period is defined as the period for which the sampler's cap is removed from the diffusion tube.

A succession of CO passive sampler prototype designs are presented in the following sections. The results of the testing of these designs reflect the history of the refinement of the technology to a workable and mass-producible design. Prototypes with designation "PS*x*" will refer to CO passive samplers of the *x*-th generation, designed to operate over a 7-day period. Likewise, the prototype designation "D*x*" will refer to the 8-hour occupational dosimeter design of the *x*-th generation. The passive samplers designated PS1 are considered to be the original proof-of-concept design which established the feasibility of the work presented here. Some of the results from the development of the PS1 are included here for completeness.

Occupational Dosimeter Development Approach

A phased approach was taken in the development of the Occupational Dosimeter. The goals were to use the concepts proven to work in the PS1 to:

1) develop an improved prototype sampler design (PS2) which could be adapted for use as an occupational dosimeter (PS3 / dosimeter 1, D1);
2) test the new prototype and compare its performance to the PS1;
3) continue testing and evaluation of sensors, in collaboration with QGI, with the goal of improvement of the chemical formulation (i.e., reduced reversibility, humidity effects) and manufacturing processes (i.e., reduction of inter- and intra-batch sensor variability).
4) design the optimal dosimeter configuration (PS4/D2) and evaluate its performance in the laboratory;
5) build and validate the final dosimeter configuration (PS5/D3)suitable for a pilot field study.

Apparatus

A list of all major laboratory equipment and instrumentation is presented in Table 4-1. All testing methods used with CO sensors required a supply of exposure gases and a CO analyzer for monitoring test atmospheres. CO was supplied from cylinders of compressed mixtures of CO in pure air, or CO in pure nitrogen. The concentration of CO supplied from the cylinders was typically 40 ppm when the gas was to be used at a low flow rate for

direct exposure of individual sensors. Exposure atmospheres where higher flowrates of gas were needed were generated by blending 5000 ppm CO with dry ultra-pure air or nitrogen using mass-flow controllers and glass mixing manifolds. The contents of the compressed gas cylinders were certified as a primary standard (contents certified to be within ±1% of stated concentration). The dilution gas was either ultra-pure air generated in the lab (AADCO Pure Air Generator Model 737) or from certified cylinders, or in some cases using certified and tested cylinders of compressed dry nitrogen. A Thermo Environmental Model 48 Gas Filter Correlation CO analyzer was used to monitor test atmospheres. This instrument was calibrated daily, and checked with a standard cylinder to ensure that its response was accurate to within ±1 percent of the standard.

Figure 4-1 depicts the experimental setup used to expose the diffusion samplers to test atmospheres. Using this system, samplers were exposed to various CO concentrations under controlled temperature and humidity conditions. Although not shown in the figure, temperature and humidity in the exposure chamber were monitored and recorded by the data acquisition system (see Table 4-1).

An ultraviolet/visible/near-infrared spectrometer was used for measurement of the sensor response at wavelengths from 400-1100 nm. The instrument was a Perkin Elmer Lambda 2 double-beam spectrophotometer with a wavelength range of 190 - 1100 nm using deuterium and tungsten-halogen lamps and solid-state optical sensors. This instrument had an onboard microcomputer and a RS-232 communication interface to a personal computer. The rated photometric accuracy of the instrument was ± 0.005 absorbance units (*A*), with a repeatability of ±0.002*A*.

Sensor Technology Development

The CO Sensor

One component essential to the occupational dosimeter was the QGI sensor. The sensor, developed and manufactured by QGI, responds to CO exposure with a proportional near-linear increase in optical density in the near-infrared region. The exact chemical formulation of the sensors is considered proprietary by QGI, however the salient features of the chemistry have been discussed in the literature (Goldstein, 1991a; Goldstein, 1991b). Figure 4-2 presents the key elements of the sensor chemistry. The sensors are made by coating the palladium and molybdenum salts ($PdCl_4$ and MoO_3), orange-yellow in color, onto a porous silica-based (VYCOR™, Corning Glass Works, Corning, NY) circular disk (6 mm in diameter, 1.3 or 2.6 mm thick). (This sensor was originally developed by QGI for use in a bio-mimetic CO breath detector (Goldstein, 1991b). The CO detecting characteristics of the chemistry are based on the oxidation of environmental CO by palladium, which in turn reduces the molybdenum (VI) to a mixed oxidation state species having a blue color (Mo_{blue}). This change was shown to be quantifiable by monitoring the sensors' absorbance of light in the visible to near-infrared. In fact, with moderate CO exposure, this change from yellow to blue is visible to the naked eye. The sensors now used in the occupational dosimeter have been found to have a peak sensitivity at around 700 nanometers (nm).

Copper in the sensor was thought to be responsible for a reverse reaction, by catalytic oxidation of the molybdenum blue species back to its original state [Mo(VI)]. Originally, this

copper was intentionally included to provide the reversibility needed in the bio-mimetic CO breath sensor. Direct oxidation of the molybdenum blue by atmospheric oxygen is also a possible source of sensor response reversal. Reversibility is not desirable for time-averaged sampling because it leads to loss of integrated information.

Re-formulations of the sensor focused on removing trace amounts of copper from the chemistry. The silica sensor substrates were analyzed qualitatively for trace metal contamination using an X-ray Fluorescence Spectrometer facility at LBNL (Giauque, 1973). The material was found to contain detectable amounts (several ppm on a mass-mass basis) of copper. Initial attempts to remove copper from the sensors were not completely successful because even very small concentrations caused unacceptable reversibility of the chemistry. After the copper contamination was identified as the cause of the reversibility, QGI was able to eliminate its effects through a chelating process developed by them. This process binds the remaining copper so it is not available for interaction with the other components of the sensor.

Methods

Theory of quantification of sensor reaction kinetics

A set of possible mechanisms of the sensor chemistry outlined in Figure 4-2 was used to develop a model for determining the forward and reverse sensor reaction kinetics. Empirically derived rate constants using this model as a guide are of use in understanding both how the sensor responds to CO and how the response is lost through reversibility as the measured analyte H_xMoO_3 (Mo blue) is re-oxidized to MoO_3 (Mo(VI)).

Spectrophotometric measurement of sensor response

The spectrophotometric analysis used to assess the sensor response is based upon the Beer-Lambert Law (Peters, 1974), which states that:, for a given wavelength of light energy,

$$A = \log\left(\frac{I_0}{I}\right) = \varepsilon\, bc \qquad (1)$$

where,
A = Absorbance (A),
I_0 = incident intensity of radiation from a light source onto a sample,
I = intensity of light radiation emerging from a sample,
ε = molar absorptivity of the sample analyte species (mole-l^{-1}-cm^{-1}),
b = path length of the sample (cm),
and
c = the molar concentration of the analyte species (mole-l^{-1}).

In the case of the QGI sensor, I and I_0 are measurable using a spectrophotometer, and a may be determined experimentally. (Note: the concentration of molybdenum blue species on the surface of the QGI sensor is the analyte to be measured for quantification of CO exposure). However, the pathlength (b) and analyte concentration (c) were not easily determined. This was because it was not feasible to measure the quantity and thickness of the coating of the QGI metal oxide sensing material on the porous VYCOR sensor substrate surface. Fortunately, the QGI sensor's response to CO could be measured empirically so it was not

necessary to know the true sampling rate or the actual concentration of analyte on the sensor surface. Empirical methods to assess the sensor response are discussed in sections below.

A forward reaction kinetic model

The literature (Goldstein, 1991a) suggests that the forward reaction presented in steps 1 and 2 of Figure 4-2 is a first-order process for CO. This was also evident in the sensor response experiments discussed below. Assuming that the production of Mo_{blue} (step 2) is in direct proportion to the concentration of CO,

$$d[Mo_{blue}] = k_f[CO]dt\,. \tag{2a}$$

where k_f = overall rate constant for steps 1 and 2:

$$PdCl_4^{2-} + CO + 2/xMoO_3 + H_2O \xrightarrow{k_f} Pd(II) + 2/xH_xMoO_3 + 4Cl^- + CO_2$$

Integrating,

$$\int_{[Mo_{blue}]_0}^{[Mo_{blue}]} [Mo_{blue}] = \int_0^t k_f[CO]dt\,, \tag{2b}$$

with $[CO]$ constant. Then,

$$[Mo_{blue}] - [Mo_{blue}]_0 = k_f[CO]t\,. \tag{2c}$$

Assuming that the optical density, measured as absorbance of light energy, of the sensor is directly proportional to $[Mo_{blue}]$, i.e.,

$$[Mo_{blue}] = KA\,, \tag{3}$$

where

K = a sensor-specific constant relating $[Mo_{blue}]$ to the optical density of the sensor (mole-$cm^{-1}A^{-1}$).

Then,

$$\frac{d[Mo_{blue}]}{dt} = K\frac{dA}{dt}\,, \text{ and} \tag{4}$$

$$\frac{dA}{dt} = \frac{k_f}{K}[CO]\,. \tag{5a}$$

Finally, the relationship between change in the optical density of the sensor and CO exposure can be described by

$$\int_{A_0}^{A} dA = \int_0^t \frac{k_f}{K}[CO]dt\,, \text{ so that} \tag{5b}$$

$$A - A_0 = \frac{k_f}{K}([CO]t). \qquad (5c)$$

Note that the quantity $[CO]t$ is the concentration-time product, otherwise termed CO exposure (units = ppm-h). Equation 5c indicates that the change in absorbance of the CO sensors is directly proportional to time-weighted average CO exposure. An effective value for k_f/K can be determined empirically and is simply the slope of the linear relationship between change in absorbance of a sensor plotted against CO exposure. The true value of k_f cannot be calculated since K is also unknown. However, an empirical value for the ratio k_f/K, henceforth termed k, can be derived directly from exposure experiments which will be presented below. The equation

$$dA = k[CO]t \qquad (5d)$$

describes the empirical relationship between CO exposure and forward sensor response. The units of k are $A \cdot ppm^{-1}hr^{-1}$.

Although the constant K is unknown, a method for empirically deriving a related quantity, the mass-balance relationship between moles (or mass) of CO and dA for a batch of sensors, is presented later.

A note on copper contamination as a competitive reaction

Figure 4-2 shows that copper can also oxidize Pd(0) to Pd(II) (see note in step 2). This reaction has the potential to compete with the desired reaction where Mo(VI) is reduced by Pd(0) to Mo_{blue}. Clearly this competition is undesirable and demonstrates the deleterious effects of copper on the CO sensing chemistry. Copper also has an effect on the chemistry as shown in Figure 4-2 equations 3a, 4a, and 4b. For these reasons a major effort was focused on totally eliminating copper from the materials used in the sensors. This is discussed in the experimental section below.

A reverse reaction kinetic model

Understanding the chemical *regeneration* of these sensors is important for the functioning of a sampler using this sensing technology because significant reversal of the reactions can lead to loss of integrated information. An effort was made to understand the reverse kinetics. The derivation of the Mo_{blue} oxidation kinetics can be derived in a similar fashion to the forward reaction kinetics discussed above. From a practical standpoint the oxidation (or *regeneration*) of Mo_{blue} to Mo(VI) on the sensor surface represents a loss measured analyte. The loss of a Mo_{blue} molecule created during CO exposure on the sensor surface translates into the loss of a CO "count" in the time-averaging integration of sampled CO molecules. This reverse chemical process is described in steps 3 and 4 of Figure 4-2.

Step 3 of the sensor chemistry outlines three potential mechanisms for loss of CO sampled by the sensor. The first two mechanisms involve either catalytic or direct oxidation of the Mo_{blue} species (H_xMoO_3) whereas the third involves the competition between Mo and Cu species for reaction with Pd(0) created in the third phase of step 1. Although the relative importance of these mechanisms are unknown, the sensor chemistry for the CO sampler has moved toward complete elimination of Cu from the formulation. Thus the direct oxidation

of Mo_{blue} is probably the primary mechanism by which the sensors used in the CO samplers will reverse.

From Figure 4-2, the equation for the direct oxidation of H_xMoO_3 (Mo_{blue}) takes the form

$$\frac{1}{x}Mo_{blue}+\frac{1}{2}O_2+H^+ \underset{k_{-5}}{\overset{k_5}{\rightleftharpoons}} \frac{1}{x}MoO_3 + H_20, \tag{6}$$

where $0 \leq \frac{1}{x} \leq 1.05$ (Goldstein, 1991).

So that

$$\frac{d[Mo_{blue}]}{dt} = -k_5[Mo_{blue}]^{1/x}[O_2]^{1/2}[H^+] + k_{-5}[H_2O][MoO_3]^{1/2}. \tag{7}$$

Assuming that $k_{-5} << k_5$ and that $[O_2]$ is a constant, in excess, so then,

$$\frac{d[Mo_{blue}]}{dt} = -k_5[Mo_{blue}]^{1/x}. \tag{8}$$

Combining Equations 3, 4, and 8,

$$\frac{dA}{dt} = \frac{-k_5}{K}A^{1/x}K^{1/x} = \left(\frac{-k_5}{K^{1-1/x}}\right)A^{1/x}. \tag{9}$$

Given $0 < x \leq 1.05$, the possible order of the reverse reaction is in the range $0.95 \leq 1/x < \infty$. Substituting an overall reverse rate constant for the combined contributions of k_5 and K,

where $k_{rn} = \left(\frac{k_5}{K^{1-1/x}}\right)$ (subscript n represents the order), and integrating, as above, the following relationships can be derived for 1st, 2nd, and 3rd order oxidation kinetics with respect to the measured analyte, Mo_{blue}:

1st order: $ln\left(\frac{A_0}{A}\right) = -k_{r1}t$; (10a)

2nd order: $\left(\frac{A_0}{A}-1\right) = A_0 k_{r2} t$; (10b)

3rd order: $\left(\frac{A_0}{A}\right)^2 - 1 = 2A_0^2\, k_{r3} t$; and in general, (10c)

nth order: $\left(\frac{A_0}{A}\right)^{n-1} - 1 = (n-1)\left(A_0\right)^{n-1} k_{rn} t$, where n>1. (10d)

Note: these integrations are straight-forward and are given in many basic chemistry textbooks. Therefore, the math has not been shown here. The solutions for orders 1, 2, 3, and n are given in Dickerson, 1984.

Given this theoretical framework for understanding the kinetics, methods for quantifying the forward and reverse reactions were developed. The methods, discussed below, involved observing the change in absorbance of the CO sensors as a function of either CO exposure (in the case of the forward reaction during which the reverse reaction is assumed negligible) or time since exposure (in the case of the reverse reaction in which [CO]= 0, so no additional Mo_{blue} is being formed). Least-squares linear regressions of the observed bivariate dA/exposure or dA/time relationships were used to determine the appropriate kinetic model to use for quantification of the forward and reverse rate constants. The linearity of the data in the fitted models was assessed through inspection of the regression correlation coefficients (R^2). In the case of the linear forward reaction, where $dA = k[CO]$ (Equation 5d), and dA is plotted against [CO]t, the slope of the response is the empirical rate constant (k) . In the case of reverse kinetics, the units of k_{rn} are a function of the order of the kinetic model used, as follows:

Order	Constant	Units	Plot	Equation
1st	k_{r1} = -slope	(hr^{-1})	$\ln(A_0/A)$ vs. t	(11a)
2nd	$k_{r2} = \text{slope} \cdot A_0^{-1}$	($A^{-1}hr^{-1}$)	$[(A_0/A) - 1]$ vs. t	(11b)
3rd	$k_{r3} = 0.5\ (\text{slope} \cdot A_0^{-2})$	($A^{-2}hr^{-1}$)	$[(A_0/A)^2 - 1]$ vs. t	(11c)
nth (general)	$k_{rn} = (n-1)^{-1}(\text{slope} \cdot A_0^{1-n})$, where n>1	($A^{(1-n)}hr^{-1}$)	$[(A_0/A)^{n-1} - 1]$ vs. t	(11d)

Experimental

Direct exposure method

The Direct Method was designed to monitor the CO sensor response to exposure in test atmospheres in near-real-time. This method was very useful for rapid determination of sensor kinetics and calibration curves for the diffusion samplers. Thus, the Direct Method provided a means to quantify and compare sensors' individual responses.

The Direct Method used a specially-constructed single-sensor flow-through cell (Figure 4-3). It was made from a machined Delrin™ sensor holder fitted into a standard 1cm spectrophotometric cuvette. Figure 4-4 depicts the system for placement of the flow-through cell into the spectrophotometer. The Delrin™ and styrene materials were tested for compatibility with the sensor and found to be inert. Small tubes entering and exiting the cell provided for a flow of exposure gases. Operating at a slight positive pressure, the exposure gases were introduced at a flowrate of 10 cc/min. The spectrophotometer was set to monitor the absorbance of light energy between 400 and 1100 nm. The scan rate of the spectrophotometer was adjusted to a frequency between 6 and 20 scans/h.

compatibility with the sensor and found to be inert. Small tubes entering and exiting the cell provided for a flow of exposure gases. Operating at a slight positive pressure, the exposure gases were introduced at a flowrate of 10 cc/min. The spectrophotometer was set to monitor the absorbance of light energy between 400 and 1100 nm. The scan rate of the spectrophotometer was adjusted to a frequency between 6 and 20 scans/h.

A test protocol was developed for the direct exposure method. The flow-through cell, loaded with a QGI sensor, was placed into the spectrophotometer. The spectrophotometer was started and set to scan automatically at fixed intervals until the end of the experiment. After the first scan, exposure gas supply tubing was connected to the cell inlet. The exposure pattern varied depending upon the objectives of the experiment, but typically the sensor was exposed to a CO environment, usually 40 ppm (±1% supplied from a certified cylinder) for several hours. The selection of 40 ppm was somewhat arbitrary, however this concentration was within in the range of concentrations of the different ambient and occupational air quality standards. Figure 4-5 shows a typical direct exposure sensor response profile at 700 nm. The sensor absorbance increased with CO exposure. At the completion of the CO exposure period the sensor was returned to storage. Occasionally a sensor's post exposure response was observed in real-time. This was useful for observing the reversal of the sensor response (regeneration). If the monitoring was continued, the exposure gas supply tubing was quickly (about 1 min) purged with pure, dry nitrogen or air, and then connected back to the cell. The sensor could be held in a CO-free environment after CO exposure for a period from hours to days in order to monitor any change in absorbance with time; however, since the sensor regeneration occurs over weeks, the method was not practical for assessing sensor reverse kinetics. After removal from the flow-through cell, individual sensors were monitored at various intervals in the spectrophotometer using the Single Scan Sensor Holder (Figure 4-4).

Analysis of the direct method data

The sensor response in the optical/near-infrared to CO exposure was assessed by measuring the absorbance spectrum of the sensors in the range of 400 nm to 1100 nm. The exposed sensor coating has strongest absorbance at about 700 nm. A typical spectrum of sensor response is presented in Figure 4-6.

Data collected from the direct method, as described above, were a series of spectra taken at frequent intervals (2.5 to 10 minutes) for up to 6 or more hours. These data yield real-time response profiles of sensors exposed to a particular concentration of CO. The slope of the response curve (as in Figure 4-5) was proportional to the sensitivity of the sensor and could be used as a calibration curve for the diffusion samplers. The response of typical QGI sensors was approximately linear below a dA of about $1.2A$. Using the direct method, sensors' response would start to become non-linear after a dA of about 1.2 was reached. The response was better modeled with a polynomial curve fit after this. For low exposures the linear model was a good approximation which could simplify characterization of the sensors. The apparent non-linearity of response observed (as in Figure 4-5) for longer exposures using the Direct Method may have been an artifact of the exposure method due to a temporary saturation of the most accessible sensor reaction sites. This is discussed below.

Quantification of reverse sensor reaction kinetics

Reverse kinetics of the sensors was quantified by first exposing the sensors to CO and then making a series of repeated measurements of their optical density over a period of several days to several months. The conditions under which the sensors were stored after CO exposure were found to affect the reverse reaction. Parameters affecting the reverse kinetics included humidity and presence of oxygen. The effects of O_2 presence could be predicted based on the role that it plays in the reverse chemistry of the sensors (see Figure 4-2). The effects of water are not as clear based on the chemistry shown in Figure 4-2, however empirical results have shown that the amount of water available to the sensors has a strong effect on the extent of the reverse reaction. Sensors were stored under humid, dry, and dry-oxygen-free conditions depending upon the purpose of the experiment.

Humid conditions were created by simply storing the sensors in glass vials containing strips of filter paper which had been conditioned at approximately 50% relative humidity. Dry conditions were maintained using tightly sealed glass vials containing fully dried silica gel desiccant for storage (no additional oxygen was added to the air in the vials once they were sealed). The dry, oxygen-free environment was maintained within glass vials with open-face caps containing Teflon™-lined rubber septa. The vials were purged with high purity nitrogen by placing two hypodermic needles into the septa. One needle was used as a vent while the second was used to provide a low flow of the nitrogen. Once purged, the hypodermic needles were removed from the septa. During storage, the nitrogen-filled vials were stored in a secondary nitrogen-purged glass vessel to further ensure that no oxygen would reach the sensors.

An example of the data collected from a regeneration experiment can be seen in Figure 4-7a which depicts the average sensor reversal profile for four QGI CO sensors (formulation MD15, the different sensor formulations are discussed later in this chapter) over a period of about 500 hours after exposure to CO. The error bars on the data points represent one standard deviation. Throughout the following discussions the kinetic models are all with respect to Mo_{blue}. Figures 7b-7f depict the application of first- through fourth-order kinetic models (see Equations 10a-10d) to the data shown in Figure 4-7a. The fit of the first-order kinetic model was clearly poor indicating that the sensor response data could not be interpreted as following first-order kinetics. The second-order model, although better, did not do a good job of fitting the response data. The third- and fourth-order models (Figures 7d and 7e) did a reasonably good job of fitting the data, indicating that the sensor kinetics was in the range of third to fourth order.

Figure 4-7f presents the application of the 3.3-order model to the data, showing very strong empirical evidence that the overall reverse kinetics of this chemistry is order 3.3 in Mo_{blue}. The interpretation of the implications of a 3.3 order kinetic model on the chemistry of the sensors is beyond the scope of this work. For the practical application of comparing rates of reversibility of these sensors was considered to be third-order.

History of the sensor technology development

Although the main focus of this work is to present the results of the more recent advances in the CO passive sampler technology, the presentation would be unclear without a discussion of the history of development of the sensor. The following data in this section are heretofore unpublished. The collaboration began in 1989 when discussions between LBNL

and QGI led to the identification of the of QGI biomimetic sensor chemistry as potentially capable of collecting a CO sample in a diffusion sampler configuration (Goldstein, 1989-1997). The first sensors supplied by QGI, designated MD1, were formulated with copper to be reversible so that they would mimic the reversible behavior of carboxyhemoglobin, the CO-hemoglobin complex formed in blood when CO is inspired. Early results showed that the reversibility was responsible for rapid post-exposure regeneration of the sensors to their original pre-exposed state. This reversibility was a liability in the development of a monitor to measure exposure to CO.

Early sensor regeneration research

Table 4-2 describes the differences between sensors from 23 batches of sensors, designated by letters D through Z, manufactured in the pursuit of a non-reversible formulation. The reversibility of the different batches of sensors was tested by observing their regeneration over several weeks after exposure. Sensors from each batch were exposed indirectly to CO, via a simple diffusion tube configuration where they were placed at the end of 10 cm length (8mm inside diameter) glass tube with a polyethylene cap covering the end. After exposure, the sensors were stored using one of the three methods discussed above; dry, humid, or in the absence of oxygen. The storage method for the different experiments is shown in the table. Also shown in the table are the parameters of the experimental sensor formulations which were changed in the different batches. Among the parameters which were tested were sensor curing temperature, choice of Pd salt, substitution of some or all of the Mo for ruthenium, removal of copper from formulation, adjustment of the pH of sensor coating solution, and the substitution of another silica-based porous substrate (Gelsil®, Geltech Inc., Orlando FL) in place of VYCOR™.

The third-order reverse rate constants, $k_{r,3}$, for sensors from batches D through K are presented in Table 4-3. The sensors used to make these calculations were stored in dry, humid, or oxygen-free conditions. For the sensors stored dry on silica gel, the value for $k_{r,3}$ ranged from 0.0009 ± 0.0003 $A^{-2}hr^{-1}$ for the "D" sensors to 0.005 ± 0.0007 $A^{-2}hr^{-1}$ for the "K" sensors. The relative standard deviation of the measured rate constants for the different batches ranged from 11 to 31%.

In general, the reformulations that were tested in these batches did not lead directly to an irreversible sensor. However three important advances were made. *First*, the effects on regeneration caused by adjusting the pH of the coating solution used to manufacture the sensors became evident. Inspection of Table 4-2 shows that lowering the pH reduced the sensors' reversibility, however this change also compromised the forward reaction making the sensors useless. *Second*, the role of oxygen in the reverse reaction was verified experimentally. *Third*, and possibly of the greatest practical importance, the role of environmental water in promoting sensor regeneration was established.

The effects of O_2-free storage conditions can be seen in Table 4-3. The N_2 stored sensors all had values of $k_{r,3}$ about an order of magnitude lower than those stored on silica gel where O_2 was available. Figure 4-8 is an example of the difference in sensor regeneration data fitted to the third-order kinetic model under these two storage regimes. Four sensors from batch K were stored in vials with dry silica gel while another set of four sensors were stored in vials in an oxygen-free nitrogen atmosphere for almost 400 hours. During the storage period their absorbance spectra were measured four times. The average of the silica gel

Mo(VI), however it does indicate that the reaction requires a source of environmental oxygen.

Table 4-2 also presents the effects of storing exposed sensors in dry versus humid environments. The average value of $k_{r,3}$ for the sensors from batch "I" stored on paper was 0.021 ± 0.012 $A^{-2}hr^{-1}$ versus $0.003 \pm .0006$ $A^{-2}hr^{-1}$ for sensors stored on dry silica gel. A similar effect can be seen for the batch "J" sensors. Figure 4-9 depicts the effect of humidity on the "J" sensors. The exact role of H_2O in the reverse chemistry is not clear, however dry storage appears to have had a strong effect on the rate at which the sensors regenerated.

Identification of copper contamination in the sensor substrate

The effect of copper on the reversibility of the sensors is clear from the chemistry discussed in Figure 4-2. Considerable effort in reformulating the sensor chemistry described above, including the use of high purity Pd and Mo salts and other components of the sensor coating did not lead to a major improvement in post exposure sensor stability. An investigation into the presence of metal contaminants on the VYCOR and Gelsil sensor substrate materials was conducted.

The VYCOR disks were manufactured by QGI from purchased cast VYCOR rods containing a micro-porous structure with a pore size about 70Å (Goldstein, 1989-1997). The rods were cut into 1.3 or 2.6 mm disks using diamond ceramic saws. The disks were cleaned in an acid wash and rinsed with pure water after cutting.

The blank (uncoated) silica disks used in the sensors were tested for metal (especially copper) contamination using LBNL's X-ray Fluorescence (XRF) Facility. This facility employs a semiconductor X-ray spectrometer. The method used is described by Giauque (Giauque, 1973). Although the equipment was not calibrated specifically for these samples, the technique's limit of detection for copper is about 1 ppm.

Samples from three different lots of the sensor blanks with small manufacturing differences were analyzed. All three lots were cleaned thoroughly using the same preparation methods used for the sensors. After these disks were tested, a fourth lot of disks, which had been "ultracleaned" using a sequence consisting of nitric acid cleaning and sonication, followed by numerous rinses with nanopure water, was also analyzed. It was hoped that the ultracleaning of the disks would remove the copper found in the first disk lots. The results of the XRF analysis for each lot are shown in below. The units were in μg/g (ppm, by weight).

Lot # (QGI designation)	Disk #1	Disk #2	Disk #3	Disk #4	Disk #5
Uncut VYCOR™ rod	<1				
1 (Lot 8 - 80°C)	20	20	20	-	-
2 (I0215 - 180°C)	1	10	1	1	1
3 (I0617 - 530°C)	3	4	10	3	15
4 (8A - 40°C) (ultracleaned)	20	15	15	20	15

The pre-cut silica rod used to make the sensor substrate disks showed no detectable amount of copper. The copper contamination must therefore have been due to the cutting or cleaning process. The cutting process was a likely source of contamination because the abrasive cutting blades were made of brass. Possibly, the copper from the brass blades

became attached to the porous surface of the silica matrix of the disks. Attempts to clean the surface after cutting were made.

These results showed a considerable amount of copper in the disks, and that there can be a large disk-to disk variation in the amount of copper present. The ultracleaning process used on lot 4 seems to have merely reduced the variation but not the amount of copper present.

A disk of Gelsil®, grown in a mold, rather than cut from a rod, was also analyzed for copper contamination using XRF analysis. The copper concentration was below the detection limits of the XRF spectrometer.

A sensor with low reversibility was developed

Table 4-4 describes a series of batches of improved sensors using two techniques to reduce reversibility, ultrapure materials, and copper chelation. Sensors AB and AC used the original MD-1 formulation (re-named MD-1*) containing ultra purified metal salts. In addition, sensors AB used ultra-cleaned VYCOR substrate in an attempt to avoid potential contamination from copper from this source. Sensors AC used QGI manufactured cast xerogel substrates. Xerogel is an ultra clean porous silica which can be cast into appropriately sized disks. The MD-1* formulation did not prove to be an improvement over the MD-1 primarily because the ultracleaning process could not remove enough copper from the substrate (AB) and the xerogel technology was excessively expensive.

After attempts to clean the sensor substrate were unsuccessful, the focus turned towards developing a method to inactivate the metal contaminants so that they would not participate in the CO chemistry. QGI found a method to bind the copper on the surface of the VYCOR™ substrate into a chelated (bonded to non-metal ions) complex which effectively removed the copper from the system. A new sensor, the MD-15, was developed using a combination of this method and ultrapure metal salts. Batches AD, AF, and AG were identical formulations of the MD-15 sensor. AE (QGI MD-15*) was a formulated with slightly different proportions of the sensor solution constituents.

Post CO exposure reversibility of the MD-15 sensors was tested for sensors stored in a dry environment. The sensors' post-exposure absorbance was tracked over a period of one to five weeks. Analysis of regeneration data, at 700nm, for 4 AD sensors, 4 AF sensors and 3 AG sensors found that the average regeneration rate for all 3 batches combined was -7.0% ± 3.8% per week. The individual regeneration rates were -5.8% ± 2.2%, -6.3% ± 2.5%, and -9.5% ± 6.6% for sensor batches AD, AF, and AG, respectively. The average third-order rate constant k_{r3} calculated for these sensors was 0.0001 ± 4.7E-05 $A^{-2}hr^{-1}$.

The forward response of the MD15 sensors AD, AF, and AG was studied in some detail. Direct Test data for 13 of these sensors are plotted in Figure 4-10. This figure shows the dA for the first four hours of direct exposure to 40 ppm CO and a linear least-squares line fitting the data. The slope (k, see Equation 5d) of the fitted line and a linear regression correlation coefficient of these of these response curve fits are also given. The average slope, for all 13 sensors exposed to 40 ppm CO, was 0.415 ± 0.118 A-hr^{-1} (RSD = 28%). The average slopes were 0.407 ± 0.088 A-hr^{-1} (RSD = 22%), 0.329 ± 0.044 A-hr^{-1} (RSD = 13%) and 0.570 ± 0.096 A-hr^{-1} (RSD = 17%) for sensors AD, AF and AG, respectively. A single factor analysis of variance indicated that these three batches were statistically different at the 95% confidence level (C.L.), however pairwise t-tests showed that

differences between AD and AG, and AD and AF were not statistically significant (95% C.L.). The reasonably low RSDs for individual sensor groups indicated that the intra-batch variation was fairly low. The high correlation coefficient values for all 13 sensors indicated that the linear model for first order forward reaction was appropriate, at least for a four-hour direct exposure to 40 ppm CO.

Discussion of sensor history

Through a long series of developmental steps, a sensor formulation was achieved that was relatively non-reversible, yet had a forward response to CO that was sensitive and fairly linear. The research clearly showed that humidity had a strong effect on the reversibility of the sensors, and that buffering the sensors' with dry silica gel environment greatly reduced this cause of reversibility. The early sensors (MD1) had third-order reverse rate constants of about 0.002 $A^{-2}hr^{-1}$ when stored dry. The MD15 sensors' dry reverse reaction rate constant was found to be about one twentieth of this with a value of 0.0001 $A^{-2}hr^{-1}$. With these advances, it was possible to proceed in the development a passive sampler. Discussion of the first passive sampler prototype, PS1, which used the MD15 sensor, is taken up below in the section discussing diffusion samplers.

Investigation of performance of non-reversible sensors for use in CO passive samplers

Improved sensor materials (Goal 3)

Once the MD15 sensors were found to meet the needs for use in a diffusion sampler, further tests were conducted to characterize their performance both directly and in situ in diffusion samplers. This section addresses Goal 3 of the *Occupational Dosimeter Development Approach* discussed earlier. This goal was related to sensor development; the other goals detailed in the approach section are addressed in the Diffusion Sampler Results section below.

Four components of the MD15 CO sensor performance were tested: (1) intra-batch sensor homogeneity; (2) inter-batch sensor homogeneity, (3) sensor response, including sensitivity, linearity, and capacity; and (4) sensor reversibility after exposure. It was possible to assess all of these factors using the direct method. As discussed above, sensor reversibility was tracked over time by observing the change in absorbance after exposure. Inter-batch sensor homogeneity was assessed by comparing sensor forward response characteristics between batches.

Batch homogeneity characterization

Due to large variability, or heterogeneity of sensor response of the early QGI sensors, QGI made an effort to improve and refine the sensor manufacturing process. To this end, they experimented with modifications in sensor chemistry to reduce sensor reversibility. They also worked on methods to reduce both intra and inter-batch sensor variability. QGI manufactured 10 batches of sensors using the MD15 formulation for performance testing. These batches are listed in Table 4-5. The first batch, AL, was found to have a large variability in sensor responses, and were subsequently only used for testing materials compatibility. Batch AM and AN were made to compare the difference between two sensor substrates of different thickness, 0.050 and 0.100 inch thick, respectively. It was found that

although treated identically, the thicker sensors (AN) were optically more consistent, and slightly more sensitive. For this reason, the thicker substrates were used for the rest of the batches of sensors prepared by QGI.

Sensors AN-AU were all made using identical formulations, although slight variations in the manufacturing process probably occurred. These sensors were used for testing sensor performance and manufacturing all samplers. Sensor AV had calcium added to the basic MD15 formulation as a stabilizer causing it to behave differently from the other sensors.

Inter- and intra-batch sensor variability in response slope and linearity

The variation in sensor response curves for three desiccated AP batch sensors shown in Figure 4-11 was typical of the sensors from batches AN-AU. Figure 4-12 shows the response-curve average of three conditioned sensors each from the 8 batches, AN-AV. It was evident that the inter-batch variability of these sensors was significant. The curves in Figure 4-12 are averaged data from the first 4-hours of exposure of three sensors to 40 ppm in direct method tests. These data indicated that, for this section of the response profiles, the sensors' responses were linear. Table 4-6 presents the slopes (and correlation coefficients) from least-square linear regression fits for each of three sensors for sensor batches AN-AV. The intercepts in these regressions were constrained to the origin, since all sensor exposures started with zero change in absorbance. Note that the slopes of these lines were quite close within batches and, as expected, varied considerably from batch to batch.

An analysis of variance of these data, excluding the AV sensors which were different, indicated that the variance in sensor response slopes was due almost entirely to inter-batch differences ($p > 0.05$), while no statistical difference ($p < 0.001$) could be detected in slopes within batches. When an analysis of variance of the linearity of the sensor response was conducted using the correlation coefficients, the variation in inter-batch linearity explained most of the variance ($p>0.05$), while intra-batch variability was also significant ($p >0.05$). Most of the intra-batch variability in R^2 values was caused by the alinearity of one sensor in the AN batch. If the AN batch data are removed from the analysis of variance, the intra-batch variance in sensor linearity was not statistically significant ($p<0.05$).

The results showed that, with current QGI manufacturing technology, it was necessary to create a separate calibration curve for each batch of sensors. This was not considered a problem, as calibration curves would be generated for quality control in any case. It was very promising that within batches the sensors were consistent.

CO capacity limits

Direct method data consistently showed that the sensors continued to respond to CO with an absolute absorbance above $3A$. This corresponded to an increase over background absorbance of about $2.5A$. At optical densities greater than $3A$ the spectrophotometer output was found to be noisy, however the sensors still continued to show an increase in absorbance with exposure. As stated above, using the Direct Test Method the linear range of the sensors was found to go up to a change in absorbance of about $1.2A$. Above this, the direct sensor response was best modeled with a polynomial curve fit. For all practical purposes, the capacity of the sensors appeared to be at a dA of about $3.0A$. Issues related to the observed deviation from linearity of the sensors during direct exposure will be discussed later.

Sensor conditioning prior to use

From a practical standpoint, sensors within a batch must be homogeneous in order to manufacture passive samplers with minimum variability. Several factors affected intra-batch sensor homogeneity, but with only one exception, they were all controlled in the manufacturing process. The one exception was the sensor moisture content. QGI shipped the sensors with the moisture level at equilibrium with ambient humidity, i.e., at about 50% relative humidity (RH). Upon receipt, they were desiccated to equilibrium with fully dried silica gel, a RH very close to zero. If sensor moisture content was not controlled, they were found to have a large variability in sensitivity. Figure 4-13 shows the effect of sensor conditioning on response of AP sensors using the direct method. The response profiles of sensors in humid and dry conditions are superimposed. The curves with the steepest slopes represent the response of the wettest sensors. When dry, the response characteristics became quite uniform. It was necessary to desiccate the sensors for a minimum of 14 days to ensure that the sensors were fully dry.

Direct Test sensor regeneration (sensor batches AP-AU)

Table 4-7 presents data on sensor regeneration for sensor batches AP-AU. The amount of regeneration that occurred in one week after sensors were exposed in Direct Method tests is shown. The third-order reverse rate constant, k_{r3} is also shown. Regeneration was tracked by re-scanning the sensors' absorbance spectra every few days. The sensors were stored on dry silica gel when not being measured. Note that sensors were exposed to 40 ppm for different amounts of time in the different tests. Note that the post Direct Test regeneration results from the AW sensors shown if Figure 4-7 had much lower rates of reversibility. These results are discussed below.

A review of the data indicates that the percent regeneration was slightly affected by the peak sensor absorbance. In contrast, the calculated values of k_{r3} within batches of sensors were clearly dependent upon the peak sensor absorbance which in turn was directly related to the extent of CO exposure. Finally, the effect of percent regeneration after one week on inferred CO exposure was strongly influenced by the peak absorbance. For example, examine the regeneration of sensors AP-01 and AP-03, which regenerated 43% and 50% and had peak absorbance measurements of 1.4A and 3.6A, respectively. The drop in absorbance of AP-01 was 0.6A, while it was 1.8A for AP-03. Translated into ppm-h of negative bias of inferred CO exposure, this would be equivalent to Direct Test exposures of 68 ppm-h and 340 ppm-h for the two sensors, respectively. This effect is strictly due to the non-linear reverse kinetics.

Although the MD15 sensors were generally far less reversible than their predecessors, the desiccation period and dryness of the sensors was an important factor in ensuring that they had low reversibility. The one-week regeneration rates for sensor batches AP-AU were found to be higher than desired for use in diffusion samplers. It is likely that this was due to an insufficient desiccation period. The rates of regeneration of sensors from AP and AW batches that were exposed in situ in diffusion samplers were found to be much lower. This will be discussed later.

Sensors used in final laboratory and field validation experiments (sensor batch AW)

A large batch (400) of fresh sensors were manufactured by QGI in August, 1995 using the same formulation as in QGI sensor batches AN-AU (Table 4-6). These sensors were

identified as batch AW. They were desiccated for close to a year before exposure. The following results were from tests that were conducted after this long desiccation period.

Direct test calibration data for AW sensors

Seven AW sensors were exposed to 40 ppm CO in pure air (normal O_2 levels) using the Direct Method. Figure 4-14 shows the individual sensor behavior from the first 2.5 hours of these exposures. The response of one sensor (k = 0.32 A-hr^{-1}, R^2 = 0.9993) was a clearly different than the average slope of the other six (k = 0.37 A-hr^{-1} , R^2 = 0.9995). All of the sensor response data were very linear over the first 2.5 hours of exposure to 40 ppm. (A quadratic curve fit $dA = -0.01t^2 + 0.39t$, R^2 = 0.9993 where t is 40 ppm direct test CO exposure in hours, fits the average sensor response well for direct exposure periods of longer than 2.5h.) The linear AW sensor response coefficient of 0.37 was very similar to the observed responses of sensor batches AS-AV (Table 4-6). The RSD of the set of 7 sensor's responses was 6%.

It can be seen from the direct test data such as those shown in Figures 11 though 14, and from the non-linear curve fit data presented above, that the forward response of the sensors did not perfectly obey the assumption of linearity. Possibly, this was due to a non-linear behavior of the forward kinetics of the sensor chemistry. However, more likely, the observed sub-linearity is an artifact of the Direct Method exposures. Such an effect could be caused by a temporary saturation of the most available reactions sites on the sensor surface due to a high rate of exposure over an extended period, while over shorter periods the saturation would not occur. This sub-linearity was not observed in the response of the sensors when exposed in diffusion samplers.

Reversibility of Direct Test exposed AW sensors

Table 4-7 contains sensor regeneration data for four AW sensors exposed to CO during Direct Tests. These sensors had been exposed to 40 ppm CO for a period of three to seven hours, resulting in peak dA values up to 3.0A. AW sensor regeneration during a one-week period was about one half of the regeneration over the same time for sensor batches AP-AU. The average one-week regeneration was 41 ± 8 percent for the AP-AU sensors, while it was 21 ± 5 percent for the AW sensors. The difference is probably due to the extremely long period of time that these sensors were stored on dry silica gel prior to exposure (almost 300 days vs. about 100 days for the AP-AU sensors).

Aging and variability of AW sensors

An unfortunately long period (more than a year) elapsed between the time when the AW sensors were manufactured, and when they were built into dosimeters. Although the sensors were stored in sealed vials within a sealed desiccator jar, their average background absorbance drifted up from 0.7 ± 0.2A to 1.3 ± 0.3A. This increase in background, or initial absorbance, caused the photometric accuracy of measurements to decrease. This was noticeable in an increase in variability of response of dosimeters assembled using these aged AW sensors.

The cause for the increased optical density of the unexposed aged sensors is unknown. Possibly, it was simply due to a slow diffusion of CO into the sealed vials during storage.

However, it was more likely that the aging was due to the desiccation of the sensors. AW sensors stored over the same period of time in sealed vials without silica gel did not darken to the same extent as those which were dried. The source of observed variability in the aged AW sensors could be related to water depletion within the sensors. Possibly, some sensors had actually reached the point where there was insufficient water to allow for the complete chain of reactions to occur on the sensor surface. The data, both collected from direct tests and from diffusion sampler experiments indicated that on average the behavior of the sensors was identical to the less aged sensors, but there was more variability between sensors.

Development of Diffusion Sampler Technology

Passive sampler concept

The QGI sensor was well suited for use in a passive sampler because 1) its response to CO was sufficiently irreversible; 2) its response was easily measured (optically) without complicated wet-chemical or gas-phase chemistry techniques; and 3) it was small enough to be configured into a very small package requiring no pump or external power. The results from application of the Direct Method described above showed that the QGI sensors performed satisfactorily for incorporation into a diffusion sampler.

The key functional elements of the LBNL/QGI sampler were the CO sensor and the diffusion tube, encased in a sealed housing. A removable cap on the end of the diffusion tube was used to control when the device was able to sample. Desiccant was added to the device so that environmental water would not affect the sensor.

The diffusion sampling approach was selected because well-established methodology exists, based by Fick's law of diffusion (Palmes, 1976; Rose, 1982), to collect time-averaged gas samples inexpensively.

An advantage of the diffusion sampler design was that sampling rates (and sampler capacity) could be varied with a simple change of the diffusion tube dimensions. Mathematically, given the assumption that the sensor has 100% collection efficiency, Fick's Law can be stated by the following equation.

$$M = \frac{D_{co} C A t}{L} \qquad (12)$$

where:

M = mass diffused to end of diffusion tube (μg);

D_{co} = diffusion coefficient for CO in air (0.245 cm^2/sec);

C = bulk air to sensor surface CO concentration gradient where the CO concentration at the sensor is assumed to be zero; i.e., ambient concentration of CO at tube entrance (μg/m^3);

A_x = cross-sectional area of tube (cm^2);

t = sampling time (sec);

and

L = length of tube (cm).

This relationship defines the parameters needed to engineer a diffusion sampler for a given application, Thus, within the limits of the rate at which the sensor interacts with CO, using a shorter tube, or one with a larger inside diameter will lead to a greater diffusion sampling rate. An optimum range of sensor response could be achieved by properly designing the sampler geometry. It was possible to configure a passive sampler to collect for 168 hours (1 week) or an occupational dosimeter to collect for 8 hours, in part, by changing the diffusion tube. The initial design for the passive sampler used a configuration suitable for 168-hour sampling.

Rearranging equation 12, and converting the time units from seconds to hours, an expression for the theoretical mass conversion rate of the diffusion samplers can be derived:

$$q = \frac{3600M}{Ct} = \frac{3600D_{CO}A_x}{L}, \qquad (13)$$

where

q = the diffusion sampler's mass conversion rate ($\mu g\text{-}ppm^{-1}hr^{-1}$).

This rate represents the mass of CO which is involved in the initial CO-Pd reaction shown in Figure 4-2, Step 1a. Note that the sampling rate of the diffusion sampler is dependent upon the CO concentration gradient between the bulk-air and the sensor surface. Also note that the actual sampling rate of this diffusion sampler cannot be directly calculated because of the nature of the QGI sensor, i.e., the exact relationship between dA and the mass, M, of CO reacted with the sensor is unknown (see Equations 3-5).

Methods

Diffusion sampler laboratory test method

The purpose of the diffusion sampler laboratory exposure method was to test the performance of passive diffusion sampler configurations, in contrast to the direct method that was developed to test individual sensors. It was a test regime where samplers were exposed to CO, and possibly other gases, under controlled conditions. Prototype passive samplers were exposed to test atmospheres in a temperature and humidity controlled environmental chamber made of a 3-liter glass reaction vessel. Figure 4-1 depicts the diffusion sampler exposure test setup. The instruments used in this setup are listed in Table 4-1.

Ports on the reaction vessel were connected to the laboratory gas flow system so that an atmosphere of exposure gas could be created. A typical flowrate for the system was 1.0 $l\ min^{-1}$. The pressure of the exposure chamber was maintained slightly above atmospheric pressure (200 Pa). CO concentration and humidity were measured downstream of the exposure chamber. All environmental parameters under control, including CO concentration, were recorded by the data acquisition system. Typically, for the diffusion method experiments, 10-minute averages of the monitored parameters were recorded.

The change in optical density of the sensors caused by CO exposure was quantified by measuring the change in the sensor's absorbance (dA) of light (400 to 1100 nm) before and

after exposure. The 700nm measurements were used for analysis. In the early sampler designs, such as Prototype #1, PS1 (see Figure 4-15), the sensors were placed individually in the single-scan holder in the spectrophotometer (see Figure 4-4). It was necessary to disassemble the sampler in order to remove the sensor for measurement. The spectrophotometer sample chamber was purged with ultra-pure air to prevent sensor contamination from ambient air. The sensor absorbance spectrum was scanned four times for each measurement. The sensor orientation was changed for each scan, and the four scans were averaged. Post-exposure changes in absorbance due to sensor regeneration were also measured using this method.

The following test protocol was developed so that different sampler configurations could be compared: Sensors were desiccated for at least two weeks prior to exposure (this desiccation period was found to be an important factor in controlling sensor response rate, as discussed above). A pre-exposure measurement of sensor absorbance spectra were taken. Samplers were assembled using the sensors to be tested. Two or more samplers, left unexposed, were used as controls. They were handled identically to the test samplers and were measured with each measurement of the exposed sensors. Various CO concentrations of between 5 and 100 ppm were used in the exposure chamber depending upon the experiment. After exposure, the samplers were removed from the exposure chamber, disassembled, and measured in the spectrophotometer.

The PS1 had to be disassembled in order to remove the sensors for each absorbance measurement, while the later prototype designs allowed for sensor measurement in situ. Typically a series of exposures were conducted on a set of samplers with sensor absorbances measured before and after each exposure. For example, in some experiments the PSx samplers were removed from the exposure chamber and measured once every 24 hours for one week. The Dx prototype occupational dosimeters were typically exposed to CO in a sequence of four 4-hour periods. Delta absorbance values were calculated by subtracting the initial absorbance prior to the first exposure from the absorbances after the subsequent CO exposures. These dA values were plotted against their cumulative CO exposures.

Analysis of the diffusion sampler laboratory test method data.

Data collected using the diffusion sampler exposure method yielded only a pair of data points at 700 nm for each exposure to CO. This was because the absorbance spectra were only measured prior to and after exposure. The change in absorbance (or the difference in absorbance between these two points) with exposure to CO, for a sensor exposed in a diffusion sampler, were used to compute the CO exposure of the sampler.

Calculating a diffusion scaling factor for comparing diffusion samplers to direct test forward response data.

An empirical calibration based on data collected from both the direct tests and a series of laboratory diffusion exposure tests at a range of exposures were made in order to compare the passive sampler response to the response characteristics of sensors from the same batch. Once this relationship was determined it was possible to superimpose the direct test response curves onto plots of delta absorbance data collected from diffusion samplers in a sequence of controlled CO exposures. The diffusion samplers were calibrated for each batch of sensors to remove the variability caused by inter-batch differences in sensor response. This calibration accounted for the increased restriction in the diffusion path

created by the diffusion tube. The assumption was that the rate at which CO molecules diffused to the sensor in the direct tests was a constant. Given this assumption it was possible to scale the response of the passive samplers relative to that of the sensors tested using the Direct Method. Normalizing to the direct exposure regime, the ratio of the response of the sensor in the sampler to what it would have been in a direct test should be a constant. This relationship will be called the diffusion scaling factor, R, calculated as follows:

$$R = \frac{e}{e_{eff}} \tag{14}$$

and

$$e_{eff} = \frac{dA}{k} \tag{15}$$

where,

R = the diffusion scaling factor (unitless),
e_{eff} = effective exposure of sensor (ppm-h),
e = actual exposure of sampler (ppm-h),
dA = delta absorbance of sensor (A),
and
k = derived forward response (slope) of sensor batch from direct tests (see Equation 5d, A-ppm^{-1}h^{-1}).

The empirically derived diffusion scaling factor was useful for comparing the observed sensor response under the direct and diffusion sampling modes, two very different exposure regimes.

Empirically derived diffusion sampler response used to calibrate passive samplers

The Diffusion Sampler Laboratory Test Method produced a sequence of two or more absorbance measurements related to CO exposures. These dA values were plotted against their respective exposure levels, e in ppm-h. In the simple case, where samplers were only exposed once, the sample response was merely dA/e. However, when a set of samplers were exposed to a sequence of exposure regimes and corresponding change in absorbances were measured, the slope of the line fitted (using a least-squares linear regression) through these points was calculated. This slope,

$$\rho = \frac{dA}{e}, \tag{16}$$

was the average response of the samplers for these exposure regimes. Once calculated for a batch of samplers ρ was used as a calibration to calculate the exposure of samplers. From Equation 16,

$$e_{calc} = \frac{dA_{sampler}}{\rho}, \tag{17}$$

where:

e_{calc} = the calculated TWA exposure of the sampler (ppm-h), and

$dA_{sampler}$ = the measured pre and post exposure difference in sensor absorbance at 700nm (A).

Note that e is the actual exposure whereas e_{calc} is the measured exposure calculated from the change in absorbance of the CO sensor.

Definition and calculation of precision, bias, and accuracy

Precision, bias, and accuracy have formal definitions set forth by NIOSH with regard to air sampling analytical method development (Kennedy, 1995). In this work they are only used to discuss the results of the fully functional occupational dosimeter. In other instances test results are presented in terms of sample mean, standard deviation, and relative standard deviation.

NIOSH defines precision as the "relative variability of measurements on replicate samples about the mean of the population measurements." In reality this is merely the relative standard deviation, the standard deviation of a set of individual measurements divided by their mean (Kennedy, 1995).

Bias is defined as the "uncorrectable relative discrepancy between the mean of the distribution of measurements from a method and the true concentration being measured, T as expressed as a fraction. It is given by $B = [(\mu/T) - 1]$." In the context of this work T is the true CO exposure as measured by the calibrated CO analyzer and μ is the mean of measured values (e) of a set of exposed dosimeters (Kennedy, 1995).

The definition of accuracy set forth by NIOSH is "the ability of a method to determine the "true" concentration in the environment sampled ...The accuracy of a method is the theoretical maximum error of a measurement, expressed as the proportion or percentage of the amount being measured without regard for the direction of the error, that is achieved with 0.95 probability of the method." NIOSH provides a method for the calculation of accuracy based upon measured bias and precision from experimental data. A nomogram providing hyperbolic curves relating bias and precision to accuracy is provided in Kennedy, 1995 (Figure 4-16). The accuracy calculations for sets of dosimeters presented in the dosimeter performance results section was simplified using this procedure.

Sensor storage and silica gel preparation for use in passive samplers

For direct measurement, or prior to assembly into passive samplers, the sensors were stored in individual glass vials with Teflon cap seals. When dry storage conditions were required, the vials were filled with dry silica gel and a paper retaining plug. When humid storage conditions were required, vials were packed with clean filter paper equilibrated at about 50% RH. The paper contains enough moisture to maintain a humid environment in the vial.

All silica gel (7-20 mesh blue indicator, Silica Gel Products, Inc., Los Angeles, CA) was conditioned prior to use by purging with dry, ultra-pure air for 24 hours at 70°C. This was done to ensure that the gel was not a significant source of volatile organic compounds (VOCs) since a concern existed that the sensors might respond to relatively high concentrations of certain VOCs. In addition to water, silica gel could adsorb a wide range of

VOCs that concentrate on its surface. If the concentration was high enough, the equilibrium VOC concentrations in an enclosed space such as a sensor storage vial could be quite high, possibly causing an increase in background exposure to the sensor.

Results: PS1 and PS2 laboratory tests

Summary of PS1 results

PS1 design

Figure 4-15 shows the features of the first prototype CO passive sampler. The key points of the design were (1) a large excess of dry silica gel to adsorb any water vapor in the sample stream, and (2) a well defined sampling rate based on Fick's Law and the geometry of the diffusion tube and sensor. The sampler body was a glass vial. The vial was filled with indicator silica gel. A porous polyethylene tube (Porex Technologies, Fairburn. GA) with the QGI sensor placed at the lower end was embedded into the silica gel in the vial. A silicon rubber and PTFE septum was placed in an open-faced cap at the top of the vial. A 16 gauge hypodermic needle was inserted into the septum protruding down into the void space inside the porous internal tube.

The needle acted as a diffusion tube, fixing the sampling rate of the sampler. The porous tubing allowed moisture to diffuse out of the sampling path before reaching the sensor. The silica gel acted to keep the entire system dry.

PS1 laboratory exposure tests

A series of three exposure tests were conducted on a very small number of PS1 prototypes. The samplers were exposed to test atmospheres in the 3-liter temperature and humidity controlled exposure chamber. The exposure concentrations in three sets of tests were 40 ppm, 18 ppm, and 0.8 ppm. These concentrations were chosen to represent 0.1*NAAQS (9 ppm for 8-hours), 2* NAAQS, and 4* NAAQS (also, the 1-hour standard is 35 ppm), a range of CO concentrations that could be found in indoor atmospheres. The following results showed that the diffusion sampler configuration could be used to measure CO exposures using the QGI sensors. The data in these tests were limited so little significance was placed on the statistics which were calculated for the PS1 performance.

In the first test, two samplers using sensors from the AD batch were exposed in two stages to about 40 ppm CO at about 60% RH for a total of 3240 ppm-hours. The sensors were measured after 1540 ppm-h, and then a second time at 3240 ppm-h. (The RSD of the two sampler's e_{eff} was about 9%.) The average value for the diffusion scaling factor, R, was calculated to be 0.066 (RSD = 9%).

In the second test, four samplers were exposed to 18 ppm during three consecutive periods for a total of 3431 ppm-h, also at about 60% RH. The RSD for the response of the samplers was 13%, 6.8%, and 5.6% for 799, 2120, and 3431 ppm-h exposures, respectively. R was calculated to be 0.063, 0.059, and 0.051 for these three exposures.

In the third test, five samplers were exposed to the very low concentration of 0.8 ppm for one-week (e = 141 ppm-h). The calculated value for e_{eff} and R were 6.5 ppm-h and 0.046, respectively. As expected the variation between samplers at this low exposure level was

larger that in the first two tests (RSD=39%). Limited results from field testing of the PS1 are presented in a later section.

Discussion of PS1 design

The PS1 results proved the CO passive sampler concept, however the device was not practical for use in large scale field tests. Analysis was very cumbersome because it was necessary to disassemble the samplers in order to remove the sensors. The samplers were prone to leakage around the cap and at the needle hole in the septa. The glass body and the hypodermic needle were unsuited for use in field studies where improper handling could lead to an injury of a participant. These issues were dealt with in subsequent prototypes.

Goal 1 - Prototype dosimeter development (passive sampler 2, PS2)

Design of critical components and enhancements

An improved CO passive sampler prototype, the PS2, suitable for use as an occupational dosimeter, was designed and constructed (see Figure 4-17) to improve the design to 1) miniaturize and reduce weight; 2) reduce blank exposure (e.g., reduce leaks); 3) improve the safety of the design for field use (e.g., remove hazardous components); 4) improve sample analysis methodology; and 5) improve precision and reduce inter-sampler variability. It was also necessary to re-configure the diffusion tube dimensions for use as an 8-hour dosimeter. The 8-hour design is referred to here as the PS3 which was the same as D1, the first occupational dosimeter.

The PS2 had several advantages over the original prototype PS1, achieving most of the goals listed above. However, its underlying principle of operation was identical to that of its predecessor. The PS2 design was small and compact, and CO exposure could be measured directly. It was rectangular in shape (1.3 cm x 1.3 cm x 4.5 cm) and was well suited for use in mailout studies, or to be worn as a personal sampler.

The PS2 design was intrinsically safer than its predecessor. The hypodermic needle previously used for a diffusion tube was replaced with a 4 cm piece of 1 mm outside diameter (OD, 0.5 mm inside diameter [ID]) PTFE, or 15.6mm OD (4.8mm ID) brass tubing for the one-week passive sampler and the 8-hour dosimeter, respectively. The diffusion tubes fixed into place and the cuvette was sealed with epoxy sealant. The glass vial was replaced with a plastic (styrene) cuvette. The new prototype design required less desiccant. PS1 had a large excess of desiccant. Based on calculations of the actual amount of silica gel needed, this amount was reduced significantly. The entire unit was permanently sealed so it could no longer be disassembled. With these improvements the samplers were essentially tamper-proof, ensuring that they would be safe for deployment in the field.

The PS2 design allowed for ease of analysis. The device was built into a standard spectrophotometric cuvette. With these improvements pre- and post-exposure measurements could be made without disassembling the passive sampler. In Figure 4-4 the "Dosimeter Holder" shows how the PS_x and D_x samplers were placed in the spectrophotometer. The sensor was permanently positioned within the cuvette so that when placed in a spectrophotometer it was automatically sealed in the optical path of the measurement beam. Analysis was accomplished simply by placing the sampler into the standard cuvette holder of a spectrophotometer (see Dosimeter Holder in Figure 4-4). Another benefit of the design was that the sensor position within the sampler was fixed.

Because the orientation of the sensor with respect to the spectrophotometer beam could not change between subsequent measurements, measurement precision was improved. The height adjustment on the cuvette holder was positioned so that the light beam would be centered on the CO sampler sensors.

Evaluation of sampler materials for use in PS2

Although the design of PS2 was fairly simple, it was necessary to select the materials used in its construction very carefully. This was because the QGI sensor was sensitive to high concentrations of plasticizers and certain volatile organic compounds. All of the materials used in the manufacturing of the sampler including the sensor holder, adhesives, and sealants were tested. Table 4-8 presents a list of the materials examined and the results of the compatibility tests. This discussion will focus on the materials which were found be compatible with the sensors, however it should be noted that their selection was not trivial, taking many months to identify them and to complete their testing.

The materials were tested by exposing QGI sensors to each them in small glass vials about the same volume as a 1 cm cuvette for 1 week. Certain materials were too large to be placed in small vials, so larger vials were used where necessary. For controls, additional sensors were stored identically, in the absence of the material being tested. The quantities of materials used were similar to those that would be used in a passive sampler. Before and after exposure to the materials, sensor absorbance measurements were made (at 700 nm). A material was considered to have a positive interference with the QGI sensor if the average change in absorbance of the exposed sensors was more than about 10% greater than the average change in absorbance of the controls.

Selection of a sealant for the open end of the cuvette was difficult. As can be seen in Table 4-8, several different materials were tested. The most effective sealant was the epoxy-based potting system, a product of 3M Corporation (St. Paul, MN). This material appears to have virtually no VOC emissions detrimental to the sensor during or after curing. It also has excellent sealing properties. After the epoxy sealant had cured, the samplers were virtually leak-free, leading to low blank values for unexposed samplers.

The PS2 sensor was housed in a porous polyethylene sleeve manufactured by Porex Technologies (Fairburn, GA). This sleeve was intended to act as a holder locating the sensor in the spectrophotometer beam and to mask light leaks which could occur at the sensor perimeter. The porous nature of the material was expected to allow a free exchange of gases, including water vapor, between the sensor and the silica gel. As received, the Porex material was found to interfere with the QGI sensors (Table 4-8). By cleaning the material in ethanol and then baking it in an oven at 40°C for 48h, while purging with pure air, this interference was completely mitigated.

Goal 2 - Evaluation of PS2

PS2 response characteristics

With the development of the PS2, an effort was made to ensure that the new design performed at least as well as Prototype #1 (PS1). Groups of five PS2 samplers configured for 1-week sampling were exposed in the laboratory under dry conditions using the diffusion sampler test method described above. The exposure ranged from 180 to 4200 ppm-hours,

at concentrations from 8 to 41 ppm and the exposure duration ranged from 8 to 168 hours. The response of the samplers is shown in Figure 4-18. The concentration- duration of CO of each consecutive exposure is tabulated on the figure. The error bars on the data points in Figure 4-19 represent ±1 standard deviation, an indication of the spread in response of five samplers at a given exposure level. The dashed curve superimposed on this figure is the scaled direct method response curve for the batch of sensors used. The solid line through the points is a least-square regression fit of the data, indicating a sampler response, ρ, of 0.0002 A-ppm^{-1}hr^{-1}. The response of these samplers was very linear ($R^2 = 0.999$), with an average RSD of 8.5% across the range of exposures. The lowest exposure level was about 200 ppm-h, equivalent to about a 1.2 ppm average for a week. The RSD of the 5 sampler measurement was 13.6% for this exposure level. On the other extreme, the samplers were exposed to the equivalent of 25 ppm for a week (4200 ppm-h) with an RSD of 7.8%. At the highest exposure level the maximum average change in absorbance was less than 1A. Direct method measurements indicated that the sensor response range goes up to a change in absorbance of about 3A. Although never tested to their limit, the PS2 should be capable of measuring a one-week average exposure of up to about 75 ppm, or 13,000 ppm-h.

The average diffusion scaling factor, R, for the PS2 across the exposure range was 33.8 (RSD=5.0%). As described in equation 12 above, this ratio is a function of the sensor kinetics and geometry of the diffusion tube configuration. With a change in sampler configuration, the range of the sampler was extendible either for use in different concentration ranges or sampling duration. The low variability in R for this sampler configuration indicates that the sampling rate was fairly uniform across a wide range of exposures.

The linearity of the sampler response when they were exposed to a range of concentrations indicated that they appear to perform independent of concentration in the range of 8 to 40 ppm. Of interest was that the sixth exposure point on the response curve (8-hr x 38 ppm, see Figure 4-18) fell slightly below both the line of best fit and the superimposed scaled direct exposure trend. This was the only exposure datum to diverge from the expected response. It was also an 8-hour exposure, a duration about one-third or less as long as the others in the test. It is possible that the observed reduced response was due to the shorter exposure duration. Recall that the PS2 samplers were configured to sample for up to one-week or more. The observed underestimate of exposure for the 8-hour exposure may indicate that the performance of the PS2 may be compromised if a sampling duration of 20-hours or less is used.

Humidity effects

Three PS2 samplers were exposed in the laboratory to CO in humid environments. Figure 4-19 shows their response. The solid curve superimposed on the figure is the scaled direct method test response from the AP sensors used in the experiment. The direct data were scaled using the value for R (33.8) calculated for the samplers under dry conditions. The RH during the exposures varied from an initial 75% to above 95% as shown in the figure. The sampler response appears to have significantly underestimated the true exposure after the RH levels reached 90%. At 5400 ppm-h of exposure, the samplers' integrated measurements averaged 23% low. Even during the 75% RH exposure period the samplers began to show a negative bias. Nonetheless, the results were promising even at RH levels approaching 100%. At the highest humidity exposures the rate of diffusion of water vapor into the sampler was

excessive, and the silica gel was unable to keep the sensor dry. However, the indicator in the silica gel did not show any evidence of water saturation (the indicator dye never changed from dark blue). Thus the problem appeared be due to restriction in the ability of water vapor to diffuse through the porous polyethylene sensor holder into the silica gel (see Figure 4-17). This design issue was resolved during the development of the final dosimeter configuration (PS4/D2), and it is discussed below.

PS2 Sensor reversibility after exposure

PS2 samplers constructed using sensors from batch AP were measured for reversibility for over 400 hours Figure 4-20 shows the average reversal of sensor response from 5 samplers that had been exposed to CO in dry conditions. These samplers had been given a total CO exposure of 600 ppm-h with [CO] ranging from 10 to 40 ppm. The average peak dA was 1.5 $\pm$ 0.15A. The third-order reverse rate constant was 9.0E-4 $A^{-2}hr^{-1}$ (RSD=12.5%). Average sensor reversal was about 1% (6 ppm-h equivalent) a day with a measured 6.8% (40 ppm-h equivalent) reduction of the peak absorbance after one week. The sensors used in these tests were desiccated for 100 days prior to exposure. Note that the reversibility of the AP sensors exposed in the samplers was almost an order of magnitude less than for sensors exposed using the Direct Method. The reason for this is not understood, however it may be related to a difference in sensor behavior due to the different exposure modes.

Response of unexposed PS2 controls

Unexposed samplers, used as controls with a group of exposed samplers, are necessary to account accurately for any background changes in sensor absorbance. The use of laboratory and field controls is standard for any pollution measurement surveys involving samplers. The most likely cause of absorbance shifts in unexposed samplers is air leakage. The design of PS1 was quite leaky. The use of the epoxy potting material as a sealant in PS2 reduced this leakage significantly, however some background increase in absorbance was still noticeable in these samplers. Figure 4-21 shows the response of passive sampler controls which remained capped, but were placed in 8 to 40 ppm CO environments for more than 650 hours. Although this background drift was quite small, possibly some of the increase was caused by a response to one or more components of the materials that were present. Small leaks in the PS2 samplers were likely the main cause of the sensor response. The sampler response is shown as a function of a nominal sensor capacity (dA of 2.5A). The average change in absorbance was about 0.1A over the 650 hour period corresponding to an equivalent CO exposure of 500 ppm-h (or 0.8 ppm average over the 650 hours).

Initial Occupational Dosimeter Configuration (PS3/D1)

After testing PS2 with a diffusion tube diameter (1mm) and length (4cm) similar to that of PS1, a small number of samplers (referred to as PS3 or dosimeter 1, D1) were constructed using inlet diffusion tubes with larger diameter (4.8 mm ID x 4 cm, 5.6 mm OD) to allow more CO mass to diffuse to the sensor in an 8-hour period, as required for occupational dosimetry. Figure 4-22 presents the results from exposing five D1 samplers. The dosimeters' exposures ranged from 40 to almost 600 ppm-h. (To place this in perspective, NIOSH recommends that a suitable measurement range for sampling should be 0.1 to 2 times the regulatory standard, i.e., a range of 40 - 800 ppm-h based on the OSHA PEL, or 25 - 500 ppm-h based on the ACGIH TLV (Kennedy, 1995)). The actual concentrations and duration of the test exposures are tabulated on the figure. The concentrations ranged

from 4 to 36 ppm. The highest exposure led to a delta absorbance average of more than 1.5*A*, which was out of the linear region of the sensor response curve. The dashed curve superimposed on Figure 4-22 is the scaled direct method response curve for AP sensors. Although the data clearly fit the calibration curve very well, the alinearity at the high-end of the response curve was evident. A least-square fit through all the data still indicates a reasonable (correlation coefficient, R^2=0.98) fit to a linear model, but the use of the polynomial fit to the calibration curve provides more precision. The RSDs for the lowest and highest exposure levels were 9.9% and 8.9%, respectively. The average RSD across the exposure levels was 8.4%. The average value for the diffusion scaling factor, R, was 2.6 (RSD = 7.4%), consistent with the much higher diffusion rate for the occupational dosimeter design. The slope, ρ, of the regression line was 0.0027 A-ppm^{-1}hr^{-1} (95% interval (CI): 0.0026 to 0.0028). The low RSD for the diffusion ratio indicated that the behavior of the sampler was very consistent over the wide exposure range. As with the PS2, the data confidence indicate that the dosimeter response to CO exposure was independent of CO concentration.

Goal 4 - Occupational dosimeter configuration (PS4/D2)

The design of the PS2 and the first dosimeter configuration (PS3/D1) had satisfactory performance characteristics with only three exceptions. The primary flaw, as discussed earlier, was humidity control. The porous polyethylene sensor holder was unable to transfer water vapor at a rate sufficient to protect the sensor from moisture. The second flaw, which has not yet been discussed, was that the porous sensor holder material was difficult to handle and machine, making the manufacture of the sensor holder very labor intensive. The third problem with the early dosimeter prototype was the inadequacy of the machined PTFE seal which centers the diffusion tube and separates the silica gel from the epoxy sealant. This seal allowed the epoxy sealant to leak into the silica gel when the samplers were being assembled, which reduced the desiccating capacity of the device and made it unattractive.

These issues were tackled when D2 was engineered jointly by LBNL and QGI. The new design is shown in Figure 4-23. A new sensor holder was designed to increase the water vapor transfer rate to the silica gel and improve the manufacturability of the device. This holder was made of a machined black polycarbonate cube, a plastic material that had been tested for compatibility with the QGI sensor. The holder contains numerous small ports on all faces except the two perpendicular to the optical path which hold the sensor. Additionally, the vertical sides of the cube were slotted to allow water vapor to diffuse up from the bottom of the cuvette into the silica gel. The sensor holder was machined to fine tolerances so that 1) it fit perfectly into the plastic cuvette and 2) the diffusion tube would snap into it. Figure 4-23 also shows the new seal that was designed to align perfectly and seal against the diffusion tube and the mating surfaces of the cuvette walls. The seal was also machined from black polycarbonate plastic. The sealing edges were cut at 12° in order to make a tight closure.

Although both of the new parts were machined using a computer programmed mill, it was anticipated that an injection mold would eventually be developed to make them in production quantities. It is not anticipated that the switch to a molding process will cause any changes in the design because injection molding is a very precise manufacturing technique. The same polycarbonate material is available for injection molding so it would not be necessary to switch materials.

Results: D2 response, precision, bias, accuracy, and humidity control verification

In order to test the response and humidity control performance of the newly designed D2, a preliminary batch of 20 pairs of sensor holders and seals were manufactured. These parts were assembled into dosimeters using 40.6±.05 mm (1.6 inch) lengths of 5.6 mm OD (i.e., nominal 7/32 inch OD, ID = 4.8 mm) brass tubing, and pre-conditioned 7-20 mesh indicator silica gel, lightly packed into the dosimeter cavity.

The primary functional change implemented in the design of D2 was the increased water vapor transfer capability of the machined sensor holder. It was necessary to test the performance of the dosimeters with this improvement. A series of three tests were conducted for this purpose. Sets of three dosimeters were uncapped and exposed using the diffusion sampler test method in the 3-liter reaction vessel. Three capped dosimeters were also placed in the vessel during the exposure experiments as controls. Table 4-9 presents the exposure conditions and average dosimeter response at 700 nm. Sets of three uncapped dosimeters and three controls were exposed in approximately 4-hour increments to 40 ppm CO (159 to 207 ppm-hours) and nominal relative humidities of 20%, 30%, 50%, or 90%. In Tests 1 and 3 the dosimeters were first exposed to low RH for 8-hours, and then high RH for 8-hours. This pattern was reversed in Test 2 where the dosimeters were first exposed to high RH and then low RH.

Figure 4-24 presents the average of three dosimeters from all three tests. Error bars represent ±1 standard deviation of the incremental (4-hr) change in absorbance of the dosimeters. The humidity exposure of each run is identifiable in the figure. A bivariate least-squares linear regression of the dosimeter response against CO exposure, with the intercept constrained to zero, indicates that the slope, ρ, of the average dosimeter response was 0.0029 A-ppm^{-1}hr^{-1}(R^2 = 0.97, 95% CI of ρ: 0.0028 to 0.0030 A-ppm^{-1}hr^{-1}).

A multivariate regression analysis of dosimeter response against CO exposure and relative humidity is presented here. This analysis, was conducted by breaking the three tests into their incremental, nominal 4-hour, exposure increases in order to look at the unbiased relationship between CO exposure, RH, and dosimeter response. The analysis uses the 36 individual dosimeter absorbance measurements and their associated exposures and RH levels. The results yielded a CO exposure coefficient of 0.0029 A-ppm^{-1}hr^{-1}($p < 0.0001$, R^2 = 0.94, 95% CI of ρ: 0.0027 to 0.0031 A-ppm^{-1}hr^{-1}) and an RH coefficient of 0.0006 (95% CI: 2.0 x 10^{-5} to 0.001). The relationship between CO exposure and dosimeter response was statistically highly significant, and the effect of RH was weak but significant at the 95% confidence level. The RH coefficient suggests a change in absorbance effect of 0.06A at 100%RH (equivalent to 20 ppm-hours). The dosimeter response coefficient, ρ, of 0.0029 A-ppm^{-1}hr^{-1} seen in these data were very close to the slope of 0.0027 A-ppm^{-1}hr^{-1} measured for the response of the D1 dosimeter prototype.

Although the RH effect was statistically significant in this analysis, its import is small (20 ppm-h compared with an 8-hr TLV of 200 ppm-h and PEL of 400 ppm-h, i.e., < 10% of TLV and 5% of PEL). Furthermore, the interpretation should be taken with caution because the high humidity data were sparse and the three dosimeters using the aged batch of AW sensors in the 90% RH test were unfortunately variable. Further testing at high humidity is needed to verify the small humidity effect observed here.

The above results, sensor variability not withstanding, indicated that the improvements in the sensor holder design had the intended effect on water vapor transfer rate. The D2 prototype was capable of operating at very high humidity without compromise to sensor performance.

Precision, bias, and accuracy of occupational dosimeter D2

Precision, bias, and accuracy calculated for the D2 prototype exposure data are also shown in Table 4-9. The samplers were exposed to four different humidity levels as discussed above. The precision of the samplers in these exposure experiments was very low (1%-5%) with the exception of the two discussed above that were exposed to 90%RH. The bias observed for all experiments was also low with an absolute value ranging from 0 to 10%. The accuracy calculated using the NIOSH nomogram (Kennedy, 1995) ranged from 5% to 16% except for the variable high-RH samplers which had accuracies of 20% and 27%. Interestingly, high-RH exposures did not bias the dosimeters (bias was 0 and 4% for these two exposures).

Discussion of D2 development results

Comparisons between the direct test forward response data and the response from the diffusion samplers shed light on the deviation from linear response seen in sensors exposed via the direct method. Figures 17 and 21 show that that the responses of the passive sampler and occupational dosimeter are both quite linear despite the non-linearity of the direct test response of sensors from the same batch. This observation bolsters the theory that the non-linearity of the direct test data is probably an artifact caused by saturation of the most available reaction sites on the sensor surface.

Although rate of reversibility of the MD15 sensor was much lower than for earlier sensors, the sensors were found to loose about one percent of their response per-day. Although acceptable for short term measurements, this reversibility was responsible for some bias due to loss of sample both during exposure, and after the samplers were capped. However, due to the empirical sampler calibration method, the sampler response slope, ρ, does include an average reverse reaction component. This is because the reverse reaction occurs during the test exposure period so long as comparable times are used. Thus, on average, calculated exposures of the samplers, e_{calc} was not likely to have been biased by reversibility. However, due to variability of the reverse reaction among sensors from the same batch, individual calculations of e_{calc} could be biased to some extent. For the 8-hour dosimeters, the error introduced by variability in reversibility should be negligible since the average daily regeneration is only about 1 percent. For the one-week passive samplers (PS*x*), slightly more error could be introduced due to variability due to the longer exposure period.

Clearly, due to the post-exposure reversibility, the samplers should be measured as soon as possible after exposure. If they were to be measured within one day the losses would be insignificant, but could be of concern over longer periods. In the case where the samplers are to be used for field studies, express mail service should be used if samplers must be mailed to a laboratory. Although less desirable, back-calculations of peak dA values could be performed if sampler reversibility for a batch were to be well characterized.

In the case of the occupational dosimeter a dedicated inexpensive field sampler reader is a desirable instrument. The benefits of such a device are clear. Initial absorbances of

samplers could be read on-site prior to the beginning of the work shift. At the end of the workshift the samplers could be re-read without requiring the service of an analytical laboratory. The measurement process is simple so that little training would be necessary for an in-house industrial hygienist to operate the device. A calibration factor could be supplied for each batch of samplers so that derivation of measured exposures would not be complicated. A major benefit of an on-site reader would be that the dosimeters could be read immediately after the end of a workshift.

The accuracy and precision of these prototypes was excellent, well below 20%, with the exception of high variability observed in the case of 90% RH exposures. The results indicate that the device performs within the design parameter of ±20% accuracy, with very little bias. The variability at high RH should be investigated.

Goal 5 - Diffusion Sampler D2/D3 Validation

Once the design improvements of the D2 sampler were verified a large batch of dosimeter parts (about 400 sets) were manufactured. These parts were very similar to the small batch of 20 sets used in D2, with the exception that dimensions in the sensor holder were slightly changed. Due to the fact that these samplers were mass produced and because of the small design changes this version of the occupational dosimeter (now model D3) was named the "LOCD", an acronym for **L**BNL/QGI **O**ccupational **C**O **D**osimeter.

Dosimeter performance at lowered and elevated temperatures

A series of test were conducted to investigate the effect of temperature on the LOCD response. Sets of 10 dosimeters were exposed to 25 ppm CO at temperatures of 10°C, 20° C, or 30°C, for 8-hours. The slope of the dosimeter response under these conditions is presented in Table 4-10. A discussion of an important observation regarding low temperature (10°C) effects on sensor chemistry will follow below. An analysis of variance between temperature treatment groups indicates that intra-temperature variance was not statistically significant at the 95% confidence level. In contrast, the variance between temperature treatment groups was statistically significant ($p=0.007$). Pairwise t-tests were conducted assuming that the variance in dosimeter response in each temperature treatment group was equal. A test of the hypothesis that the mean dosimeter response for the 10°C group was no different from the 20°C group was rejected ($p < 0.001$). The 10°C group was also statistically different from the 30°C group ($p = 0.027$). The hypothesis that the mean response of the 20°C group was not different from the 30°C group was accepted ($p = 0.14$). An interesting finding was that the slope of 0.0034 for the 10°C group was about 26% higher than the 20°C group. This finding indicates that a temperature correction was necessary for dosimeters exposed in colder environments. Further study of temperature effects is needed.

Analysis of sensor behavior at 10°C

An important observation not discussed above was that when the dosimeters were exposed to CO at 10°C, they did not immediately show their full response. Absorbance measurements taken immediately after the 8-hour, 25 ppm CO exposures translated into a response slope, ρ, of 0.0023 ± 0.0002 A-ppm^{-1}hr^{-1} (see Table 4-10). However after 12 hours

of post-exposure storage at approximately 20°C the absorbance of the sensors increased to indicate the response slope discussed above (ρ = 0.0034 A-ppm^{-1}hr^{-1}). Understanding this phenomenon is important because it sheds light on the behavior of the chemistry of the QGI sensors.

It was clear from the ultimate (12 hour storage) sensor response that the sensors continued to interact normally with CO throughout the 10°C exposure. This indicates that the initial $PdCl_3$ oxidation of CO must not be affected by the lower temperature. The CO oxidation is thought to be a fast reaction, so it is likely that the change in reaction rate caused by the 10 degree temperature drop did not significantly affect the sensor performance. However, the sensor condition at the initial post-exposure measurements indicate that the final concentration of the blue, mixed-oxidation state Mo, had not yet been reached. This verifies that the rate-limiting step in the sensor kinetics was the Pd-Mo forward reaction, and that the rate at which the Mo(VI) was reduced to the Mo blue species was significantly affected by temperature. Figure 4-25 presents an Arrhenius plot, i.e., log sensor response plotted against inverse temperature, (Johnston, 1966), of the immediate-post exposure data, showing that the rate-limiting sensor kinetic was affected by temperature as would be expected. Note that the *ultimate* sensor response, reflecting the dA value once the dosimeters were moved to 20°C and the Pd-Mo reactions had completed, is also plotted on Figure 4-25.

Discussion: implications of temperature effects.

An important observation that the sensor was able to "store" the CO reaction, probably as an intermediate complex, either $PdCl_3(CO)$, $PdCl_3(CO_2H)^{2-}$, or as Pd(0), until the oxidation of Pd by the Mo occurred (see Figure 4-2). Another important implication in this chain of reactions is that the reverse reaction of Mo blue to Mo(VI) during CO exposure must have been reduced in proportion to the reduction in the forward reaction. This explains the 26% higher average sensor response slope observed in the sensors which had been exposed at the low temperature.

The variability of sensor response as a function of temperature seen in Figure 4-25 is striking. The RSD of the response of the 10 dosimeters was 10%, 16%, and 20% for the 10° C, 20°C, and 30°C exposure tests, respectively. If this trend were to prove consistent in future experiments, it would indicate that intra-batch sensor variability was a function of chemistry, not variability in the optical qualities of the sensor substrate. One hypothesis is that the observed variability was due to the variability in the reverse Pd-Mo rate constant, possibly due to trace amounts of contaminants.

Another important implication of these results is that samplers that have been exposed in environments colder than 20°C should be allowed to react to completion at room temperature prior to making a final absorbance measurement. If necessary, a series of post exposure measurements should be conducted until the sensor response stabilizes.

Interferent Screening Tests

Dosimeter interferent screening test method

A protocol was developed for testing the occupational dosimeter for interferent response from individual gases and evaporated liquids. This protocol was used late in the occupational dosimeter project (D3 dosimeters, LOCD) after the dosimeters had been well characterized in the absence of potentially interfering compounds. The method was used to screen the dosimeters for a response from relatively high concentrations of potential interferents. The concentrations of interferents were quantified.

A 500 liter stainless steel and glass glove box (Protector®Multi-Hazard Glove Box, Model 50655-004384) was used as an environmental chamber. Two 100 CFM mixing fans were placed in the chamber to ensure thorough mixing. One glove port was permanently sealed and the second port was sealed except when it was used as access to the inside of the chamber. A stainless steel injection tube, connected by a 6mm (¼-inch) outside diameter (OD) polyethylene tubing, to a 0-20 slm mass flow controller was used to inject CO and interfering gases into the chamber. The injection tube outlet was directed into the inlet stream of one of the mixing fans in order that injected gases would mix rapidly. In addition, the chamber was also equipped with a number of bulkhead fittings suitable for withdrawing gas samples for analysis. The chamber was equipped with a ventilation system capable of fully purging its contents within about 3 minutes. The ventilation system supply and exhaust ports were fitted with ball valves which sealed the chamber when they were closed. The exhaust port was plumbed into the laboratory fume hood so that the contents of the chamber would not enter the laboratory air upon venting.

Three dosimeters were exposed simultaneously for each test atmosphere under investigation. The exposure duration was nominally 2 hours. Three dosimeters were dedicated for exposure to each gaseous test species, first exposed to the gas alone, and then exposed again to the same gas in combination with 100 ppm CO. Initial and final dosimeter absorbance measurements were recorded for each exposure. Three unexposed dosimeters were used as controls, also measured before and after each interferent exposure test. Their blank delta absorbance values were subtracted from the dA values measured for the exposed dosimeters.

Creation of test atmospheres in the chamber was accomplished by a number of means depending upon the nature of the chemical species under investigation. The standard target CO concentration of 100 ppm was achieved by injection of 10 liters of 5000 ppm (flow rate = 2.5 liters/minute) CO from a compressed gas cylinder into the chamber injection port. The same method was used to establish test atmospheres of the test species which were available as compressed gases. Some gas species which were available in pure (99% or higher purity) form were measured into a gastight syringe and subsequently injected into the chamber injection line. The injection line was always purged with air to force any residual test gas into the chamber.

Test species, such as organic solvents, which are normally liquid at standard temperature and pressure, were evaporated into the chamber. A simple evaporation apparatus was devised by placing a heated (about 150°C) 1 kg block of brass in the chamber. A glass petri dish was placed on top of the hot brass block. The volume of liquid material required to evaporate in

the chamber to achieve a target test atmosphere concentration for a particular test gas was calculated (Table 4-11). In order to evaporate the required amount of liquid into the chamber, the correct volume was drawn into a calibrated liquid chromatography syringe and then injected into the hot petri dish. The chamber access port was immediately closed after the liquid injection. Evaporation times were typically less than 10 minutes to completion.

Table 4-12 lists the quantitative verification methods for the test atmospheres. CO, nitric oxide (NO), temperature and relative humidity were continuously monitored (Metrasonics, Inc., Model AQ-501) and data were collected by a computerized data acquisition system every minute. CO and NO were detected using electrochemical sensors which were calibrated after every third day of exposure testing. Carbon dioxide (CO_2) data were monitored in real-time and recorded every minute using a non-dispersive infrared analyzer (Metrasonics, Inc., Model AQ-501). Nitrous oxide (N_2O) was monitored in real-time using a variable wavelength long-path infrared spectrometer set to a wavelength of 4.48 μm (Foxboro Miran).

Gas chromatography was used to quantify the concentration of the organic species in the test atmospheres. Two methods were necessary to detect the range of organic compounds under investigation. Gas chromatographs (GC, Hewlett Packard Model 5980) used in both methods were equipped with flame ionization detectors (FID). Samples were collected up to four times during a two-hour exposure period in the chamber. Both methods included calibration using standards prepared in the lab. Fresh standards were prepared for each experiment. The simpler method involved collection of a 50cc grab sample of gas from the chamber using a glass syringe. This sample was immediately injected onto the GC column (Alltech GasPro Column, length=5 meters, film thickness=0.32mm). The FID response was quantified by comparison of the appropriate peak area of the peak area measured with the prepared calibration standards. This method was found to work well with all but the strongly polar organic compounds.

The second method (NIOSH, 1994), see Table 4-12, GC= Hewlett Packard Model 5980, column = Hewlett Packard type HP-1) required sample collection using charcoal sorbent cartridges. Samples of up to 2.0 liters of test atmosphere air were collected at a rate of 50 to 200 cc/min depending upon the compound. The samples were extracted from the charcoal cartridges with 2.0 ml of carbon disulfide solvent containing an internal standard of butanol, 1% by volume. A 1.0 μl aliquot of the extracted sample was injected onto the GC column. It was found that no butanol was lost on the charcoal cartridge. Again, the FID response areas from the samples were compared to the laboratory generated standards and sample concentrations were calculated.

Commercial stain-length sampling tubes were used to quantify two of the test species, ammonia and ethylene (see Table 4-12), which could not be easily measured using any of the methods discussed above. Measurements using these tubes were made at least three times during the test atmosphere exposure period.

Results: Dosimeter performance in the presence of potential interferents

A series of tests were conducted to assess the performance of the dosimeter in the presence of potential interferents. In general, these tests were conducted using relatively high

concentrations of the potential interferent. The philosophy of the experiment was that if the dosimeter did not respond to a high concentration of a concomitant species, it would be unnecessary to test it at lower levels. The work presented here should be considered a screening experiment. Although the fifteen different molecular species tested here represent a fairly large range of the types of gas-phase pollutants commonly found in occupational and residential environments, it was by no means an exhaustive study. Table 4-13 presents the experimental conditions of the interference testing. (Three potential interferent/interferent classes clearly missing from these experiments were environmental tobacco smoke (ETS), aldehydes, and nitrogen dioxide (NO_2). These experiments have not been conducted, but should be in further investigations of the performance of the passive sampler/dosimeter.) The potentially interfering inorganic gases that were tested included carbon dioxide, and nitrogenous gases (nitrous oxide, nitric oxide, and ammonia). Organic compounds that were tested include alcohols (ethanol and isopropanol), aromatic hydrocarbons (toluene), alkanes (butane, methane, heptane), alkenes (ethylene), halogenated alkanes (trichloroethane), ketones (acetone), and esters (ethyl acetate). In addition a commercial acrylic cement containing a mixture of organic solvents (including methylene chloride and methyl ethyl ketone) was tested.

Paired t-tests were used to compare the mean electrochemical CO detector response (assuming an accuracy of ± 5%) to the mean dosimeter response (H_0: $\mu_1 = \mu_2$). Figure 4-26 and Table 4-13 indicate that with two exceptions there was no strong interfering effect from the compounds tested. The two exceptions were NO and ethylene. A concentration of 50 ppm of NO, without CO, over the 2 hour exposure period caused an average decrease in absorbance of 0.24±0.03*A*, corresponding to an apparent "negative" CO concentration (-80 ±10 ppm-h). Interestingly there was no statistically significant negative bias to the dosimeter response when CO and NO were both present in the test atmosphere ($p=0.22$). In the case of ethylene, the response to a two hour, 200 ppm exposure in the absence of CO produced an apparent dosimeter response of 200±90 ppm-h. When exposed to the combination of 200 ppm ethylene and 100 ppm CO the resulting apparent dosimeter response was 370±40 ppm-h. Ethylene appears to be a strong positive interferent for the dosimeter. No other interferent + CO combinations yielded statistically significant differences between actual CO concentrations and the apparent dosimeter measurements.

A number of the interferents appear to have caused small effects on the dosimeter in the absence of CO. Methane, heptane, and isopropanol appear to have caused a statistically significant ($p < 0.05$), slightly negative dosimeter response. CO_2, N_2O, and ethyl acetate had slightly positive, statistically significant ($p < 0.05$) dosimeter response. Possibly, the effects seen here were an artifact of the small sample size (3 dosimeters) used in these tests. Certainly, the practical significance of these small effects is likely to be negligible. Recall that the concentrations of these potential interferents were quite high relative to those found in typical occupational settings.

Ethylene in the environment

Little information on indoor and occupational concentrations of ethylene is available. The ACGIH does not recommend a threshold limit value for the substance but does consider it a simple asphyxiant. Ethylene is commonly present in air in the natural environment, typically in the parts-per-trillion to the parts-per-billion concentration range, since it is emitted from plant materials, especially ripening fruit. It was measured to be 3-4% of the total

hydrocarbon emissions from automobile engines and observed at a concentration of 1.4 ppm in a heavily used highway tunnel. Jet engines had ethylene concentrations of .27 to 731 ppm in their exhaust. NIOSH estimates that about 12,000 workers are exposed to ethylene in the U.S. at some level above background (Chem-bank, 1997). Interference from ethylene may be an issue in environments with very high levels of internal combustion engine emission. It may be speculated that fruit ripening warehouses and ship holds with large amounts of bananas or other fruit may have considerably elevated concentrations that could bias the CO dosimeter readings.

Preliminary Field Testing

Field test methods and protocol

To test the overall performance of the prototype CO passive samplers, field tests were conducted over one-day to one-week periods using the following protocol: Two to five passive samplers or occupational dosimeters and one or more field and laboratory controls were used at each site. An air sample reflecting the integrated (time-weighted-average) concentration overTo test the overall performance of the prototype CO passive samplers, field tests were conducted over one-day to one-week periods using the following protocol: Two to five passive samplers or occupational dosimeters and one or more field and laboratory cotant 0.5 cc-min-1, so in the course of a week about 5 liters of air were collected.

The air samples in the bags were analyzed directly using the Thermo Environmental Model 48 Gas Filter Correlation CO Analyzer. This analyzer operates at a flowrate of 1.0 l-min^{-1} and provides updated concentration readings every 10 seconds. When sampling from the air sample bags, the measurement reaches steady-state within two minutes. The one-week integrated air sample concentration was determined from the average of twelve 10-second-average analyzer readings over the third-through fourth minutes of measurement.

The absorbance of passive sampler sensors exposed in the field were measured using the spectrophotometer before and after deployment. The change in absorbance of the sensors was used to determine the exposure (Equation 17).

Preliminary Field test results for PS1 and PS2

Figure 4-27 summarizes the available field performance data using both PS1 and PS2. One field site was tested using two PS2 samplers and one PS2 control. The results of this test, in a day-use parking garage were excellent and consistent with the measurements conducted using the PS1. The one-week average CO concentration in the garage was 5.2 ± 0.2 ppm as measured in bag samples. The average concentration measured by the passive samplers was 4.6 ± 0.9 ppm. The RSD of the two sampler measurements, after adjusting for the control was 19.8%. The mean concentration as measured by the samplers was about 0.6 ppm lower than the bag sampler. It should be noted that the RH in the garage was about 50% indicating that humidity does not seem to have interfered with the sensor. Also, it is likely that a wide mix of organic compounds and combustion products were present in the garage since a large number of automobiles were parked in or drove through the space. These compounds do not appear to have interfered with the performance of the sampler.

Preliminary Field test results for LOCD in residential environments

Three field tests were conducted using the D3 occupational dosimeter in residential environments prior to conducting tests in true occupational environments. The dosimeters were operated as area samplers for periods of two to three days during these tests. At each site three dosimeters were exposed and one bag sample was collected. Once deployed, the dosimeters were mounted on the bag sampler case next to its inlet port. Three additional dosimeters, used as controls, were placed next to the bag sampler but were not exposed.

Figure 4-28 presents the results of the bag sampler measurements compared to those from the dosimeter. All three residences; one cabin in a rural setting, and two urban houses, had potential CO sources, however the average CO concentrations at all three sites were quite low during the measurement periods. The cabin was heated with a non-airtight woodstove while the two houses used floor furnaces. The exposure, e_{calc}, was calculated by applying equation 17, and using the empirically derived value of $\rho = 0.0027$ A-ppm^{-1}hr^{-1}. The time-weighted average CO concentrations were 0.69 ± 0.08 (RSD = 12%), 0.66 ± 0.06 (RSD = 9%), and 0.68 ± 0.22 (RSD = 33%) for the cabin, House #1, and House #2, respectively. Although humidity levels were not monitored during any of these tests they were probably quite high because they were conducted during rainy weather in the 1996-97 winter season.

These results indicated that the dosimeters could be accurate at very low CO exposures and could be operated over longer periods of time than the 8-hour period that they were designed for. No noticeable change was evident in the color of the dosimeters' blue indicator desiccant after these protracted exposures, indicating that the drying capacity of the gel had not diminished.

Sampling Rate Validation

Method for measurement of QGI sensor's mass conversion rate and calculation of volumetric sampling rate.

The empirical methods for calculating the passive sampler response characteristics discussed above were all that was needed to calibrate the device. However, that technique provides no information on the mass of CO that was involved in the reactions at the sensor surface. Actual sampling rates could not be calculated unless these molecular quantities were known. A controlled mass balance experiment was devised to measure the relationship between mass of CO molecules reacted in the forward reaction, to the observed change of sensor absorbance. Theoretically, this relationship should be constant for a batch of sensors:

$$\beta = \frac{dA}{M} \qquad (18)$$

where,

β = change in sensor absorbance per microgram of CO (A-μg^{-1}),

dA = change in absorbance of QGI sensor at 700nm (A),

and,

M = mass of CO reacted at the sensor surface (μg).

The slope, ρ, of the actual passive sampler response to CO exposure is an important parameter. Symbolically it is expressed as the ratio presented in Equation 16:

$$\rho = \frac{dA}{e}.$$

In the case of multiple CO exposures of one or more samplers, ρ (A-ppm^{-1}hr^{-1}) is the slope of a regression line fitted to the relationship between dA and exposure (ppm-h).

An empirical mass conversion rate can be calculated for the diffusion samplers once a value for β is determined:

$$q_{emp} = \frac{\rho}{\beta} = \frac{dA/e}{dA/M} = \frac{M}{e} \qquad (19)$$

where,

q_{emp} = the empirical, dosimeter mass conversion rate (µg-ppm^{-1}hr^{-1}).

When the units of exposure are expressed in terms of mass, a volumetric sampling rate can be calculated:

$$q_{empv} = \frac{M}{e} = \frac{\mu g}{(\mu g \cdot m^{-3})hr} = \frac{10^6 \cdot cm^3}{hr} \qquad (20)$$

where the units of q_{empv} are cm^3 hr^{-1}.

Note that volumetric concentrations in *ppm* can be converted to *mass* concentrations by applying the Ideal Gas Law. Given the molecular weight of CO is 28 g-mole^{-1}, and assuming a temperature of 20°C and 1 atmosphere, 1 ppm of CO = 1162 µg-m^{-3}.

Dosimeters constructed using the final mass-producible configuration (LOCD) were exposed to a measured volume of CO using the following protocol. A rubber GC septum was fitted to a port on a 1-liter glass desiccator vessel with ground glass sealing flanges. The initial absorbance of ten dosimeters was measured. They were then placed in the vessel. A precision gastight syringe was filled with 10.00 ml of 5000±50 ppm (5.8 µg) CO (Matheson Primary Standard grade gas mixture). This gas was injected into the vessel. Preliminary experiments using a similar method, which allowed for direct measurement of the dosimeter without interruption of the exposure, showed that one dosimeter fully reacts 2.00 ml of 5000 ppm CO within 4 days. Thus, once the CO was injected into the vessel, the dosimeters were exposed, uninterrupted, for 4 days. At the end of the fourth day the dosimeters were removed and their final absorbance at 700 nm was measured. The average mass of CO consumed by each dosimeter was calculated using the Ideal Gas Law (1 ml CO (pure) = 1162 µg at 20°C and 1 atmosphere). The ratio, β, was calculated for each dosimeter.

Results: Measurement of QGI sensor's mass conversion rate, calculation of dosimeter (LOCD) sampling rate, and comparison of empirical and sampling rates

The experimental method for determining dosimeter sampling rates is discussed above. A set of 10 LOCD were exposed in the desiccator. On average, each sensor reacted with 1000 ml of the gas mixture, equivalent to 5.81 μg of CO. The sensor absorbance at 700nm changed by an average of 0.35 ± 0.07 A. Thus, the empirical mass conversion rate, β, was 0.060 ± 0.011 (A-μg^{-1}) and the empirical mass conversion rate, $q_{emp.}$, from Equation 19 was 4.5 x 10^{-2} ± 0.9 x 10^{-2} μg-hr^{-1}ppm^{-1}. Using Equation 20 this translates into a volumetric sampling rate of 39.0 cm^3-hr^{-1}.

The theoretical mass conversion rate, q, for a diffusion sampler configured (L = 4.065 cm and A_x = 0.18 cm^2) as a D3 dosimeter, calculated using Equation 13, is 4.6 x 10^{-2} μg-ppm^{-1}hr^{-1} (39.6 cm^3-hr^{-1}). Clearly, $q_{emp.}$ and q were very close: the measured CO sampling rate was within 2% of the theoretical rate indicating that the overall efficiency of the dosimeters was about 98% in laboratory testing.

References

ACGIH. (1991). *Documentation of the Threshold Limit Values and Biological Exposure Indices*, American Conference of Governmental Industrial Hygienists, Cincinnati, OH.

Chem-bank (1997). "Chem-bank: databank of potentially hazardous chemicals. Entry on ethylene in the Hazardous Substances Data Bank (HSDB) from the National Library of Medicine," SilverPlater Information Services, Wellesley Hills, MA.

Dickerson, R. E., Gray, H. B., Darensbourg, M., Y., and Darensbourg, D. J. (1984). *Chemical Principles, Fourth Edition*, Benjamin/ Cummings Publishing Co., Menlo Park, CA.

Giauque, R. D., F. S. Goulding, et al. (1973). "Trace Element Determination with Semiconductor Detector X-ray Spectrometers." *Analytical Chemistry* **45**(4): 671-681.

Goldstein, M. K. (1989-1997). Personal telephone conversations between Michael G. Apte of Lawrence Berkeley Laboratory and Mark Goldstein, President of Quantum Group, Inc.

Goldstein, M. K., T. Anderson, et al. (1991a). *Chemical CO Detector for an Automatic Gas Safety Shutoff Valve.* Chicago, IL, Gas Research Institute.

Goldstein, M. K. (1991b). *Biomimetic Sensor that Simulates Human Response to Airborne Toxins.* U.S. Patent Office. USA, Quantum Group, Inc., San Diego, CA: Pat. No. 5,063,164.

Johnston, H. S. (1966). Gas Phase Reaction Theory. New York, NY, Roland Press.

Kennedy, E. R., Fischback, T. J., Song, R., Eller, P. M., and Shulman, S. A. (1995). *Guidelines for Air Sampling and Analytical Method Development and Evaluation*, A NIOSH technical report, U.S. Department of Health and Human Services, Centers for Disease Control and Prevention, National Institute for Occupational Safety and Health., Cincinnati, OH.

NIOSH. (1972). *Criteria for a recommended standard: Occupational Exposure to Carbon Monoxide.* NIOSH Publication Number 73-11000, NTIS Publication Number PB-212-629, U.S. Department of Health, Education, National Institute for Occupational Safety and Health, National Technical Information Service, Springfield, VA.

NIOSH (1994). NIOSH Manual of Analytical Methods. Cincinnati, OH, U.S. Department of Health and Human Services, Centers for Disease Control and Prevention, National Institute for Occupational Safety and Health.

OSHA. (1993). "29 CFR Part 1910.1000 Air Contaminants, Table Z-1"; Amended by *Federal Register* 58:35308, 35340 (June 30, 1993); corrected by *Federal Register* 58:40191 (July 27, 1993), U.S. Department of Labor, Occupational Safety and Health Administration.

Palmes, E. D., A. F. Gunnison, et al. (1976). "Personal Sampler for NO_2." *American Industrial Hygiene Association Journal* **37**: 570-577.

Peters, D., J. Hayes, et al. (1974). *Chemical Separations and Measurements, Theory and Practice of Analytical Chemistry.* Philadelphia, PA, W.B. Saunders Co.

Rose, V. E. and J. L. Perkins (1982). "Passive dosimetry - state of the art review." *American Industrial Hygiene Association Journal* **43**(8): 605-621.

Tables

Table 4-1. Instrumentation used for laboratory testing of the QGI CO sensors and the LBNL/QGI Passive Sampler and Occupational Dosimeter prototypes.

Function	Device	Specifications	Manufacturer/Model
Pure air generation	Catalytic pure air generator	Output: 0-20 lpm Hydrocarbons < 5 ppb, CO < 5 ppb, Dewpoint <-60°C	AADCO model 737
Gas flow control	Mass flow controller	Range:0-200 sccm, 0-2 slm, 0-20 slm Accuracy: ±1%	Brooks /5800 series Matheson / FC200
Gas mixing	Glass gas mixing manifolds	2 to 1 and 6 to 1 multi-ported glass manifolds	LBNL Glass Shop
Thermal exposure control	Temperature controller water bath	Temperature range: 0-100 °C	Forma-Scientific Model 2067
Humidity generation	Fritted glass bubblers in gas wash bottle.	Two glass gas wash bottles with fritted bubblers. Splitter valve used to adjust amount of water vapor flowing into exposure stream.	LBNL
Exposure chamber	Glass reaction vessel	3 liter glass reaction vessel with clamped ground glass cover flange. Stainless steel cover plate with 10 threaded ports	ACE Glass Co. LBNL
Data acquisition	16 channel data acquisition system	12 bit, 16 channels, RS-232 interface to PC. LBNL SAM software.	LBNL/Fawlkes Engineering
Temperature	Sealed, waterproof AD590 temperature probes	Range: 0-100°C Accuracy: ±0.2°C	Analog Devices/AD590 LBNL packaging and calibration.
Humidity	Chilled Mirror Dewpoint Hygrometer	Range: 0-50°C Accuracy ±1°C	General Eastern/DEW10
Pressure	Magnehelic pressure gauge	Range: 0-2000 Pa Accuracy: ±50 Pa	Dwyer/2008c
CO concentration	Gas filter correlation infrared analyzer	Range: 0-1000 ppm CO Accuracy: ±1%	Thermo Environmental/48
Spectral absorbance	UV-Near infrared spectrophotometer	Spectral range 180-1100 nm Absorbance range 0.001 - 6.000 *A* Accuracy: ± 0.005 *A*	Perkin Elmer/Lambda 2

Table 4-2. Sensor and test summary for early formulations of CO sensors.

Sensor type LBNL(QGI)	Purpose of sensor	Formulation	Characteristics	Date Rec'd	Exposure conditions	Storage conditions
D(MD-1)	General evaluation of sensor	Standard MD-1	Large sensor-to sensor variation, strong humidity effects, high reversibility	12/90	Diffusion Tube- Dry Air with 35 ppm CO. Direct- 40 ppm CO, Dry nitrogen.	Si gel (dry) and paper (wet).
E (MD-1 LBL)	Attempt to lower reversibility	Low temperature (70°C) curing.	Similar to D Sensors	4/91	Diffusion Tube. Dry Air with 35 ppm CO	Si gel (dry)
F (MD-1 Na LBL)	Attempt to lower reversibility	NaPdCl2 replaced KPdCL2 salt in MD-1	Similar to D sensors, but more reversible	4/91	Diffusion Tube. Dry Air with 35 ppm CO	Si gel (dry)
G (28Y #1)	Attempt to lower reversibility and humidity effects	Contains Ru as well as Mo.	Similar to D sensors, but more reversible	5/91	Diffusion Tube. Dry Air with 35 ppm CO	Si gel (dry)
H (28Y #2)	Attempt to lower reversibility and humidity effects	Contains Ru as well as Mo.	Similar to D sensors, but much more reversible	5/91	Diffusion Tube. Dry Air with 35 ppm CO	Si gel (dry)
I (MD-3)	Attempt to make more stable and less reversible and humidity-sensitive	Different metal salts. Removed copper.	Less humidity-sensitive than D sensors. Non-reversible in absence of 0_2	6/91	Diffusion Tube. Dry Air and dry N_2 with 35 ppm CO	Si gel (dry) and paper (wet). Also in dry N_2
J (RU-1)	Test of ruthenium sensor	Ruthenium based sensor	Similar to D sensors	8/91	Diffusion Tube. Dry Air and dry N_2 with 35 ppm CO	Si gel (dry) and paper (wet). Also in dry N_2
K (MD-6)	Test use of high purity materials.	High purity Pd. Higher pH version of MD-3	Very reversible due to higher pH.	7/91	Diffusion Tube. Dry N_2 with 35 ppm CO	Si gel in air(dry) and dry N_2
L (MD-3)	Test for control of reversibility by adjusting pH lower	MD-3 with pH 1.344 (control)	Same as I sensors	1/92	Diffusion Tube. Dry Air with 35 ppm CO	Si gel (dry)
M (MD-3)	Test for control of reversibility by adjusting pH lower	MD-3 with pH 1.004	Less reversible than I sensors	1/92	Diffusion Tube. Dry Air with 35 ppm CO	Si gel (dry)
N (MD-3)	Test for control of reversibility by adjusting pH lower	MD-3 with pH 0.803	Virtually non-reversible, lower sensitivity, large variation.	1/92	Diffusion Tube. Dry Air with 35 ppm CO	Si gel (dry)
O (MD-3)	Test for control of reversibility by adjusting pH lower	MD-3 with pH 0.515	Non reversible, very low response.	1/92	Diffusion Tube. Dry Air with 35 ppm CO	Si gel (dry)

Table 4-2. Sensor and test summary for early formulations of CO sensors (continued)

Sensor type LBNL(QGI)	Purpose of sensor	Formulation	Characteristics	Date Rec'd	Exposure conditions	Storage conditions
P (MD-3)	Test for control of reversibility by adjusting pH lower	MD-3 with pH 0.187	Non reversible, very low response.	1/92	Diffusion Tube. Dry Air with 35 ppm CO	Si gel (dry)
Q (MD-3)	Test for control of reversibility by adjusting pH lower	MD-3 with pH 0.078	No response to CO	1/92	Diffusion Tube. Dry Air with 35 ppm CO	Si gel (dry)
R (MD-3)	Test Gelsil Si matrix	Gelsil Si matrix. Standard MD-3 formulation	Gelsil structurally weak—one sensor broke. Responded to CO but had low capacity because of small size	1/92	Diffusion Tube. Dry Air with 35 ppm CO	Si gel (dry)
S (MD-3)	Test for control of reversibility by adjusting pH lower	MD-3 with pH 1.382. Control MD-3	Same as I sensors	2/92	Diffusion Tube- Dry Air with 35 ppm CO. Direct- 40 ppm CO, dry nitrogen,	Si gel (dry)
T (MD-3)	Test for control of reversibility by adjusting pH lower	MD-3 with pH 0.998		2/92		
U (MD-3)	Test for control of reversibility by adjusting pH lower	MD-3 with pH 0.944	Irreversible, lower sensitivity, variable response	2/92	Diffusion Tube. Dry Air with 35 ppm CO	Si gel (dry)
V (MD-3)	Test for control of reversibility by adjusting pH lower	MD-3 with pH 0.910	Irreversible, lower sensitivity	2/92	Diffusion Tube- Dry Air with 35 ppm CO. Direct- 40 ppm CO, dry pure air.	Si gel (dry)
W (MD-3)	Test for control of reversibility by adjusting pH lower	MD-3 with pH 0.850	Irreversible, lower sensitivity, variable response	2/92	Diffusion Tube. Dry Air with 35 ppm CO	Si gel (dry)
X (MD-3)	Test for control of reversibility by adjusting pH lower	MD-3 with pH 0.799		2/92		
Y (MD-3)	Test for control of reversibility by adjusting pH lower	MD-3 with pH 1.004	Slightly reversible, reasonable response, showed positive response to exposure to moisture	2/92	Diffusion Tube- Dry Air with 35 ppm CO. Direct- 40 ppm CO, dry pure air.	Si gel (dry) and paper (wet)
Z (MD-3)	Test for control of reversibility by adjusting pH lower	MD-3 with pH 0.803	Irreversible, lower sensitivity, variable response. Reversible when wet.	2/92	Diffusion Tube- Dry Air with 35 ppm CO. Direct- 40 ppm CO, dry pure air.	Si gel (dry) and paper (wet)

Table 4-3. Early sensor performance investigations. Third-order oxidation kinetics for sensors stored in dry, humid, or oxygen-free conditions. The average reverse rate constant k_{r3}, standard deviation (Std. Dev.) and relative standard deviation (RSD) are shown.

Sensor Designation	Number of Sensors tested	Storage[a] Conditions	Average k_{r3} ($A^{-2}h^{-1}$)	Std. Dev. ($A^{-2}h^{-1}$)	RSD (%)	QGI Designation
D	8	Si-Gel	9.2E-04	2.8E-04	31	MD-1 1989
E	6	Si-Gel	1.2E-03	2.1E-04	18	MD-1; 70C; 28 #1
F	6	Si-Gel	2.2E-03	5.1E-04	23	MD-1 Na; 70C; 28 #2
G	8	Si-Gel	1.8E-03	1.9E-04	11	28Y #1; 180C
H	7	Si-Gel	3.3E-03	6.9E-04	21	MD-1 1989
I (test 1)	4	Si-Gel	1.9E-03	2.2E-04	12	MD-3; 180C; 33W
I (test 1)	4	Paper	2.1E-02	1.2E-02	39	MD-3; 180C; 33W
I (test 2)	4	Si-Gel	2.8E-03	5.7E-04	21	MD-3; 180C; 33W
I (test 2)	4	Nitrogen	2.4E-04	1.0E-04	39	MD-3; 180C; 33W
J (test 1)	4	Si-Gel	1.2E-03	1.9E-04	16	RU-1; 530C
J (test 1)	4	Paper	2.9E-03	1.0E-04	36	RU-1; 530C
J (test 2)	4	Si-Gel	1.1E-03	2.7E-04	24	RU-1; 530C
J (test 2)	4	Nitrogen	3.0E-04	1.0E-04	41	RU-1; 530C
K	4	Si-Gel	5.1E-03	7.8E-04	16	MD-6; 70C
K	4	Nitrogen	4.8E-04	9.6E-05	20	MD-6; 70C

[a]Storage conditions between measurements during post CO exposure regeneration period: "Si-Gel" indicates that the sensors were stored on dry silica gel in glass vials; "Paper" indicates that the sensors were stored in glass vials a humid environment on filter paper strips that had been pre-conditioned at approximately 50% relative humidity; "Nitrogen" indicates that the sensors were stored in glass vials that had been purged with oxygen-free, dry nitrogen.

Table 4-4. Early CO sensor development summary, MD15 sensors. These sensors were manufactured with a new chelating process which reduced post CO exposure sensor regeneration.

Sensor type LBNL(QGI)	Purpose of sensor	Formulation	Characteristics	Date Rec'd	Exposure conditions	Storage conditions
AB (MD1*)	Test ultrapure materials for lower reversibility	Ultrapure materials	Reversibility not reduced over MD1	11-5-92	Direct test. 40 ppm CO.	Si gel (dry)
AC (MD1*)	Test Zero-gel	As AB but in small Xerogel pellets	Low response	11-5-92	Direct test. 40 ppm CO.	Si gel (dry)
AD (MD15)	Low reversibility	Ultrapure materials and chelating process to bind Cu	Low reversibility when humidity controlled low	12-7-92	Direct test. 40 ppm CO.	Si gel (dry) and paper (wet)
AE (MD15*)	Modified MD15 test for low reversibility	Slightly different formulation than MD15	More sensitive than MD15	3-1-93	Direct dry and at 23% and 45% relative humidity and 40 ppm CO	Si gel (dry)
AF (MD15)	Same as AD	Same as AD	See AD	3-1-93	40 ppm CO Direct test and 18 ppm and 0.8 ppm CO prototype passive sampler tests	Si gel (dry)
AG (MD15)	Same as AD	Same as AD	See AD	4-27-93	40 ppm CO Direct test .	Si gel (dry)

Table 4-5. QGI CO sensors used for dosimeter development. and validation. All of these sensor batches were manufactured with the MD15 formulation. Sensors AL-AM, and sensors AN-AW were made on 1.3 mm thick or 2.6mm thick VYCOR™ disk substrates, respectively

LBNL designation	QGI designation	Date of Manufacture	Size of Batch (Count)	Research Application
AL	MD15	3/7/95	200	Test k, k_{r3}
AM	MD15-9a	3/7/95	20	Test k, k_{r3}
AN	MD15-9a	3/7/95	20	Test thick sensor substrate
AP	MD15-9a	3/7/95	100	Test k, k_{r3}, Dosimeter Development
AQ	MD15-10A*	3/7/95	20	Test k, k_{r3}, and batch differences
AR	MD15-10D*	3/7/95	20	"
AS	MD15-15B	3/7/95	20	"
AT	MD15-16D2	3/7/95	20	"
AU	MD15-17A2	3/7/95	20	"
AV	MD15-16A2	3/7/95	20	Test with calcium added to MD15 formula
AW	MD15/WH-25abc	8/25/95	400	Dosimeter validation

Table 4-6. MD15 sensor response characteristics. Inter- and intra-batch differences. Sensor response slope (A-hr^{-1}) and correlation coefficient from least-squares linear regression. Forward sensor kinetics were measured using the Direct Method with [CO] = 40 ppm and absorbance measured at 700nm. Std is standard deviation of three individual values. Note that batch AV was formulated with calcium added as a stabilizer.

	Response of Sensors Within a Batch k_{r3} (R^2)			
Batch	1	2	3	Average±Std
AN	0.348 (0.999)	0.333 (0.934)	0.376 (0.995)	0.352±0.022 (0.976)
AP	0.308 (0.998)	0.282 (0.998)	0.313 (0.997)	0.301±0.017 (0.998)
AQ	0.273 (0.998)	0.272 (0.999)	0.283 (0.999)	0.276±0.006 (0.999)
AR	0.296 (0.997)	0.308 (0.996)	0.302 (0.997)	0.302±0.006 (0.997)
AS	0.364 (1.000)	0.359 (0.997)	0.323 (0.996)	0.349±0.022 (0.998)
AT	0.381 (0.995)	0.384 (0.992)	0.389 (0.996)	0.385±0.004 (0.995)
AU	0.366 (0.998)	0.386 (0.997)	0.368 (0.998)	0.373±0.011 (0.998)
AV	0.185 (0.990)	0.117 (1.000)	0.104 (0.999)	0.135±0.044 (0.996)

Table 4-7. Sensor regeneration after exposure to 40 ppm CO in direct exposure tests. Regeneration is given as percent drop from peak delta absorbance. Sensor response measured at 700nm. The empirically-derived third-order kinetics reverse rate constant, k_{r3}, calculated for each sensor is shown.

Sensor	Exposure to 40 ppm (Hours)	Peak Abs. (A)	One-week Regeneration (%)	k_{r3} x10^{-3} ($A^{-2}hr^{-1}$)	Duration of desiccation[a] (Days)
AP-01	4	1.4	43	3.3	98
AP-02	6	1.7	34	1.9	99
AP-03	17	3.6	50	1.4	99
AQ-01	6	1.4	31	4.5	100
AQ-02	6	1.5	29	3.1	100
AQ-03	11	2.7	38	1.3	100
AR-01	6	1.6	31	3.8	101
AR-02	16	3.4	37	0.8	101
AR-03	4	3.4	37	0.8	102
AS-01	5	1.6	31	3.7	105
AS-02	16	3.5	56	0.7	105
AS-03	5	1.4	44	2.9	106
AT-01	17	3.7	52	0.5	106
AT-02	5	1.7	48	2.3	107
AT-03	18	3.7	50	0.6	107
AU-01	5	1.6	41	1.5	108
AU-02	18	3.8	43	0.4	108
AU-03	4	1.6	37	1.4	109
AW51	7	3.0	18	0.2	292
AW52	3	1.9	16	0.3	292
AW53	5	3.0	21	0.2	295
AW54	4	2.5	28	0.4	295

[a]Duration of sensor desiccation period prior to CO exposure and subsequent regeneration measurements.

Table 4-8. Materials compatibility tests for LBNL/QGI carbon monoxide passive samplers.

Material/Test Condition		Function in sampler	Results	Difference relative to control	Comments
Styrene		Sampler body. styrene disposable cuvette	Non-interfering	-10±40%	Melted styrene caused interference
Porex™	Aged: New: Baked 24h: Baked 48h:	Diffusive sensor holder	Interfering Interfering Interfering Non-interfering	-40±40% 40% 40±10% 2±2%	Cleaned in ethanol and baked at 40°C for 24 - 48 hours
Neoprene		Seal	Interfering	60±20%	
Sealing wax		Sealant	Interfering	120±20%	Interfering with and without addition of cuvette
Hot melt glue	Low Temp: High Temp:	Sealant	Interfering Interfering	500±60% 600±40%	Both low/ high temperature settings
Melted paraffin wax		Sealant	Interfering	-20±30%	Appeared to interact with epoxy
Water-based putty		Sealant	Interfering	-80±40%	Possible negative interference with water released during curing
Epoxy Sealant	Epoxy only: Wax layer:	Sealant	Non-interfering Interfering	3±9% 30±30%	Low viscosity potting system. Less interference without paraffin wax layer.
Silica gel		Desiccant	Non-interfering	NA	Baked out at 110°C for 24 hours.
Teflon		Diffusion tube and support	Non-interfering	NA	Cleaned in ethanol and baked out at 40° C for 24 hours
Nylon		Inlet fittings and plugs	Non-interfering	NA	Cleaned and baked out at 40° C for 24 hours

*Mean percent difference (± relative standard deviation) in delta absorbance between sensors exposed to materials and sensors stored in identical conditions without materials (controls). A difference of 10% in absorbance from the control value indicates an incompatible material.

Table 4-9. LBNL/QGI occupational dosimeter (D2) humidity effects tests. These exposure tests were conducted in a 3-liter reaction vessel at 40ppm CO and 20°C. Three series of four 4-hour exposure runs were conducted. Each test was conducted at a low and a high relative humidity (RH) level. The sequence of low and high RH exposures were alternated. Three dosimeters were concurrently exposed in each test. Average dosimeter response (± standard deviation), less average of 3 unexposed controls, at 700nm are presented. Incremental response is between successive runs in each test. Precision, bias, and accuracy using the NIOSH definition (Kennedy, 1995) for each of the elapsed CO exposures are also included.

Test #	Run #	Average Relative Humidity (%)	Incremental CO exposure (ppm-hours)	Average Dosimeter Response[a] (*A*)	Elapsed CO exposure (ppm-hours)	Average Dosimeter Response (*A*)	Precision	Bias	Accuracy (%)
1	1	20	160	0.43 (±0.00)	160	0.43 (±0.00)	0.01	-0.06	7
	2	20	160	0.45 (±0.02)	320	0.88 (±0.02)	0.02	-0.05	8
	3	50	180	0.59 (±0.01)	490	1.47 (±0.03)	0.02	0.03	6
	4	50	210	0.70 (±0.04)	700	2.17 (±0.03)	0.01	0.07	9
2	1	50	160	0.52 (±0.01)	160	0.52 (±0.01)	0.02	0.10	14
	2	50	190	0.56 (±0.06)	350	1.09 (±0.06)	0.05	0.07	16
	3	20	160	0.31 (±0.02)	510	1.39 (±0.08)	0.05	-0.05	13
	4	30	160	0.34 (±0.00)	670	1.73 (±0.07)	0.04	-0.10	16
3	1	30	160	0.46 (±0.01)	160	0.46 (±0.01)	0.02	-0.01	5
	2	30	180	0.52 (±0.03)	340	0.98 (±0.03)	0.03	-0.01	8
	3	90	170	0.55 (±0.13)	510	1.53 (±0.14)	0.09	0.04	20
	4	90	160	0.42 (±0.14)	670	1.94 (±0.27)	0.13	0.00	27

[a]Response to individual consecutive incremental (4-hour) exposures during exposure tests.

Table 4-10. Effect of temperature during 25 ppm CO exposure on sensor response of LBNL/QGI Occupational Dosimeters. Ten dosimeters were exposed for each test.

Exposure Temperature	Average Slope (*A*/ppm-h)	Relative Standard Deviation
10°C	0.0023[a]	10%
10°C	0.0034[b,c]	11%
20°C	0.0027[a]	16%
30°C	0.0029[a]	20%

[a]Slope calculated using sensor absorbance measured immediately after exposure test at 10°C.

[b]Slope calculated using sensor absorbance measured 12 hours after exposure test at 10°C.

[c]Statistically different from 20°C ($p<0.001$) and 30°C ($p = 0.027$) slopes at the 95% confidence level.

Table 4-11. Preparation of target gas species from liquids at 20°C: Calculation of liquid volumes for evaporation in the 500 L chamber.

Species	MW (amu)	Density (g/ml)	Target concentration (ppm_v)	Mass conc. ($\mu g\text{-}m^{-3}$)	Required liquid volume (ml)
Ethyl acetate	88.1	0.901	200	709	0.39
Isopropanol	60.1	0.785	200	492	0.31
Acetone	58.1	0.792	200	475	0.30
Ethanol	46.1	0.789	200	377	0.24
Toluene	92.1	0.867	200	754	0.43
Trichloroethane	133.4	1.343	200	1091	0.41

Table 4-12. Target gas concentrations to be used in test atmospheres for CO interference tests.

Gas Species	Target Conc.	Verification Technique (Reference Method)	Sample Duration (min)
Carbon monoxide	100 ppm_v	Electrochemical Sensor	Continuous
Methane	500 ppm_v	Charcoal tube/GC (NIOSH 1500) [a]	30
Butane	300 ppm_v	Charcoal tube/GC (NIOSH 1500) [a]	60
Heptane	500 ppm_v	Charcoal tube/GC (NIOSH 1500) [a]	30
Ethyl acetate	200 ppm_v	Charcoal tube/GC (NIOSH 1457) [a]	60
Isopropanol	200 ppm_v	Charcoal tube/GC (NIOSH 1400) [a]	60
Carbon dioxide	1000 ppm_v	Non Dispersive Infrared (NA)	Continuous
Ammonia	100 ppm_v	Stain Length Tube (Dräger 5/a)	5 pump strokes
Acetone	200 ppm_v	Charcoal tube/GC (NIOSH 1300) [a]	60
Ethylene	200 ppm_v	Stain Length Tube (Dräger 50/a)	60
Ethanol	200 ppm_v	Charcoal tube/GC (NIOSH 1400) [a]	30
Toluene	200 ppm_v	Charcoal tube/GC (NIOSH 1500) [a]	30
Trichloroethane	200 ppm_v	Charcoal tube/GC(NIOSH 1003) [a]	30
Nitric oxide	50 ppm_v	Electrochemical Sensor	Continuous
Nitrous oxide	200 ppm_v	Infrared Spectroscopy @ 4.48mm (NIOSH 6600) [a]	Continuous

[a](NIOSH, 1994)

Table 4-13. Prototype D3 LBNL/QGI Occupational Carbon Monoxide Dosimeter (LOCD) response in the presence of potentially interfering gases. Exposures were conducted in a 500 liter stainless steel and glass glove box.

Interferent or interferent +CO	Interferent Concentration (ppm)	Actual CO Exposure (ppm-hours)	Apparent CO Exposure, LOCD (ppm-hours)	Average Relative Humidity (%RH)	Average Temperature (°C)
CO alone	0	110	83±30	30	25
CO alone	0	280	280±60	10	26
carbon dioxide†	1100	0	10±0	30	27
carbon dioxide + CO	1000	200	200±20	30	26
nitrous oxide†	230	0	10±0	20	27
nitrous oxide + CO	200	220	260±30	20	26
nitric oxide††	50	0	-80±10	20	26
nitric oxide + CO	50	220	200±20	20	25
ammonia	80	0	0±10	30	26
ammonia + CO	100	220	220±20	20	26
ethanol	150	0	10±0	10	26
ethanol + CO	150	250	190±70	10	25
isopropanol†	160	0	-10±0	20	27
isopropanol + CO	160	220	260±110	20	26
ethylene††	200	0	200±90	NA	NA
ethylene + CO††	200	210	370±40	30	26
toluene	170	0	10±10	20	26
toluene + CO	170	190	200±20	20	26
butane	270	0	10±0	30	25
butane + CO	300	200	200±10	20	27
methane†	480	0	-10±10	30	26
methane + CO	530	220	230±40	30	27
heptane†	470	0	-10±0	30	25
heptane + CO	470	210	230±30	30	27
trichlorethane	270	0	0±0	30	28
trichloroethane + CO	280	230	230±60	20	26
acetone	200	0	0±0	30	26
acetone + CO	180	210	220±40	20	26
ethyl acetate†	190	0	10±0	30	26
ethyl acetate + CO	190	210	220±10	20	26
acrylic cement[a]	b	0	10±0	30	24
acrylic cement + CO	b	220	230±10	30	25

[a] Commercial product containing a mixture of organic solvents including methylene chloride and methyl ethyl ketone.

[B] Estimate: 2300 ppm DCM and 2000 ppm MEK generated by spreading 20 grams of acrylic cement on a metal foil surface in exposure chamber.

† $p < 0.05$, results of paired t-tests with H_0: $\mu_1 = \mu_2$.

†† $p < 0.005$ results of paired t-tests with H_0: $\mu_1 = \mu_2$.

Figures

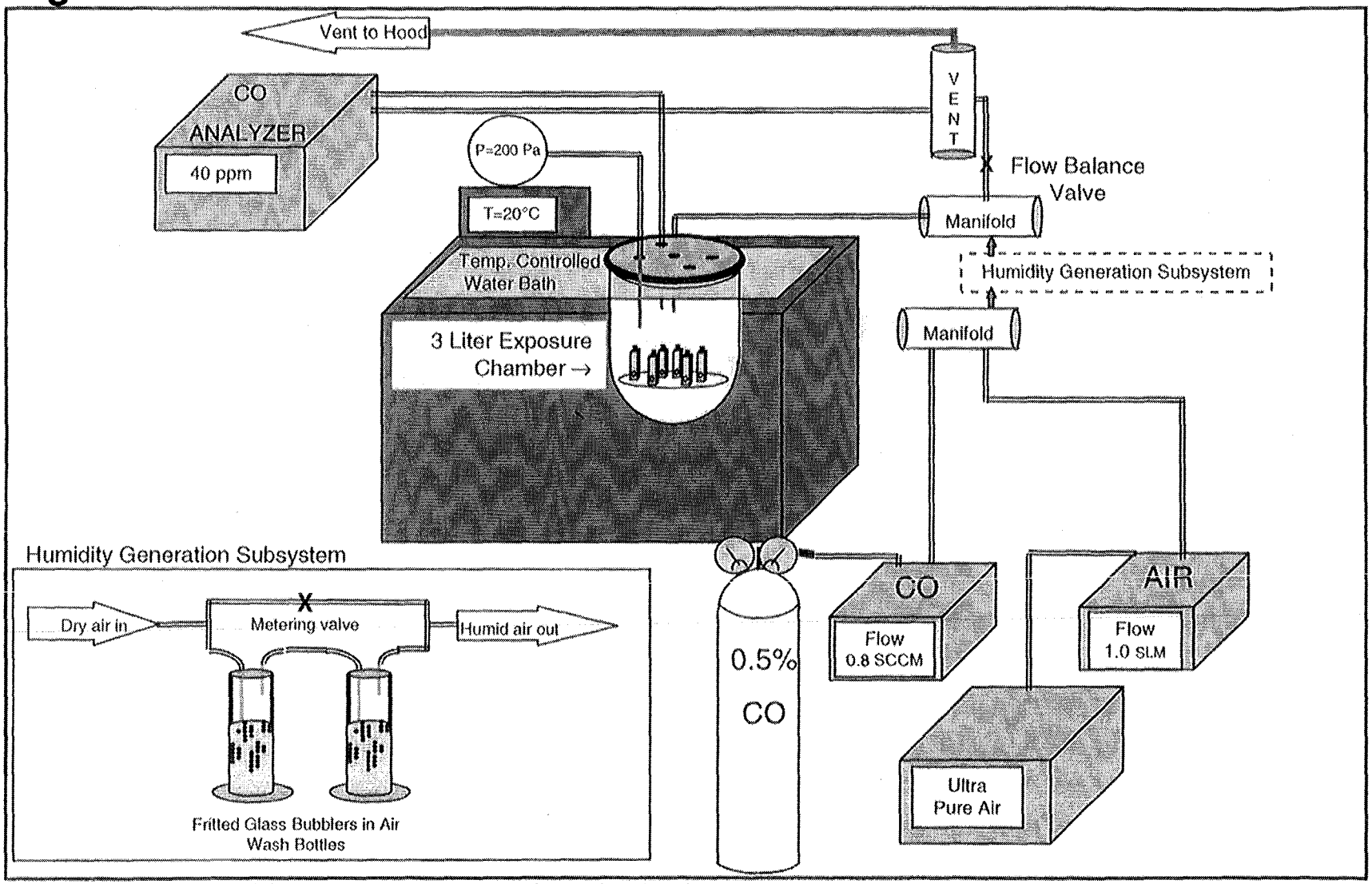

Figure 4-1. Diagram of laboratory exposure system for testing CO diffusion samplers.

Step 1: The homogeneous water-gas shift reaction via the intermediacy of palladium.

(forward) $PdCl_4^{2-} + CO \underset{k_{-1}}{\overset{k_1}{<=====>}} PdCl_3(CO)^- + Cl^-$ 1a

$PdCl_3(CO)^- + H_2O \xrightarrow{k_2} PdCl_3(CO_2H)^{2-} + H^+$ 1b

$PdCl_3(CO_2H)^{2-} \xrightarrow{fast} Pd(0) + 3Cl^- + H^+ + CO_2$ 1c

Step 2: The reduction by Pd(0) of Mo(VI) to mixed valent molybdenum species with an intense blue color, molybdenum blue. **Note**: possible competitive reaction when copper is present.

(forward) **(Measured Analyte)**

$Pd(0) + 2/xMoO_3 + 2H^+ \underset{k_{-4}}{\overset{k_4}{<=====>}} Pd(II) + 2/x[H_xMoO_3]_{Blue}$ 2a ($0 < x \leq 1.05$)

$Pd(0) + 2Cu(II) \longrightarrow Pd(II) + 2Cu(I)$ (competitive reaction)

Step 3: Oxidation of the molybdenum blue species by Cu(II) or O_2.

(reverse) $1/x[H_xMoO_3]_{Blue} + Cu(II) \xrightarrow{H^+} 1/xMoO_3 + H^+ + Cu(I)$ 3a (catalytic)

$1/x[H_xMoO_3]_{Blue} + \frac{1}{2}O_2 + H^+ \xrightarrow{k_5} 1/xMoO_3 + H_2O$ 3b (direct)

Step 4: Air oxidation of Cu(I) to give Cu(II) and water.

(reverse) $CuCl_2^- + O_2 \longrightarrow CuCl_2(O_2)^-$ 4a

$CuCl_2(O_2)^- + 4H^+ \longrightarrow Cu(II) + 2H_2O + 2Cl^-$ 4b

Figure 4-2. Key elements of the QGI carbon monoxide sensor chemistry. The proprietary QGI CO sensor technology is based upon the following set of four discrete chemical steps. Although QGI's "MD" sensor series used in the LBNL/QGI CO dosimeter follows the chemistry presented here, the actual formulation is more complicated, involving molecular encapsulants and a Cu chelating process that deactivates the reverse reactions (steps 3 and 4). Further details of the chemistry are available in the literature (Goldstein, 1991a, 1991b). Modified from Goldstein *et al.*, 1991a.

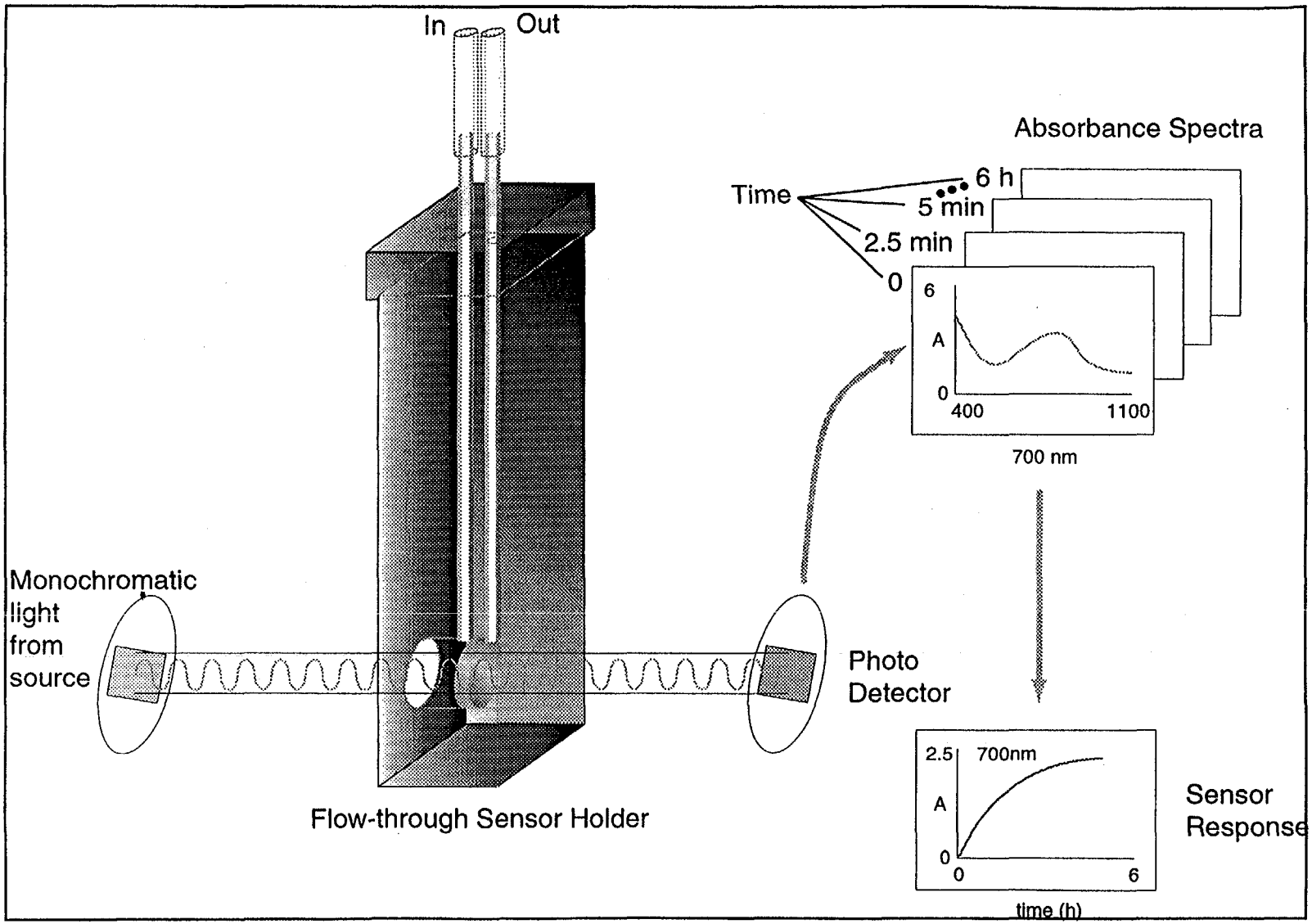

Figure 4-3. Diagram of a flow-through sensor holder for use in the Direct Method tests. These tests monitor QGI sensor response to CO in real-time, and are useful in determining CO sensor characteristics. The sensor holder is placed in a spectrometer light beam.

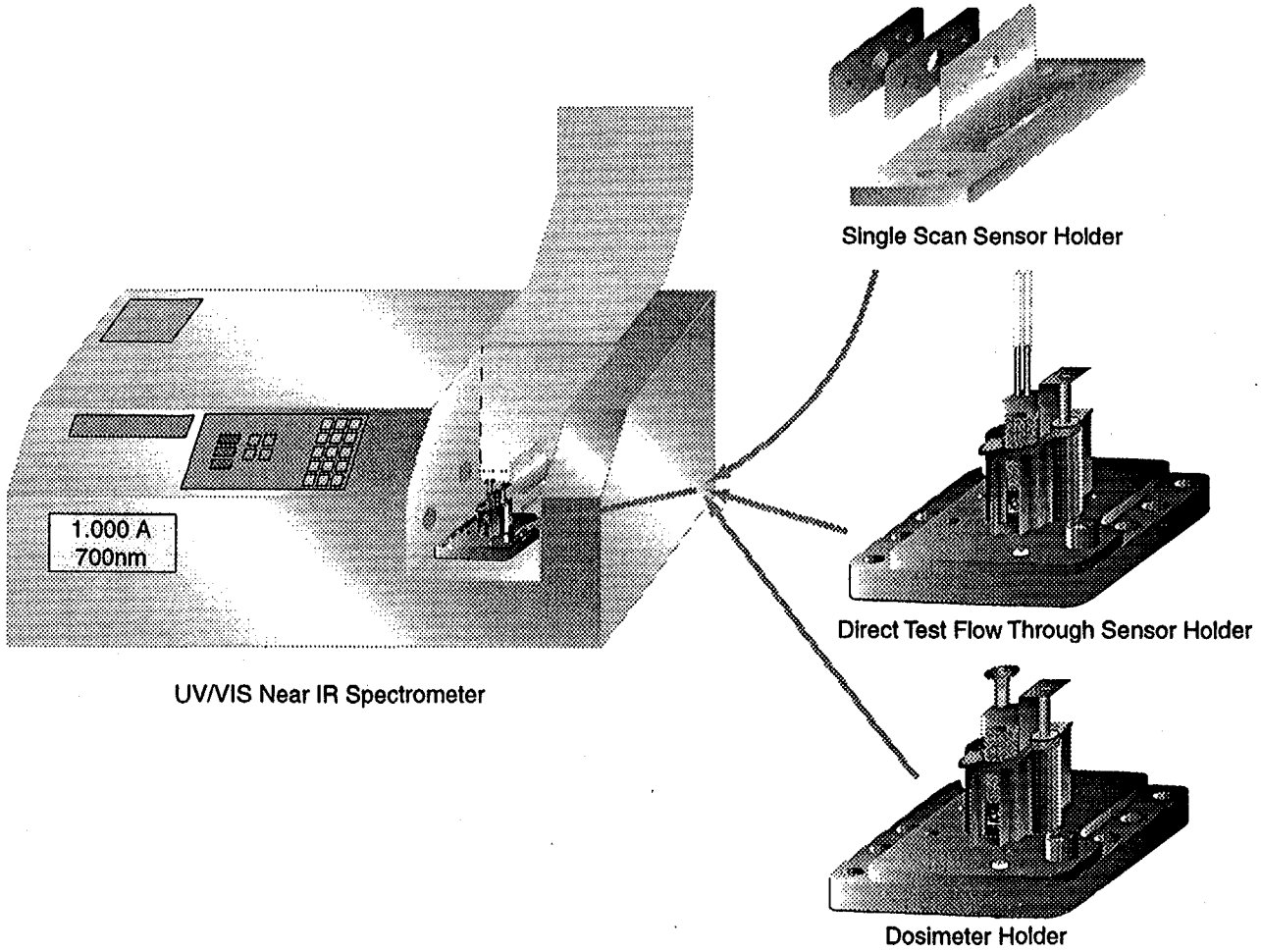

Figure 4-4. Diagram depicting three different systems for measuring the absorbance spectra of the QGI CO sensor. All three holders were designed to be fit into the light path of the spectrophotometer with the sensor positioned in the light beam. The Single Scan Sensor Holder was used to measure sensor absorbance where single measurements were needed. The Direct Test Flow Through Sensor Holder was used for real-time monitoring of sensor response in the flow-through exposure system. The Dosimeter Holder was used for measuring the absorbance of sensors in situ in the LBNL/QGI Passive Samplers and Occupational Dosimeters.

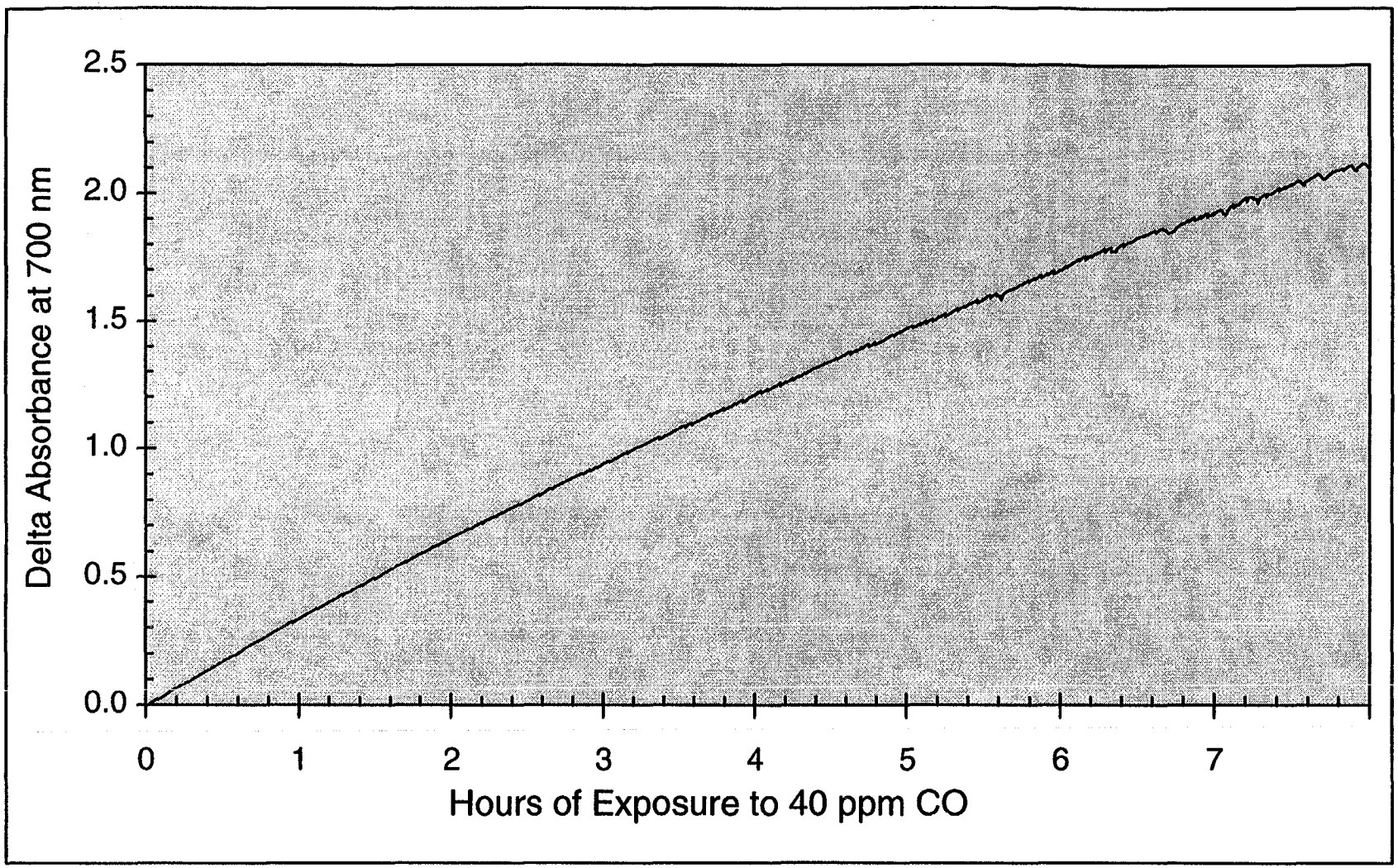

Figure 4-5. A typical "direct method" experiment response profile showing the change in absorbance of a sensor vs. duration to 40 ppm CO, measured at 700 nm. Note that CO *exposure* of the sensor can be calculated by multiplying the time on the x-axis by 40 ppm.

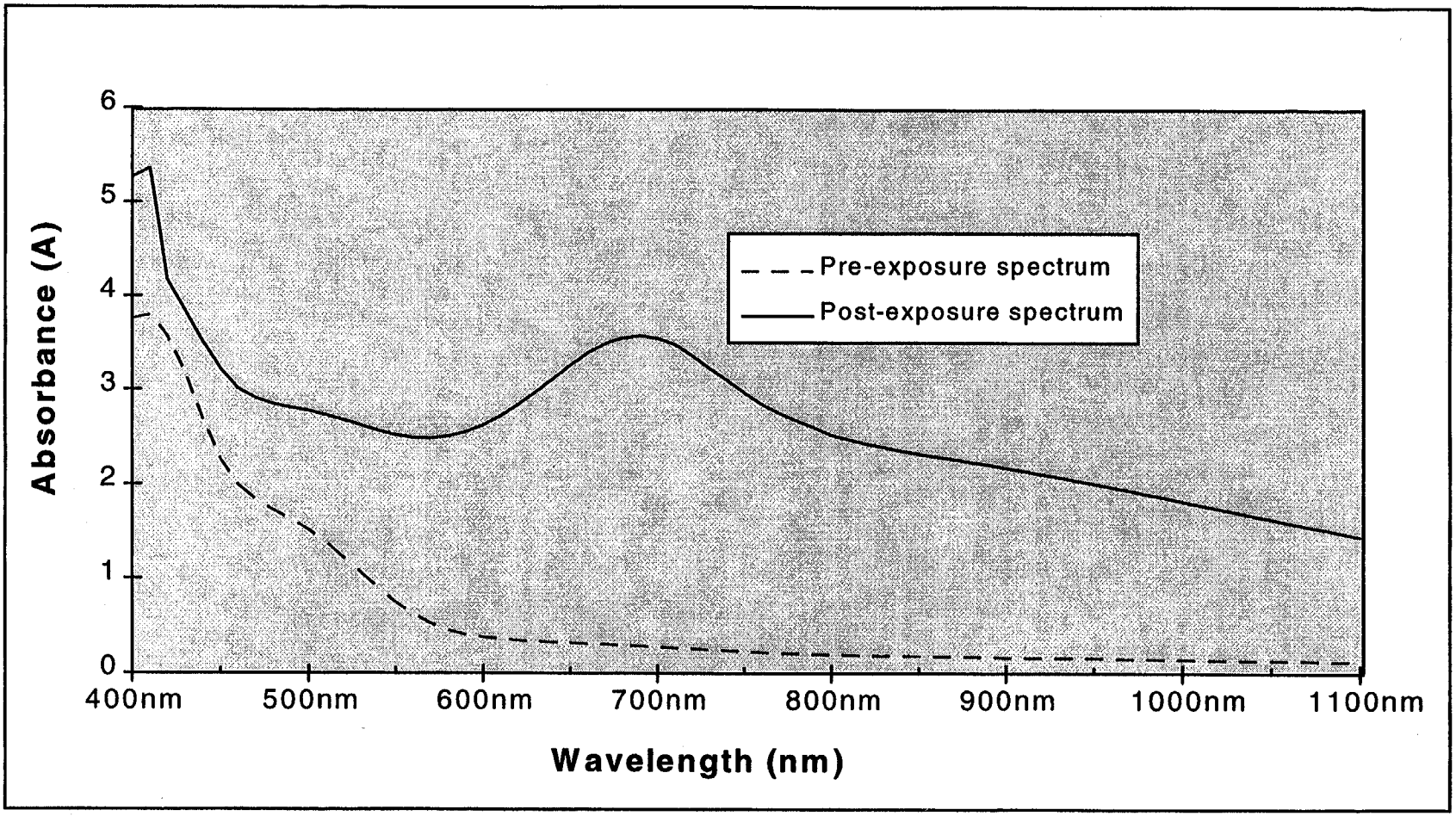

Figure 4-6. Typical sensor response spectrum from 400 to 1100 nm. This sensor was exposed to 40 ppm CO for 11 hours. The lower curve is the pre-exposure spectrum and the upper curve is the post-exposure spectrum. Note that the peak response is at 700 nm.

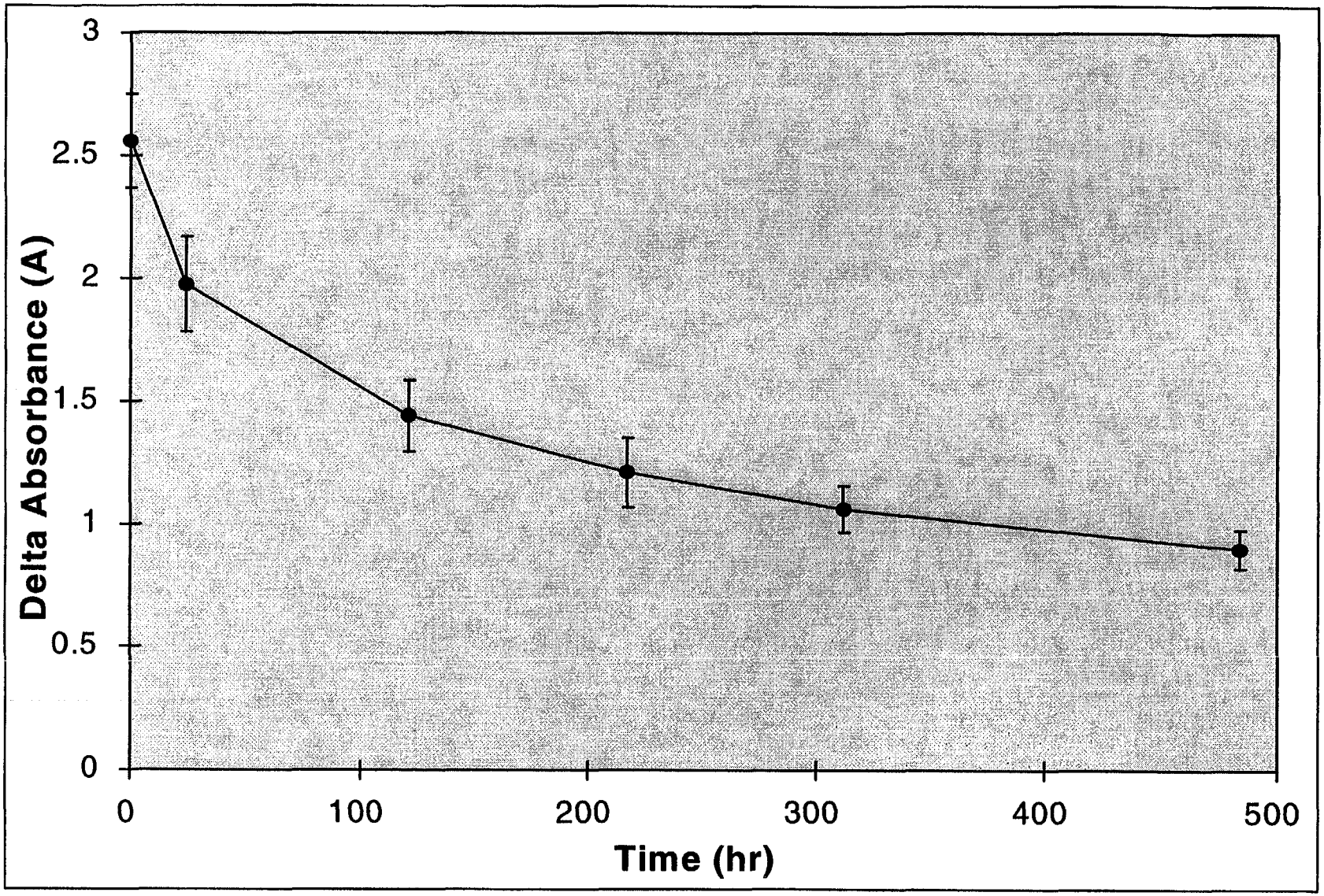

Figure 4-7a. Observed average change in 700nm absorbance of four MD15 QGI CO sensors over a 500 hour period after exposure to CO. The error bars represent ± 1 standard deviation.

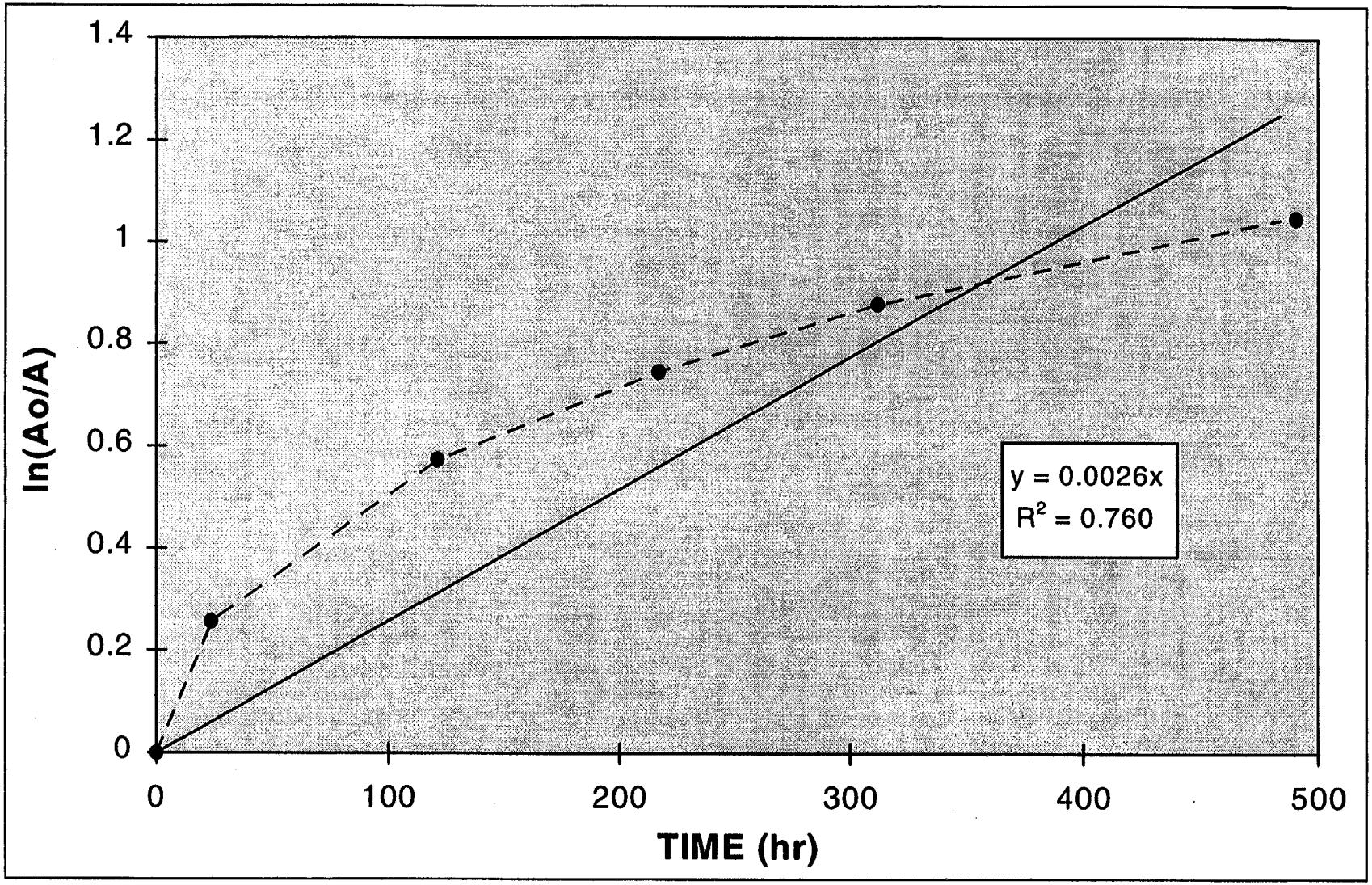

Figure 4-7b. First order kinetics in Mo_{blue} of observed change in 700nm absorbance of four MD15 QGI CO sensors during a 500 hour period after exposure to CO. The solid line on the graph is a linear least-squares regression fit through the plotted data. A good regression fit as evidenced by a high R^2 value (0.99 or higher), indicates that the kinetic model is appropriate for the data.

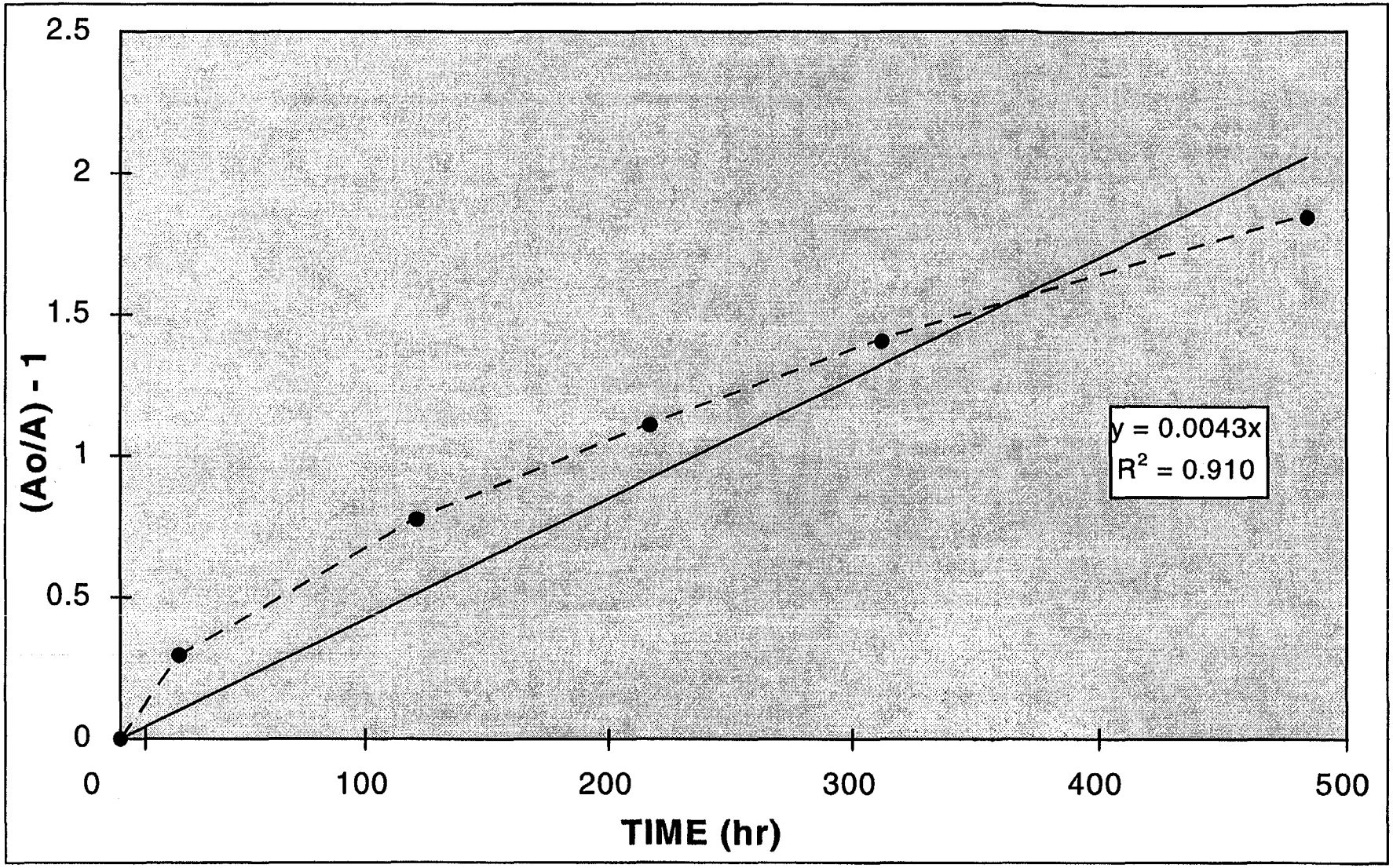

Figure 4-7c. Second order kinetics in Mo_{blue} of observed change in 700nm absorbance of four MD15 QGI CO sensors during a 500 hour period after exposure to CO. The solid line on the graph is a linear least-squares regression fit through the plotted data. A good regression fit as evidenced by a high R^2 value (0.99 or higher), indicates that the kinetic model is appropriate for the data.

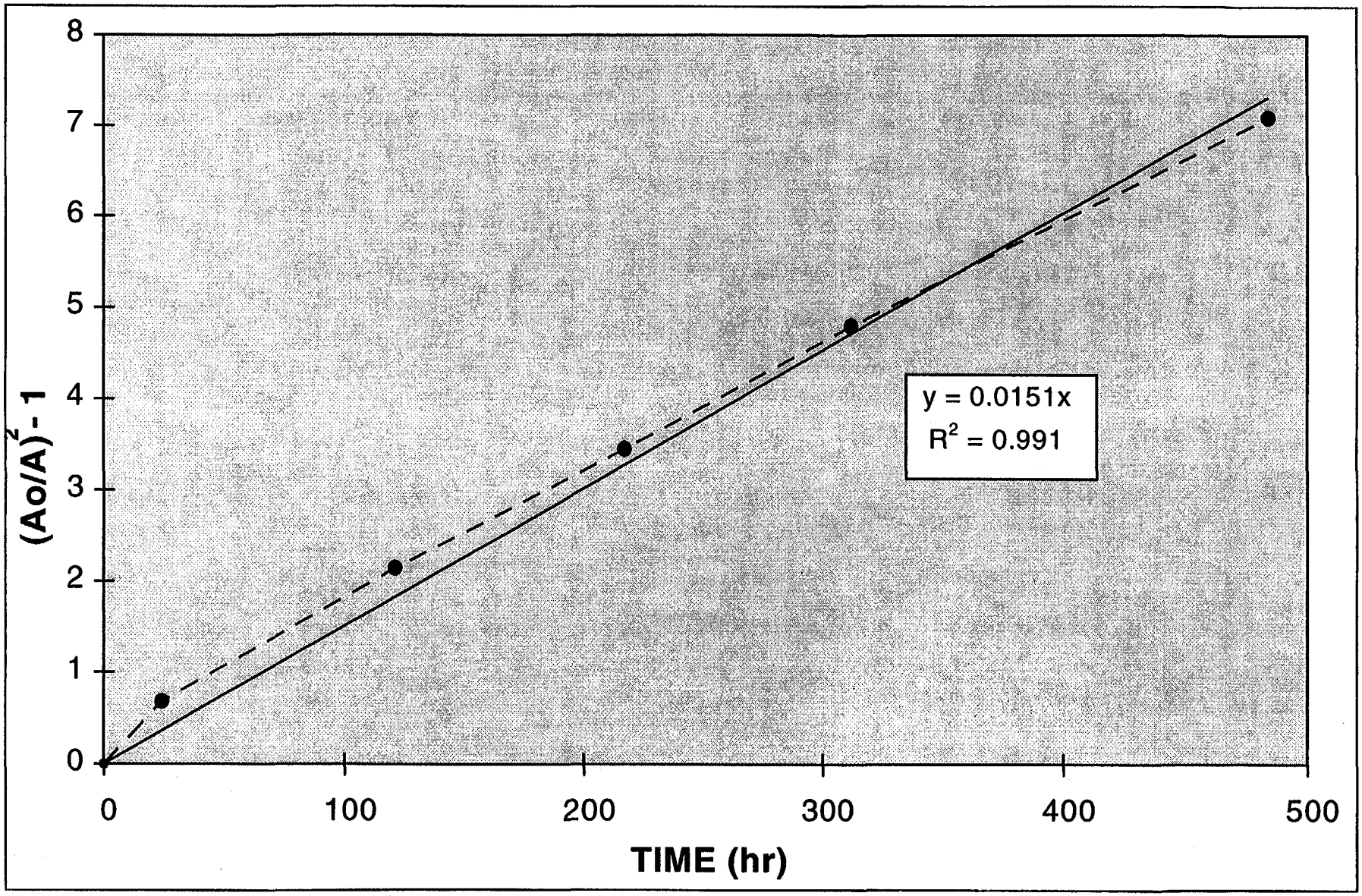

Figure 4-7d. Third order kinetics in Mo_{blue} of observed change in 700nm absorbance of four MD15 QGI CO sensors during a 500 hour period after exposure to CO. The solid line on the graph is a linear least-squares regression fit through the plotted data. A good regression fit as evidenced by a high R^2 value (0.99 or higher), indicates that the kinetic model is appropriate for the data.

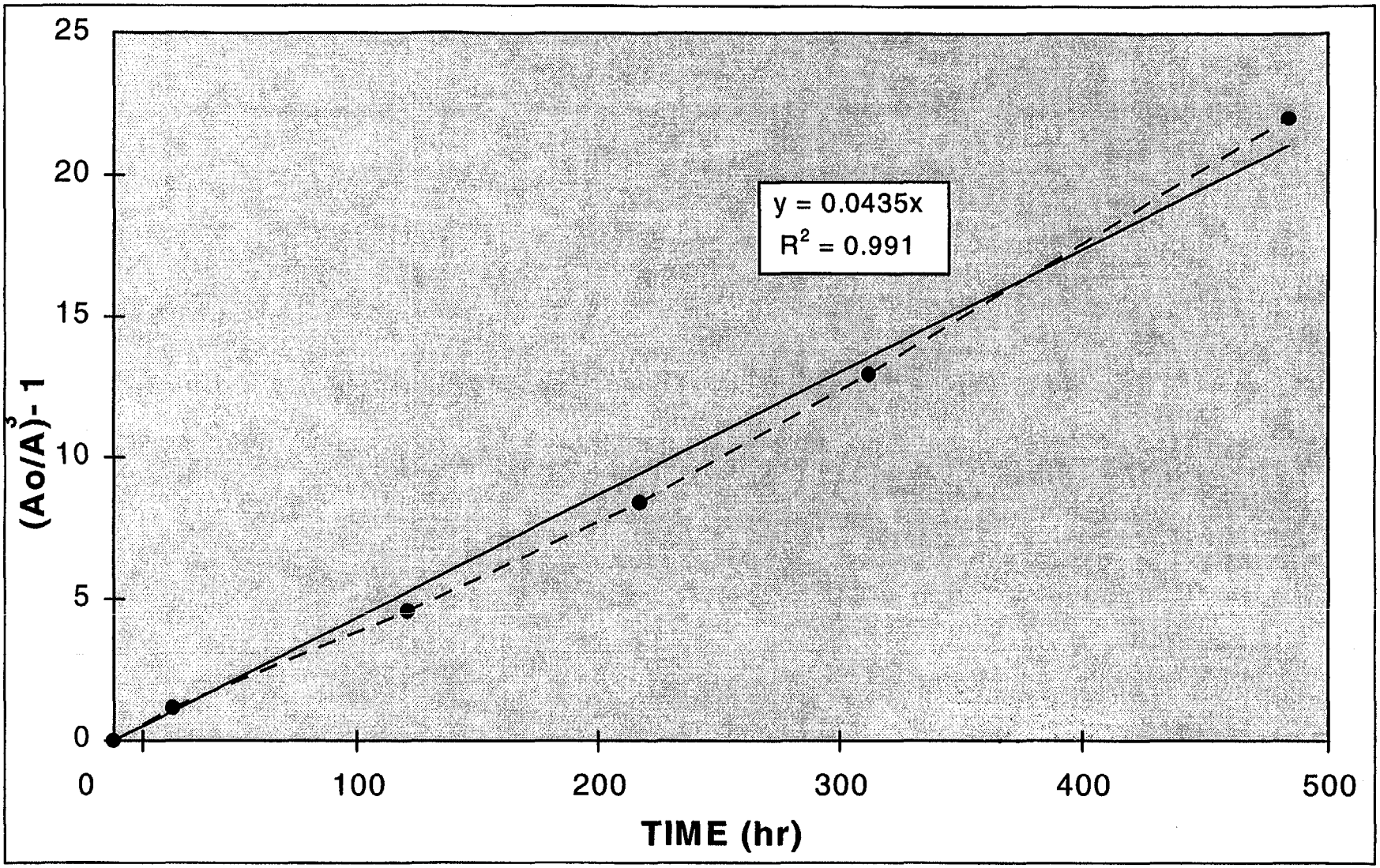

Figure 4-7e. Fourth order kinetics in Mo_{blue} of observed change in 700nm absorbance of four MD15 QGI CO sensors during a 500 hour period after exposure to CO. The solid line on the graph is a linear least-squares regression fit through the plotted data. A good regression fit as evidenced by a high R^2 value (0.99 or higher), indicates that the kinetic model is appropriate for the data.

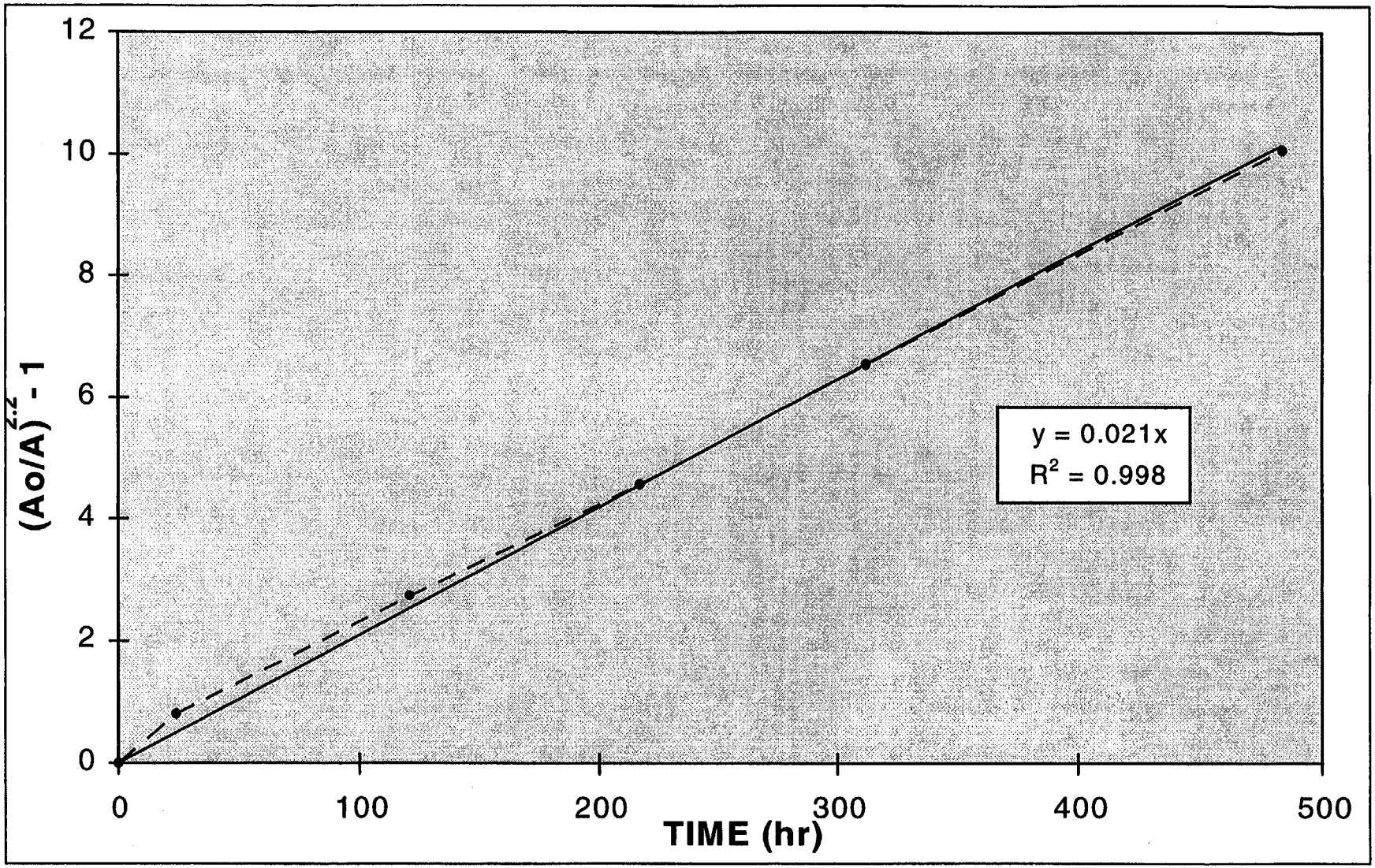

Figure 4-7f. 3.3 order kinetics in Mo_{blue} of observed change in 700nm absorbance of four MD15 QGI CO sensors during a 500 hour period after exposure to CO. The solid line on the graph is a linear least-squares regression fit through the plotted data. A good regression fit as evidenced by a high R^2 value (0.99 or higher), indicates that the kinetic model is appropriate for the data.

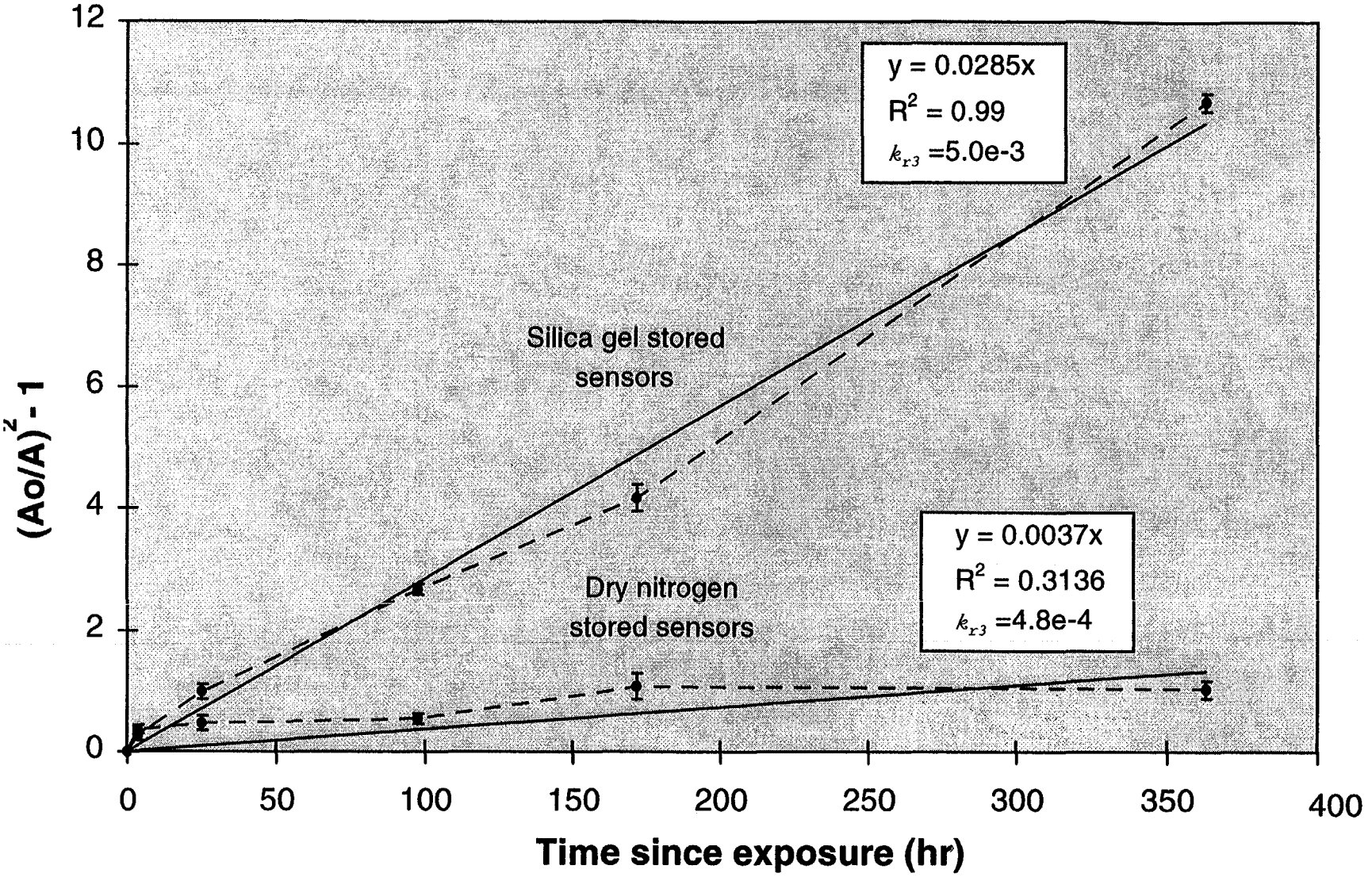

Figure 4-8. Third order oxidation kinetics in Mo_{blue} of the reversal of four CO sensors each from batch K, stored dry on silica gel and stored in dry, oxygen-free nitrogen. Note the marked difference in the rate constant k_{r3} between the sensors stored under the two conditions. The solid lines represent a least-square regression line of best fit through the data.

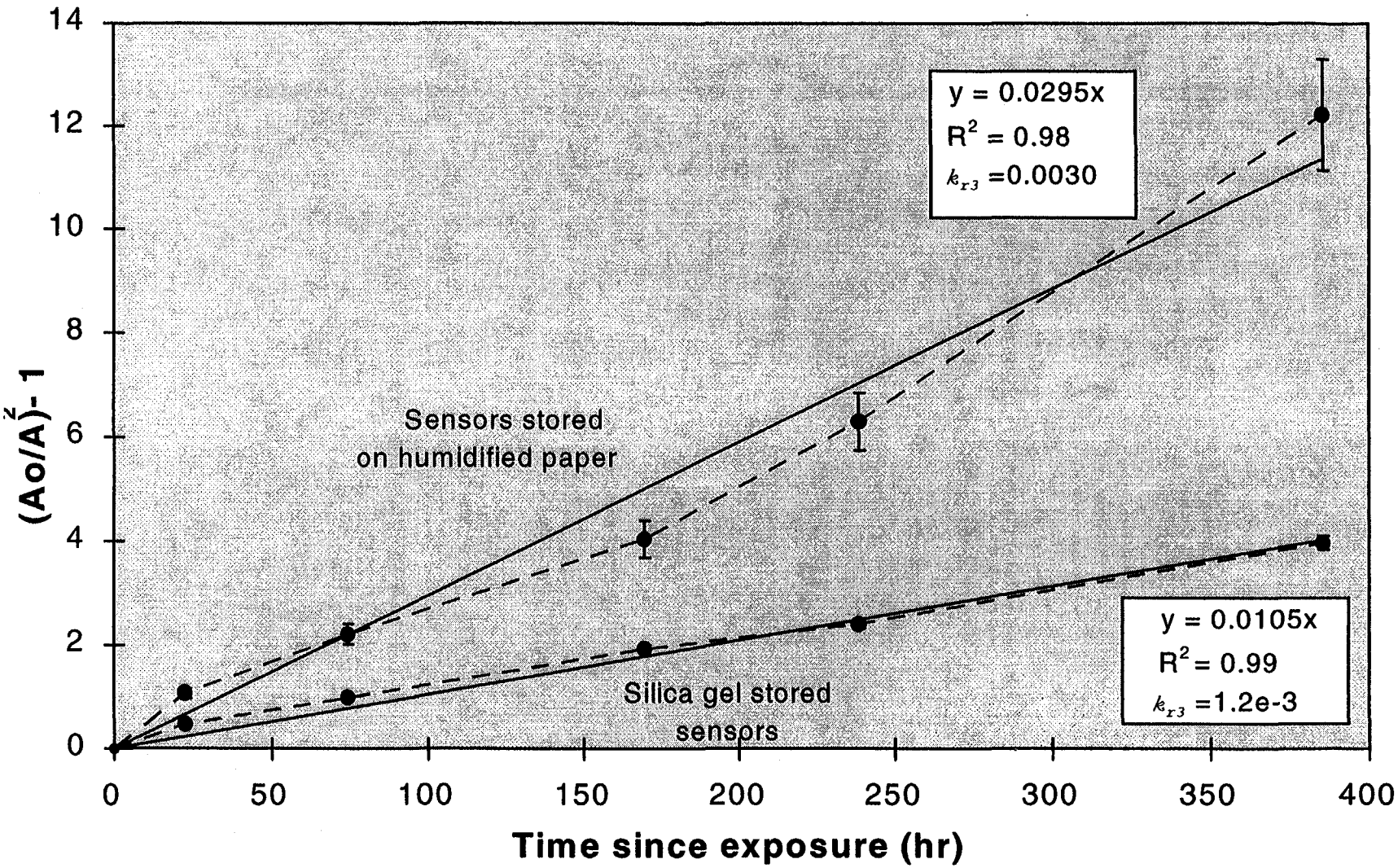

Figure 4-9. Third order oxidation kinetics in Mo_{blue} of the reversal of four CO sensors each from batch J, stored dry on silica gel and stored under humid conditions on paper. Note the marked difference in the rate constant k_{r3} between the sensors stored under the two conditions. The solid lines represent a least-square regression line of best fit through the data.

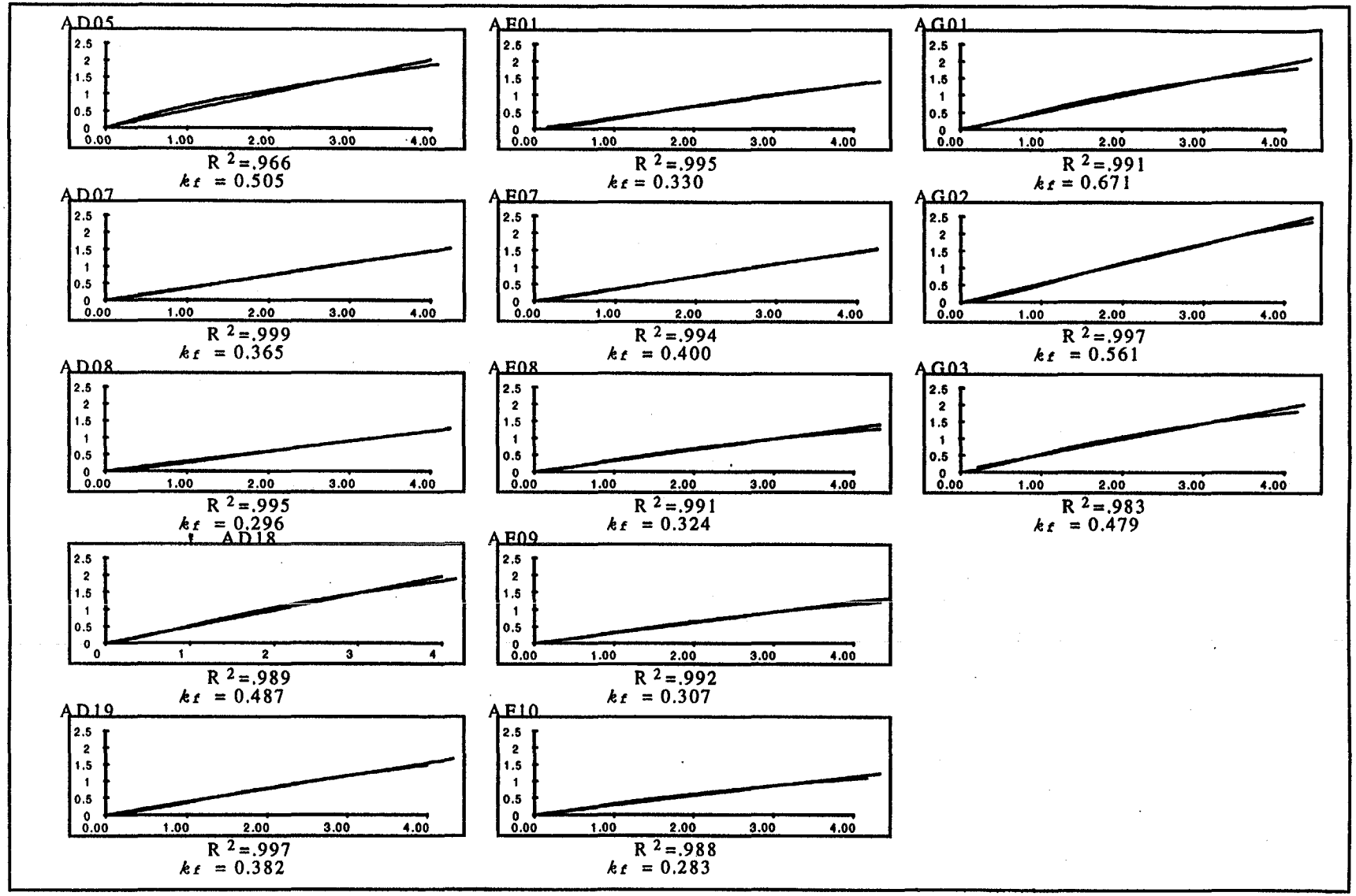

Figure 4-10. Forward sensor response to CO and curve fit for MD-15 sensors using the Direct Method. The x-axes represent duration of 40 ppm CO (hours). The y-axes represent delta absorbance at 700nm. The correlation coefficient (R^2) of a least-squares linear regression and the slope of the fitted curves are given. The *exposure* of the sensor can be calculated by multiplying the time on the x-axis by 40 ppm.

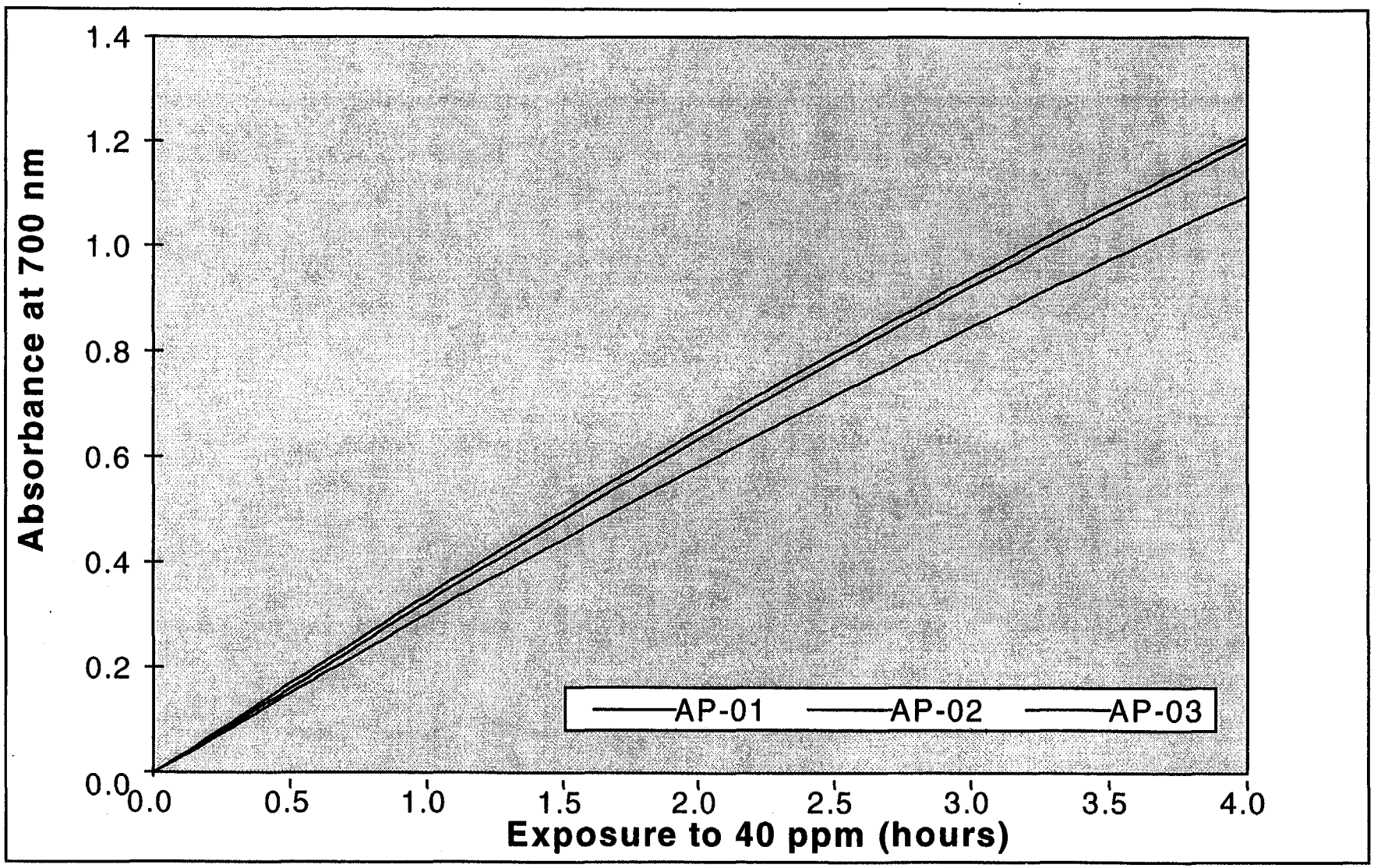

Figure 4-11. Individual sensor response curves at 700 nm from three QGI sensors from a single batch The sensors are conditioned by drying over desiccant for at least two weeks at about 20°C. Intra-batch (AP sensors) differences in sensor response can be seen. Note that CO *exposure* of the sensor can be calculated by multiplying the time on the x-axis by 40 ppm.

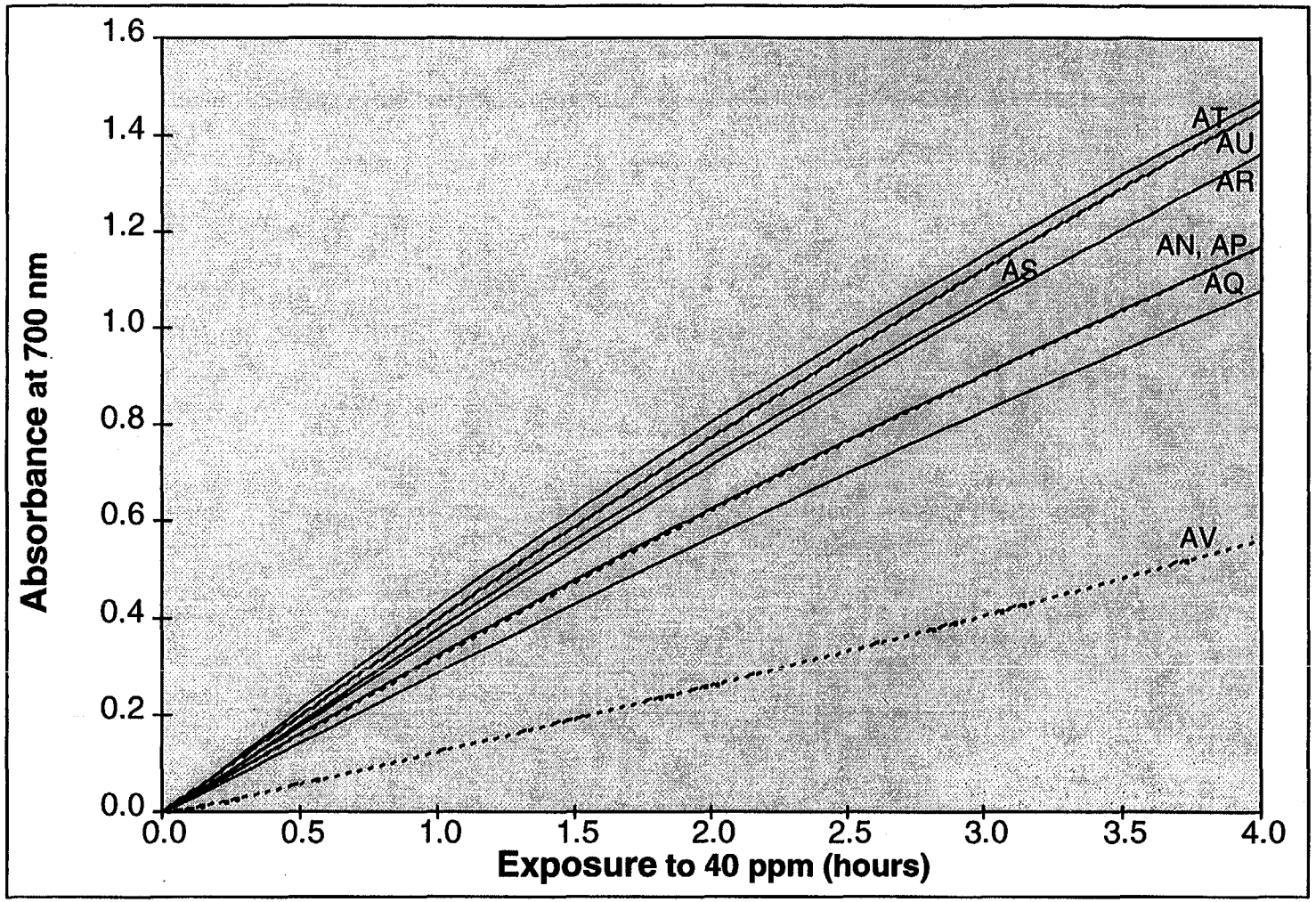

Figure 4-12. Average sensor response curves at 700 nm for 8 batches of sensors. Inter-batch differences in response can be seen. All batches except "AV" were manufactured using the same chemical formula. Variability in MD15 sensor manufacturing procedure may account for some of the variation seen. The "AV" sensors had a small amount of calcium added to the MD15 formulation, explaining the large difference in response of these sensors. Note that CO *exposure* of the sensor can be calculated by multiplying the time on the x-axis by 40 ppm.

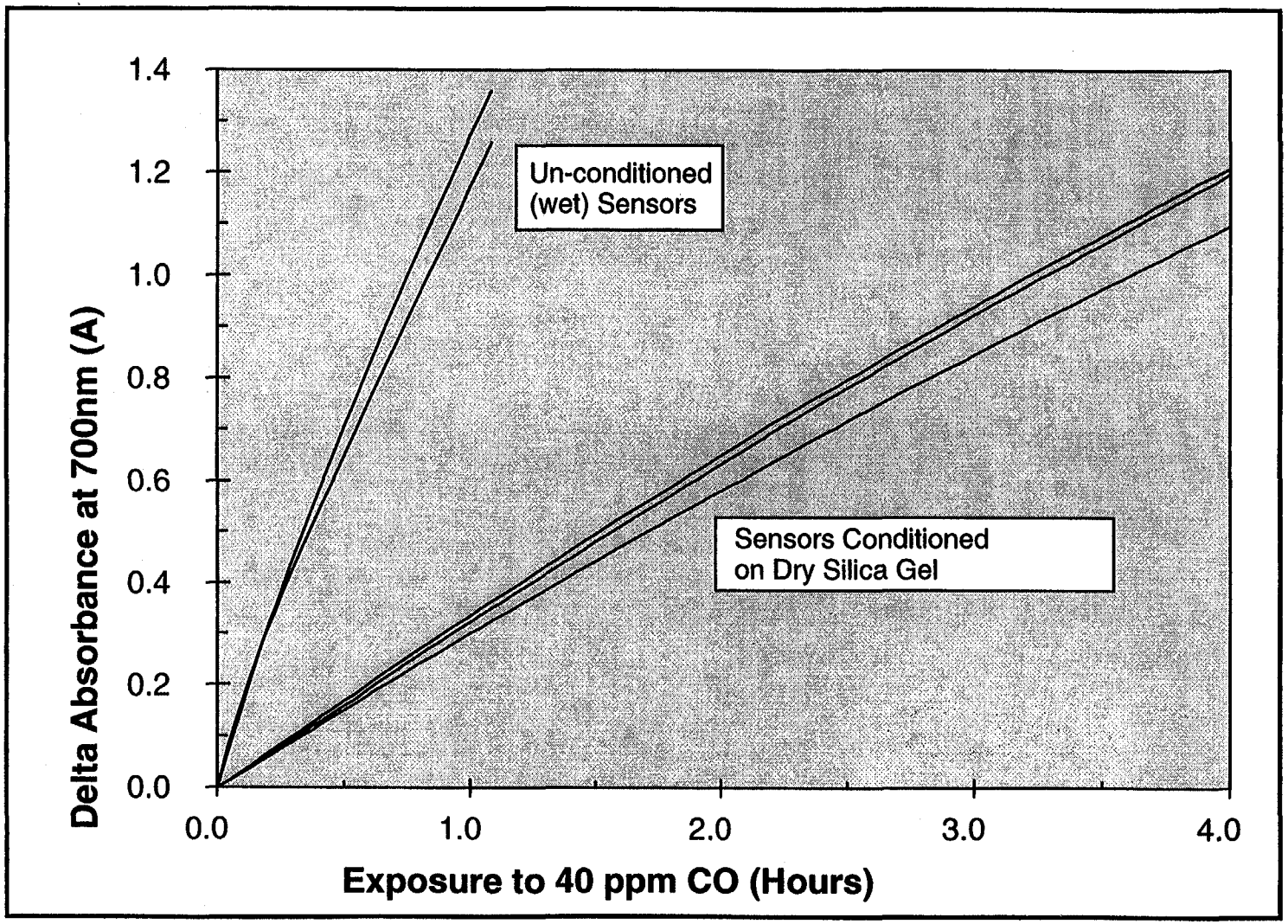

Figure 4-13. A comparison of Direct Method response curves for conditioned (desiccated) and unconditioned (wet) AP sensors exposed to 40 ppm. The MD15 sensor response was found be dependent upon sensor dryness. In order to ensure sensor homogeneity it was necessary that they be desiccated on silica gel for a minimum of 14 days prior to CO exposure. Note that CO *exposure* of the sensor can be calculated by multiplying the time on the x-axis by 40 ppm.

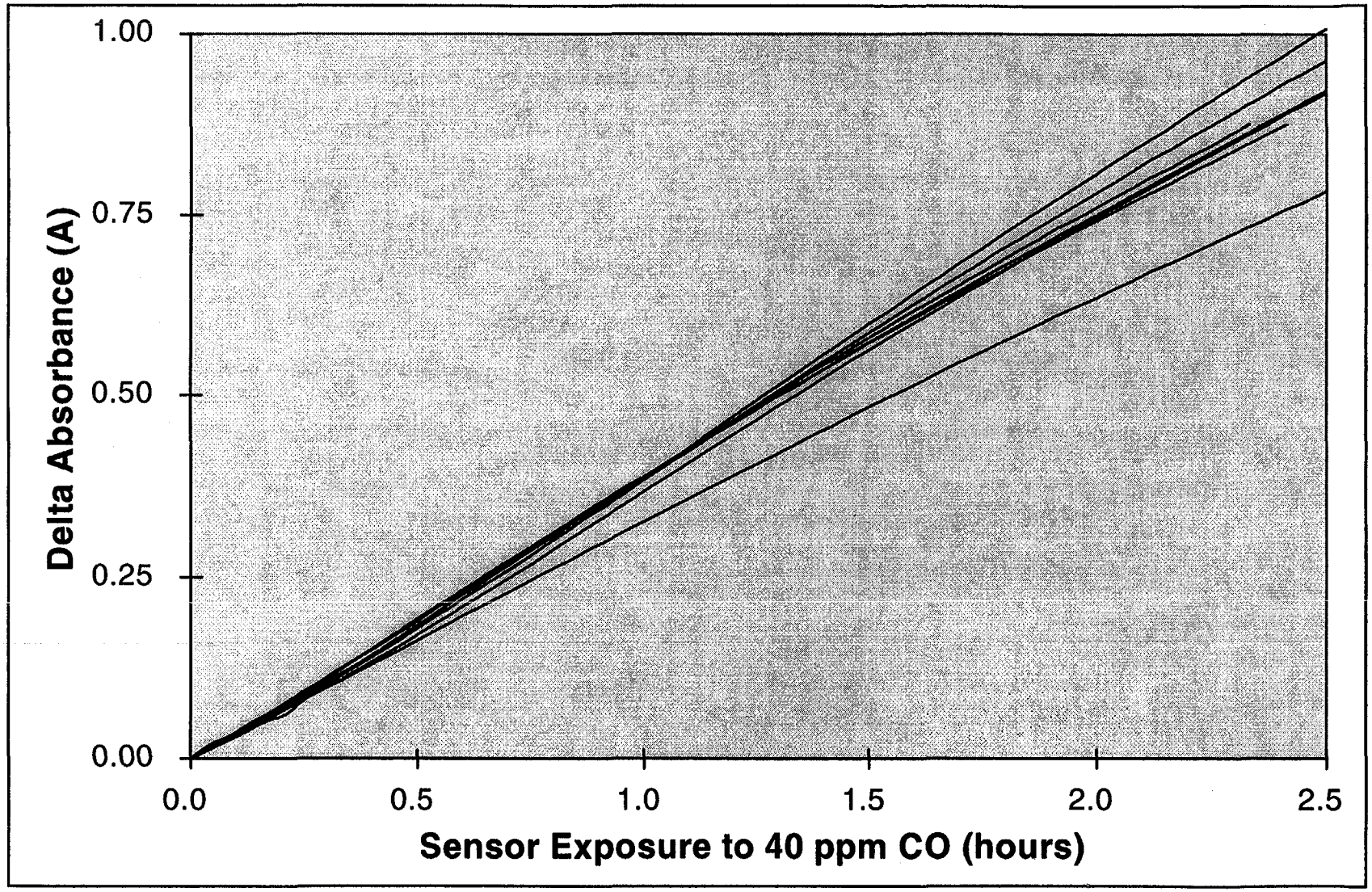

Figure 4-14. Direct Test response curves for seven batch AW QGI sensor MD15. Sensors were exposed to 40 ppm CO. Note that CO *exposure* of the sensor can be calculated by multiplying the time on the x-axis by 40 ppm.

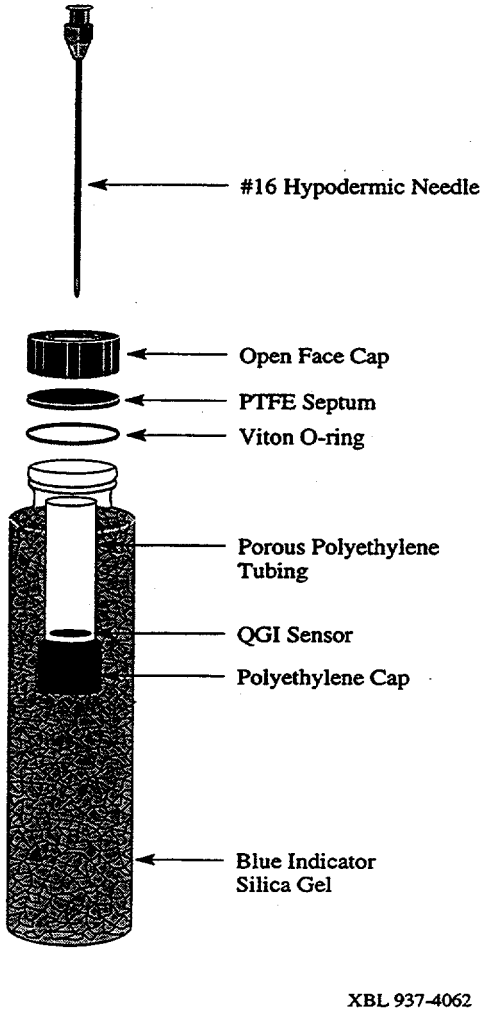

Figure 4-15. Diagram of the first prototype LBNL/QGI passive sampler (PS1).

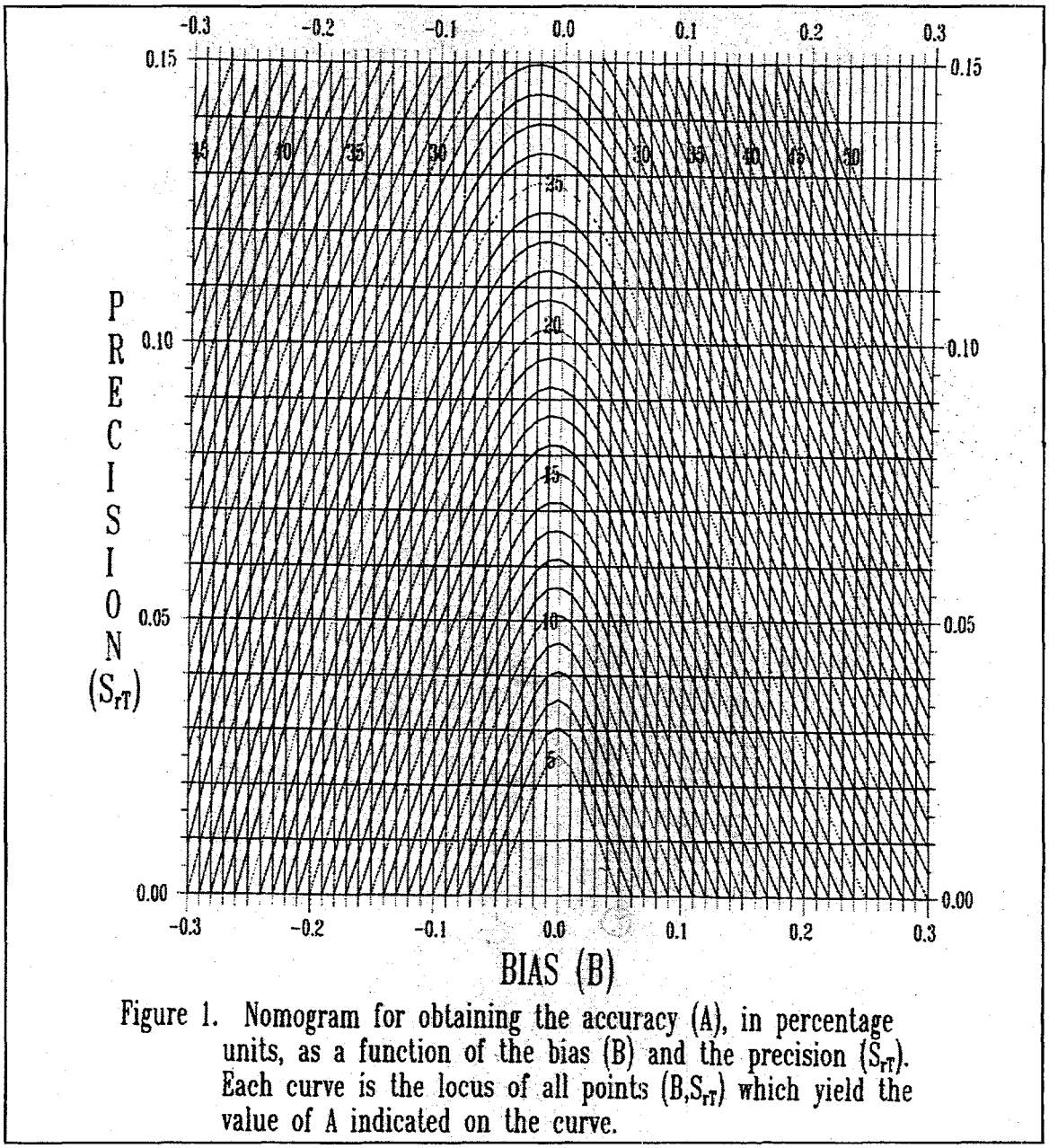

Figure 1. Nomogram for obtaining the accuracy (A), in percentage units, as a function of the bias (B) and the precision (S_{rT}). Each curve is the locus of all points (B,S_{rT}) which yield the value of A indicated on the curve.

Figure 4-16. See explanation in figure. Nomogram from NIOSH guidelines for air sampling and analytical method development and evaluation (Kennedy, 1995).

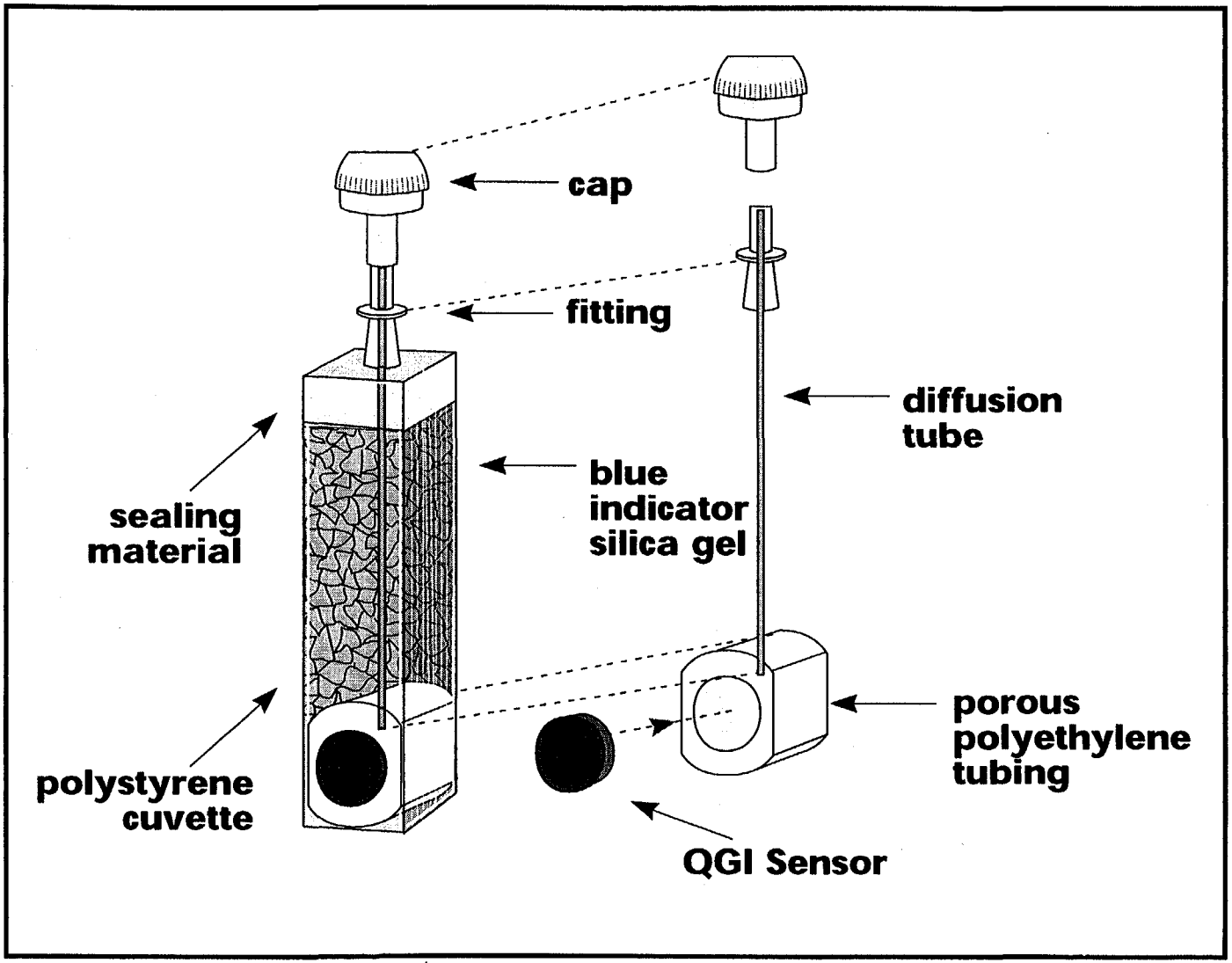

Figure 4-17. Schematic of the LBNL/QGI Passive Sampler #2 (PS2)

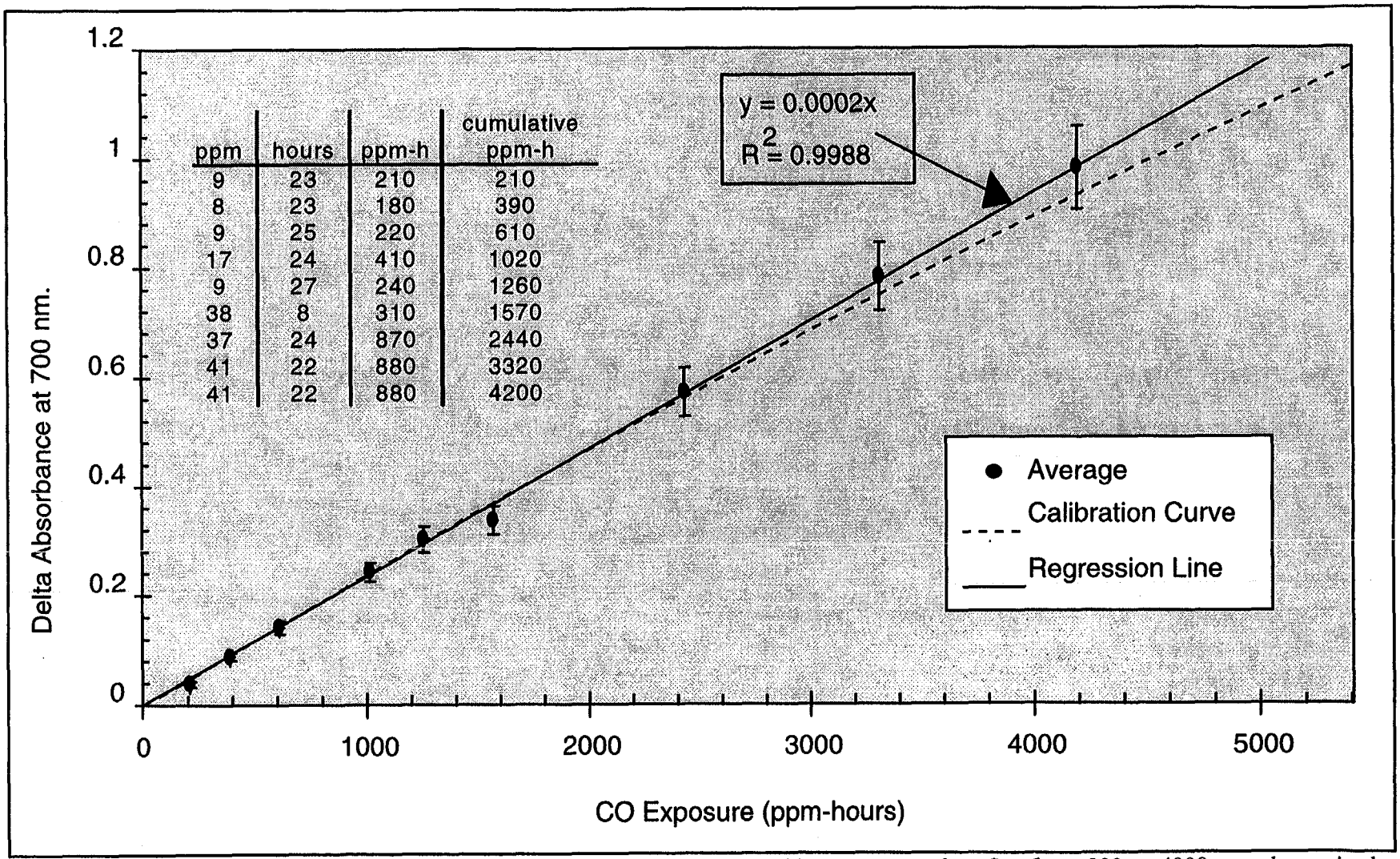

Figure 4-18. LBNL/QGI PS2 passive sampler laboratory test results. Five PS2 were exposed to CO from 200 to 4000 ppm-hours in dry conditions. The dashed line indicates the sensor calibration curve derived from direct method tests. The solid line is a least-square regression fit to the average sampler response. The CO exposure data are presented in order in the superimposed table. Note that exposure concentrations ranged from 8 to 41 ppm.

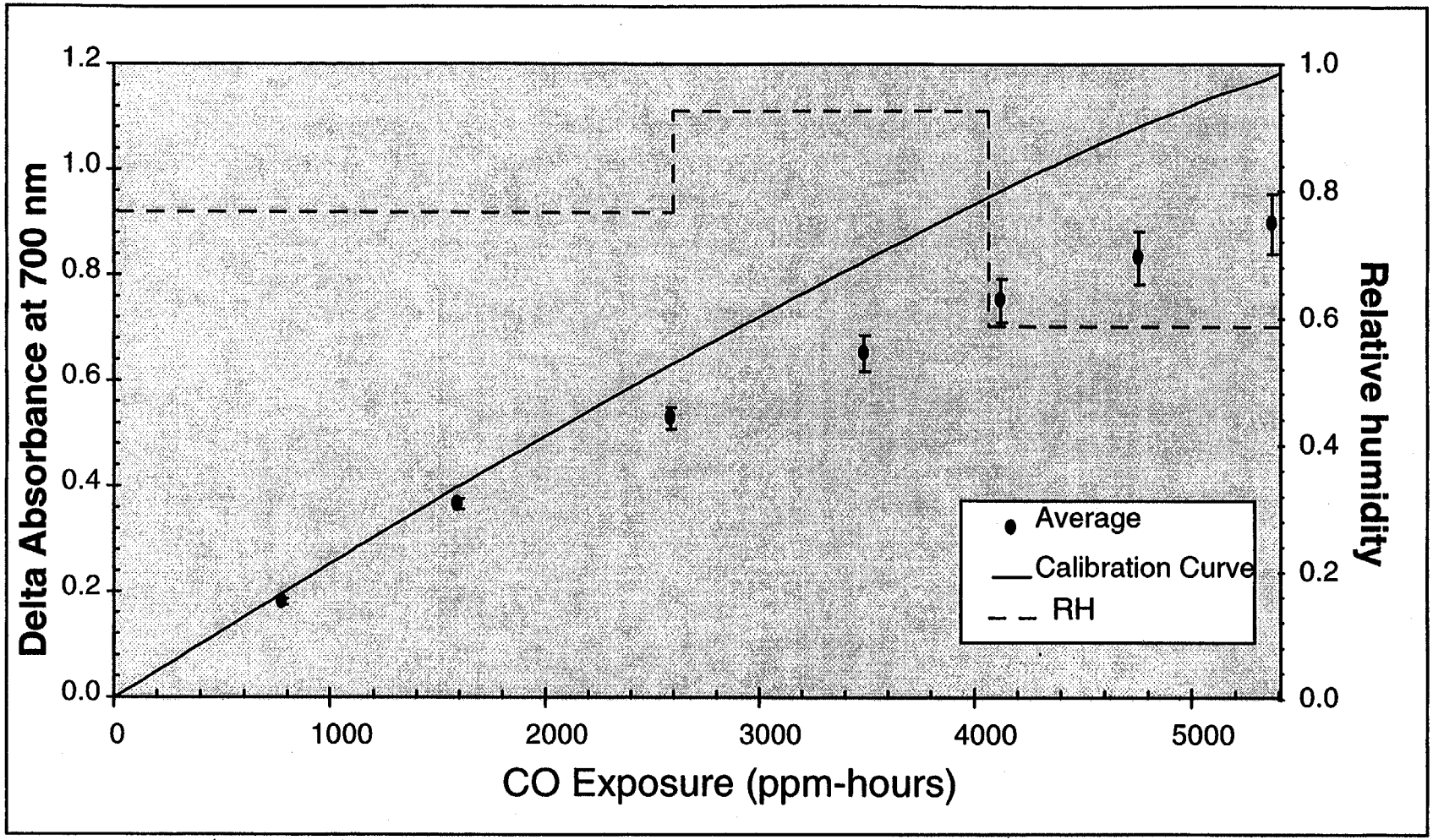

Figure 4-19. LBNL/QGI PS2 laboratory test results. Three PS2 samplers were exposed to CO from 800 to 5400 ppm-hours in varying high-humidity conditions as shown. The line indicates the sensor calibration curve derived from direct method tests. The relative humidity (RH), indicated by the dashed line was varied during the experiment.

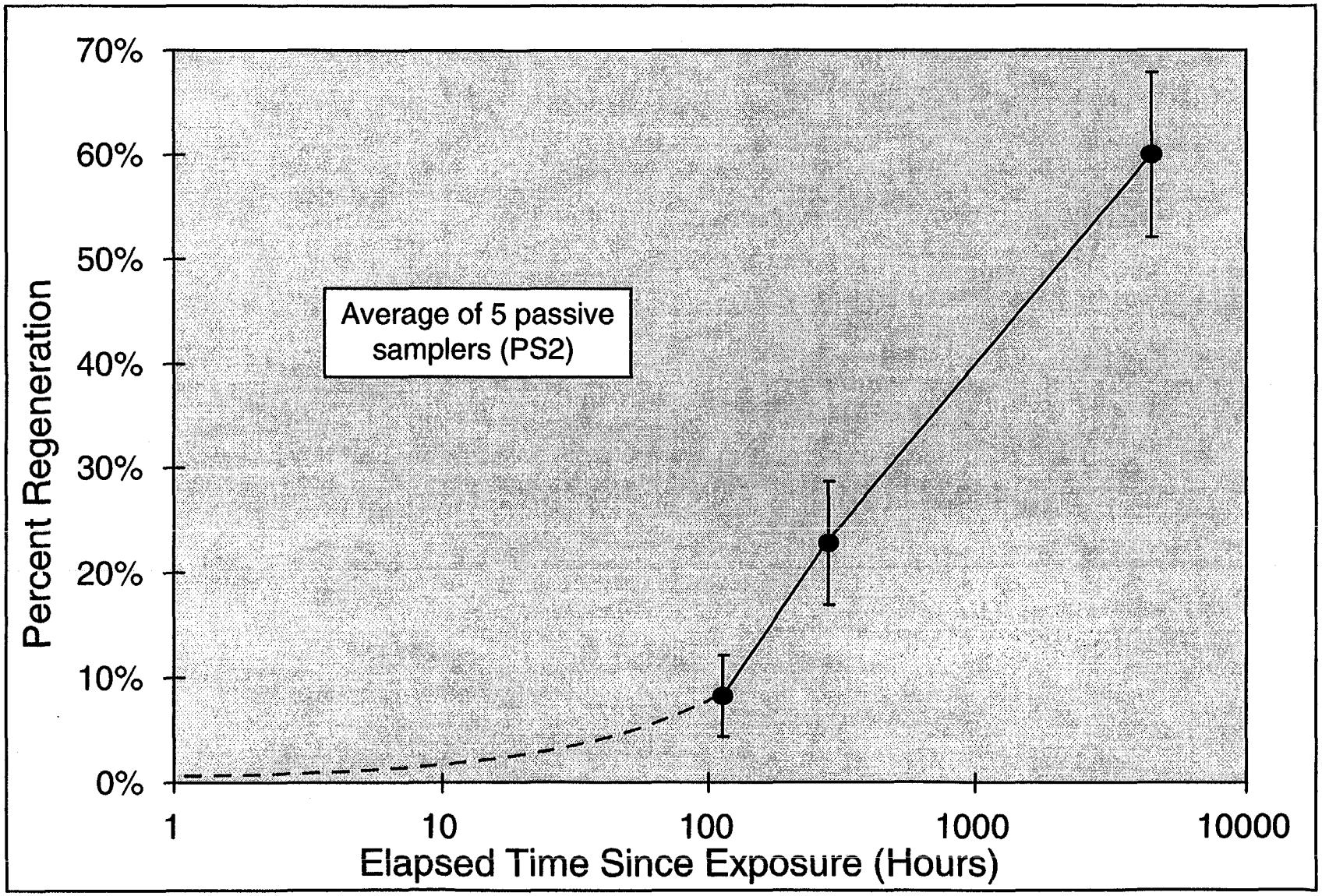

Figure 4-20. Percent regeneration of five QGI sensors in LBNL/QGI PS2 samplers in storage after exposure to CO. Error bars represent 1 standard deviation. Dashed curved indicates interpolated regeneration for times less than 100 hours.

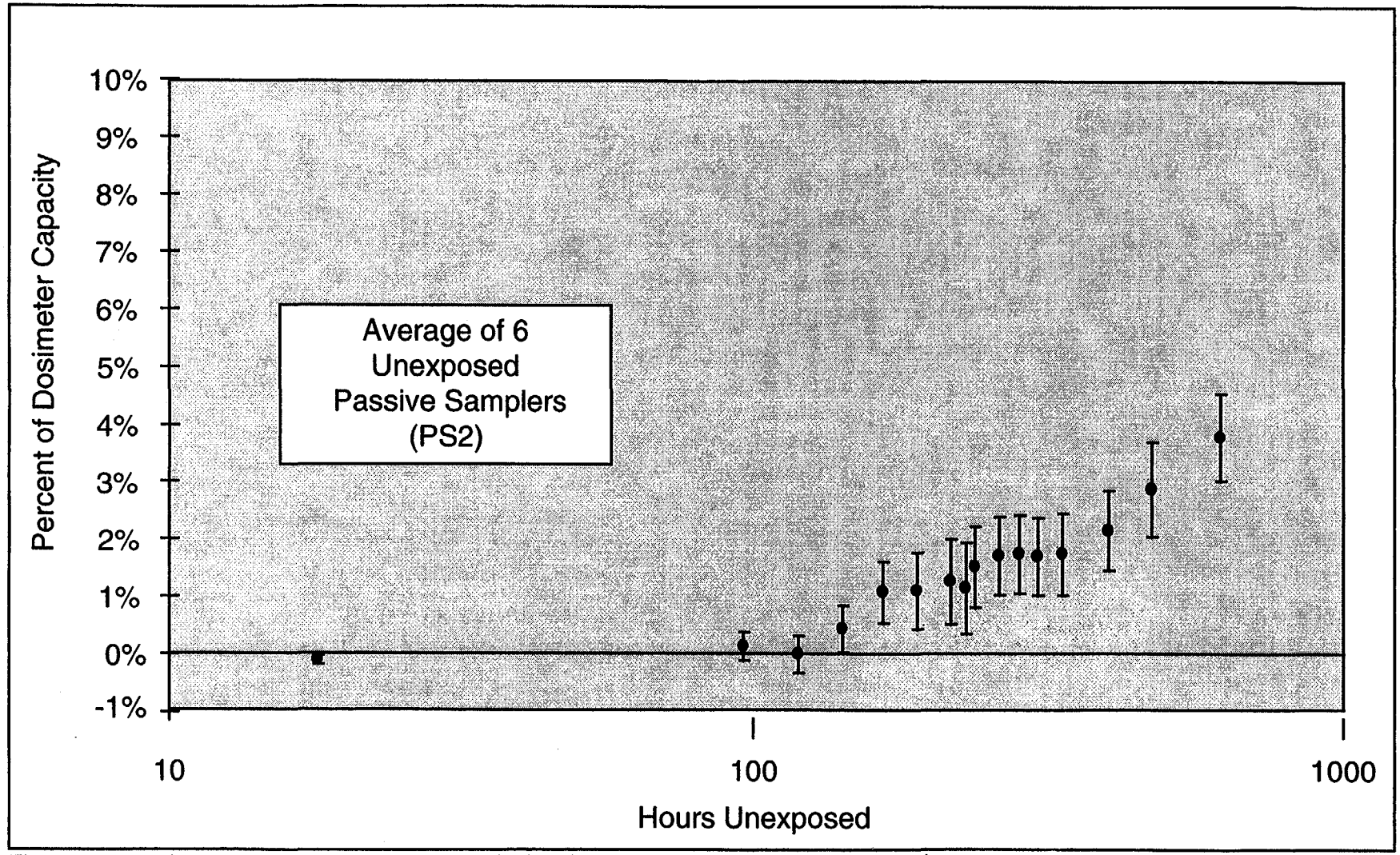

Figure 4-21. Average increase in background absorbance of six capped PS2 LBNL/QGI CO passive samplers exposed to CO environments as controls over more than 600 hours. Error bars represent 1 standard deviation.

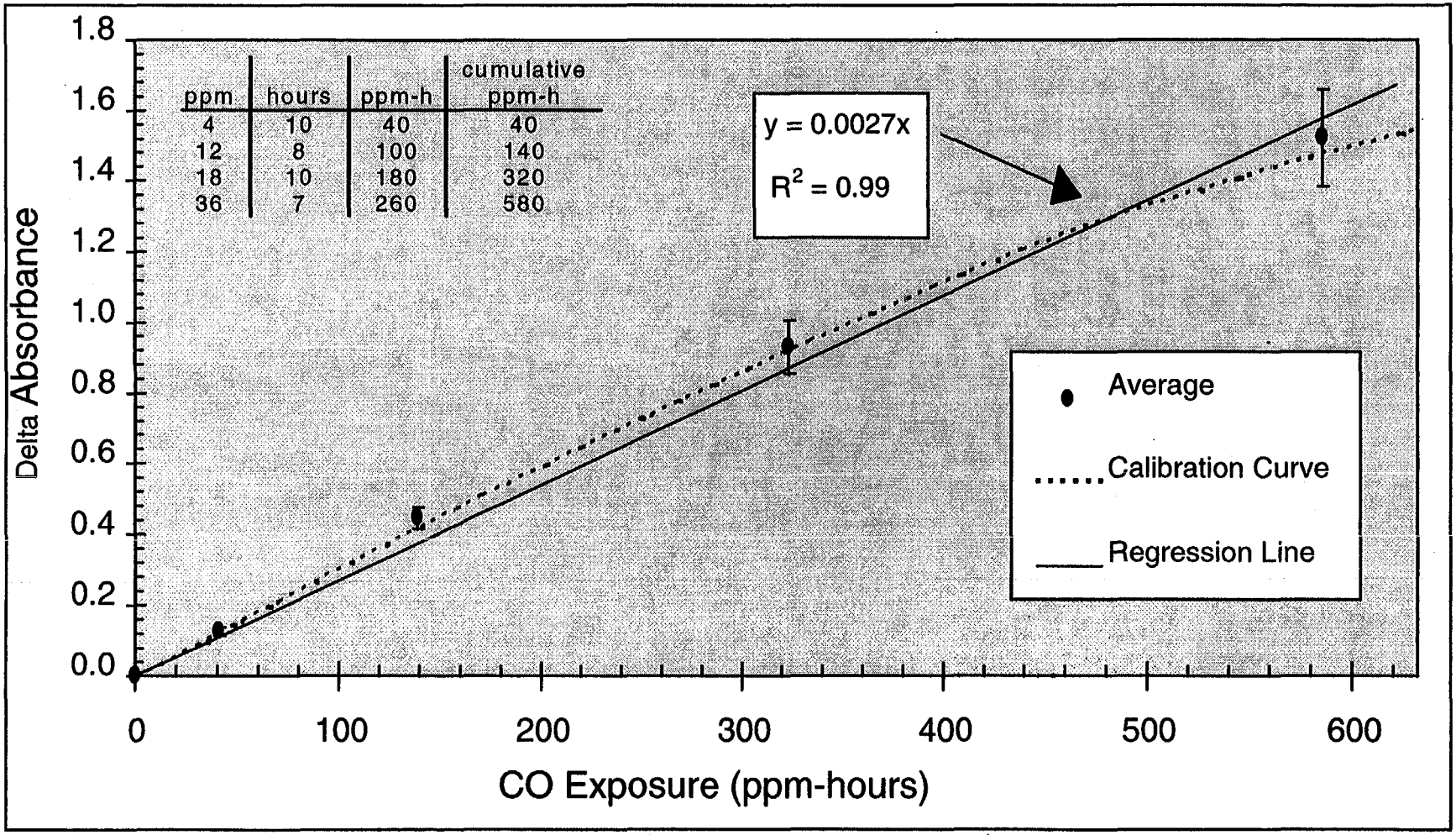

Figure 4-22. Laboratory test results for the occupational dosimeter configuration of PS3/D1 passive samplers. Five samplers were exposed to CO from 40 to 600 ppm-hours in dry conditions. The dashed line indicates the sensor calibration curve derived from direct method tests. The solid line is a least-square regression fit to the average sampler response. The CO exposure data are presented in order in the superimposed table. Note that exposure concentrations ranged from 4 to 36 ppm.

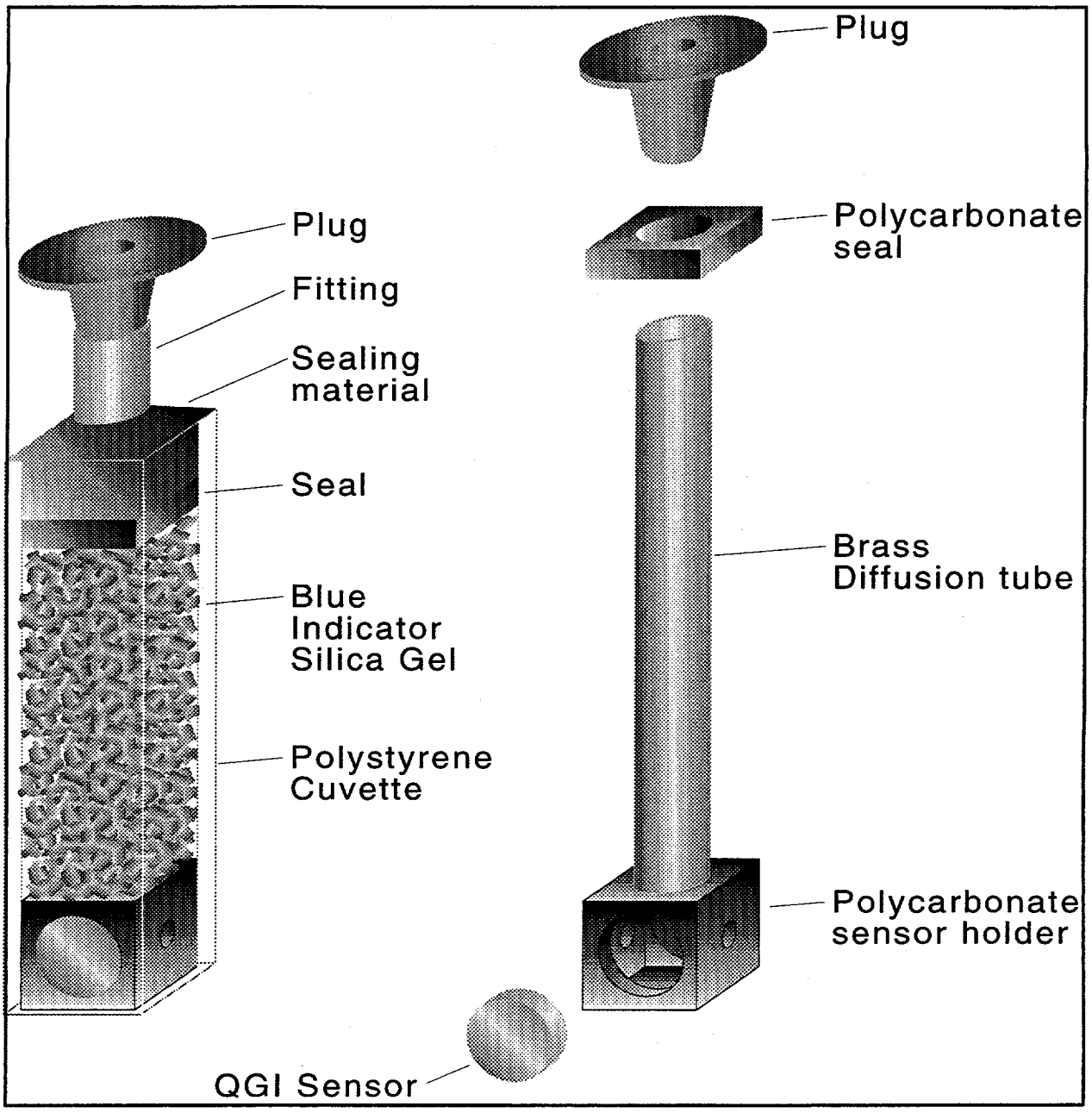

Figure 4-23. Exploded view of LBNL/QGI occupational dosimeter (D2 and D3) showing the manufactured sensor holder and seal. This design incorporated modular pieces, which snap together and fitted into the polystyrene cuvette with tight tolerances. The sensor holder was designed to optimize mass transfer of water vapor to the silica gel in order to keep the sensor dry.

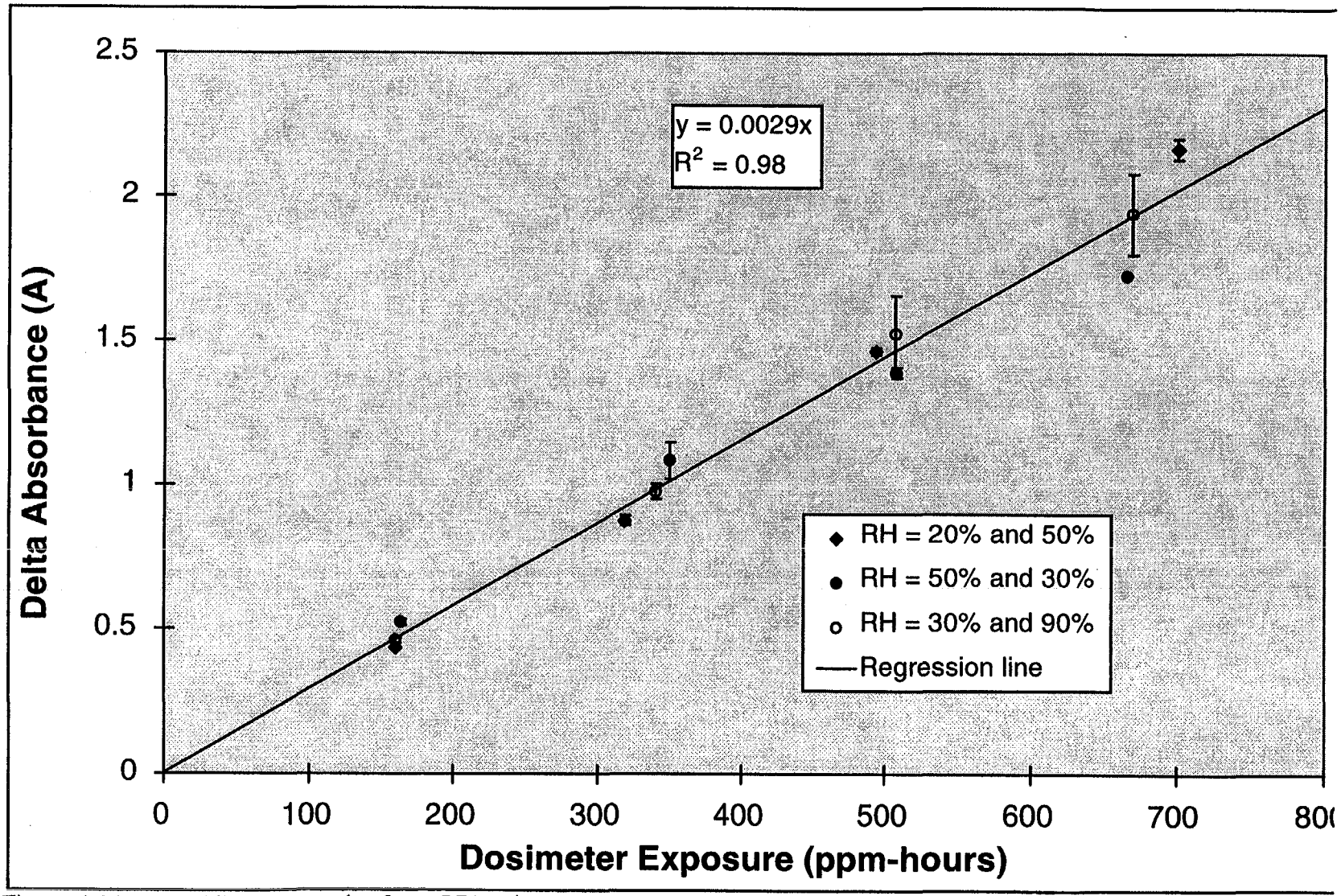

Figure 4-24. Humidity test results from LBNL/QGI CO Occupational Dosimeter D2. Sets of three dosimeters were incrementally exposed to 40 ppm CO and 20%, 30%, 50%, or 90% relative humidity for two 4-hour periods. The variability in dosimeter response does not appear to be related to humidity.

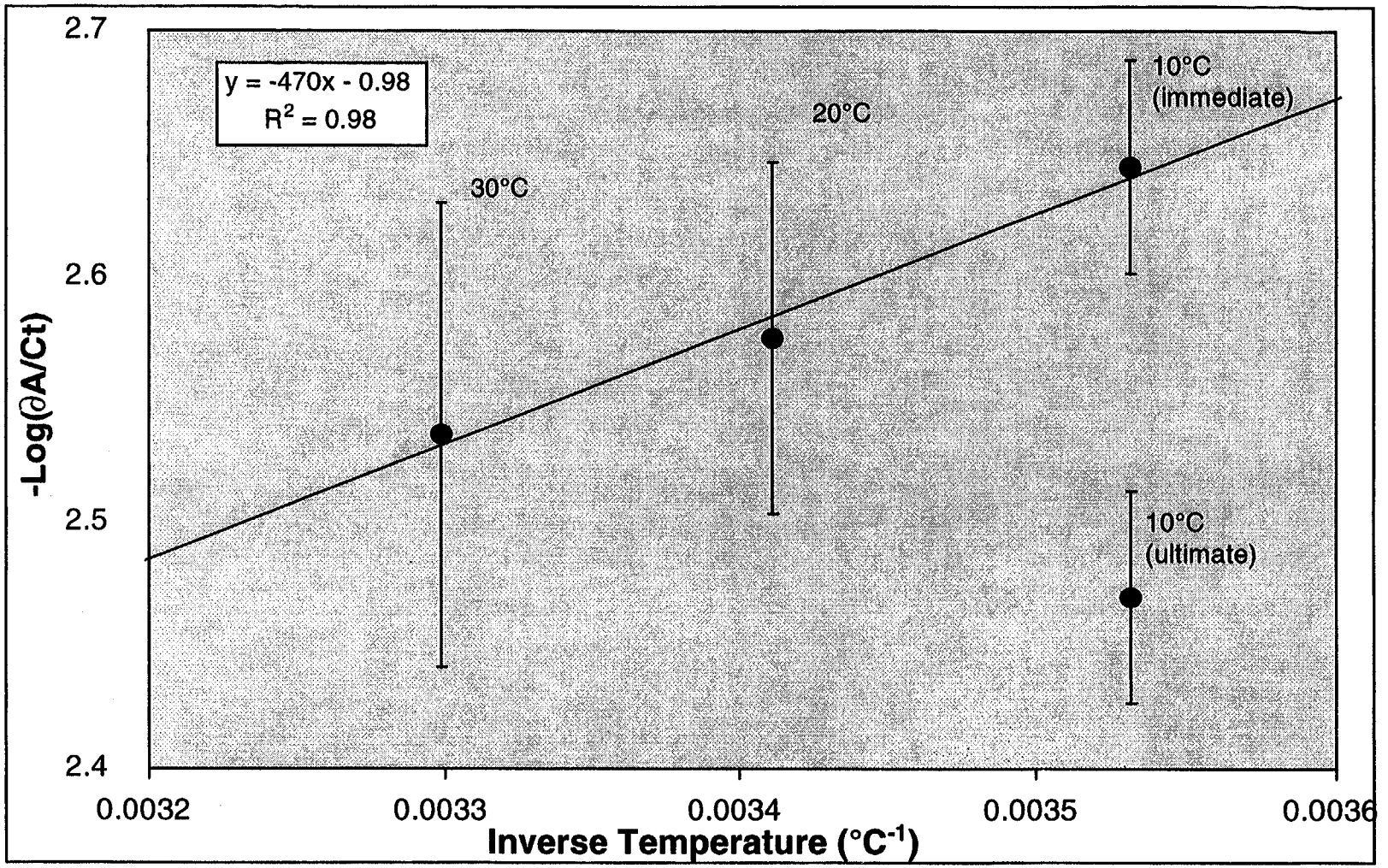

Figure 4-25. Arrhenius plot of D2 CO dosimeter response as a function of temperature. A clear relationship can be seen between sensor kinetics and temperature if response (dA) is measured immediately after exposure. A latent reaction occurs in the dosimeters exposed at 10°C once they are allowed to warm to 20°C (see "ultimate" response at 10°C). The (slow) Pd-Mo reaction, leading to sensor color change, is identified here as the rate-limiting step in the sensor chemistry. The CO-Pd catalytic reaction does not appear to be hampered at 10°C. A CO-Pd "complex" appears to be stored until the Pd-Mo reactions occur.

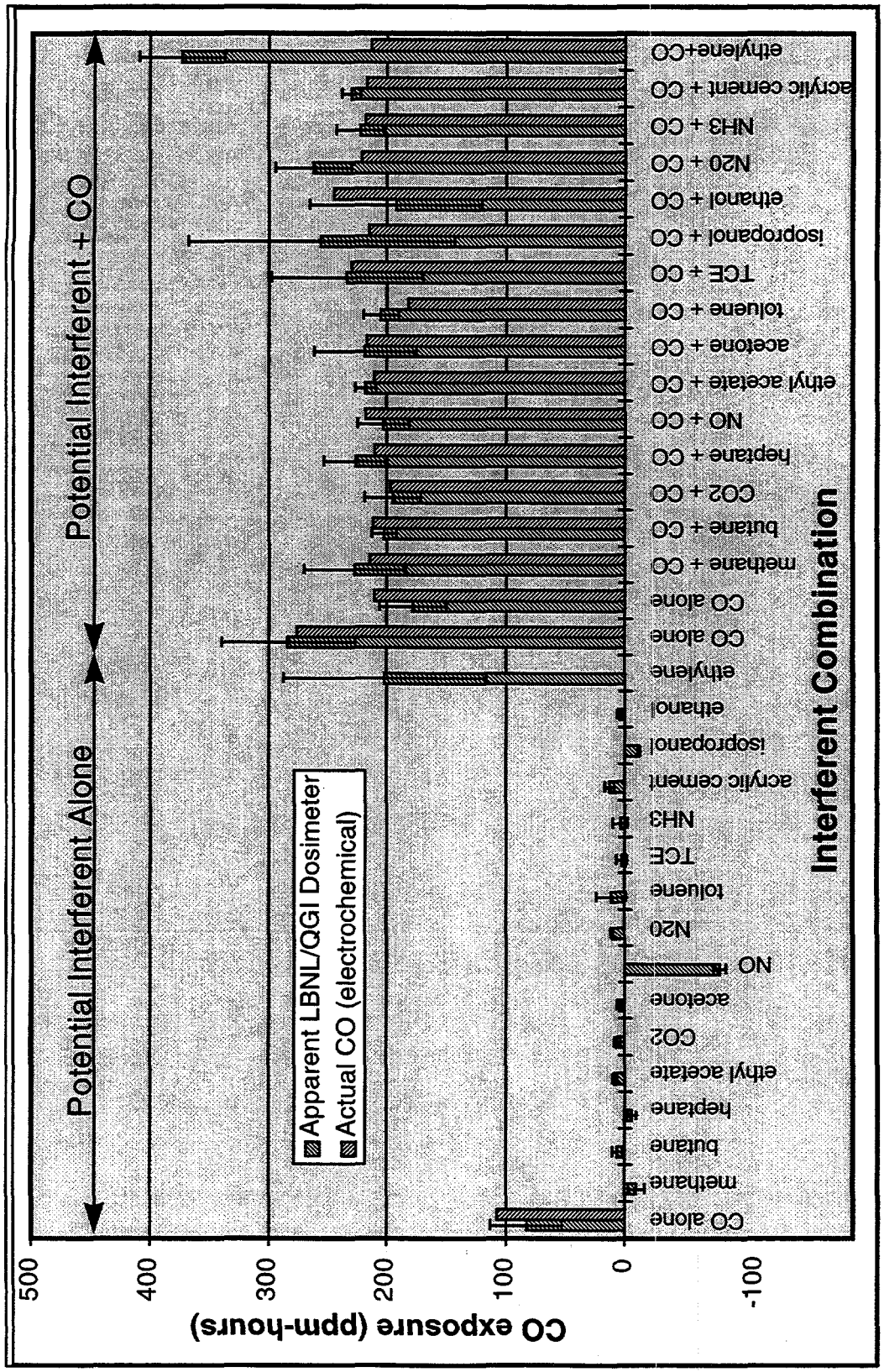

Figure 4-26. Interference screening test results. Three D2 CO dosimeters were exposed first to a potential interferent (left side of figure) for 2 hours, and then to the same interferent + 100 ppm CO for 2 hours. Different sets of dosimeters were used for each interferent. "True" dosimeter CO exposures (measured with and electrochemical CO sensor) are compared to the dosimeters' apparent CO exposures. High concentrations of nitric oxide (NO, 50 ppm) and ethylene (200 ppm) both appear to compromise the performance of these dosimeters. See text for exposure conditions for the other interference test experiments shown here.

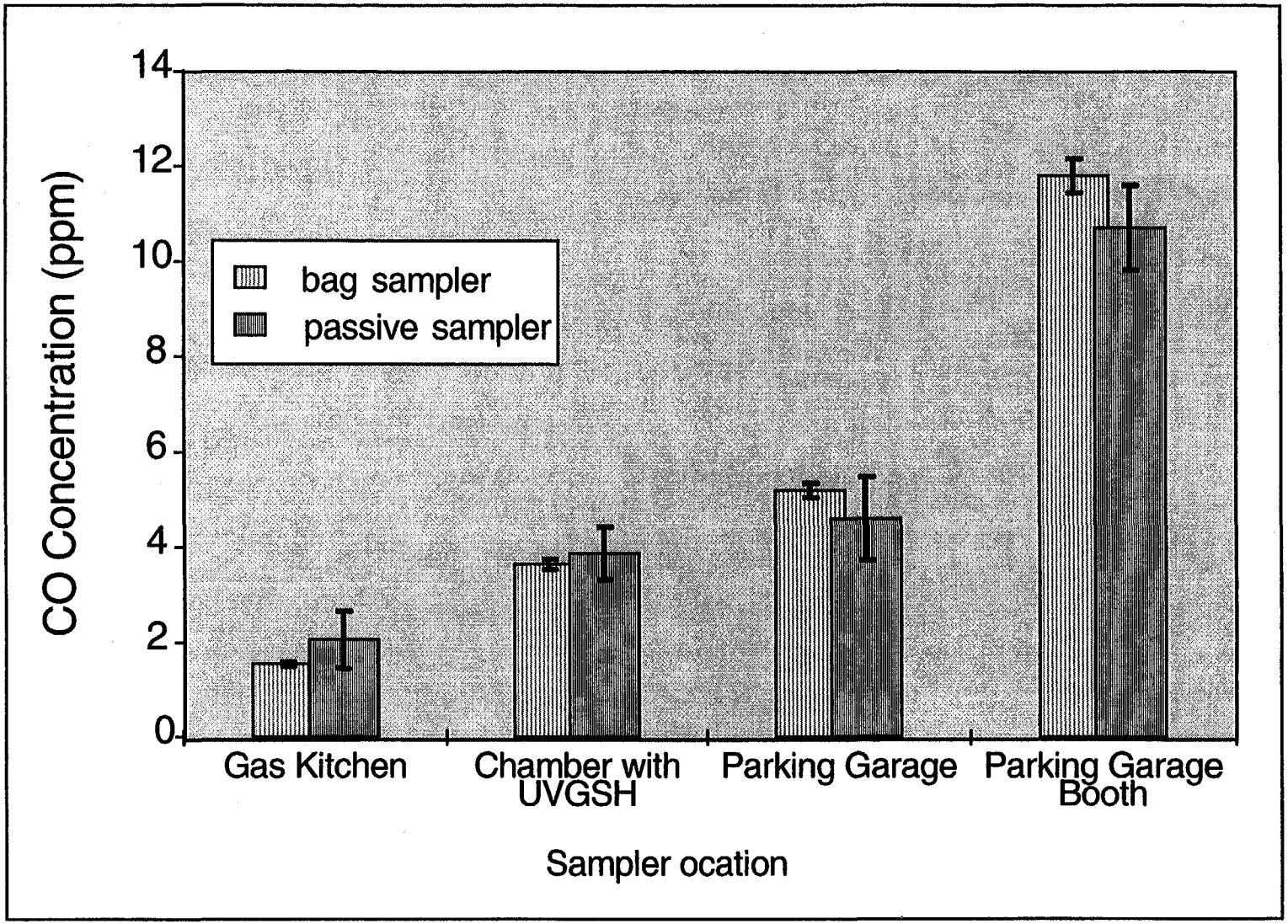

Figure 4-27. Combined preliminary field test results from PS1 and PS2 LBNL/QGI CO passive samplers in four indoor environments. These results are compared to average CO concentrations collected using bag sampler and analyzed using a gas-filter-correlation CO analyzer.

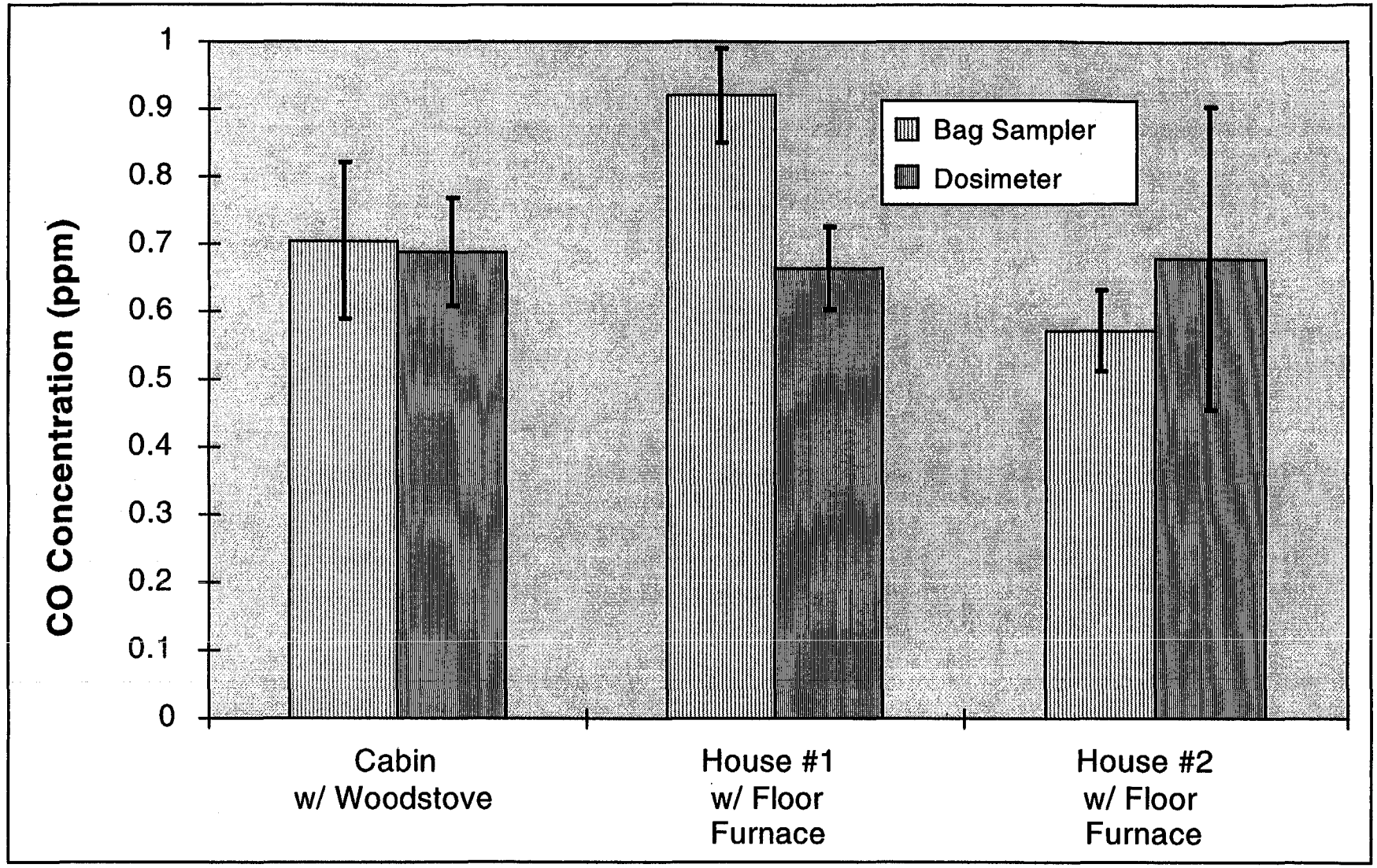

Figure 4-28. Comparison of LBNL/QGI Occupational Dosimeter measurements and bag sampler measurements made in three residences. The dosimeter results are the average of three dosimeters in each case. The error bars indicate plus and minus 1 standard deviation. The bag and dosimeter samples were collected concurrently at the same location for a period of approximately three days at each site.

Chapter 5: A Study of Occupational Carbon Monoxide Exposures

Introduction

The previous chapter discussed laboratory and preliminary field testing results of LBNL/QGI carbon monoxide occupational dosimeters. These results indicated that the D3 prototype dosimeter (called *LOCD* here) was ready to be used in a field validation study to assess its performance through actual industrial hygiene measurements and comparison against a standard CO measurement method. This chapter presents results from such a study.

An assessment of worker CO exposures and indoor CO concentrations was conducted at the Moscone Convention Center (MCC) in San Francisco, CA during the setup of the Mac World trade show. The study was conducted on January 3, 5, and 6, 1997 in collaboration with Crawford Risk Control Services (Crawford), an industrial hygiene firm, contracted by MCC management. Through this arrangement, measurements using the LOCD were collected in parallel with those collected by Crawford. As discussed in the previous chapters, the LOCD was designed to measure workers' time- averaged CO exposures or time-averaged fixed-site CO concentrations. In this survey we used the LOCD in three modes: they were used to measure personal CO exposures on workers who were also monitored by Crawford using conventional CO passive samplers; they were used to sample in parallel with real-time CO monitors that Crawford placed on a number of workers; and they were used to measure time-averaged fixed-site CO concentrations in parallel with air samples collected in gas-tight bags by LBNL. The results of these measurements are presented here.

Ventilation of the MCC poses some unique challenges. The main exhibition areas of the center are underground, with three major loading docks internal to the structure. Considerable concern has been expressed regarding the quality of air, including CO levels, in the MCC during periods when convention exhibits are setup and removed (Blackwell, 1997; Katz, 1997). During peak work periods, some forty propane-powered forklifts are operated nearly continuously throughout the building. Additionally, large numbers of diesel trucks, driven through an interior tunnel system, pull up to the interior docks to move materials in and out of the building. A small number of gasoline- and propane-powered utility lifts are operated intermittently during the decoration of the convention halls.

Measures to improve the indoor air quality of the building were already in place prior to the study reported here (Katz, 1997). These improvements included fitting of catalytic converters to the forklifts, modifications in the building ventilation system, and gaining cooperation from the truck drivers in minimizing unnecessary engine operation.

The relevant occupational health standards should be mentioned in order to put the following discussion into perspective. The current Federal OSHA Permissible Exposure Limit (PEL) for CO is set as a time-weighted-average (TWA) of 50 ppm for an 8-hour shift (OSHA, 1993). The Cal/OSHA PEL for CO is 25 ppm TWA over an 8-hour workshift (Cal/OSHA, 1997). The Biological Exposure Index (BEI) recommended by the American

Congress of Governmental Industrial Hygienists, is designed to ensure that blood carboxyhemoglobin (COHb) levels remain below 3.5% (ACCGIH, 1991). The TLV of 25 ppm is set so that an 8-hour CO exposure will not allow the BEI of 3.5% COHb to be exceeded.

The ultimate COHb level achieved in a CO exposed individual is a function of a number of factors including CO concentration, duration of exposure, and level of physical activity. Thus, it is necessary to consider more than just the 8-hour TWA concentration when assessing whether a worker is protected against CO exposures that could cause them to develop a blood COHb concentration of 3.5% or greater. Consideration of the length of workshift is especially important in the case of the MCC because extended workshifts are common, with workers often working 12 or even 16 hours at a time. Simulations of worker carboxyhemoglobin levels based on CO exposures measured at the MCC were conducted to assess the biological impact of combined CO exposures and extended workshift duration. The results of these simulations are presented here.

Methods

Study Design

The object of this study was twofold. LBNL aimed to assess the behavior of the LOCD under real operating conditions; also, the results were used to help the workers, unions, and management assess the working conditions at the MCC relative to CO exposure levels. Several types of measurements were conducted by LBNL: time-averaged personal sampling of participating workers using the LOCD; time averaged (Dräger diffusion tubes) and real-time personal CO sampling methods (STX70 real-time electrochemical CO dosimeters) used by Crawford, and LOCD/bag sample fixed-site measurement comparisons conducted by LBNL. Figure 5-1 is a diagram of the LOCD, and Figure 5-2 depicts the procedure by which it is deployed and analyzed.

Moscone Convention Center Physical Characteristics

The Moscone Convention Center is located in downtown San Francisco, California. It occupies the space of two city blocks, with halls to the North and South of Howard Street. The main exhibition hall space of the North and South sections are one floor below ground and are interconnected. Overall the MCC contains over 110,000 m^2 (1.2 million ft^2) of floor area. The main underground exhibition hall space of North and South Halls have 17,000 m^2 (181,000 ft^2) and 25,000 m^2 (261, 000 ft^2) of floor area. This space is depicted in Figure 5-3. A tunnel system leading from Howard street down to the subterranean hall level provides truck access to three loading docks with a total of 20 docking bays. The Red Dock, serving the North Hall contains slots for about ten full-sized trailer rigs to back up to. The South Hall is serviced by the Blue and Green Docks, which each can handle about five full-sized rigs at once.

The North and South Halls have separate ventilation systems (Katz, 1996). The truckway tunnel and Red Dock (North) have an air exhaust capacity of 1800 m^3min^{-1} (62,000 cfm) and an air supply capacity of 1300 m^3min^{-1}(45,000 cfm). The Green and Blue docks (South) each have an air exhaust capacity of 900 m^3min^{-1} (32,000 cfm) and an air supply capacity of

600 (22,000 cfm, Katz, 1996). The Heating, Ventilation, and Cooling (HVAC) system of the North Hall provides up to 6000 m^3min^{-1} (206,000 cfm) of airflow to the building, using 100% outside air under normal operating conditions. The HVAC system of South Hall can provide up to 18,000 m^3min^{-1} (607,000 cfm) of outside air. The MCC engineering department is reported to have stated that 100% outside air is used in South hall during exhibition move-in/move-out periods (Katz, 1996).

One particular ventilation condition was considered a potential problem by the MCC engineers and DHS industrial hygienists: Backdrafting of the dock and tunnel air into the MCC halls. This condition had been observed in the past (Katz, 1996), and was a function of unmatched static air pressures between the dock and hall spaces. In particular, a series of large entrances between the Red Dock and North Hall are controlled by huge "elephant" doors. Katz reported that when this condition occurred, an increased amount of diesel exhaust was observed to enter into the structure.

Protection of Human Subjects

The protocol for this study was approved by the University of California Committee for Protection of Human Subjects (CPHS). The protocol was exempted from a full review by the CPHS because the study, as designed, posed no known risk, physical, psychological, or financial to the participants. The risk of physical harm was minimal because the investigation was non-invasive: worker participation in the study was limited to wearing CO monitors during their workshift. The LOCD was designed as a small (1.3 cm x 1.3 cm x 4.5 cm), light-weight, intrinsically safe unit which could be clipped unobtrusively to the lapel of the worker (Chapter 4). No known risk of psychological or financial harm to the participants was anticipated because the participants were selected from a pool of volunteers, and because the protocol was designed to collect the data anonymously. Participants anonymity was ensured because their names were not linked to the CO sample identification.

The protocol proposed to the CPHS, and subsequently employed in the study, included collection of a signed information sheet and consent form prior to enlistment into the survey, and a survey questionnaire to be completed at the end of the workshift. Although the workers' names were collected on the consent form, no personal identification of the participants was made on the survey questionnaire. The survey questionnaire was used to correlate the CO measurements with the workers' job classifications and assignments, employer, and union affiliation; and the current day's location of work within the MCC.

Moscone Convention Center Employer, Union, and Worker Classifications

The study was designed to assess the workers' CO exposure as a function of job classification and union membership. Table 5-1 lists the Job categories included in the study, the unions representing the workers, and the number of participants from each category. An initial interview of participants was conducted when they were recruited. Information on the participant's job classification, union affiliation or management position, employer, and job assignments was collected and correlated with CO measurement identification numbers. After the study was completed this information was compared with the data from the survey questionnaire for quality control.

MCC Employers and Unions

During this study the MCC workforce consisted of employees of Spectator Management Group (SMG), Freeman Decorating Company (FDC), and Sullivan Transfer Co. (STC). The unions which represented these employees were Service Employees International (SEI) Local 14, Sign Display and Allied Crafts (SDAC) Local 510, and Teamsters Local 85, respectively. A total of 154 personal samples were collected during the study. Individuals may have been monitored on one, two, or three of the study days. The total number of individual participants is unknown since the participants were not tracked by name.

MCC Workforce

The *Attendants* (Table 5-1) at the MCC were employed by SMG to assist in the upkeep of the facility. They performed such services as security, housekeeping, trash removal, and trash compaction. Depending upon their assigned tasks they were either stationed at a single location or moved throughout the center during their workshifts. Although many of the workers were located on the exposition hall floors and loading docks in close proximity to forklifts and trucks potentially emitting CO, others were located in areas such as the mezzanine, upper floor meeting rooms, and rest rooms which were distant from direct CO sources.

A number individuals, classified as *Desk Workers,* were employed by SMG in various desk jobs. These workers were located in various offices located throughout the MCC facility. Some of the Desk Workers were located in offices which were in close proximity to a loading dock.

Supervisors were employed by FDC and STC management to oversee work at the docks and on the exhibition hall floor. The nature of the Dock Supervisor position was such that they interacted with forklift and truck operators and were in constant close proximity to the engine exhaust from their machines. Other supervisory positions required these participants to be located on the exhibition hall floor where considerable fork-lift traffic was present throughout the workshift. The *Dock Foreman* was a union position parallel to the Dock Supervisor, and *General Foreman* and *Shop Steward* were union positions which paralleled their respective supervisor categories in terms of location and interaction with forklift and truck operation.

The *Installer/Decorator, Handyman, Dumpmeister* and *Rigger* Job categories primarily involved work on the MCC exhibition hall floors. Their jobs involved construction of the exhibitions and decorations within the hall. These participants were intermittently in close proximity to forklifts as they moved around the exhibition halls. The Riggers operated gasoline powered lifts which were used to reach attachment points on the high ceilings and walls of the building. These lifts were potentially an additional CO source within the building. The Dumpmeister was in charge of coordinating the removal of trash from the exhibition sites as they were constructed.

The *Forklift Operator* operated the Forklifts, while the *Walker* worked on foot next to the forklifts. Obviously, these workers were in constant close proximity to the emissions from the propane powered forklifts. Forklift Drivers and Walkers were observed to work together with the forklift running within the confined space of the long diesel truck rigs. The *Truck Driver* position involved operation of a diesel truck for the MCC, spending considerable time at the loading docks.

Participant Selection

Participants for personal sampling were selected within a rough monitoring strategy established by Crawford in order that approximately the following numbers of workers from each category would be monitored: Decorators 40%; Teamsters 40%; and Attendants/Security 20%. Participants from each category were taken on a first-come, first-serve basis until the number for each category was reached. The participants were notified of the survey by union and management representatives and offered the opportunity to volunteer. Due to the high level of concern over the MCC air quality that had developed among the workers, many individuals came forward as volunteers. No strict quota was set for participants from any particular employer, union, or job category. However, due to the nature of the teamsters' work shifts, it was necessary to seek out these workers as they signed on for the day, and ask them if they would volunteer to participate in they study.

Measurement Methods

Methods Used by LBNL

The LBNL/QGI Occupational Carbon Monoxide Dosimeter (LOCD)

The LOCD, the LBNL/QGI CO Occupational Dosimeter prototype D3, is fully described in the previous chapter. Figure 5-1 depicts the configuration of the device and Figure 5-2 presents the conceptual procedure for its use in exposure assessment.

Eighty-five sensors (QGI MD15, batch AW) which had been stored in individual glass vials on dry silica gel for 45 days were used to manufacture the LOCD for this study (see Chapter 4). The AW sensors had been stored in batches of 50 within sealed glass vials and stored on dry silica gel for about 6 months prior to decanting into individual vials. By the time these LOCD were assembled the AW sensors had been in storage for about 15 months since the date that they were manufactured.

Eighty-five LOCD were assembled from these sensors. Wire clip holders were embedded into the dosimeter sealant during assembly to allow the device to hang from lapel clips. Each LOCD was labeled with a unique identification number. The LOCD caps were pressed firmly in place to ensure that they would not leak prior to deployment. Metal lapel clips with vinyl straps were looped through the LOCD clip holders and snapped into place so that the LOCD could be attached to the lapels of the participants.

Once manufactured, each LOCD was placed in the spectrophotometer for replicate 700 nm absorbance measurements. Prior to these measurements the spectrophotometer had been adjusted to read 0.000A with a LOCD containing no sensor. The average of the initial absorbance measurements was about 1.5A.

During the three days of the study, the LOCDs were reused each day. This was possible since the LOCD could be reused reliably until the capacity of the sensor was reached (an absolute absorbance of about 2.5A - 3.0A), or the silica gel desiccant in the devices was depleted (blue indicator in gel turned clear). Five LOCD were used as controls each day. Of the remaining 80 samplers about 55 were exposed as personal monitors attached to the breathing zone of the study participants, 10 were attached to STX real-time dosimeters worn on the waist of 10 of the participants and the remaining 15 LOCD were attached, in sets of three each, to five bag samplers for fixed-site measurements within the MCC.

At the time of deployment, the LOCDs were uncapped, and the sample identification numbers and deployment times were recorded in conjunction with the anonymous participant information. At the end of the workshift sampling period the LOCDs were retrieved from the participants and capped. Sampling finish times were recorded. The LOCD identification numbers were recorded on the anonymous survey questionnaire, as described above.

LOCD analysis

At the end of each day's workshift the LOCDs were transported back to LBNL for analysis. The 700 nm final absorbance of all of the dosimeters were measured within 3 hours of the end of measurement. Since the devices were re-used each day, the final 700 nm absorbance measurement for the previous day was used as an initial absorbance measurement for the next set of exposures. The exception to this was on January 5, where initial absorbance measurements were made on the night of January 4 because no sampling was conducted that day.

CO exposures were calculated by dividing the measured change in absorbance, dA by the empirically derived response slope ρ (see Equation 17, Chapter 4). The value $\rho = 0.0029$ A-ppm^{-1}h^{-1} was derived from laboratory exposures at 20 °C of the D3 dosimeters using the AW sensors (see Chapter 4). This value was used to calculate CO exposures from the response of dosimeters used for personal monitoring. As discussed in Chapter 4, when the D3 dosimeters were exposed at 10°C the effective slope of the dosimeter response was $\rho = 0.0034$. This value was used to calculate the CO exposures of dosimeters, which were used at fixed sites in parallel with bag samplers because the temperature inside the MCC was considerably lower than 20°C during the sampling periods.

The Bag Sampler

The bag sampler is a very simple device used to collect a sample of CO laden air into an inert gas sample bag over a period of time. The sampler draws at a constant rate so that the concentration of CO in the bag at any time is the average of the sampled bulk-air concentration over that time. Since CO is a non-reactive gas, the sample is not subject to wall loss due to surface reactions. Thus, as long as the bag does not leak, bag samples of CO can be stable over a long time.

The bag samplers used in this study were designed and constructed at LBNL. They were outfitted with peristaltic pumps (Masterflex™, Cole Parmer, Niles, IL) with a flow rate setting of about 10 cc-min^{-1}. The bag samplers were built into a small plastic suitcase and were powered externally using 110 VAC. The internal cavity of the suitcase was large enough to hold an inflated 10 liter air sampling bag (Air Sampling Bag, Tedlar, SKC Inc., Eighty Four, PA.). The inlet tubing of the pump was connected via a bulkhead fitting to the side of the sampler case. The inlet fitting contained a coarse metal screen used to keep insects and large particles from entering the sampler. Tubing from the outlet of the pump was fitted with a luer compression fitting which could be directly connected to a valved fitting on the sampling bag. Tedlar air sampling bags were purged twice with dry pure air and evacuated in preparation for sampling.

During this study the bag samplers were placed at a selected fixed site within the MCC and power was provided via an extension cord. Samplers were prepared by placing a bag into the

sampler case and connecting it to the outlet of the pump. Sampling commenced when the bag valve was opened, allowing a constant flow of ambient air to enter the bag.

Once an air sample was collected it was analyzed using a gas-filter correlation CO analyzer which is maintained in the laboratory (see Table 4-1). This analyzer was calibrated prior to each use. The analyzer draws gas sample at a rate of about 1 lpm. The bags of gas samples collected at the MCC were analyzed within one day of collection. The gas-filter correlation CO analysis method is certified by the U.S. EPA for ambient air monitoring. It is documented to be accurate to ±1 percent for normal CO samples. The bag sampler and CO analyzer measurement combination was considered to be the "Gold Standard" for this study. One problem with the bag samplers used in this project is that they occasionally leak or fail to fill, causing a loss of data.

Methods Used by Crawford

Dräger Diffusion Tubes

The Dräger diffusion tube (Drägerwerk, Lübeck, Germany) is a standard device for measurement of workplace CO exposure. It is a sealed glass tube packed with silica gel beads impregnated with a CO sensitive color indicator. It has a graduated scale printed on it, which represents CO exposure in ppm-h, with a minimum graduation of 50 ppm-h. The device is not recommended for exposures times beyond 8-hours. It is deployed by breaking the glass seal at the inlet end of the tube. The tube is typically worn by the worker throughout the work shift. Although these devices are easy to use, they have been found to have poor accuracy and statistically significant humidity effects (Hossain and Saltzman, 1989). These were placed on the lapel of each participant and a LOCD was paired to each one.

Real-time Datalogging Personal Monitors

The STX70 datalogging CO monitor (Industrial Scientific Corp., Oakdale, PA) was used by Crawford for measuring personal exposures in real-time. This device uses an electrochemical sensor which must be calibrated daily to maintain optimum performance. The internal datalogger in the instrument collects and stores a CO exposure profile at sampling rates as frequent as 1 Hz. Their lower limit of detection is 1 ppm and the monitoring range is 0 to 999 ppm. These monitors were calibrated with CO-free air and 100 ppm CO each day prior to use. In this study they were set to record CO concentrations every minute. An LOCD was taped to each STX70 unit before each shift. The paired devices, weighing about 200g, were attached to the belts of the workers. Each of the 10 participants who wore a real-time datalogger also wore a Dräger diffusion tube and an LOCD in the breathing zone. At the completion of each sampling session, the collected data were uploaded to a computer for analysis. TWA CO exposures were calculated from the data for the workshift period.

Extended Workshifts

During the study a number of the workers worked shifts of up to 12 or 16 hours in duration. Due to these extended workshifts occurring at the MCC some concern has arisen regarding the appropriate guideline with which to compare the workers' measured exposures (Katz, 1997). The logic used for setting of occupational exposure limits for inhaled toxicants is

based upon the assumption that there is a maximum concentration of a contaminant in workplace air to which persons can be exposed with no adverse effect. If this assumption is correct then there is also a threshold for the body burden of these toxicants below which adverse effects would not be likely. The PEL and TLV, and BEI were developed in an attempt to set values for these thresholds. Federal OSHA, Cal/OSHA and the ACGIH all acknowledge the need to analyze the potential that unusual work shifts could push the body burden from environmental exposures above this threshold (ACGIH, 1991; Cal/OSHA, 1983; OSHA, 1980).

Paustenbach has carefully reviewed the currently available methods for determining an appropriate exposure limit for workplace exposures where extended workshifts occur (Paustenbach, 1994). These methods range from applying a simple adjustment factor based upon the ratio of 8-hours to the actual duration of the workshift (the OSHA and Cal/OSHA suggested method) to a series of methods involving the use of physiologically-based pharmacokinetic (PBPK) models. For example, using the OSHA adjustment method the PEL for 16hr exposure to CO would be reduced by a factor of 8hr/16hr, or 0.5. Such adjustments are only recommended for use with chemicals where the exposure limits were set based on their acute (i.e., CO) or cumulative (i.e., lead) nature (OSHA, 1979 and 1993).

Paustenbach compared the adjustment factors produced by the different methods and showed that the differences could be significant. The differences were primarily due to the fact that the simple adjustment method does not account for the time constant for the biological retention of the toxicant, expressed in terms of half-life. The simple adjustment methods tend to be conservative because they do not take into consideration the rate at which the toxicant is released or metabolized. The half lives of various gaseous contaminants can range from 16 minutes for trichlorofluoroethane to 86 hr for nitrobenzene, while the biological half-life for inhaled CO is 1.5 hr (Paustenbach, 1994). Paustenbach states that as a rule of thumb: "Adjustments to TLVs or PELs are not generally necessary for unusual work shifts if the biological half-life of the toxicant is less than 3 hr or greater than 400 hr" (Paustenbach, 1994).

As discussed earlier, the Cal/OSHA PEL is a 25 ppm TWA for an 8-hour workshift. Application of the Cal/OSHA adjustment for 12 and 16 hour workshifts would reduce the PEL to 16.7 ppm and 12.5 ppm, respectively. In the following presentation of results the percent of the measured workers that exceeded the 8 hr, 12 hr and 16 hr PELs will be shown. The biological significance of these measured exposures will then be explored using a PBPK model that simulates COHb levels.

Carboxyhemoglobin Simulation

A PBPK model, *EPAPUF* version 1.3, developed into a computer program and validated by the U.S. Environmental Protection Agency (Benignus, 1994a; Benignus, 1994b; Benignus, 1995) was used to simulate the effects of inhaled CO on development of carboxyhemoglobin (COHb) on MCC workers. The program, run on a personal computer, uses the Coburn-Forster-Kane equation (CFKE; Coburn, 1965) to convert CO exposures in ppm to blood COHb concentrations. The CFKE algorithm is incorporated into a blood gas simulator which can simultaneously vary inhaled oxygen (O_2) and carbon dioxide (CO_2) and CO concentrations in successive iterations, based on 61 blood gas and pulmonary dependent variables (Benignus, 1994). Input parameters for the program include exposure duration,

average CO, CO_2, and O_2 concentration during exposure, body weight, age, height, level of physical exertion, alveolar ventilation, state of physical fitness, etc. The program reports the predicted COHb level reached at the end of each iteration of the program. It is ideal for predicting COHb changes over iteration step duration of one-half hour to eight-hours.

One drawback to the EPAPUF v1.3 program was that it was not possible to change the level of physical exertion from one iterative step to the next. Thus, a single exertion level was constant throughout a simulation run. A new version of EPAPUF which allows for control of the physiological exertion rate for each iteration is forthcoming but was not available for the simulations conducted here.

Results

Throughout the study the level of interest and cooperation from the MCC management, the unions, and the participants was high. The workers showed considerable attention to their work environment, and concern over how it might be affecting their health. Additionally the MCC management showed interest in ensuring that the workers were protected from emissions from CO sources. All of the MCC ventilation systems were clearly operating at a high rate during our visit, based on the palpable movement of air in many parts of the building.

Area Measurements Using Bag Sampler and LOCD

Table 5-2 presents summary data from the fixed-site CO monitoring in the MCC. The measurements were time-weighted 8-hour averages taken during the work days indicated in the table. Figure 5-3 is a map of the underground exhibition hall level of the MCC. It shows the sampling locations for the bag sampler/LOCD data for all three days.

As discussed in the methods section, the temperature in the MCC was colder than 20°C during the study. Unfortunately, detailed temperature measurements were not recorded during the study. Several spot temperature measurements, taken at the Crawford and LBNL operations desk, ranged from 17.8°C to 18.9°C. However, the operations desk was located in an enclosed internal hallway and had less ventilation air supplied, and so was observed to be considerably warmer than the loading docks and interior of the building (see Figure 5-3 for locations of LBNL and Crawford operations desks). The average outside air temperatures for San Francisco, CA on January 3, 5, and 6 were 13°C, 9°C, and 11°C, respectively (NOAA, 1997). During the study, the ventilation systems were set to supply 100% outside air and were operating at a noticeably high rate, providing a continuous supply of cold air. It is estimated that the indoor temperature in the MCC was between 10°C and 15°C during the study. Thus, the value of $\rho = 0.0034$, derived for exposures at 10°C was used to calculate the CO exposures for the fixed-site dosimeters.

The data in the Table 5-2 indicate that the level of agreement between the bag samples, analyzed using a CO analyzer, and the average of 3 LOCD was within 2 ppm and all but 1 were within 1 ppm. The highest fixed-site CO measurements were all at the docks, the highest of which were observed on the Green Dock on January 3 and 6. The bag sampler data (LOCD data) were 11 ppm (11 ppm) and 13 ppm (15 ppm) on these days, respectively. The lowest workday CO averages were observed in the North and South Halls. The set of

three LOCD attached to bag sample number 5, located at the North end of South Hall, averaged 7±2 ppm (the bag sampler at this location failed).

The bag sampler vs. LOCD data are plotted in Figure 5-4. The error bars represent ± one standard deviation about the mean of the three LOCD measurements. The average LOCD data clearly fitted the bag sample data well with essentially no bias: the slope of the fitted regression line was 1.01 (95% confidence interval 0.92 to 1.1). The response was also very linear within the range of measurements ($R^2 = 0.97$).

The average absolute difference between all individual LOCD measurements and the bag samplers was 1.2 ± 1.0 ppm. The average absolute difference between the average of three LOCD measurements and their corresponding bag samplers was 0.7 ± 0.4 ppm. Finally the average of all thirteen pairs of the fixed-site LOCD and bag samples were extremely similar, being 4.8 ± 3.8 ppm and 4.8 ±3.5 ppm, respectively.

Personal Monitoring of Workers Using the LOCD

Occupational exposures often follow a log-normal distribution. Log-normality in the distribution of exposures to air pollutants in space and time arises from the multiplicative interaction of a series of random variables such as source, ventilation and worker mobility (Rappaport, 1991). It was expected that CO exposures measured in this study might follow a lognormal distribution. This was investigated in order to determine the appropriate statistical model with which to present the data.

The distribution of all personal CO exposures measured in this study using the LOCD can be seen in Figure 5-5. The long right hand "tail" of high CO concentrations seen in Figure 5-5 is characteristic of a log-normal distribution (a normal distribution would appear to be more symmetrical about the mean value). These data were tested to verify whether they were better represented by a normal or log-normal model using a graphical method (Becker, Chambers and Wilkes, 1988). In Figure 5-6, the ranking percentiles of each CO datum was calculated. The data were plotted against their corresponding standard normal (Gaussian) quantiles (*i.e.*, zero indicates the mean value and each unit on the x-axis represents one standard deviation away from the mean). A normally distributed dataset would lay on a straight line when plotted in this manner. It clear from the non-linearity of the data in the figure ($R^2 = 0.80$) that the CO exposure data deviated from normality. In order to test the data for log-normality, the natural logarithm of the data were plotted using the same process. The result can be seen in Figure 5-7. The log-transformed data are quite linear ($R^2 = 0.98$), indicating that the data are approximately log-normally distributed and that geometric statistics are probably appropriate for representing the data presented here. The following discussion will focus on the geometric statistics. However, the arithmetic statistics are also included in the tables. In most cases there is only a small difference (1 ppm) between the geometric mean and arithmetic mean.

Statistics presented from the monitoring of worker exposures at the MCC using the LOCD include arithmetic mean (AM) and standard deviation (ASD), geometric mean (GM) and standard deviation (GSD), maximum observed CO TWA, and number of workers monitored on each day.

Personal dosimetry by date

Table 5-3 presents a summary of the LOCD 8-hour workshift TWA personal monitoring data for three monitoring days in January, 1997. Over the three days of the study, 154 8-hour workshifts were monitored using the LOCD; 52, 51, and 51 individuals were monitored on January 3, 5, and 6, respectively.

The GM of all the workers' TWA CO exposures for the three days was 7 ppm (GSD = 1.6). Since the GM of a distribution approximates its median, this means that 50 percent of the workers had average workshift CO exposures greater than 7 ppm. Figure 5-5 shows the actual distribution of TWA CO exposures for all three days of measurements. The histogram bin labels on this figure and those following indicate the midpoint of the bin range. For example a "9" indicates the bin range >8 through <= 10.

Recall that the TWA 8-hr TLV and Cal/OSHA PEL = 25 ppm, and the OSHA PEL = 50 ppm. Roughly 8%, 5% and 1% of the participants had workshift average exposures above 12.5, 16.7, and 25 ppm, respectively. Only one worker had an exposure above the 25 ppm standards and no worker was exposed above the 50 ppm PEL.

Figures 5-8 through 5-10 show how the actual measured exposures were distributed for the days of January 3, 5, and 6, respectively. The highest average and highest individual exposure value both occurred on January 3, when the GM was 8 ppm (1.6) and the maximum TWA was 34 ppm (Table 5-3). On January 3 about 13% of all the workers that were monitored were exposed to TWA CO concentrations above 12.5 ppm, 10% were exposed above 16.7 ppm, and 2% (one individual) was exposed above 25 ppm (Table 5-3).

Personal dosimetry by job category

Table 5-4 presents the dosimetry data summarized by job category. Figures 5-11 through 5-14 present how the actual measured exposures were distributed for the Job categories of Attendant, Forklift Operator, Installer/Decorator, and Supervisor. The highest GM of 8-hour workshifts was observed in the group of Forklift Operators. This group of workers had a GM of average shift exposures of 9 ppm (1.6), and the maximum 8-hour exposure was 34 ppm. About 12%, of the Forklift Operator shift exposures were above 16.7 ppm and one of these workers (6% of Forklift Operators) had a measured 8-hour exposure in excess of the 25 ppm 8-hour PEL.

After the Forklift Operators, Dock Foreman, and Walker and Handyman Job categories had the highest maximum observed 8-hour TWAs of 20 - 21 ppm. About 25% of the exposures of Dock Foreman and about 20% of the Walker exceeded 16.7 ppm. From Table 5-4 it is evident that the Dock Foreman, Walkers, and Handyman categories [GMs of 8 (1.7) and 9 ppm (1.7), 8 ppm (1.8), respectively] were similar to those of the Forklift Operators [GM 9 (1.6)] in terms of exposure. Although only one workshift measurement was made of the exposure of a Truck Driver, the TWA exposure for this worker was 18 ppm. The Dumpmeister and Supervisor categories also had similar exposure means but lower variability and maximum values. The combined data for Dock Foreman and Walker and Handyman jobs were not statistically different from the Forklift Operators (Students two-tailed t-test, p = 0.89).

Workers in the Installer/Decorator and General Foreman Job categories were exposed to lower TWA CO concentrations, both with a GM of 7 ppm (1.4). However, the maximum 8-

hour TWA for the Installer/Decorators was 16 ppm. The Attendants had a similar exposure distribution with a GM of 6 ppm (1.6) and a maximum TWA worker exposure of 17 ppm. About 2% of the Installer/Decorators, and 3% of the Attendant Job categories were exposed to workshift TWA CO concentrations above 16.7 ppm. Attendants exposures were not significantly different from Installer/Decorators (Student's two-tailed t-test test, $p = 0.89$).

The job category with the lowest exposures was the Desk Workers with a GM of 5 ppm (1.8), and a maximum of 10 ppm for one participant. Of the four participants in this category, 25%, or one of them, had a workshift average CO exposure of 10 ppm.

Student's two-tailed t-tests comparing the combined Dock Foreman, Walker, Handyman, and Forklift Operator categories against the Installer/Decorators showed that they were significantly different ($p = 0.005$).

Personal dosimetry by location

Table 5-5 presents the exposure study by location. The participants in the study worked in areas throughout the MCC. The majority of workers (71%) worked predominantly in one of the following areas throughout their work shift: North Hall, South Hall, Blue Dock, Green Dock, or Red Dock. A number of participants (13%) reported that they worked predominantly in an area other than those just listed, which include the Mezzanine and Esplanade areas of the South MCC structure. Additionally 32 of the participants (21%) reported that they worked in several of the locations listed above, or throughout the building during their work shifts.

The dock workers appeared to have the highest workshift average exposures. The GM TWA at the Green Dock was 12 ppm (1.7), with a maximum exposure of 21 ppm for an 8-hour period. The highest exposure occurred at the Red Dock where one worker was exposed to a TWA of 34 ppm. Figures 5-15 through 5-17 present the exposure distribution of participants who worked at the Red Dock, Green Dock, and Blue Dock, respectively. From the figures and table, 34% of the workers at Green Dock had workshift CO exposures above 16.7 ppm. Similarly, a TWA of 16.7 ppm was exceeded by 8% of the workers at the Red Dock. No workers at the Blue Dock had exposures above 12.5 ppm.

The exposure distribution data for North and South Hall are presented in Figures 5-18 and 5-19. The CO distributions in the two halls were not dissimilar with GMs of 6 ppm (1.5) and 7 ppm (1.3) for North and South Halls, respectively. No workers' exposures in North Hall or South Hall exceeded 12.5 ppm.

Participants working in the areas such as the Mezzanine and Esplanade appear to have the lowest exposures with a GM of 6 ppm (1.3) and a maximum TWA CO exposure of 9 ppm. Those individuals who reported that they worked "all over" had a GM of TWA exposures of 7 ppm and a maximum for a worker of 17 ppm.

Personal dosimetry by union affiliation

Table 5-6 presents the worker exposures by union affiliation. Workers affiliated with the Teamsters Union Local 85 appear to have had the highest TWA CO exposures with a GM of 8 ppm (1.7) and a maximum TWA exposure of 34 ppm. Interestingly the Management category also had a GM of 8 ppm (1.4), however, the maximum exposure for this group was

15 ppm. Figures 5-20 and 5-21 present the observed CO distribution for the Teamsters and Management. It can be seen that about 16% and 14% of the Teamsters had TWA exposures above 12.5 and 16.7 ppm, respectively.

Members of SDAC Local 510 and the SEI Local 14 had their CO exposures distributed very similarly, with GMs of 7 and 6, respectively (See Figures 5-22 and 5-23). Maximum CO exposures for workers in these unions were 17 ppm in both cases.

Personal dosimetry by employer

Table 5-7 presents the exposure summary data by employer. The workers employed by Sullivan Transfer Co. received the highest CO exposures, on average, with a GM of 8 ppm (1.6). The maximum TWA CO exposure of 34 ppm was experienced by an employee of this company. Additionally, about 15% and 12% of the STC employees experienced TWA exposures above 12.5 and 16.7 ppm, respectively (see Figure 5-24).

Employees of SMG and FDC experienced a similar exposure distribution, with GMs of 6 ppm (1.6) and 7 ppm (1.5), and maximum exposures of 17 ppm and 16 ppm, respectively. About 3% of the SMG employees and 11% of the FDC employees experienced a workshift TWA above 16.7 ppm (see Table 5-7 and Figures 5-25 and 5-26).

Real-time Personal Monitoring of Workers

Table 5-8 presents a comparison of exposure measurements made using the Crawford real-time monitors, an LOCD attached to a real-time monitor, and the LOCD attached to the lapel of the participant wearing the real-time monitor. With the exception of the example used below, the real-time profiles collected by Crawford are not included here. The workshift TWA calculated from the real-time data are presented in Table 5-8. There are a number of disagreements between the real-time data and the LOCD measurements. The real-time monitors' calibrations appear to have been biased low. This caused a number of the instruments to give falsely low averages: a number of the calculated TWA values were low enough to be inconsistent with the observed levels in the MCC during the days of this study as measured using the bag samples, the Dräger tubes, and the LOCD. It should be noted that the LOCD measurements are not likely to be in error to the extent of their disagreement with the real time monitors. The LOCD indicated a consistent agreement with the bag sampler measurements in the MCC during the same sampling period. The average LOCD measurements were within 1 ppm of the bag samplers on all but one comparison, in which the difference was 2 ppm. In contrast, the difference between the LOCD and the TWA real-time measurements were as great as 13 ppm. The averages of all 29 pairs of usable real-time and LOCD TWA data were 3.4 ppm and 6.3 ppm, respectively. An analysis of the data shows that the real-time TWA was greater than 2 ppm lower than the LOCD 70% of the time and 5 or more ppm lower 28% of the time.

A comparison of the waist-level LOCD vs. the lapel LOCD measurements indicates that the TWA CO levels at the lapel (breathing zone) tend to be several ppm higher in most cases. On average the lapel measurements were 8.5 ± 4.5 ppm versus 6.3 ± 3.5 at waist height. The reason for this is unknown, and the following discussion is speculative. It is possible that it is related to the location of the exit of the forklift exhaust pipes, which are above waist height but below lapel height. Because hot engine exhaust is buoyant until cooled, it would rise as

it mixed with the bulk air. Thus the undiluted exhaust may have disproportionately exposed the lapel samplers rather than the waist-high samplers.

One interesting observation is that four of the five forklift operators' waist LOCD measurements were greater than or equal to the lapel measurement. In contrast, only 3 of 24 of the other worker categories' measurements followed this pattern. This may be because the seated forklift operators were positioned above the exhaust outlet of their machines so that both the waist and the lapel were in the plume of undiluted exhaust. Whatever the cause of the waist/lapel height discrepancy, the difference indicates that it is important to measure worker CO exposure at breathing level rather than the waist level.

Figure 5-27 depicts a real-time CO exposure profile of one of the participants in the CO study (job category: Walker; location: Green Dock; date: 1/6/97, on Table 5-8). This monitoring session is representative of the types of exposure profiles expected from the MCC workers, however, the one presented here had the highest observed 8-hour average CO concentration of those with real-time monitors: 16.4 ppm. The data in the figure have been smoothed by plotting 5-minute average concentrations. In the case of this worker, a 5-minute average peak CO concentration of about 55 ppm was observed. In fact, the 1-minute peak reached about 160 ppm. The LOCD which was attached to this real-time monitor measured a TWA of 13 ppm and the LOCD attached to the worker's lapel measured a TWA of 21 ppm.

Comparison of parallel LOCD and Dräger diffusion tube exposure measurements.

Figure 5-28 presents a plot comparing 8-hour TWA LOCD vs. Dräger exposure measurements conducted by Crawford for the 136 instances where both types of dosimeters were worn simultaneously by participants. The LOCD measurements were a subset of the 154 from which the data above are presented. Ten additional Dräger Tubes that had been paired with LOCD were lost because they dropped loose from their lapel clips during the workshift. Unfortunately, one important Dräger Tube sample that was lost was the mate to the highest LOCD measurement of 34 ppm worn by a Forklift Operator. Eight LOCD were deployed on participants without paired Dräger tubes.

The Dräger Tube data in Figure 5-28 fall into discrete values relating to the graduated scale printed on the tubes. The lowest graduation on the tubes is 50 ppm-h which corresponds to an 8-hour TWA of 6.3 ppm (i.e., 50 ppm-h/8-hr = 6.3 ppm). The discrete levels of Dräger data below 6.3 ppm indicate attempts at visual interpolation between zero and 50 ppm-h.

The overall scatter of Dräger data (Y axis) of Figure 5-28 shows that the correlation between the Dräger data and the LOCD data was quite poor. A regression line for all 135 data points had a slope of 0.63 (R^2 = 0.37). A regression of the Dräger data below 6.3 ppm and their corresponding LOCD data had an even poorer correlation (R^2 = 0.44) and a slope of 0.61. When only the paired data with Dräger Tube TWA values of 10 ppm or more were considered the slope was 0.80 (R^2 = 0.58). The average absolute value of the difference between the Dräger and the LOCD was 3.1 ± 2.5 ppm. This can be compared to the similar statistic for the LOCD comparison to the bag samplers presented above which showed that the average difference between bag samples and individual LOCD measurements was 1.2± 1.0 ppm.

If the assumption that the LOCD data are more accurate than the Dräger at low exposures is correct, the above comparison indicates that attempts to interpolate below the 50 ppm-h minimum graduation of the Dräger tubes does not yield accurate information. Even for the Dräger TWA measurements (≥ 10 ppm) the correlation coefficient was only 0.58. Additionally the slope of the Dräger-LOCD relationship indicates that the Drägers' measurements were about 60% of the LOCD values. This improved slightly for the Dräger measurements above 10 ppm where the Dräger values were about 20% lower than the LOCD.

Three of the 10 Dräger data points where the LOCD TWA was above 15 ppm gave measured values which were about 30% of the LOCD value. The reason for these low values is not clear, but may be due to variability in the Dräger tubes. Such low response from measurements well above the limit of detection is disconcerting.

Simulation of Worker Carboxyhemoglobin Concentrations

In order to place the CO exposures observed in this study in perspective, COHb simulations were conducted. As discussed above, these simulations were run on a personal computer using the EPAPUF v1.3 program. The program was set to simulate a 35 year old male subject, 90 kg (200 pounds), non-smoker, in good physical shape. These simulations were run in order to assess the biological burden of the workers' CO exposure and to compare it to the BEI of 3.5% set by the ACGIH. The COHb data produced in the simulations were also intended to be used to assess the need to apply extended workshift adjustments to the Cal/OSHA PEL.

Figure 5-29 presents two simulations, one at rest (33 watts) and one at light exertion (50 watts) over a 16 hour workshift. The real-time CO exposure profile measured at the MCC, as shown in Figure 5-27, was used to drive these simulations. However, the CO exposure profile was run through twice in order to create the 16-hours of input data. The 8-hour and 16-hour average concentrations for these input data are both 16.4 ppm. It can be seen that at about 500 minutes (8 hours) the simulated COHb levels had reached approximately 2.4% and 2.6% COHb for the light and moderate exertion models, respectively. Over the next 8 hours the COHb levels did not rise significantly, peaking at 2.7% and 2.8%, respectively. The COHb levels dropped to less than 0.6% over the 8-hour rest period after work exposures had ceased.

Figures 5-30, 5-31,and 5-32 depict COHb simulations using 10 ppm, 16.4 ppm, and 25 ppm TWA exposures, respectively. Each figure presents a superimposed COHb profiles for 8-hr, 12-hr, and 16-hr workshifts for three consecutive days. These simulations used the same physical characteristics as in Figure 5-29, and a slight to moderate level of physical activity (approx. 33 Watts). They assumed an average CO exposure of 4 ppm during the non-working periods, which was probably conservative. It can be seen that the dominating effect on ultimate COHb levels was the TWA CO exposure, not the length of work shift or the number of days of consecutive work. In fact, the peak COHb levels for the 16-hour work day were only slightly greater than those for the 8-hour day.

Discussion

Both fixed-site measurements and personal sampling indicate that the highest exposures occurred at the docks, particularly, the Green Dock. In general, the personal exposures appeared to be higher than the area measurements. This is not surprising since worker activities often tend to include time spent in close proximity to the forklifts, whereas, by nature the fixed-site samplers are located safely out of the way of the forklift traffic. The CO concentrations observed at the fixed-sites may be considered the baseline levels (reflecting the air mixed with engine emissions) to which all workers in an area were exposed. In contrast, the personal exposures were likely to include the added CO due to direct exposure to engine exhaust which has not yet mixed into the bulk air of the room.

Personal Monitoring

The personal exposures experienced during 154 individual workdays have been presented from several different perspectives. It is clear that a considerable amount of CO was present in the MCC, and that the potential for high personal CO exposures is real. One TWA exposure (34 ppm) exceeded the 25 ppm Cal/OSHA PEL. If the rate at which ventilation with clean outdoor air were to be set lower than it was during this study, as it had been in previous years, higher CO exposures would be expected.

There does not appear to be a large difference between the exposure distributions of the three days of the study, although those on January 3 were slightly higher. In contrast, there do appear to be big differences in exposure distributions between different job categories, different locations, different union affiliations, and different employers. Obviously, the forklift and truck exhaust are the source of the CO in the MCC. All of the above differences can be explained through understanding how the various work patterns involve interaction with these machines and their exhaust.

By job category, those workers who directly interacted with the forklifts and trucks are the highest exposed. This includes the Forklift Driver, the Walker, Truck Driver, and Dock Foreman. Not surprisingly, this is reflected in the analysis by location, union, and employer: these workers are based at the docks, they belong to the Teamsters union and they are employed by STC.

One task was observed which probably results in the highest CO exposure: a forklift is driven into the trailer of a big rig truck for the purpose of unloading materials. This activity constitutes operation of an internal combustion engine in a confined space. The Forklift Operator, or a Walker on foot alongside a forklift, inside the truck may be exposed to very high CO levels.

The Job categories with the lowest exposures appeared to be Attendant, Installer/Decorator, and General Foreman. Workers in these categories were mostly on the floor in North and South halls. The workers in these categories are mostly represented by the SDAC and SEI unions, and employed by FDC and SMG.

Methods comparison: Dräger vs. LOCD

Based on the results, the LOCD appears to have been able to provide considerably more accurate CO exposure data than the Dräger Dosimeter Tubes. The overall accuracy of

TWA measurements of the Dräger tubes appears to be about ± 3 ppm in the range of exposures whereas the LOCD accurate to about ±1 ppm. Based upon the comparisons with bag samples, the average of three LOCD samplers was in almost perfect agreement with the bag sampler. In contrast, the Dräger data were on average 60% lower than the LOCD, underestimating CO concentrations by about 40%.

Simulated Carboxyhemoglobin Concentrations

Due to the widespread use of extended work hours during convention setup and removal period consideration of an adjustment to the Cal/OSHA PEL was prudent, to ensure that no workers develop COHb blood concentrations in excess of BEI of 3.5%. The Cal/OSHA Hygiene Manual recommends recalculated exposure limits based on workshift duration. The COHb simulations presented above allow us to place the exposure data into perspective relative to the BEI. However, it is important to remember that the simulations are not real COHb measurements, but derived from knowledge of the physiology of CO uptake and removal in the human body; these particular simulations should be validated with careful COHb measurements prior to using them in any way that might adversely affect worker exposures.

The implication of the COHb simulations is that the duration of workshifts beyond 8-hours makes little difference in the ultimate COHb concentration. Carboxyhemoglobin concentrations reach steady-state after about 8 to 10 hours, bringing into question the need to apply Cal/OSHA recalculation of the PEL for CO for extended workshifts. The three-day simulations shown in Figures 5-30 through 5-32 clearly show that that the ultimate COHb levels are dictated by average concentration. Peak COHb levels reach roughly 1.5% at 10 ppm workshift exposures and 4 ppm off-shift exposures. The COHb peaks at about 2.5% when the workshift exposures are raised to 16.4 ppm. Finally, COHb levels approach 3.5% when 25 ppm exposures are simulated. Exposures to 25 ppm appear to be required to approach 3.5% COHb, regardless of the duration of the workshift. This is consistent with the rule-of-thumb suggested by Paustenbach discussed earlier: the half-life for retention of CO in the body is about 1.5 hours which is less than the 3 hour minimum half-life suggested as a threshold for applying adjustment to the PEL for unusual workshifts. Thus, most likely a downward adjustment of the 25 ppm PEL would be overly protective since the BEI itself has been designed to ensure that worker health and safety are preserved.

Conclusions

With regard to the primary goal of the study, the LBNL/QGI occupational dosimeter technology appears to have performed well. The LOCD was able to withstand the rigors of workplace sampling without failing. Over 154 8-hour personal samples were monitored on workshifts over three days. Exposure distributions were calculated with an estimated precision of ± 1 ppm. None of the LOCD failed or were lost. The LOCD was used to compare results with the Dräger Diffusion Tube, a standard industrial hygiene tool for monitoring workplace CO exposures. The comparison suggests that the Dräger device read about 40% low overall, and 20% low for observed TWA concentrations ≥ 10 ppm.

Operations in the MCC expose workers CO levels above those normal for non-working conditions. However, computer simulations suggest that most of the workshift CO

exposures are not sufficient to cause worker blood COHb concentrations to reach the BEI of 3.5%. Nonetheless, all of the participants in the study were exposed to CO concentrations well above background levels. Seemingly small changes in the operation of forklifts and trucks, or the ventilation system may have a large impact on CO exposures. If a change in forklift emissions or ventilation patterns were to occur CO exposures could easily cross the threshold from "compliance" to "exceedence" of occupational health and safety standards.

One issue not discussed in this report is worker exposures to engine pollutant emissions other than CO. Although not the focus here, other pollutants including nitrogen dioxide, particles, or volatile organic compounds, emitted from diesel or propane engines may cause irritation to the respiratory systems and mucous membranes of exposed workers. The MCC ventilation may be sufficient to protect against excessive CO levels and be insufficient for removing these other compounds to safe and non irritating levels.

It is a tribute to the MCC operations that given the large number of forklifts and trucks that operate in the facility, that the workers' CO exposures do not exceed the exposure limits. This is particularly true given the task of ventilating a structure with an internal, underground loading dock. Nonetheless, an ongoing effort must be made to ensure that the working conditions in the MCC remain safe and that the workers remain healthy. This task will require continual vigilance on the part of the MCC building operators.

References

ACGIH (1991). *Documentation of the Threshold Limit Values and Biological Exposure Indices.* 6th ed. Cincinnati, Ohio. American Conference of Governmental Industrial Hygienists.

Becker, R. A., Chambers, J. M., and Wilks, A. R. (1988). *The New S Language. A Programming Environment for Data Analysis and Graphics*, Wadsworth & Brooks/Cole Advanced Books & Software, Pacific Grove, CA.

Benignus, V. A. (1994a). *EPAPUF A Blood-Gas and Pulmonary Simulator Users Manual, Version 1.3.,* U.S. Environmental Protection Agency, Research Triangle Park, NC.

Benignus, V. A., Hazucha, M. J., Smith, M. V., and Bromberg, P. A. (1994b). "Prediction of carboxyhemoglobin formation due to transient exposure to carbon monoxide," *Journal of Applied Physiology*, 76(4), 1739-1745.

Benignus, V. A. (1995). "A Model to Predict Carboxyhemoglobin and Pulmonary Parameters After Exposure to O_2, CO_2, and CO." *Aviation, Space, and Environmental Medicine*, 66, 369-74.

Blackwell, S. (1997). "Moscone Maladies." *San Francisco Bay Guardian*, San Francisco, CA, March 5,11.

Cal/OSHA. (1983). *State of California Division of Occupational Safety and Health Industrial Hygiene Technical Manual*, California Department of Health Services, Occupational Safety and Health Administration, Sacramento, CA.

Cal/OSHA. (1997). "Title 8 - General Industry Safety Orders, Section 5155 - Airborne Contaminants." *California Code of Regulations,* Register 97 No. 22; 5-30-97, Sacramento, CA.

Coburn, R. F., Forster, R. E., and Kane, P. B. (1965). "Considerations of the physiological variables that determine the blood carboxyhemoglobin in man," *Journal of Clinical Investigation*, 44, 1899-1910.

Hossain, M. A., and Saltzman, B. E. (1989). "Laboratory Evaluation of Passive Colorimetric Dosimeter Tubes for Carbon Monoxide." *Applied Industrial Hygiene*, **4**, 119-125.

Katz, E., and Osorio, A. M. (1997). "Letter to J. Moerschbaecher, Convention Facilities, City and County of San Francisco." , Department of Health Services, Occupational Health Branch, Berkeley, CA.

NOAA. (1997). "Global Summary of the Day Data set on NOAA Worldwide Website." , National Oceanic and Aeronautic Administration, Hyattsville, MD.

OSHA. (1993). "CFR Part 1910.1000 Air Contaminants, Table Z-1; Amended by Fed. Reg. 58:35308, 35340 (June 30, 1993); corrected by Fed. Reg. 58:40191 (July 27, 1993)," U.S. Department of Labor, Occupational Safety and Health Administration.

OSHA. (1980). *Industrial Hygiene Field Operations Manual*, Volume VI, OSHA 3058, U.S. Department of Labor, Occupational Safety and Health Administration, Washington, D.C.

Paustenbach, D. J. (1994). "Occupational Exposure Limits, Pharacokinetics, and Unusual Work Schedules." In: *Patty's Industrial Hygiene and Toxicology, Vol. 3A, The Work Environment*, Chap. 7, R. L. Harris, L. J. Cralley, and L. V. Cralley, eds., John Wiley and Sons, Inc., New York, NY., 198-348.

Rappaport, S. M. (1991). "Assessment of Long-term Exposures to Toxic Substances in Air." *Annals of Occupational Hygiene*, **35**(1), 61-121.

Tables

Table 5-1. Job categories for which workers were monitored for CO during 1/3, 1/5, and 1/6/1997 at the Moscone Convention Center

Job Title	Union	Employer	Number of personal samples collected[1]
Attendant	SEI 14	SMG	33
Desk Worker	Management	SMG	4
Dock Foreman	Teamsters 85	STC	12
Dumpmeister	SDAC 510	FDC	2
Forklift Operator	Teamsters 85	STC	17
General Foreman	Teamsters 85	STC	7
Handyman	Teamsters 85	STC	6
Installer/Decorator	SDAC 510	FDC	49
Rigger	SDAC 510	FDC	4
Shop Steward	SDAC 510	FDC	3
Supervisor	Management	FDC, STC	11
Truck Driver	Teamsters 85	STC	1
Walker	SDAC 510	FDC	5

[1]Some participants were monitored on one, two or three days so that the actual number of participants was less than the number of workshifts monitored.

Table 5-2. LOCD and Bag Sampler Fixed-site Monitoring Carbon Monoxide Data from the Moscone Convention Center CO Study, January, 1997.

Bag Sample Number	LOCD Average Concentration (ppm)[a]	Bag Concentration (ppm)	Location[b]	Date
1	4±1	3.5	Red Dock	1/3/97
2	11±1	11	Green Dock	1/3/97
3	5±2	5.4	Red Dock at trash Compactor	1/3/97
4	3±1	2.2	North Hall (Hall E)	1/3/97
5	7±2	NA	South Hall (North end)	1/3/97
6	1±1	NA	North Hall	1/5/97
7	3±1	3.6	Green Dock at desk	1/5/97
8	3±3	2.8	Red Dock (East end)	1/5/97
9	2±1	3.0	Breezeway between Green Dock and South Hall	1/5/97
10	2±2	2.9	Floor 1 Lobby	1/5/97
11	15±3	13	Green Dock at desk	1/6/97
12	3±1	4.1	Red Dock at Supervisor Desk	1/6/97
13	4±1	3.5	Red Dock (East end)	1/6/97
14	4±1	5.2	Breezeway between Green Dock and South Hall	1/6/97
15	3±0	2.1	North Hall (Northwest corner)	1/6/97

[a]Average of three LBNL/QGI Occupational Carbon Monoxide Dosimeters
[b]Figure 5-3 shows the locations within the MCC.

Table 5-3. Moscone Center CO exposure survey summary statistics by date of measurement. These data were collected using the LBNL/QGI CO Occupational Dosimeter and reflect time-weighted-average 8-hour workshift concentrations.

Measurement Date	Arithmetic Mean (ppm)	Arithmetic Standard Deviation (ppm)	Geometric Mean (ppm)	Geometric Standard Deviation	Max (ppm)	>12.5 ppm (%)	>16.7 ppm (%)	>25 ppm (%)	Num. Obs. (N)
All 3 Days	8	4	7	1.6	34	8	5	1	154
1/3/97	9	5	8	1.6	34	13	10	2	52
1/5/97	7	2	7	1.4	15	2	0	0	51
1/6/97	8	4	7	1.6	21	4	2	0	51

Table 5-4. Moscone Center CO exposure survey summary statistics by job category. These data were collected using the LBNL/QGI CO Occupational Dosimeter and reflect time-weighted-average 8-hour workshift concentrations.

Job Category	Arithmetic Mean (ppm)	Arithmetic Standard Deviation (ppm)	Geometric Mean (ppm)	Geometric Standard Deviation	Max (ppm)	>12.5 ppm (%)	>16.7 ppm (%)	>25 ppm (%)	Num. obs (N)
All job categories	8	4	7	1.6	34	8	5	1	154
Attendant	7	3	6	1.6	17	9	3	0	33
Desk worker	6	3	5	1.8	10	0	0	0	4
Dock foreman	9	5	8	1.7	21	25	8	0	12
Dumpmeister	9	0	9	1	9	0	0	0	2
Forklift operator	10	7	9	1.6	34	12	12	6	17
General foreman	7	3	6	1.5	11	0	0	0	7
Handyman	10	6	8	1.8	20	17	17	0	6
Installer/decorator	7	3	7	1.4	16	2	2	0	49
Rigger	8	3	8	1.4	11	0	0	0	4
Shop steward	7	1	7	1.1	8	0	0	0	3
Supervisor	8	2	8	1.3	11	0	0	0	11
Truck driver	18	NA	18	NA	18	100	100	0	1
Walker	10	6	9	1.7	21	20	20	0	5

Table 5-5. Moscone Center CO exposure survey summary statistics by work location. These data were collected using the LBNL/QGI CO Occupational Dosimeter and reflect time-weighted-average 8-hour workshift concentrations.

Moscone Center Location	Arithmetic Mean (ppm)	Arithmetic Standard Deviation (ppm)	Geometric Mean (ppm)	Geometric Standard Deviation	Max (ppm)	>12.5 ppm (%)	>16.7 ppm (%)	>25 ppm (%)	Num. Obs. (N)
All Locations	8	4	7	1.6	34	8	5	1	154
North Hall	7	3	6	1.5	15	2	0	0	45
South Hall	8	2	7	1.3	12	0	0	0	24
Blue Dock	8	4	7	1.9	12	0	0	0	3
Green Dock	13	6	12	1.7	21	50	34	0	12
Red Dock	9	6	8	1.5	34	8	8	4	25
All other indoor areas	7	2	6	1.3	9	0	0	0	13
All over	8	4	7	1.7	17	9	3	0	32

Table 5-6. Moscone Center CO exposure survey summary statistics by union. These data were collected using the LBNL/QGI CO Occupational Dosimeter and reflect time-weighted-average 8-hour workshift concentrations.

Unions at Moscone Center	Arithmetic Mean (ppm)	Arithmetic Standard Deviation (ppm)	Geometric Mean (ppm)	Geometric Standard Deviation	Max (ppm)	>12.5 ppm (%)	>16.7 ppm (%)	>25 ppm (%)	Num. Obs. (N)
All Unions	8	4	7	1.6	34	8	5	1	154
SEI Local 14	7	3	6	1.6	17	9	3	0	33
Teamster Local 85	10	6	8	1.7	34	16	14	2	44
SDAC Local 510	7	3	7	1.5	17	2	0	0	63
Management	9	3	8	1.4	15	7	0	0	14

Table 5-7. Moscone Center CO exposure survey summary statistics by Employer. These data were collected using the LBNL/QGI CO Occupational Dosimeter and reflect time-weighted-average 8-hour workshift concentrations.

Employer	Arithmetic Mean (ppm)	Arithmetic Standard Deviation (ppm)	Geometric Mean (ppm)	Geometric Standard Deviation	Max (ppm)	>12.5 ppm (%)	>16.7 ppm (%)	>25 ppm (%)	Num. Obs. (N)
All Employers	8	4	7	1.6	34	8	5	1	154
FDC.	7	2	7	1.5	16	2	0	0	67
SMG	7	3	6	1.6	17	6	3	0	35
STC.	9	6	8	1.6	34	15	12	2	52

Table 5-8. Time-weighted average CO exposures measured at the Moscone Convention Center using Crawford Risk Control Services real-time CO monitors, LBNL/QGI CO Occupational Dosimeter (LOCD) attached to the real-time monitor, and an LOCD attached to the lapel of the worker wearing the real-time monitor.

Worker Job Classification	Location	TWA CO Real-time (ppm)	TWA CO LOCD w/Real-time (ppm)	TWA CO LOCD on Lapel (ppm)	Date
Attendant	All over	0	2	3	1/5/97
Attendant	North Hall	2	3	8	1/3/97
Attendant	North Hall	1	2	3	1/5/97
Attendant	North Hall	4	5	6	1/5/97
Attendant	North Hall	3	3	15	1/6/97
Attendant	North Hall	1	3	3	1/6/97
Attendant	Red Dock	Failed	6	17	1/3/97
Attendant	South Hall	2	7	8	1/6/97
Attendant	S. Mezzanine	1	3	3	1/3/97
Dock Foreman	Red Dock	1	5	8	1/5/97
Dock Supervisor	Green Dock	0	5	8	1/3/97
Dock Supervisor	Green Dock	6	10	15	1/5/97
Forklift Operator	North Hall	3	6	lost	1/3/97
Forklift Operator	North Hall	6	7	6	1/3/97
Forklift Operator	North Hall	5	7	12	1/3/97
Forklift Operator	North Hall	11	9	4	1/5/97
Forklift Operator	North Hall	3	8	6	1/6/97
Forklift Operator	South Hall	2	10	10	1/5/97
General Foreman	North Hall	0	3	5	1/5/97
Handyman	Red Dock	1	6	5	1/6/97
Installer/Decorator	North Hall	1	13	7	1/3/97
Installer/Decorator	North Hall	0	3	7	1/5/97
Installer/Decorator	North Hall	0	5	5	1/6/97
Installer/Decorator	South Hall	0	3	8	1/5/97
Installer/Decorator	South Hall	8	9	10	1/6/97
Manager	All over	1	7	8	1/3/97
Rigger	North Hall	5	8	11	1/3/97
Rigger	North Hall	0	3	5	1/6/97
Walker	Green Dock	16	13	21	1/6/97
Walker	Green Dock	15	15	20	1/6/97

Figures

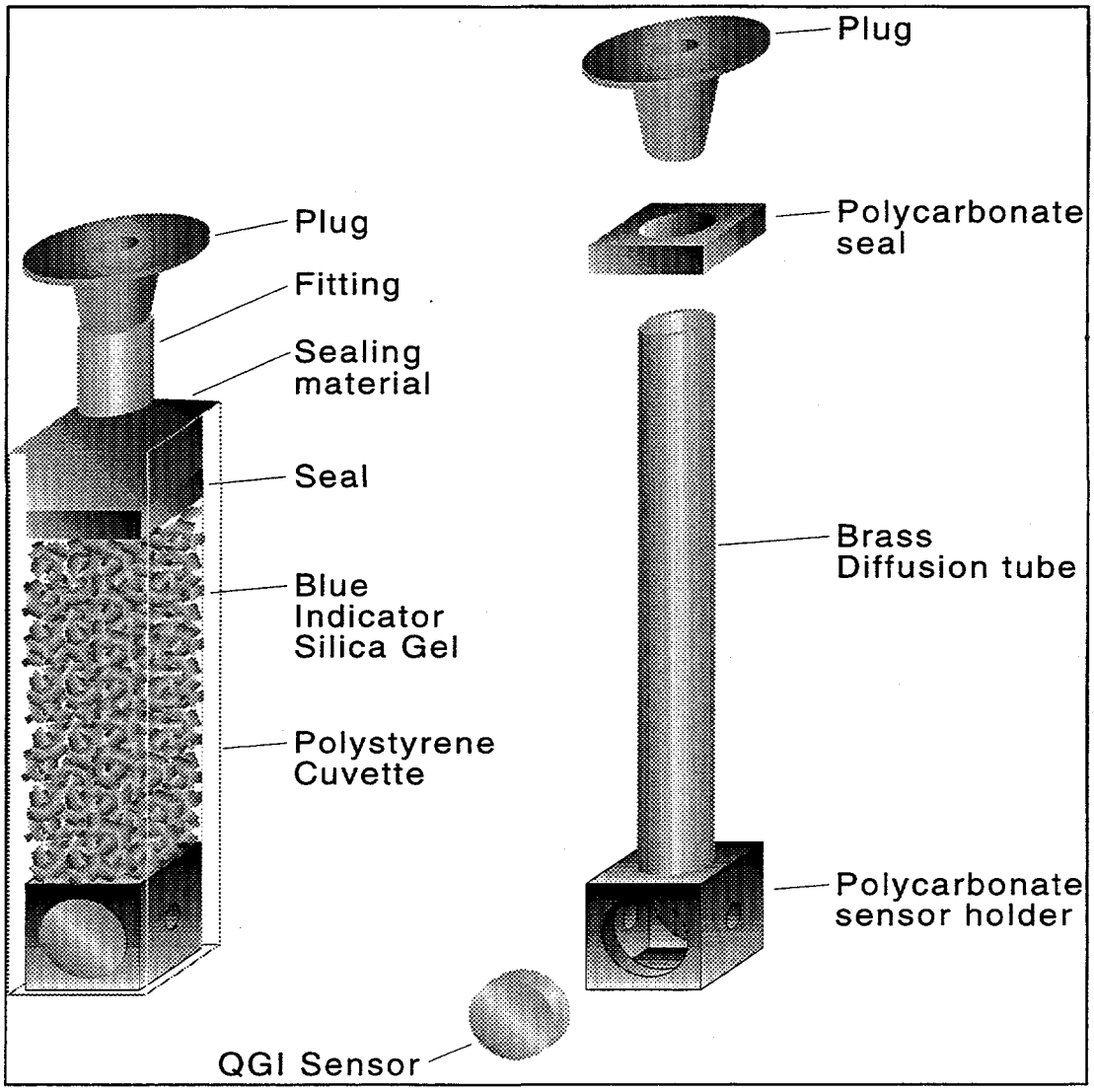

Figure 5-1. Diagram of the LBNL/QGI Carbon Monoxide Occupational Dosimeter (LOCD) and an expanded view of its internal components.

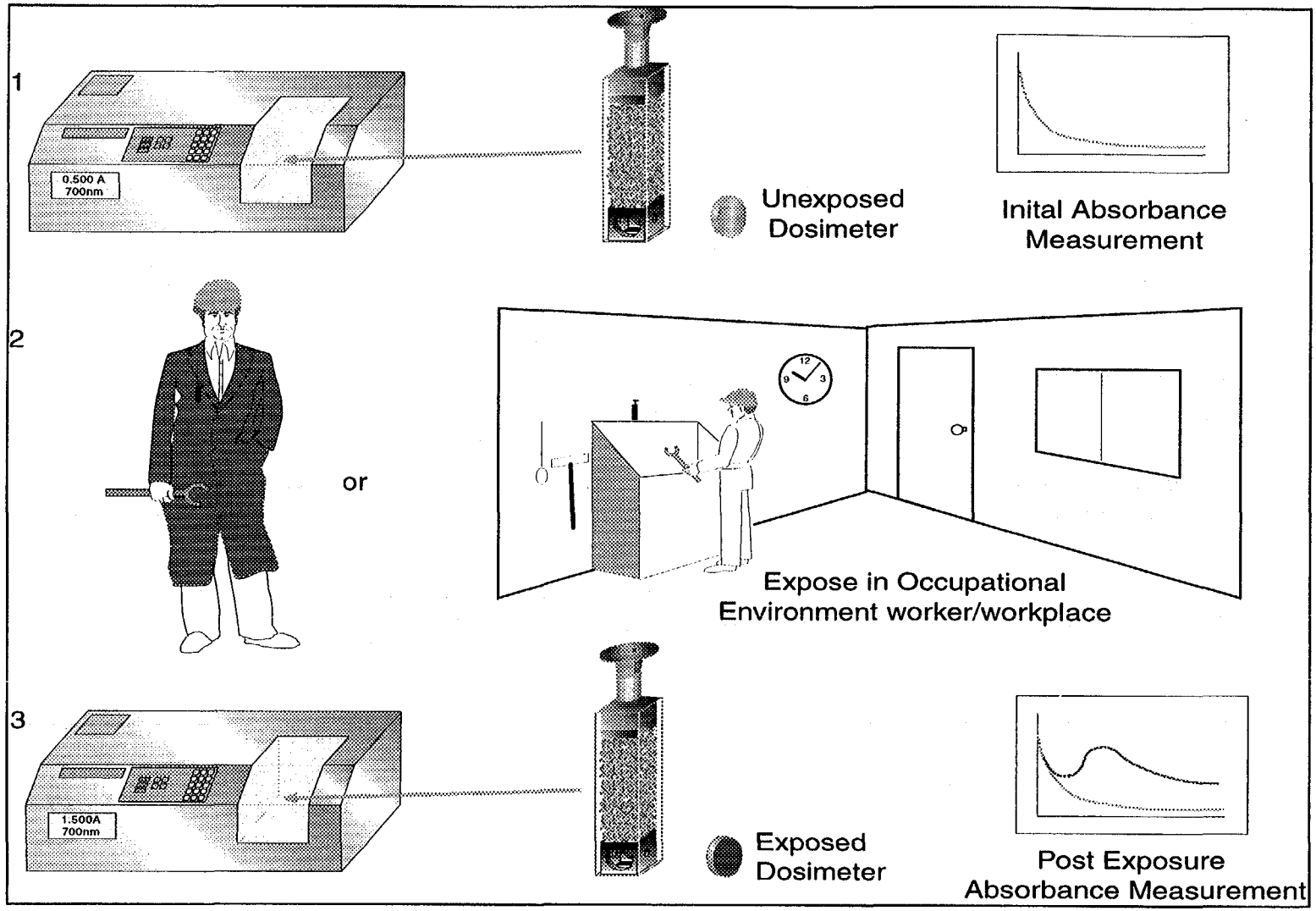

Figure 5-2. Conceptual design for use of the LBNL/QGI Carbon Monoxide Occupational Dosimeter (LOCD): 1) Initial sensor darkness measurements are made; 2) The LOCD is deployed by uncapping and attaching to lapel of worker, or by placing it in an area that is to be measured; 3) After sampling (8 hour work shift) the LOCD is capped and re-measured - the TWA worker exposure is calculated from the change in darkness and the elapsed time of sampling.

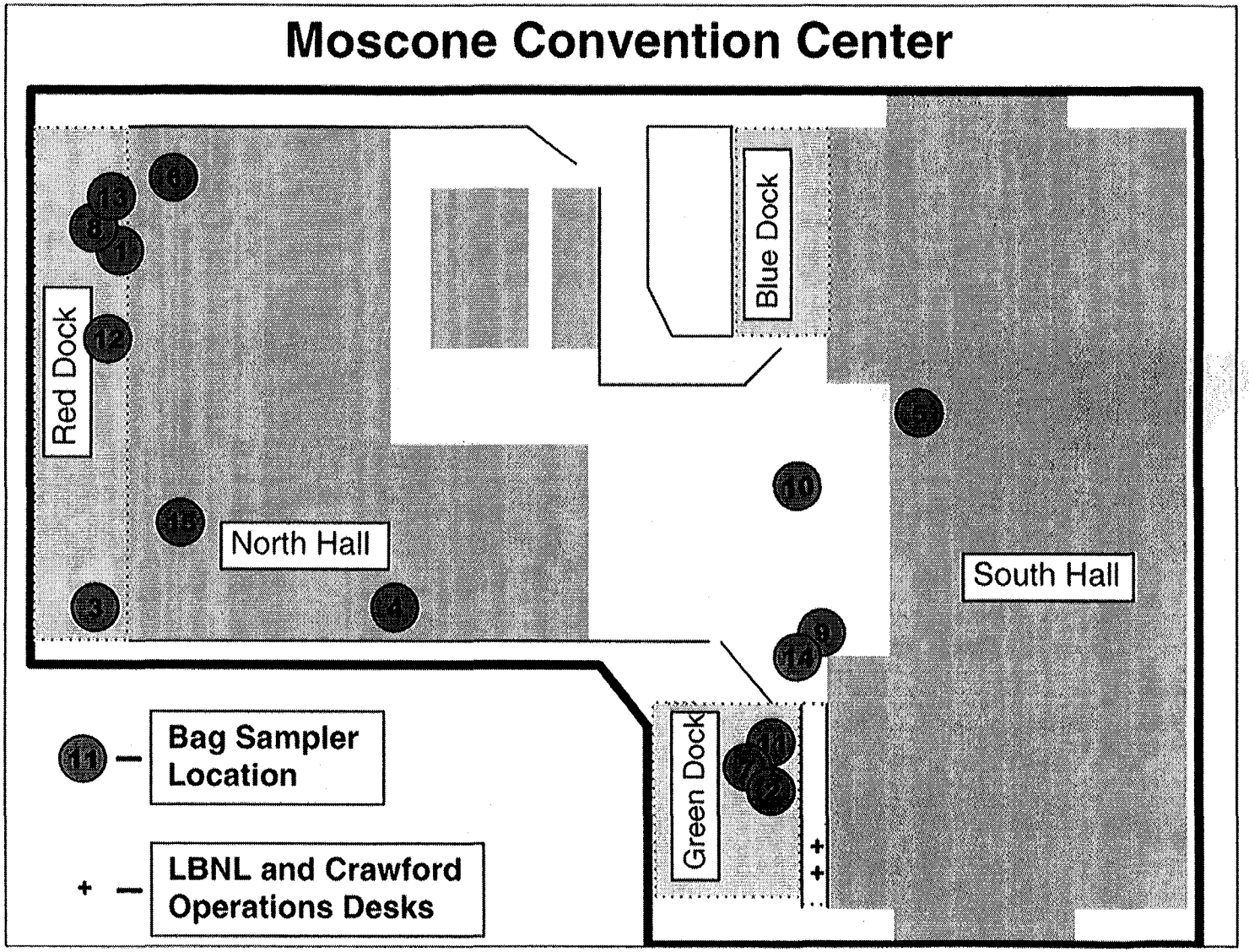

Figure 5-3. Fixed-site locations for bag sampler/LOCD monitoring. Numbers indicate the bag sampler number.

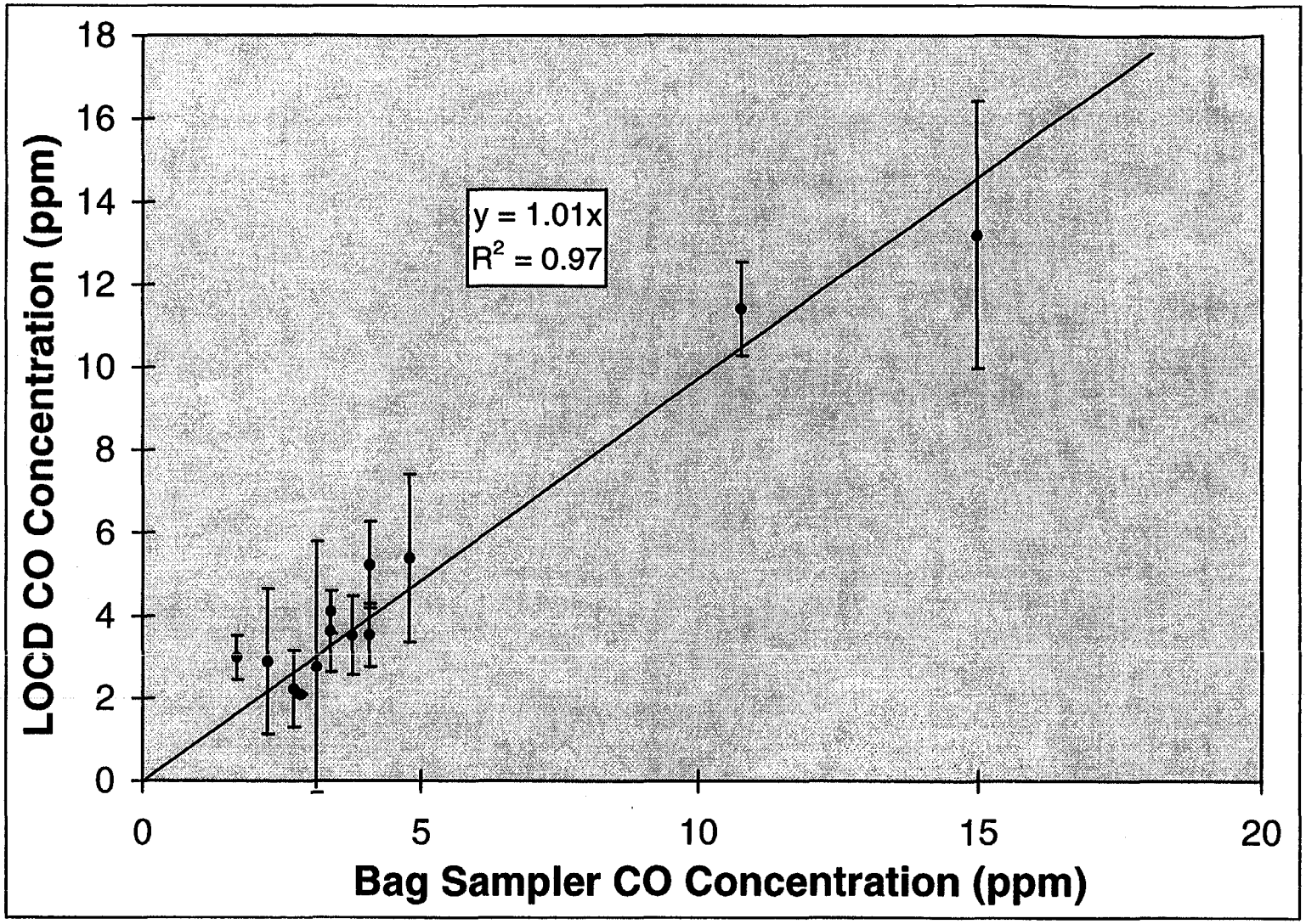

Figure 5-4. LBNL/QGI CO Occupational Dosimeter (LOCD) vs. Bag Sampler Data collected at fixed-sites throughout the Moscone convention Center during the CO exposure study. Air samples were collected in Tedlar Bags over an 8-hr period, and analyzed using a Gas Filter Correlation CO analyzer. Three LOCDs were deployed at the site of each bag sampler. The error bars represent ± one standard deviation about the mean LOCD value.

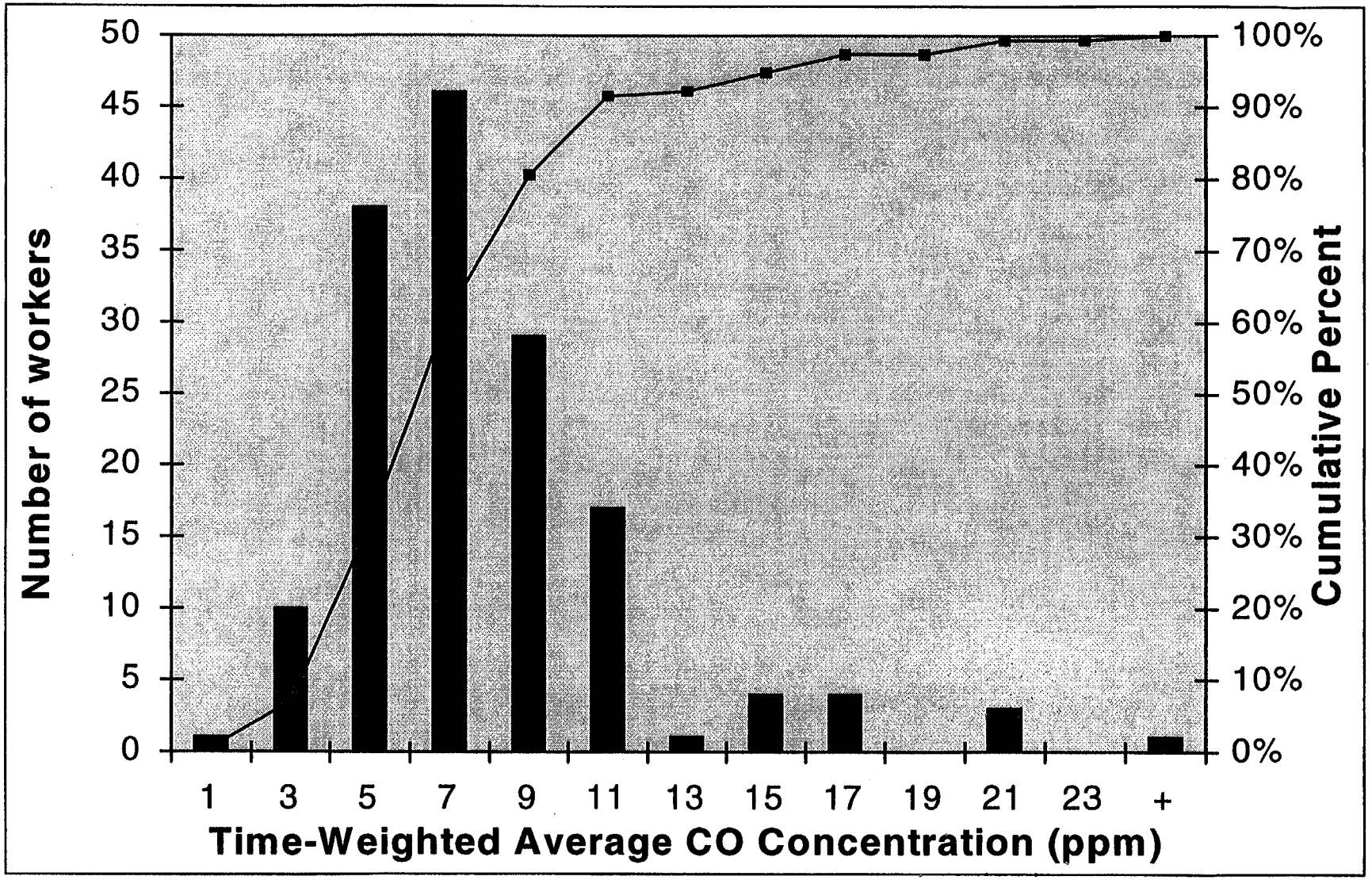

Figure 5-5. Carbon Monoxide Exposure Distribution at the Moscone Convention Center - MacWorld Setup. All job titles, all three days of the CO exposure study.

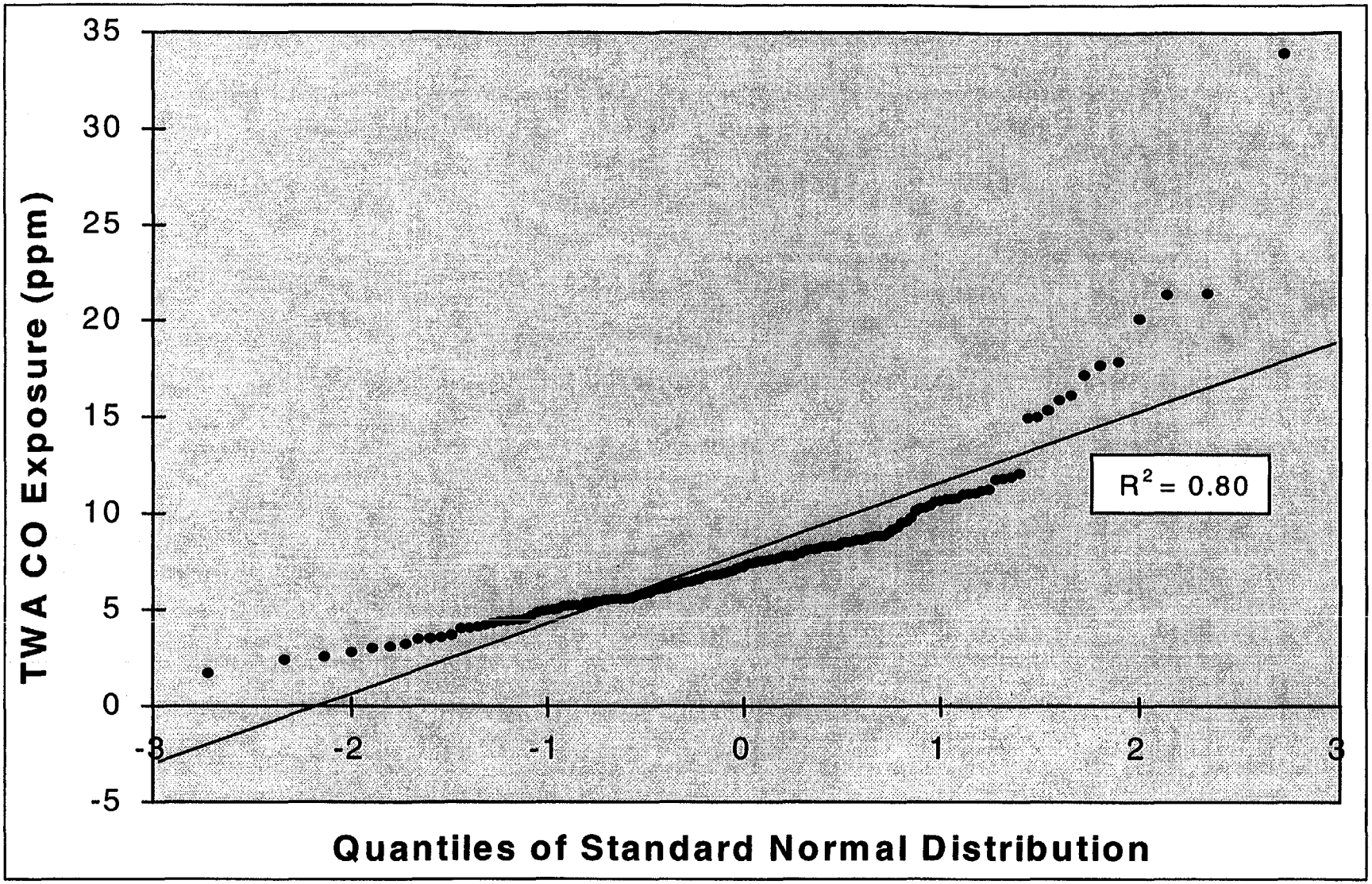

Figure 5-6. The probability distribution of measured time-weighted average CO exposures at the Moscone Convention Center plotted against the corresponding quantiles of the normal distribution. The non-normality of these data is reflected in the poor fit of the superimposed regression line ($R^2 = 0.80$). Each quantile represents one standard deviation away from the mean.

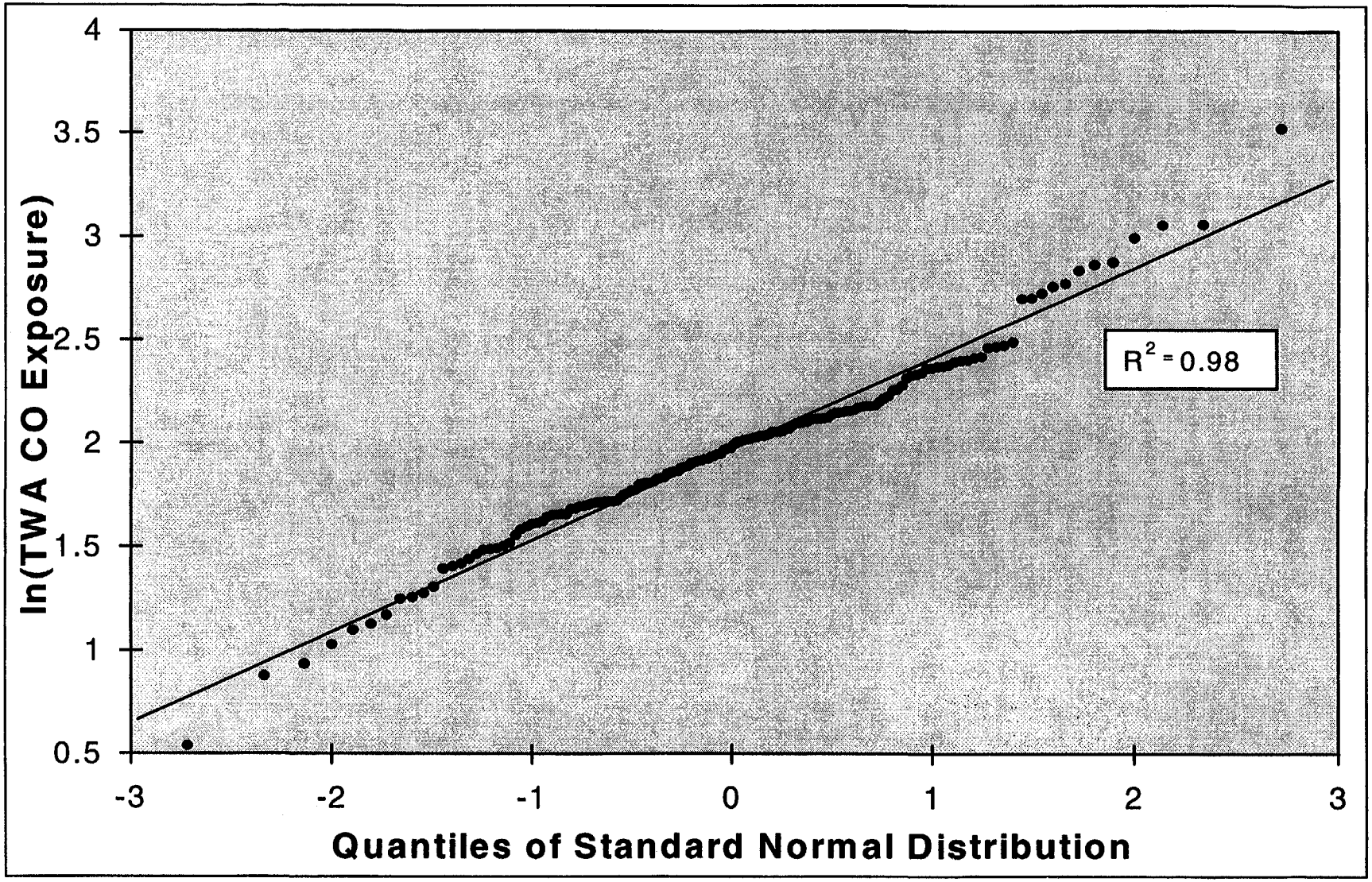

Figure 5-7. The probability distribution of the natural logarithm of measured time-weighted average CO exposures at the Moscone Convention Center, plotted against the corresponding quantiles of the normal distribution. The-normality of these data is reflected in the good fit of the superimposed regression line ($R^2 = 0.98$). This plot indicates that the untransformed CO exposure data are approximately log-normally distributed. Each quantile represents one standard deviation away from the mean.

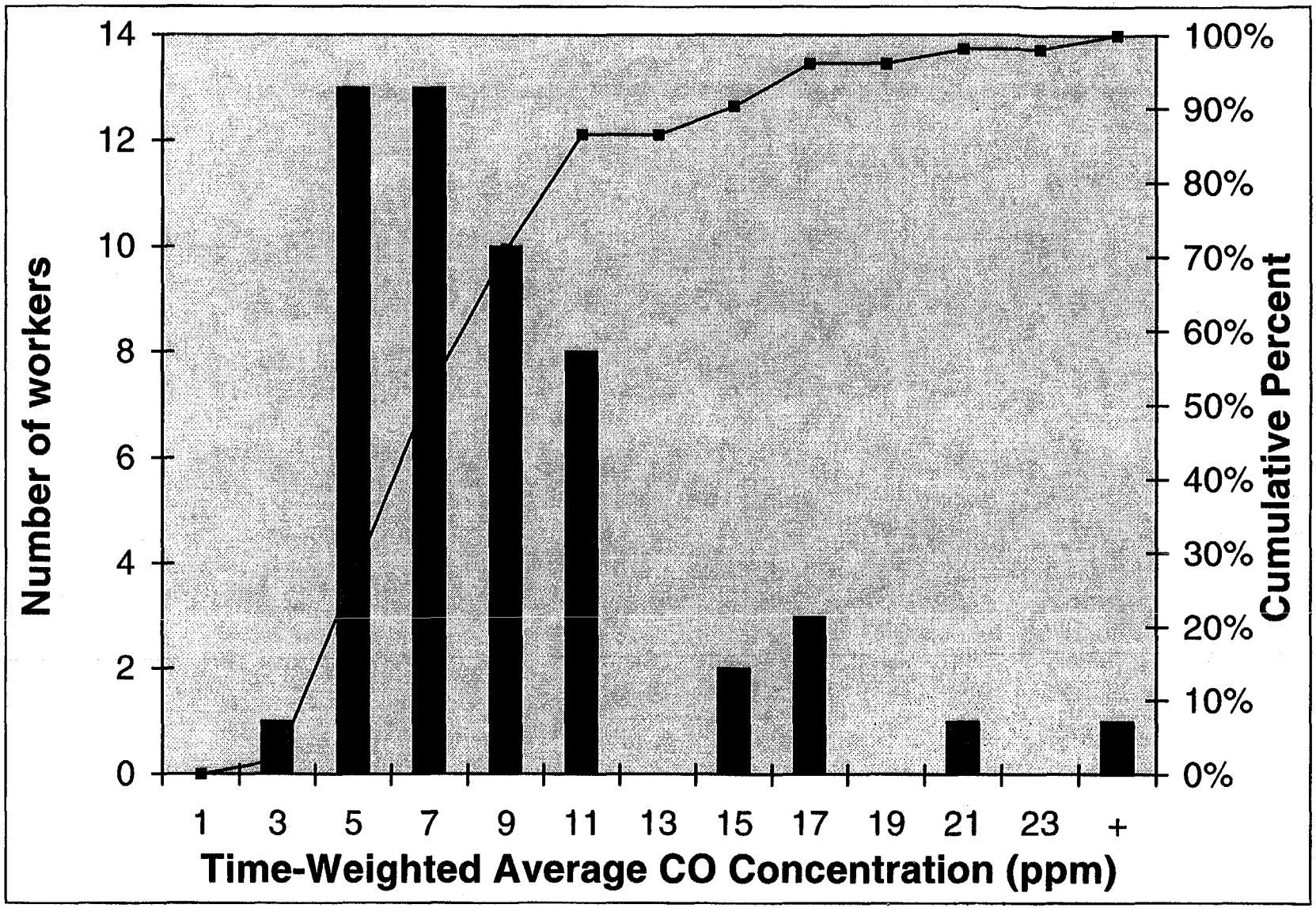

Figure 5-8. Carbon monoxide exposure distribution, Moscone Convention Center-MacWorld setup. All job categories on January 3, 1997.

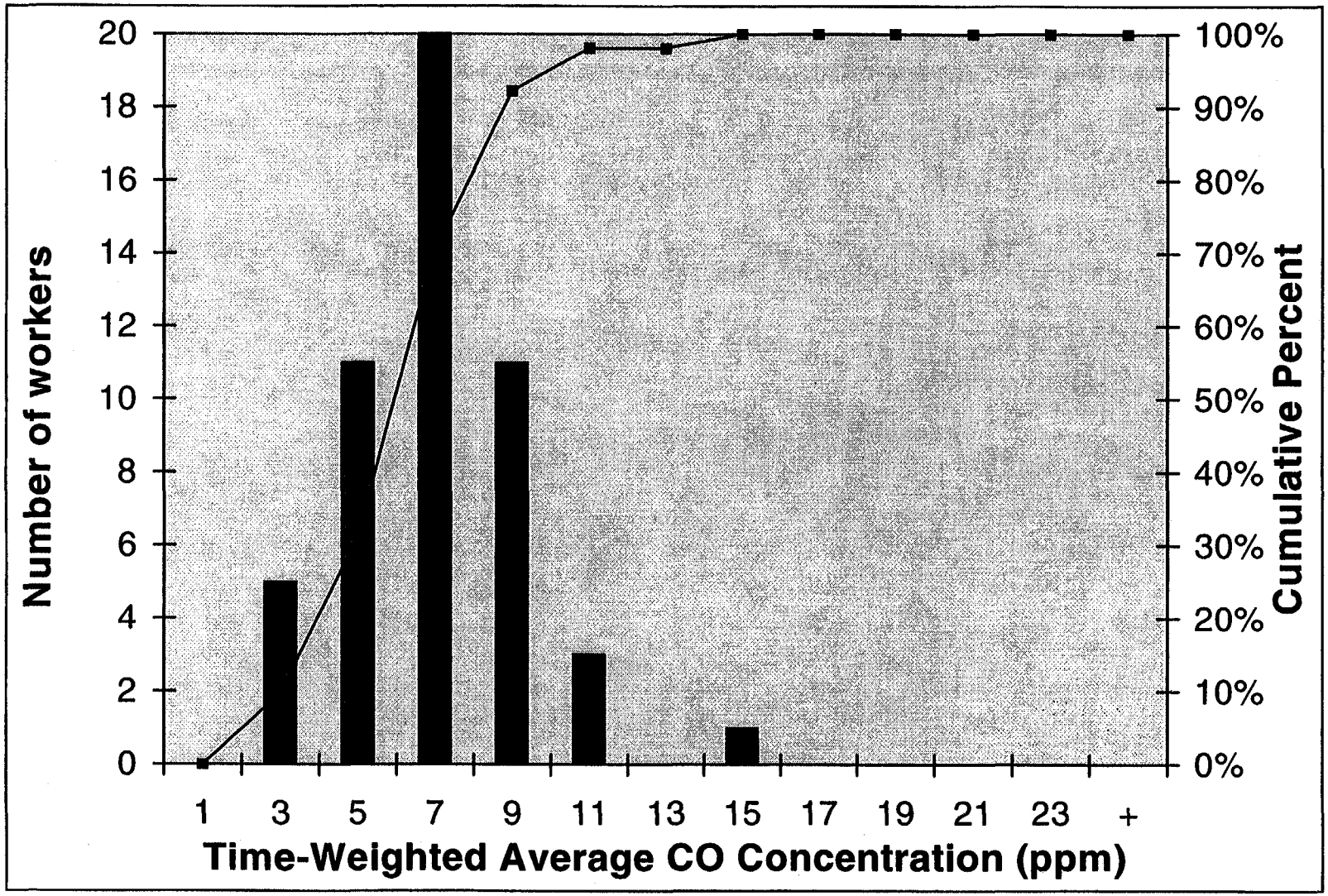

Figure 5-9. Carbon monoxide exposure distribution, Moscone Convention Center-MacWorld setup. All job categories on January 5, 1997.

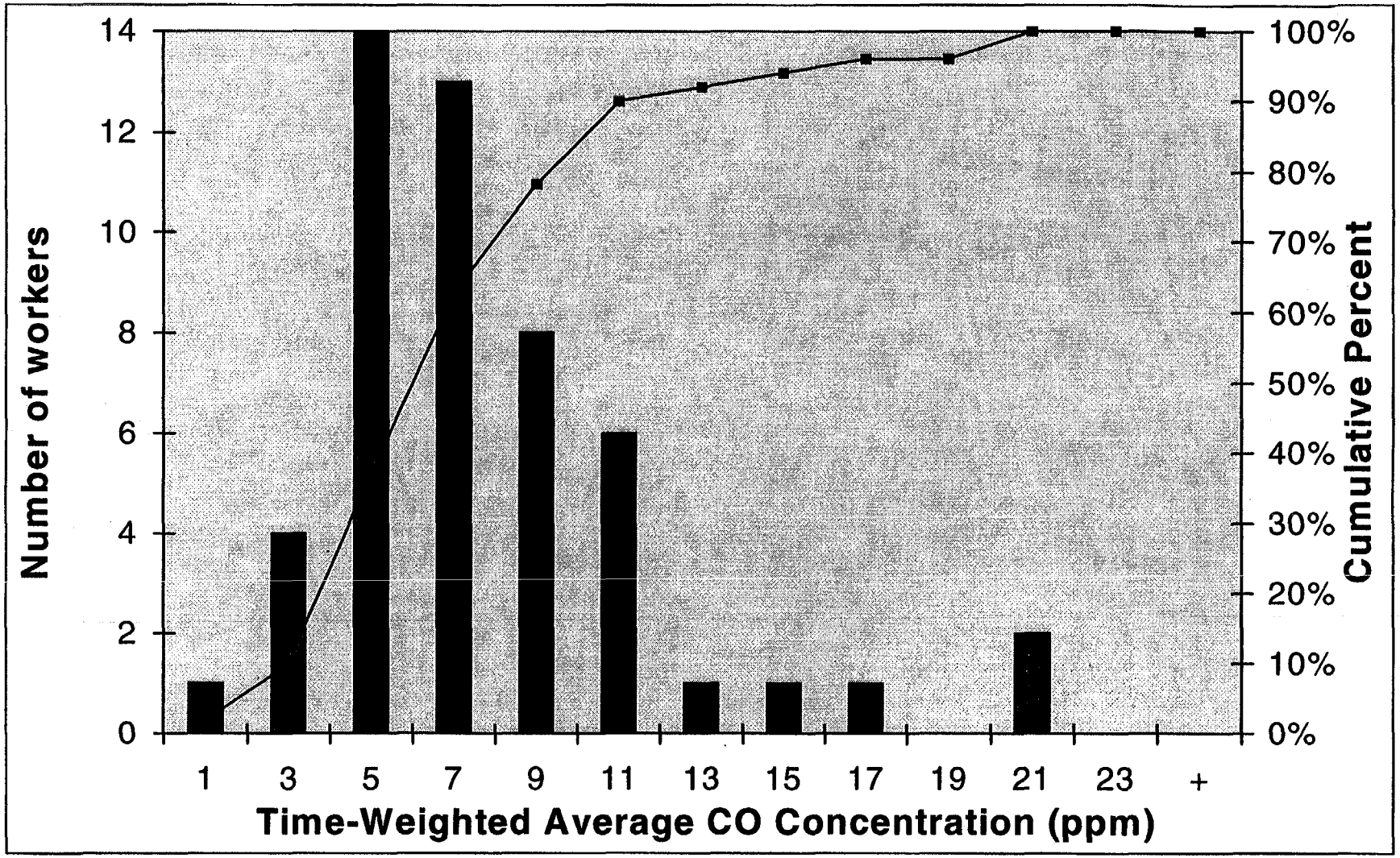

Figure 5-10. Carbon monoxide exposure distribution, Moscone Convention Center-MacWorld setup. All job categories on January 6, 1997.

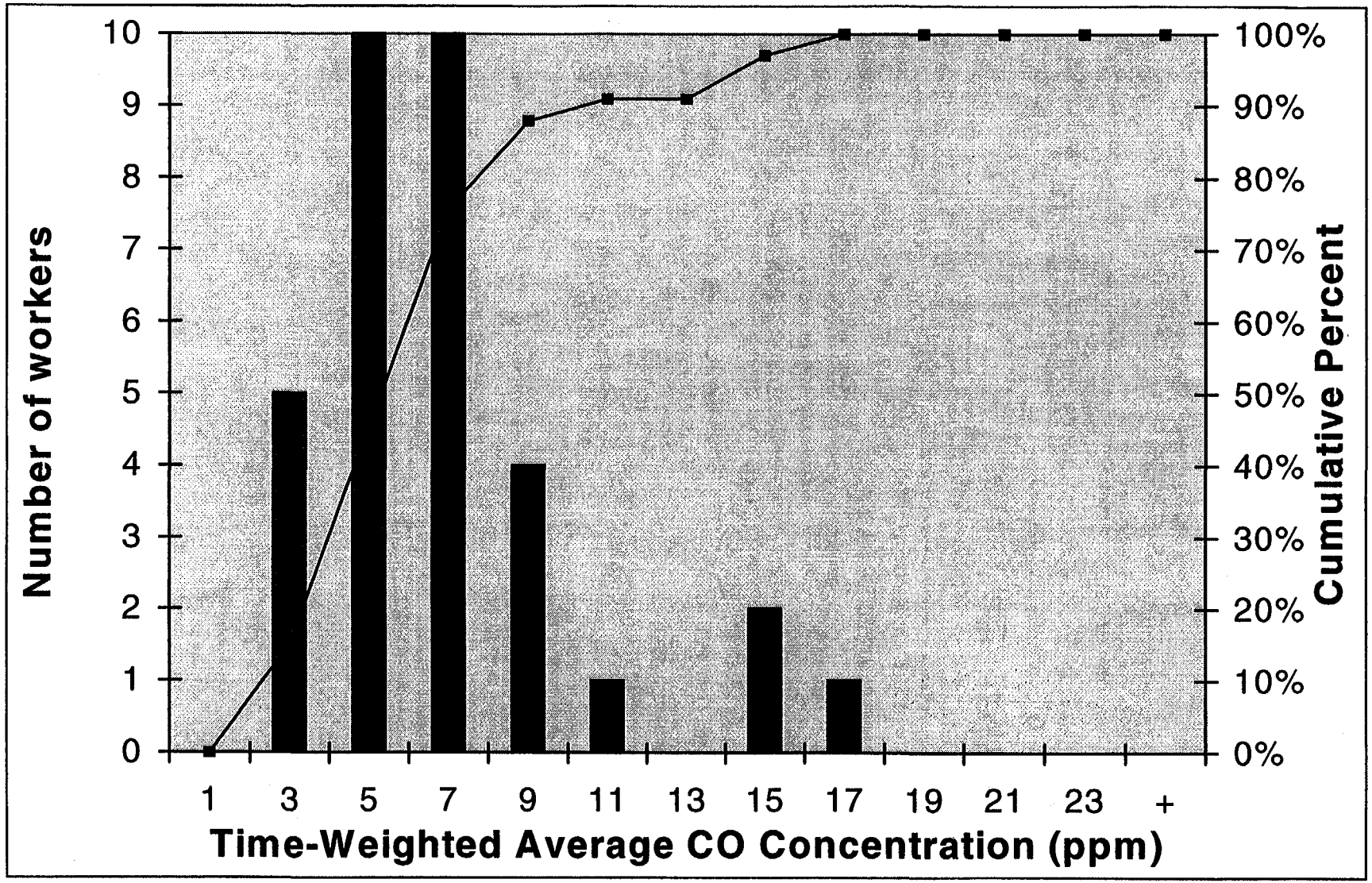

Figure 5-11. Carbon monoxide exposure distribution, Moscone Convention Center - MacWorld setup. By job category – Attendant

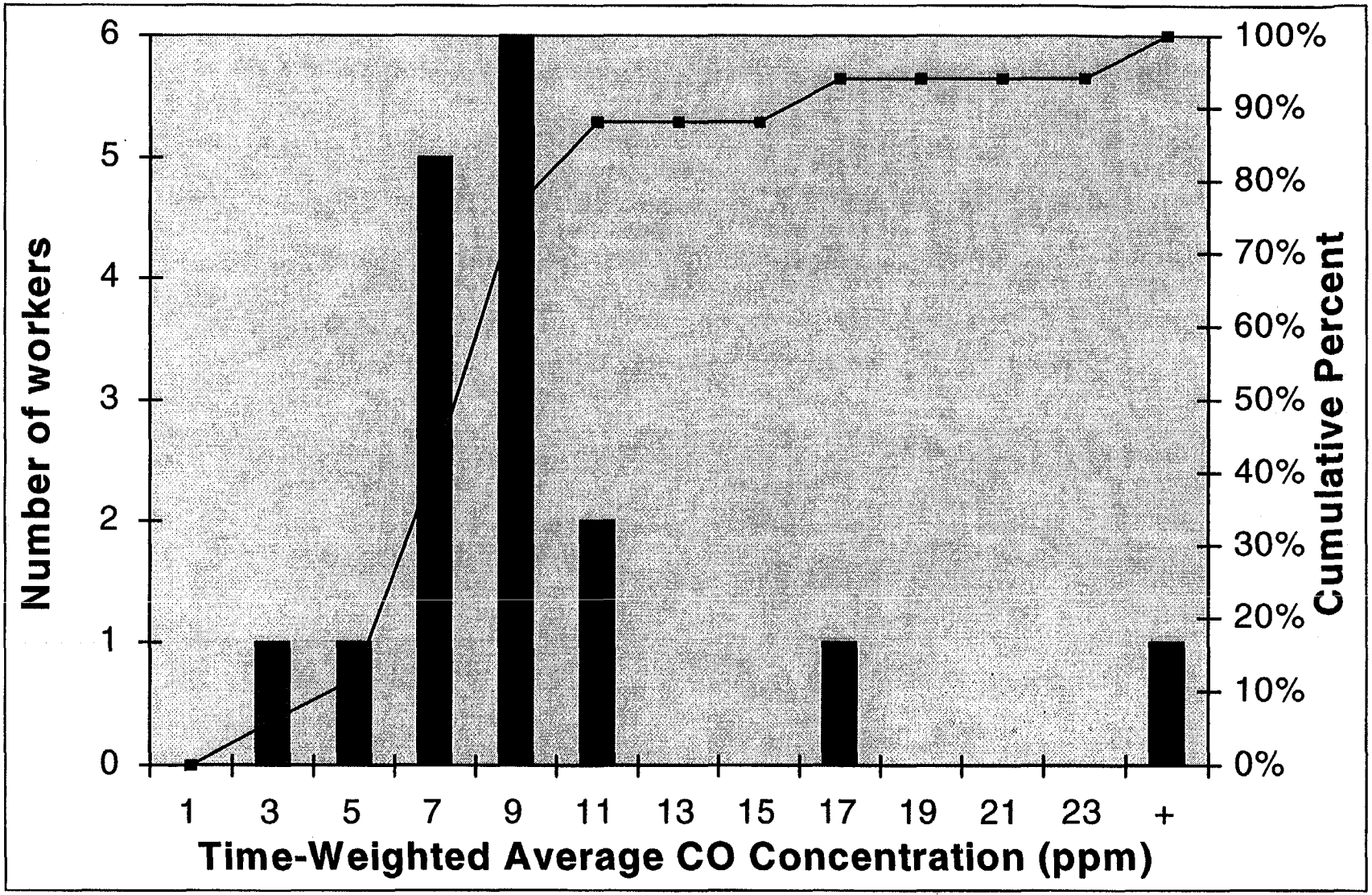

Figure 5-12. Carbon monoxide exposure distribution, Moscone Convention Center - MacWorld setup. By job category - Forklift Operator.

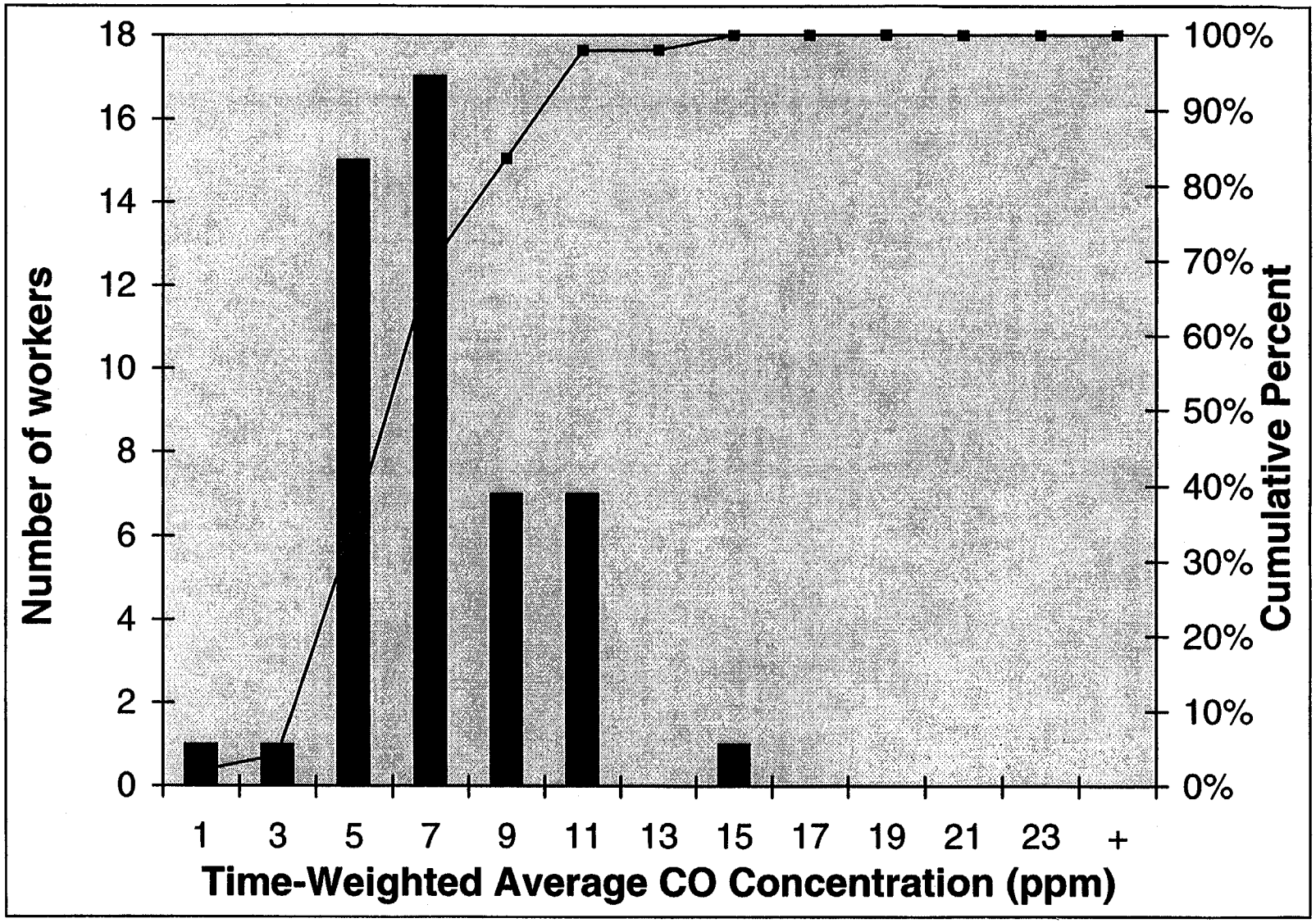

Figure 5-13. Carbon monoxide exposure distribution, Moscone Convention Center - MacWorld setup. By job category - Installer/Decorator.

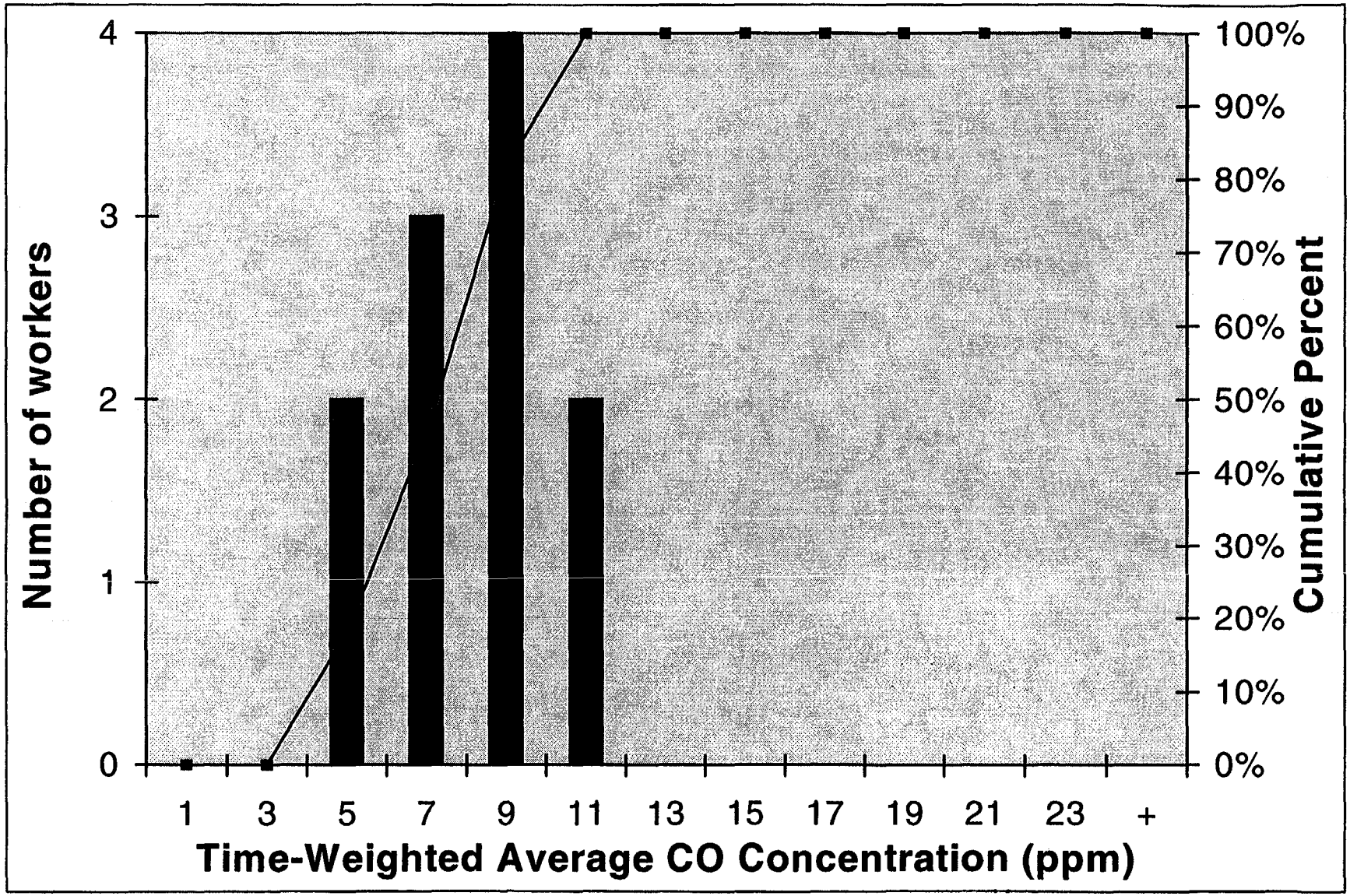

Figure 5-14. Carbon monoxide exposure distribution, Moscone Convention Center - MacWorld setup. By job category - Supervisor.

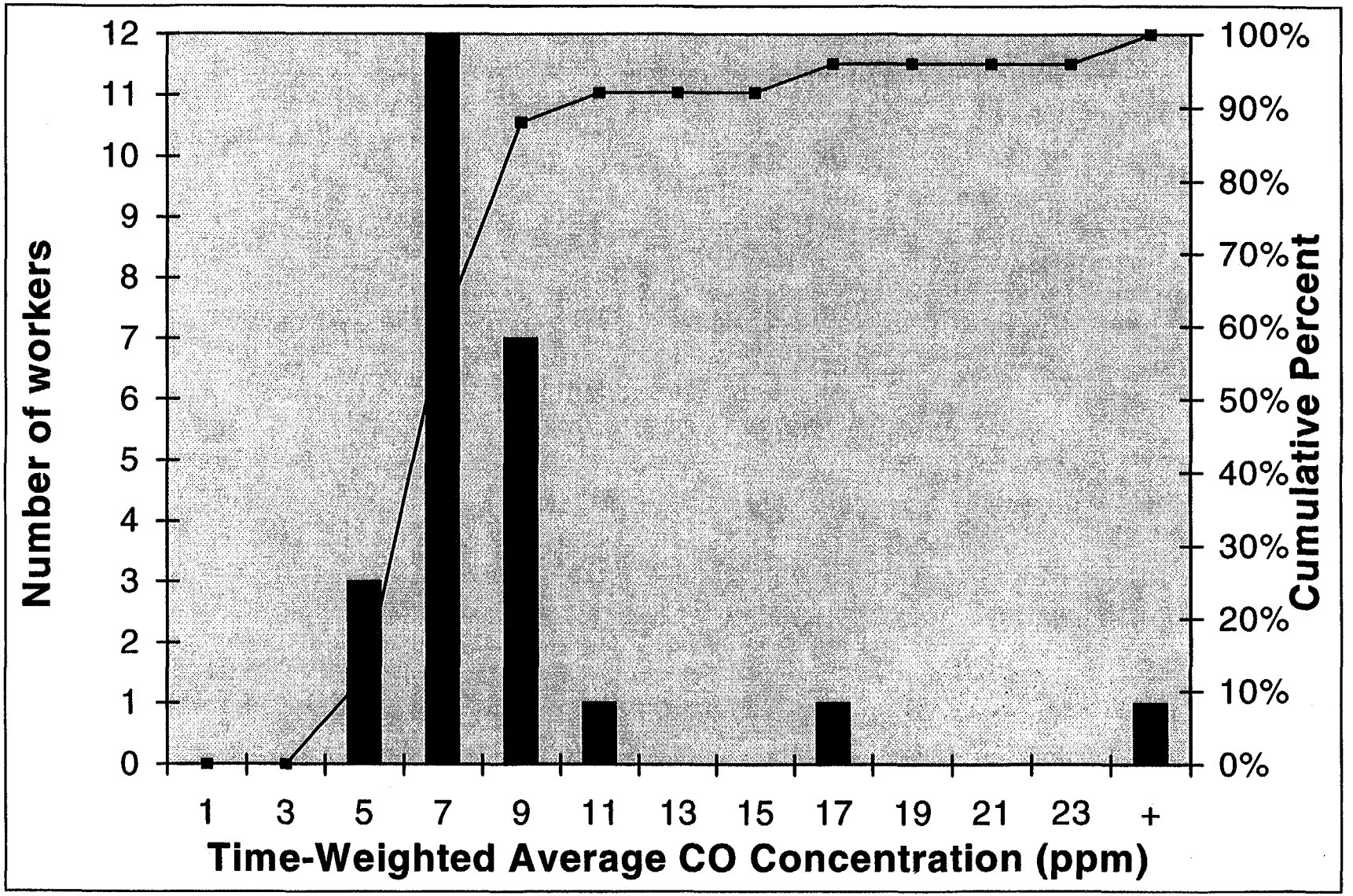

Figure 5-15. Carbon monoxide exposure distribution, Moscone Convention Center - MacWorld setup. By job location - Red Dock.

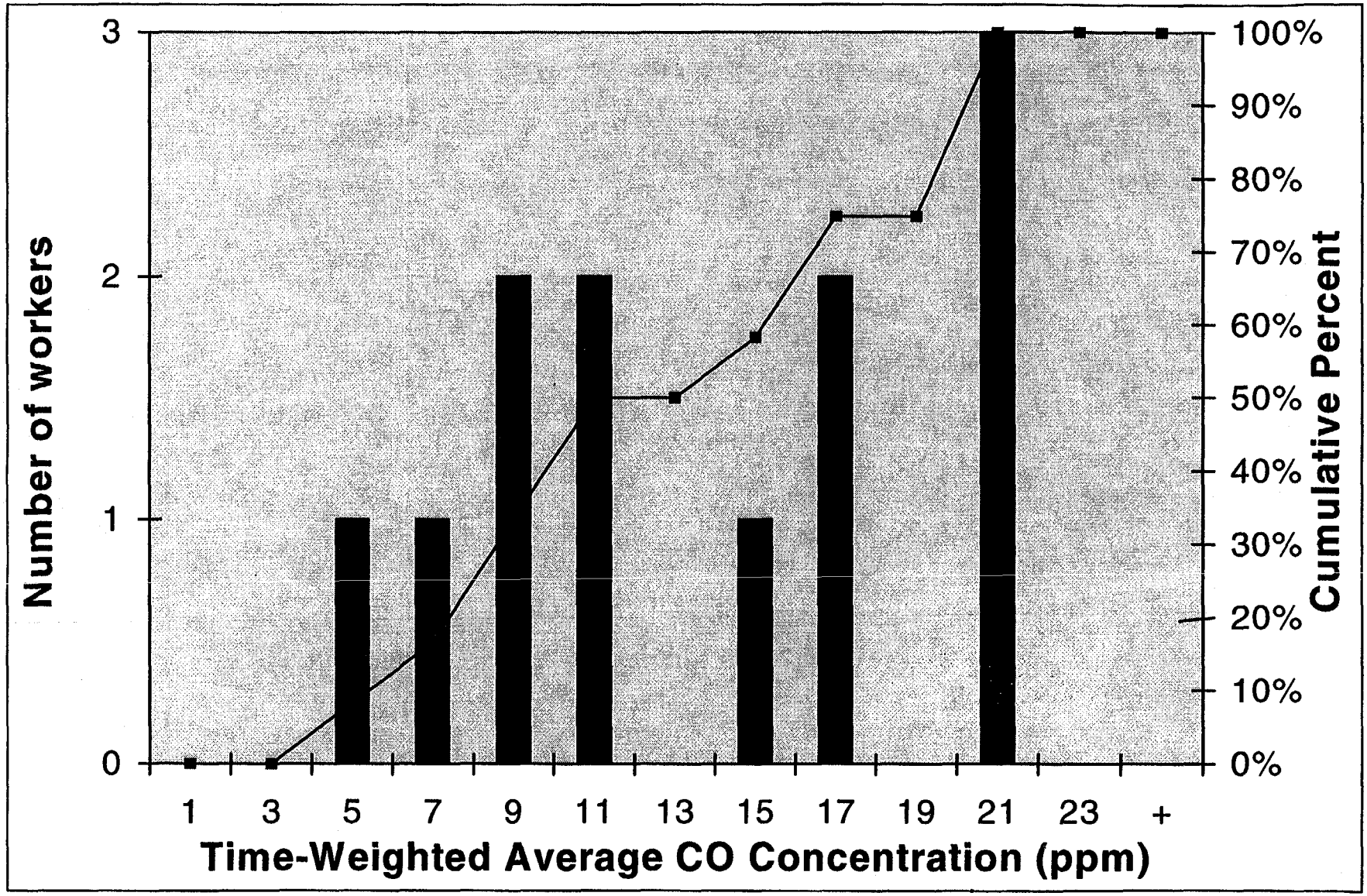

Figure 5-16. Carbon monoxide exposure distribution, Moscone Convention Center - MacWorld setup. By job location - Green Dock.

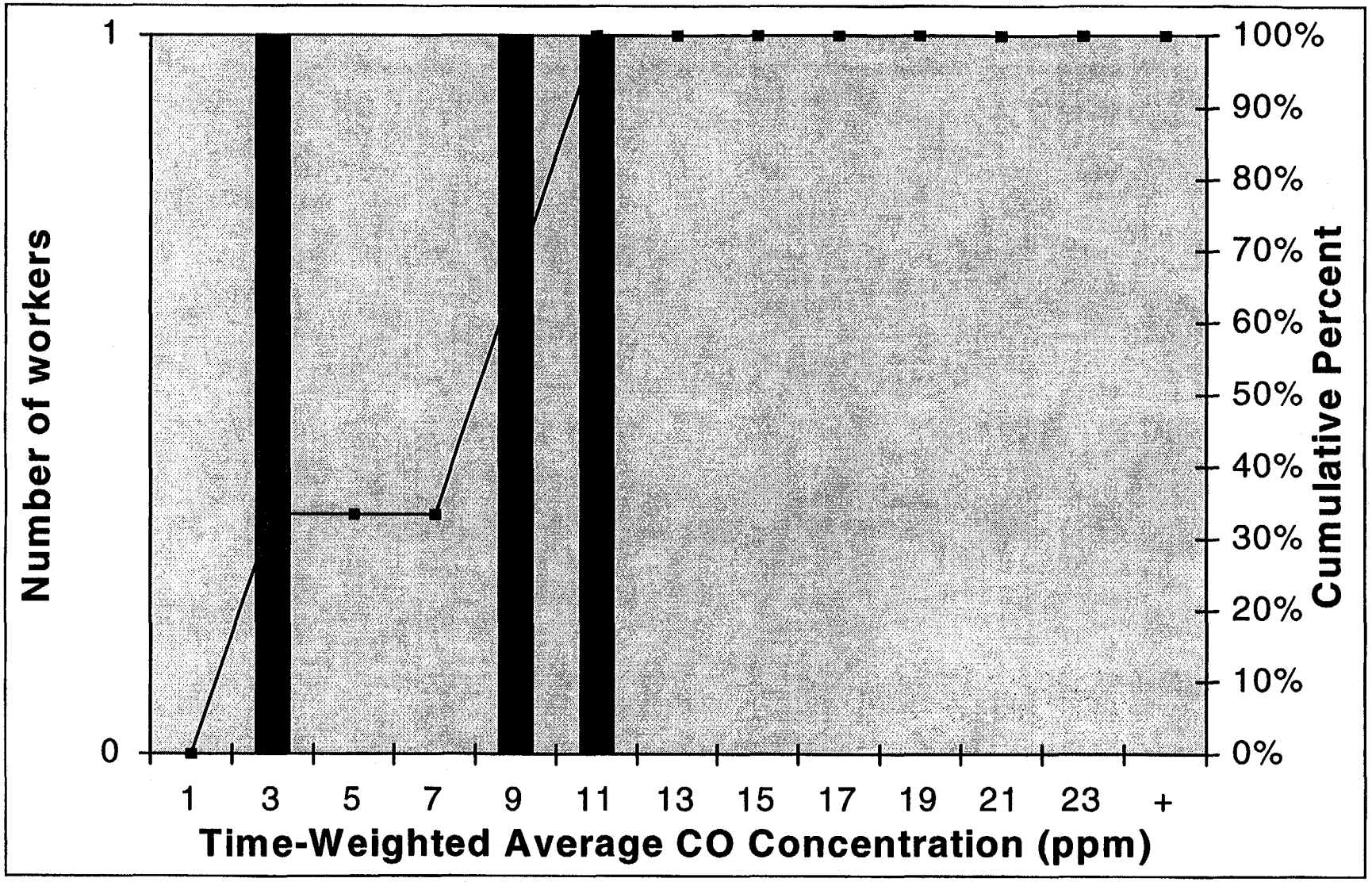

Figure 5-17. Carbon monoxide exposure distribution, Moscone Convention Center - MacWorld setup. By job location - Blue Dock.

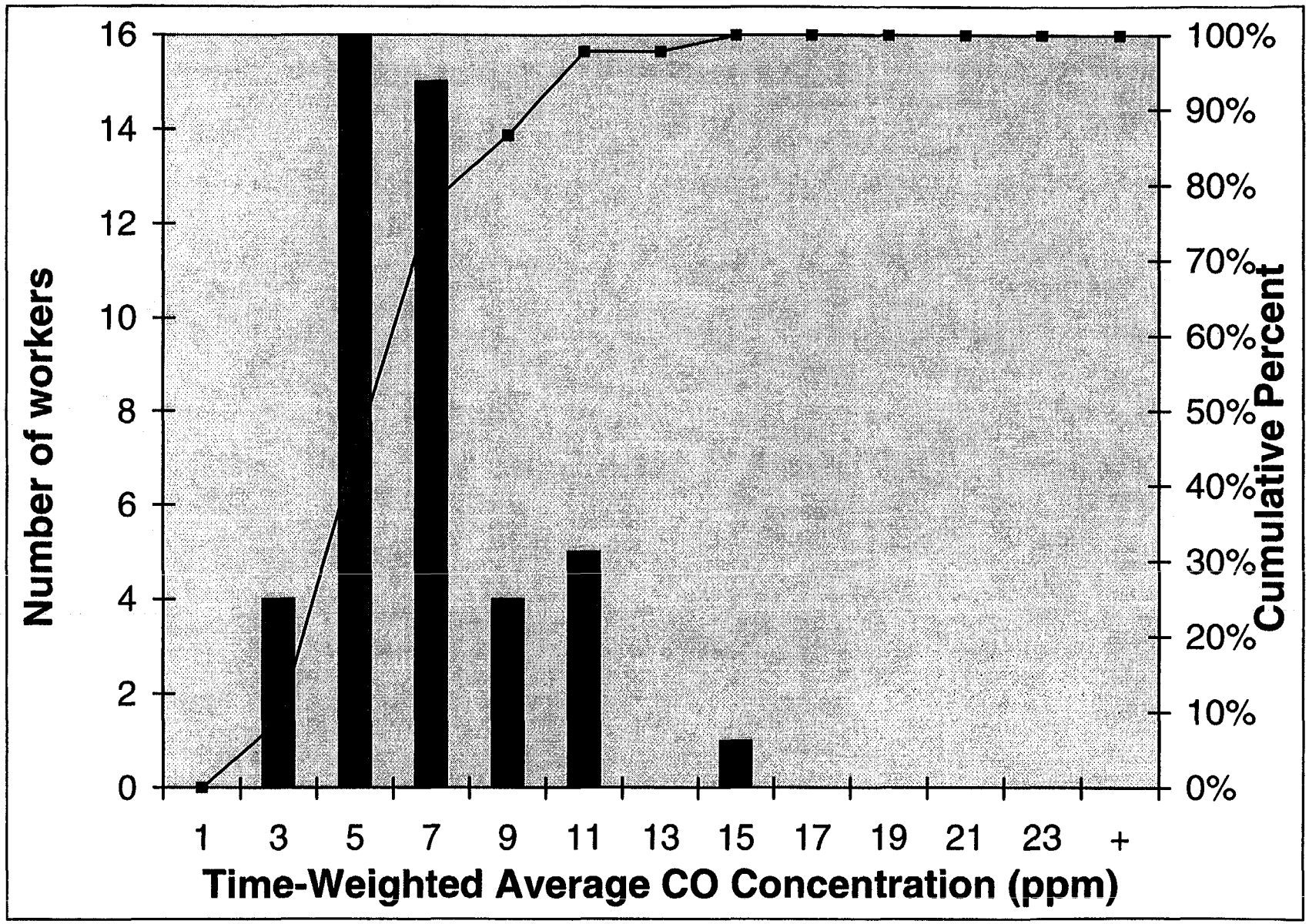

Figure 5-18. Carbon monoxide exposure distribution, Moscone Convention Center - MacWorld setup. By job location - North Hall.

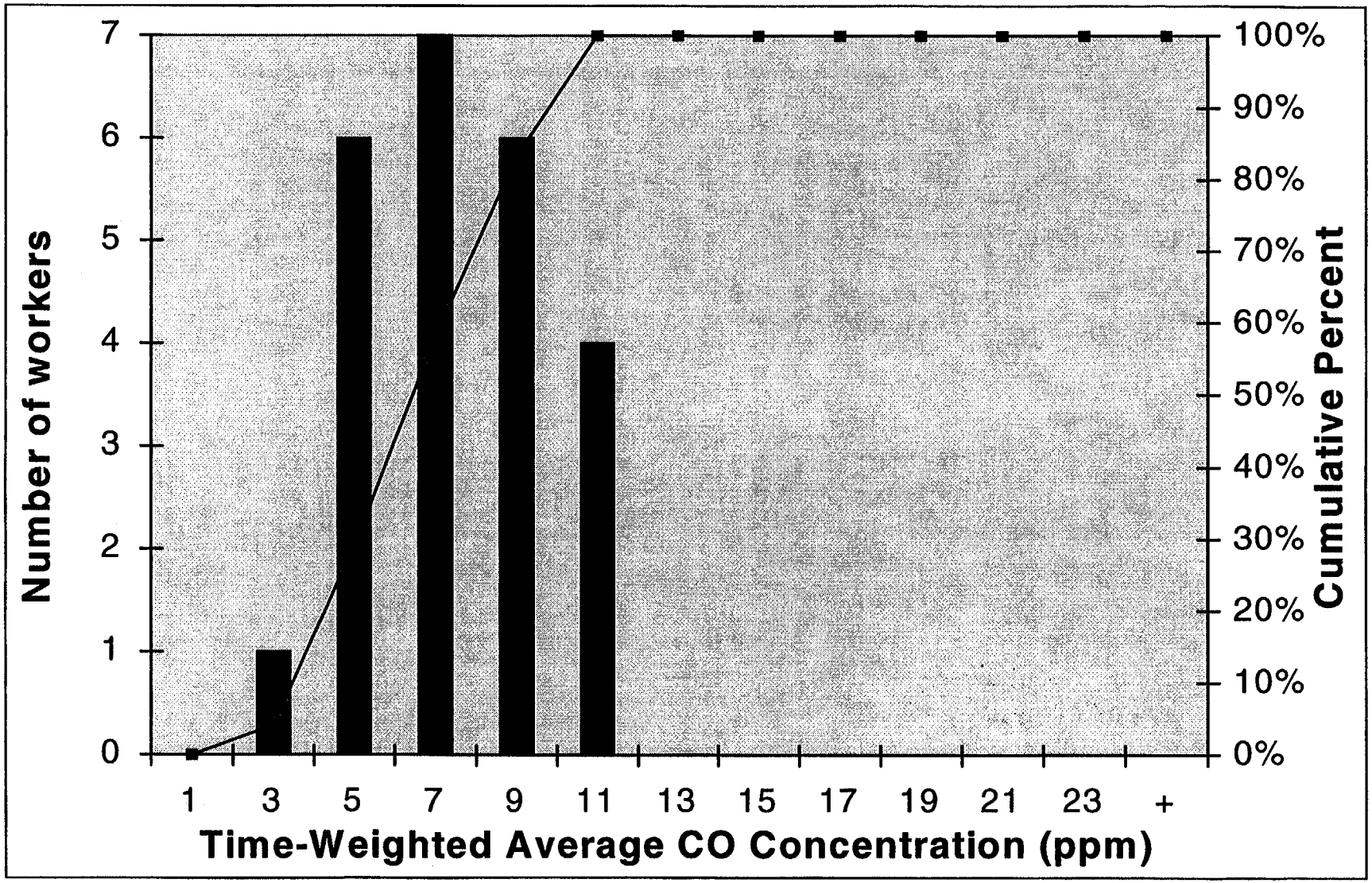

Figure 5-19. Carbon monoxide exposure distribution, Moscone Convention Center - MacWorld setup. By job location - South Hall.

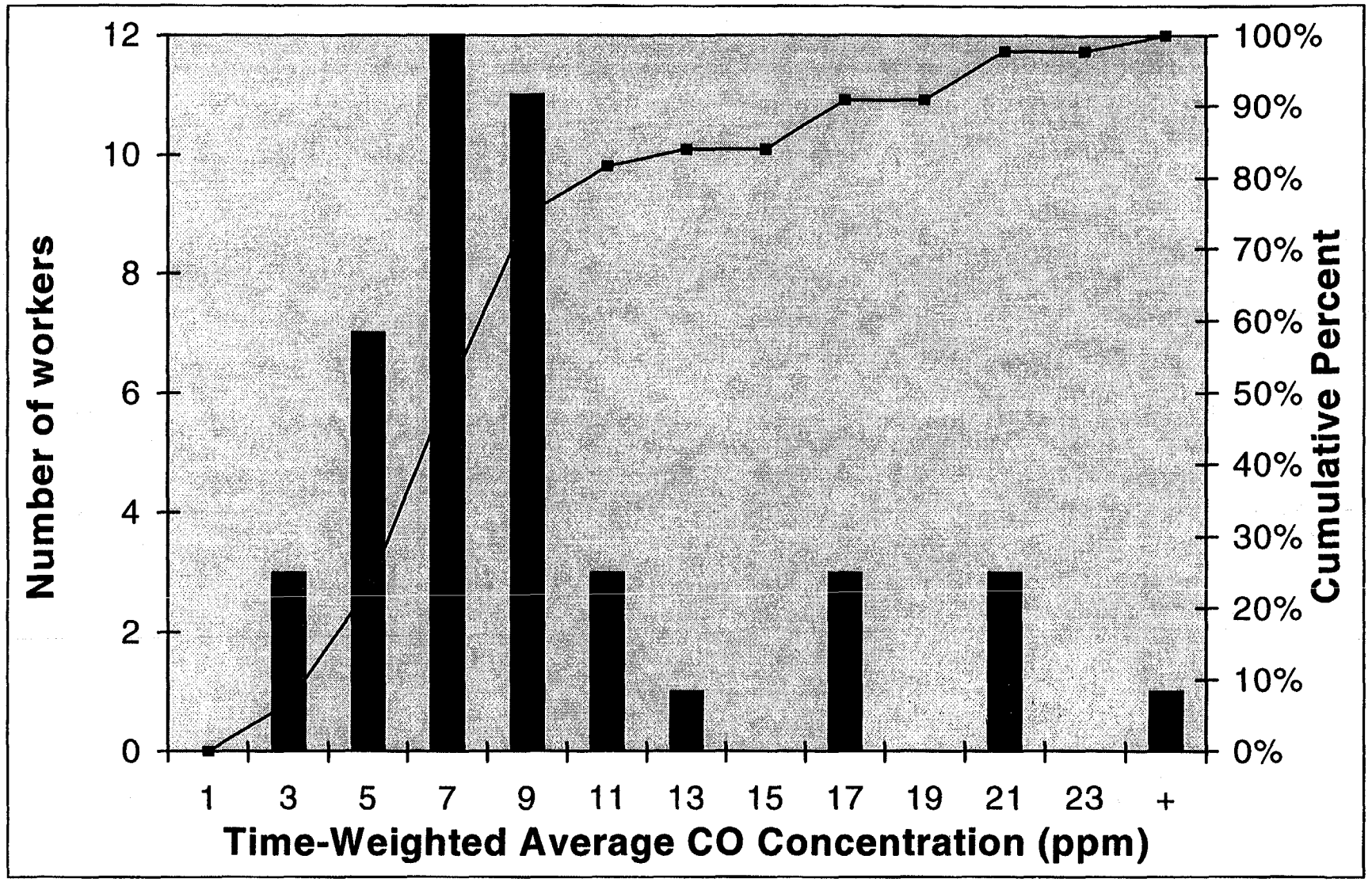

Figure 5-20. Carbon monoxide exposure distribution, Moscone Convention Center - MacWorld setup. By union, Teamsters Local 85.

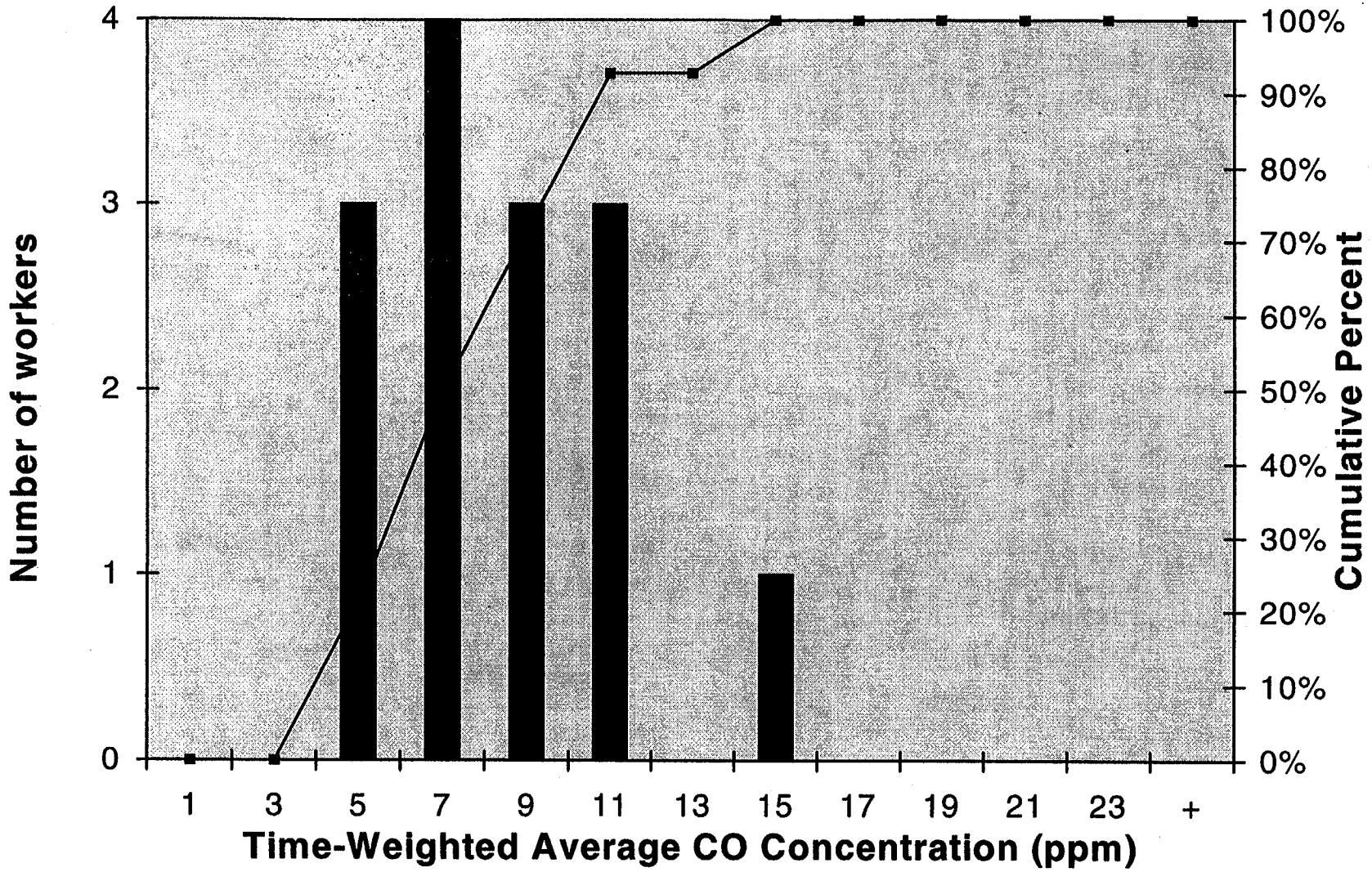

Figure 5-21. Carbon monoxide exposure distribution, Moscone Convention Center - MacWorld setup. By union, Management.

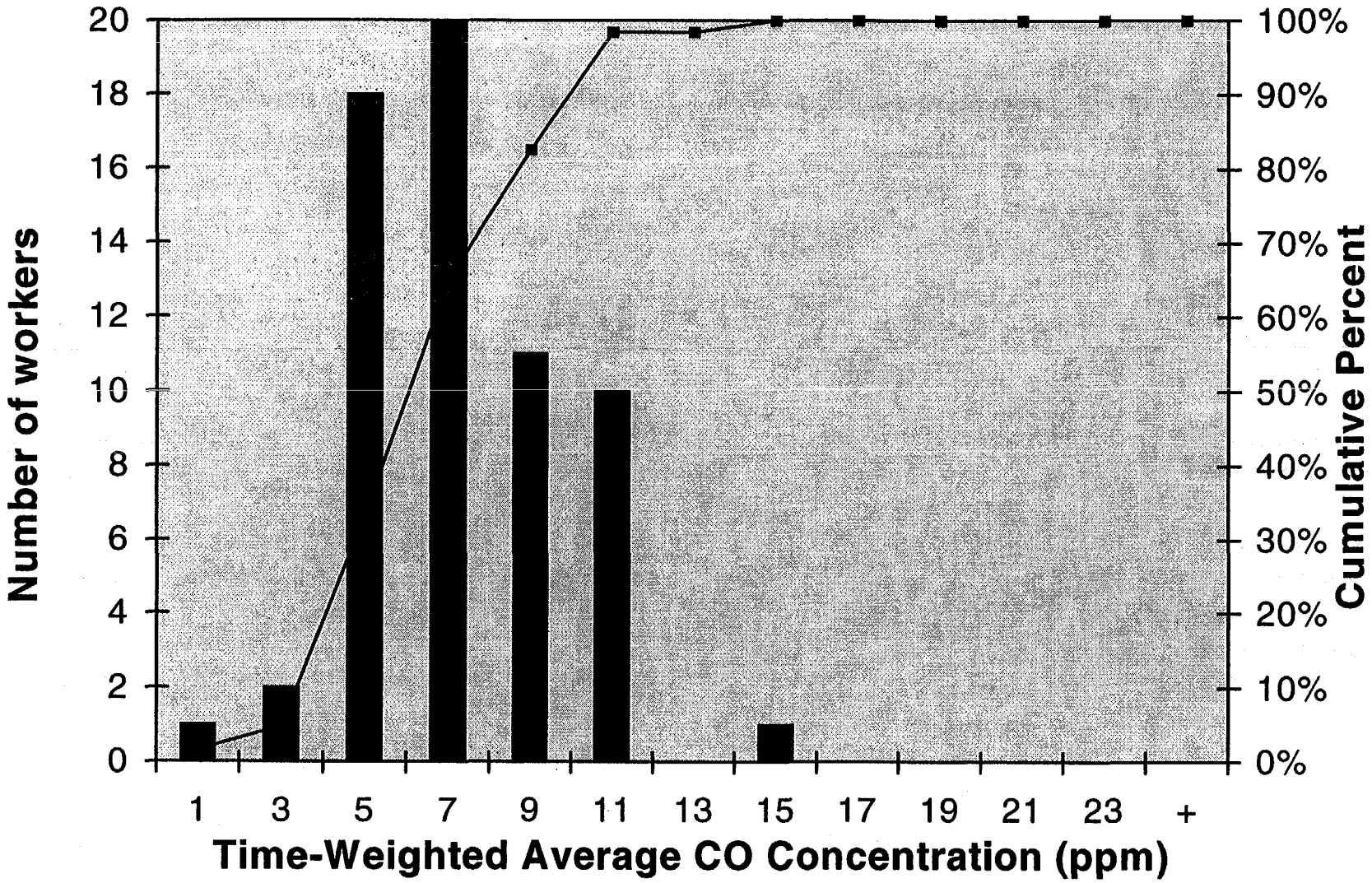

Figure 5-22. Carbon monoxide exposure distribution, Moscone Convention Center - MacWorld setup. By union, SDAC Local 510.

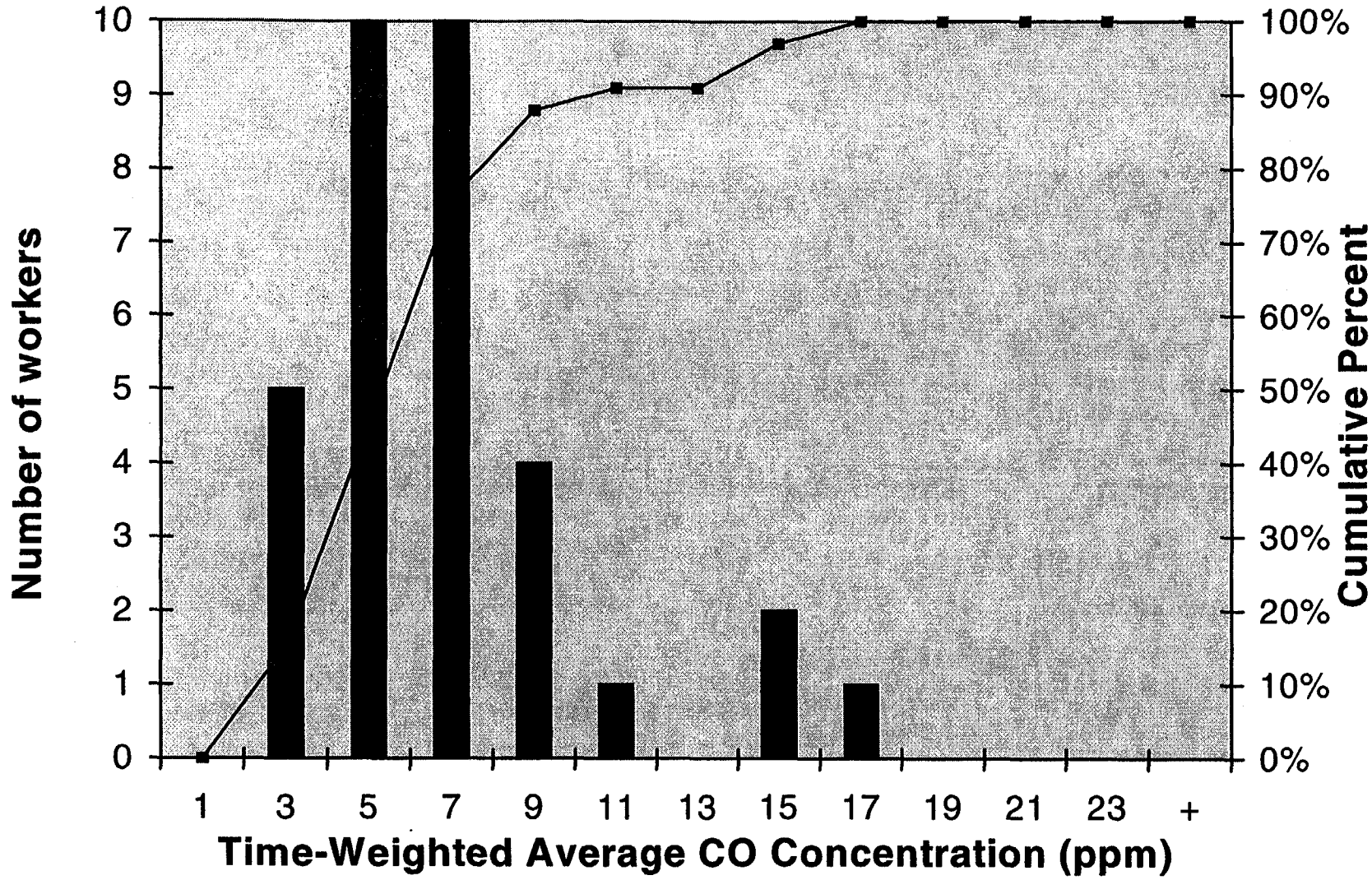

Figure 5-23. Carbon monoxide exposure distribution, Moscone Convention Center - MacWorld setup. By union, SEI Local 14.

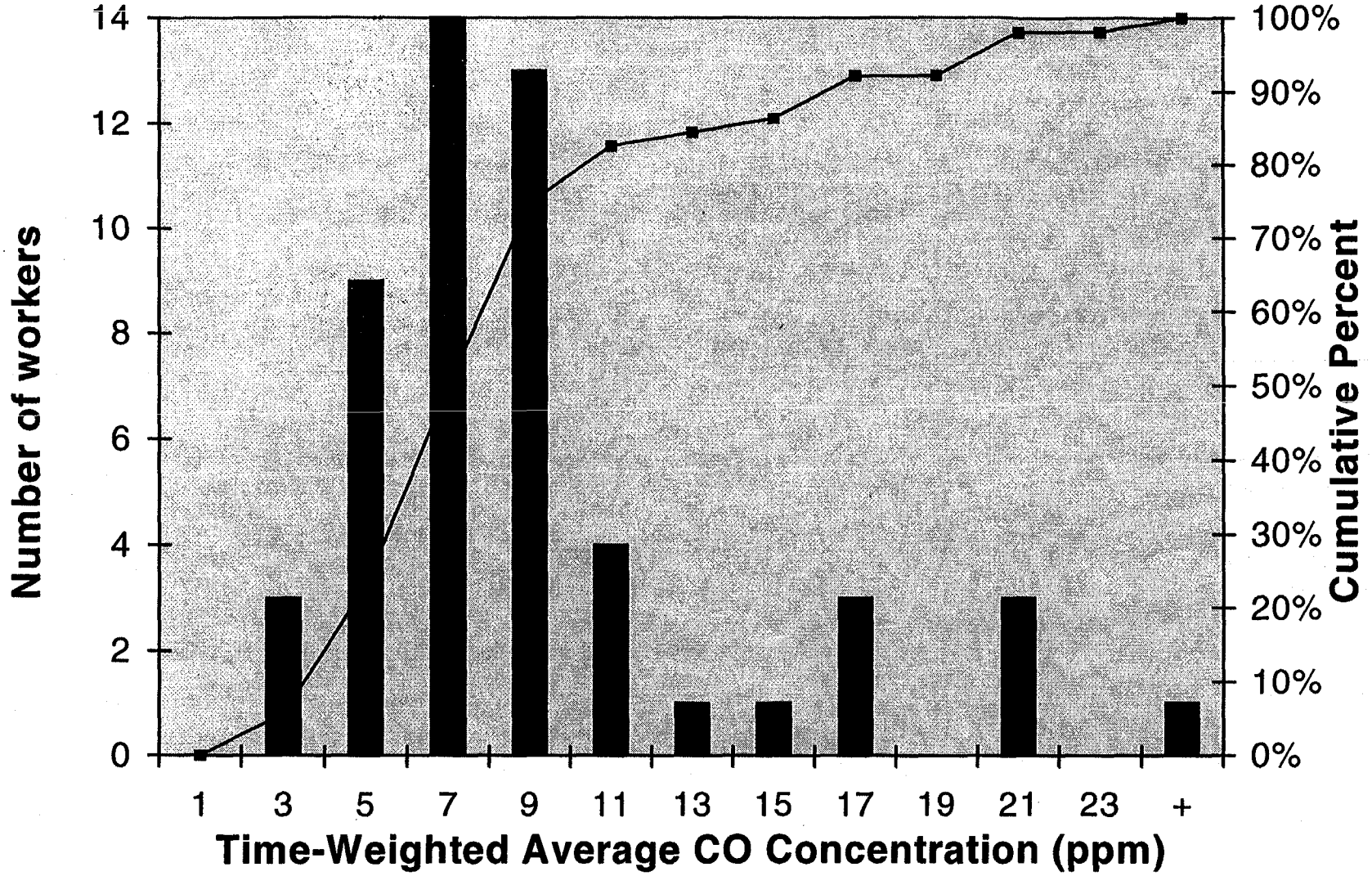

Figure 5-24. Carbon monoxide exposure distribution, Moscone Convention Center - MacWorld setup. By employer, Sullivan Transfer Co.

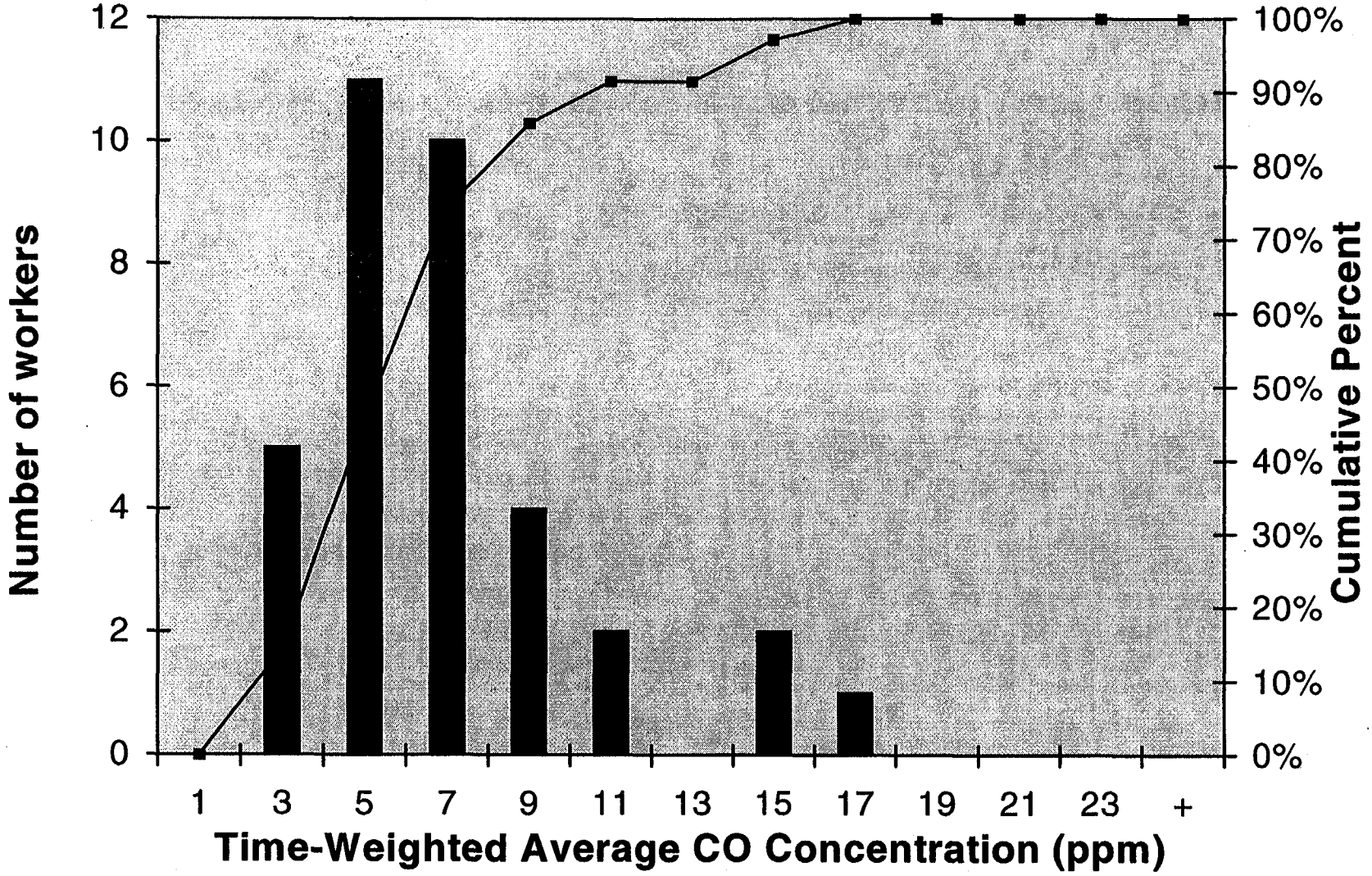

Figure 5-25. Carbon monoxide exposure distribution, Moscone Convention Center - MacWorld setup. By employer, SMG.

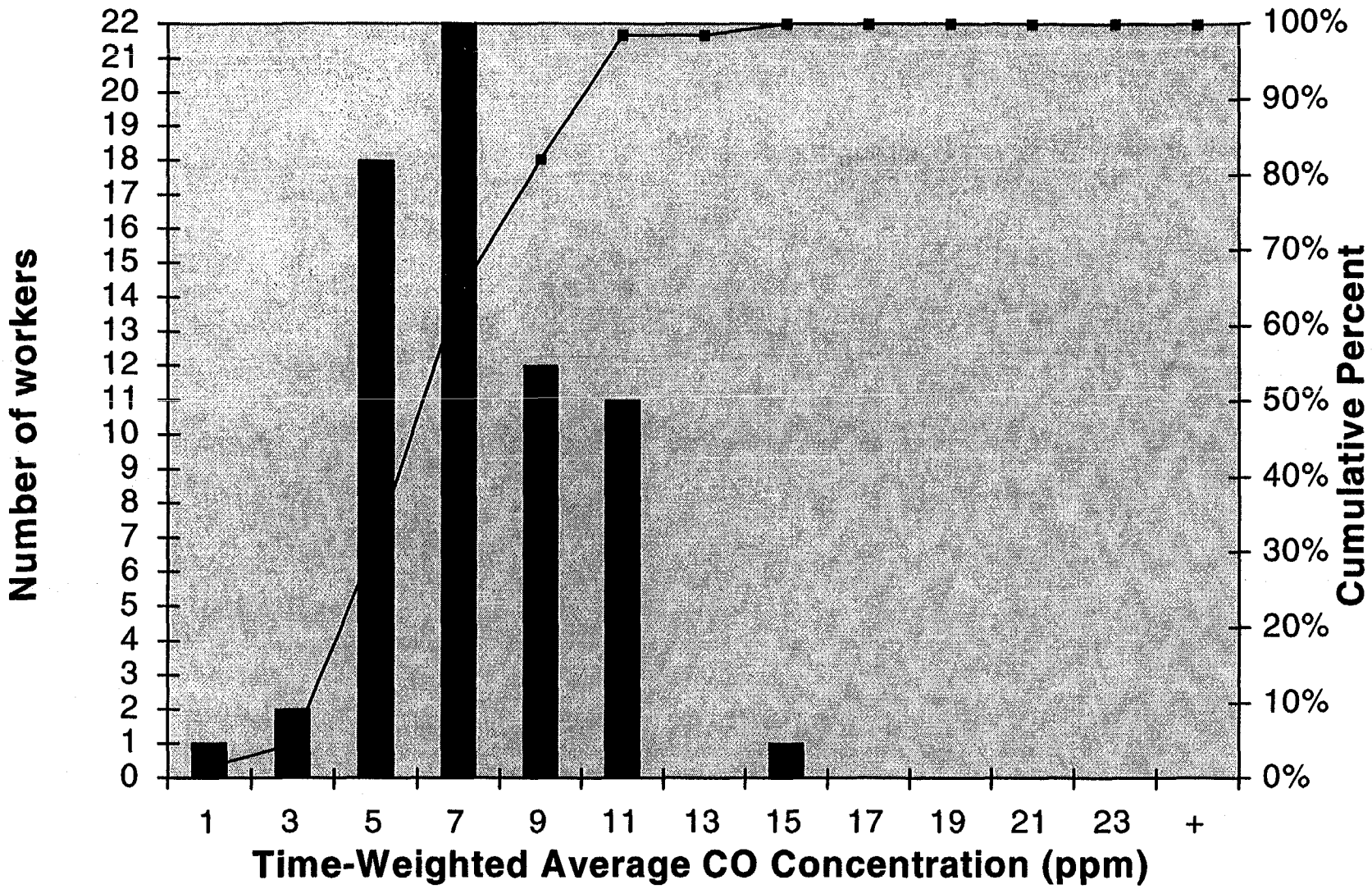

Figure 5-26. Carbon monoxide exposure distribution, Moscone Convention Center - MacWorld setup. By employer, Freeman Decorating Co.

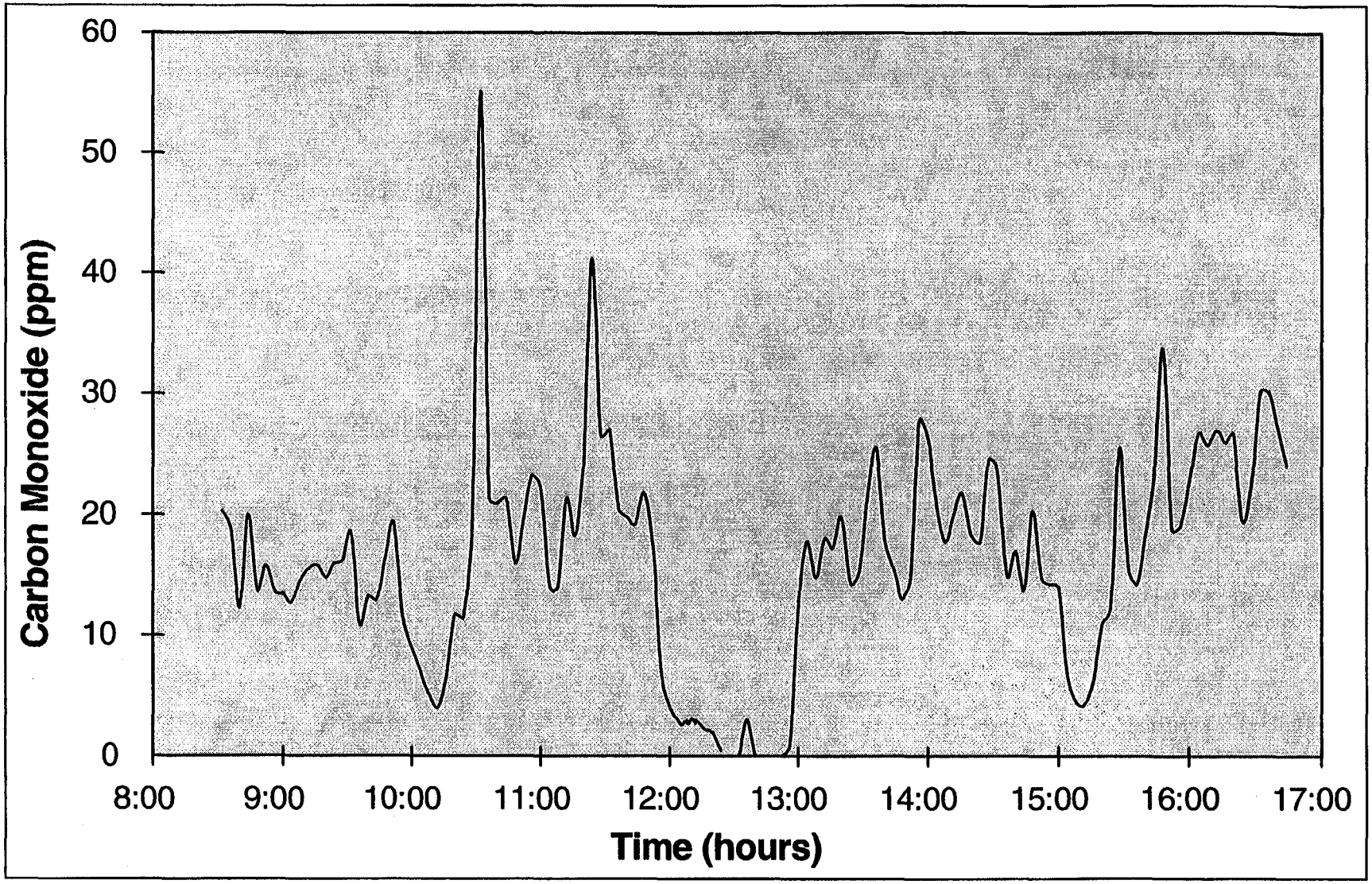

Figure 5-27. Real-time carbon monoxide exposure profile, Moscone Convention Center - MacWorld setup. Crawford Inc. Data.

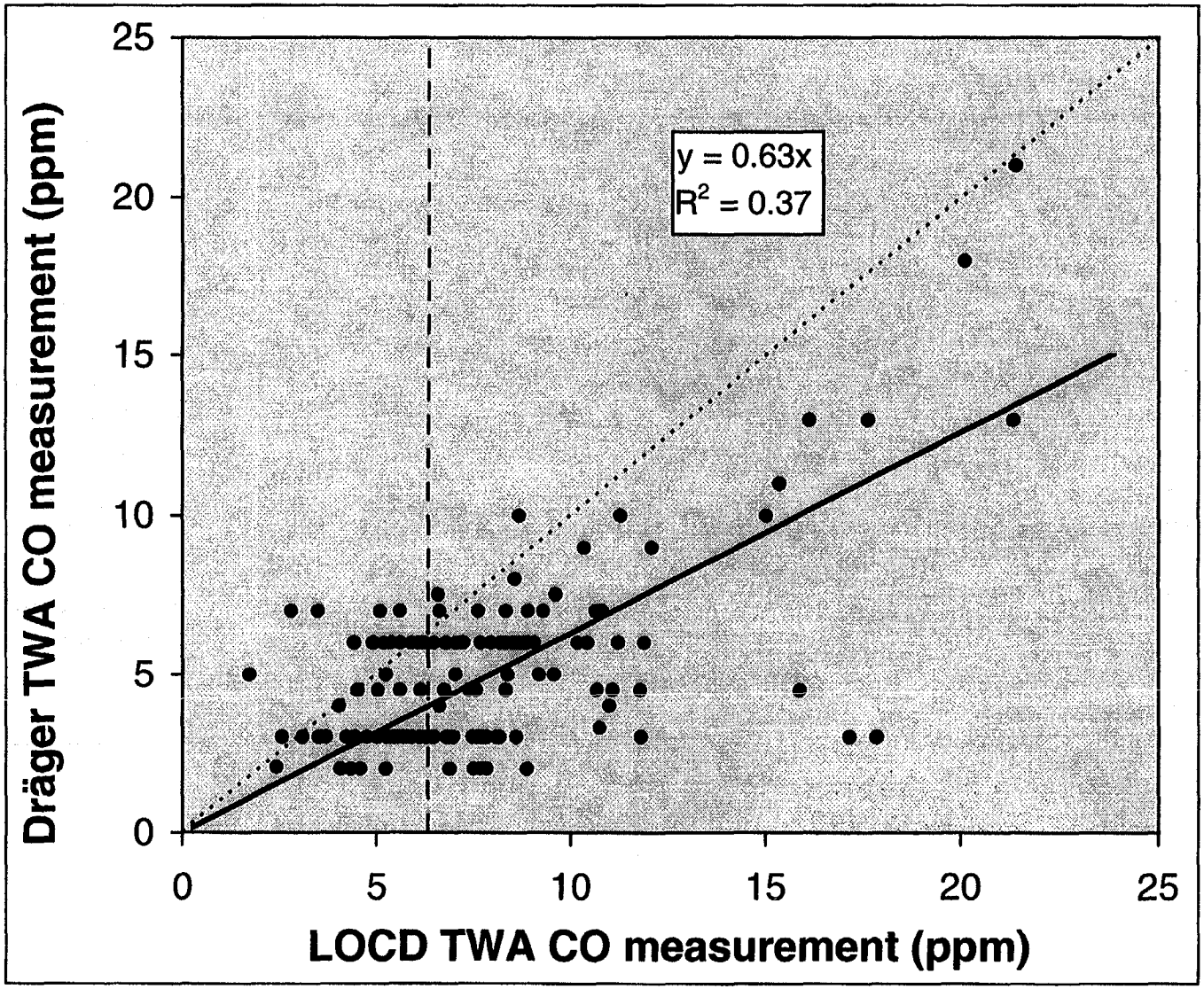

Figure 5-28. Comparison between parallel 8-hour TWA LOCD and Dräger diffusion tube CO measurements from the MCC CO exposure study. The dashed vertical line represents the Dräger diffusion tube limit of detection of 6.3 ppm. The dotted diagonal line is a 45° line representing theoretical perfect correspondence between the two measurement methods.

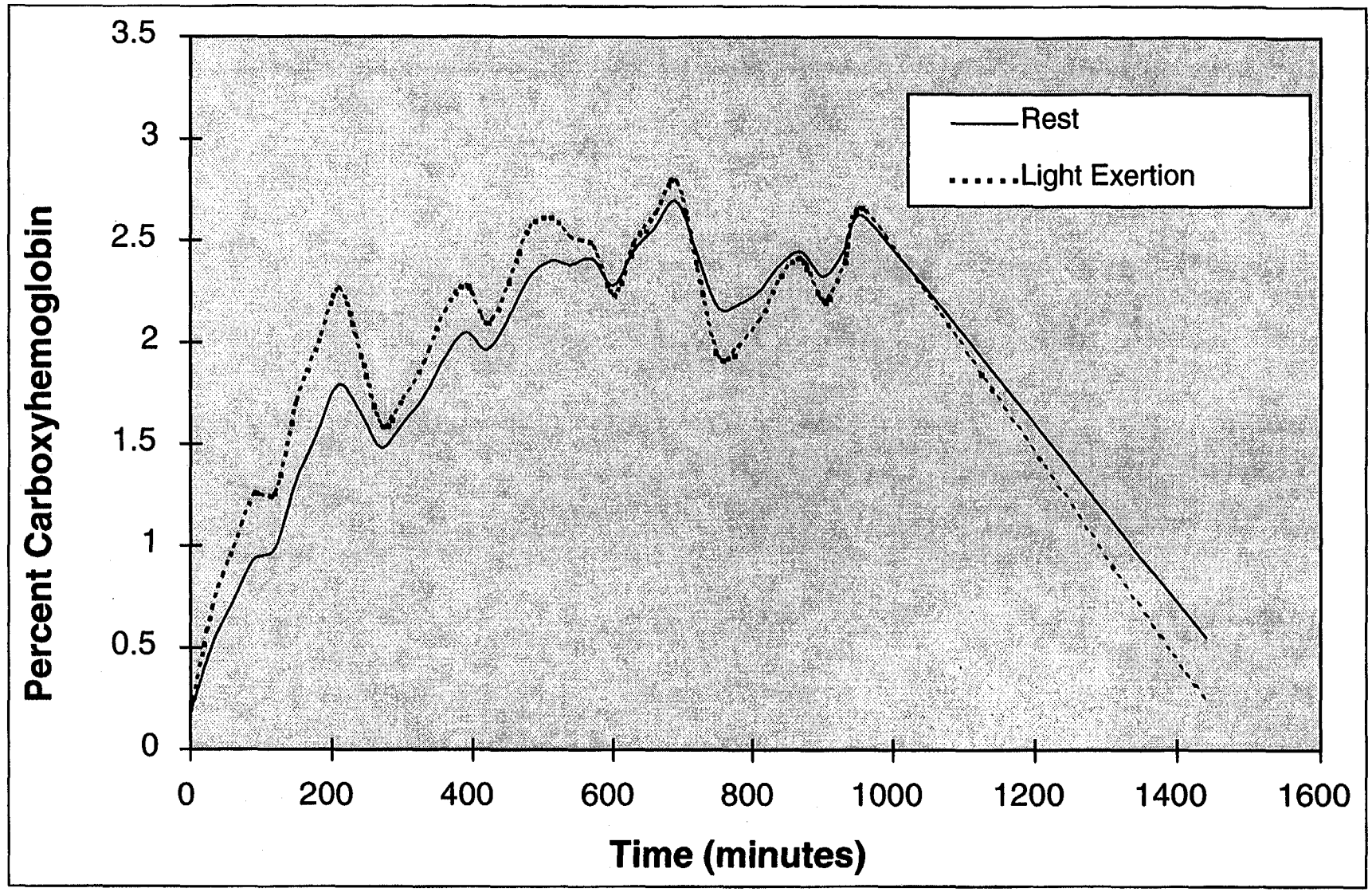

Figure 5-29. Simulated carboxyhemoglobin concentrations derived from Crawford Inc. real-time data. Moscone Convention Center - MacWorld setup.

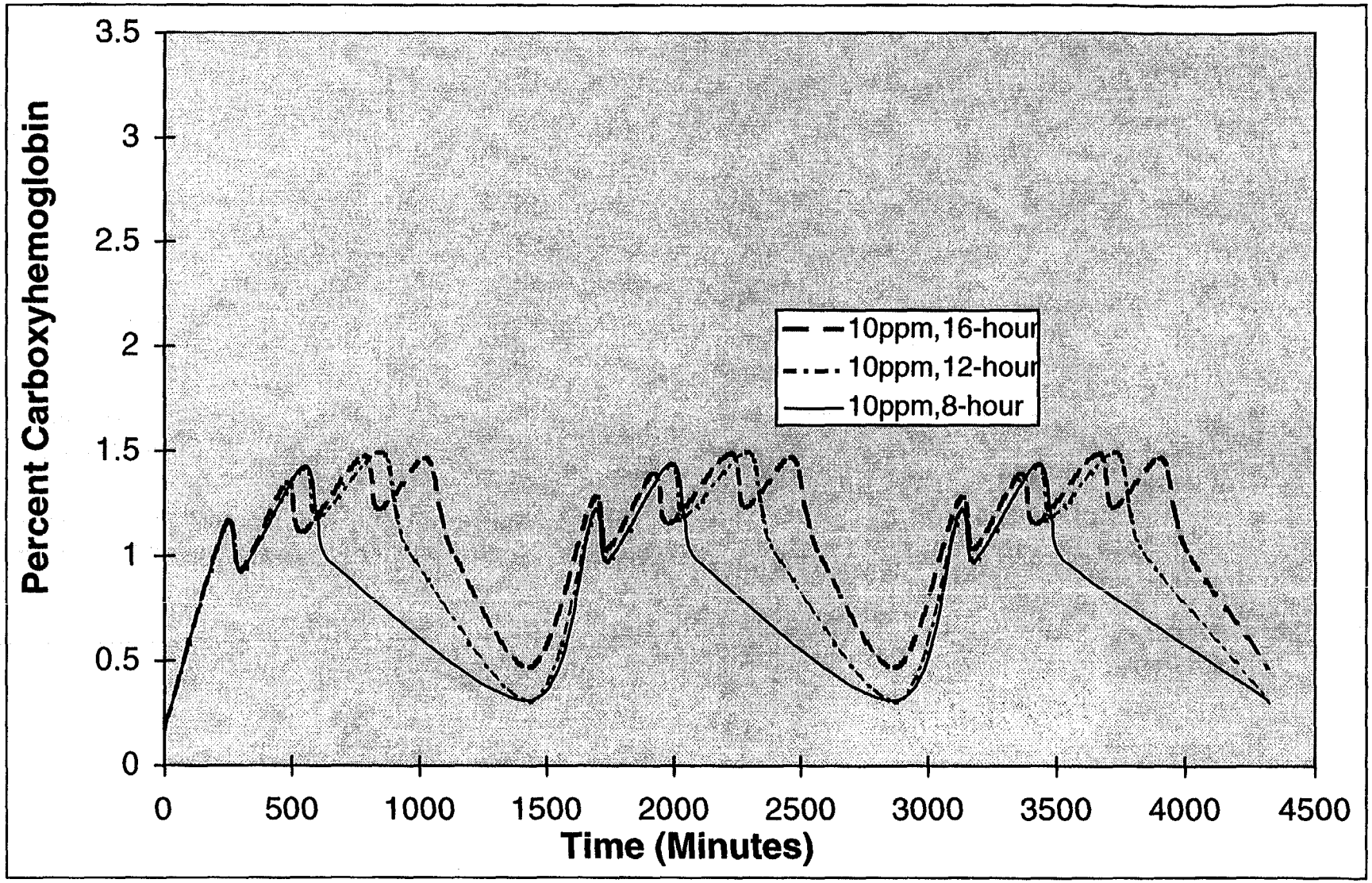

Figure 5-30. Simulated carboxyhemoglobin concentrations. Assumptions: moderate physical activity, non-smoker, male, 200 pounds, 10 ppm CO/8-hr workshift TWA, 4 ppm average CO during non-work hours.

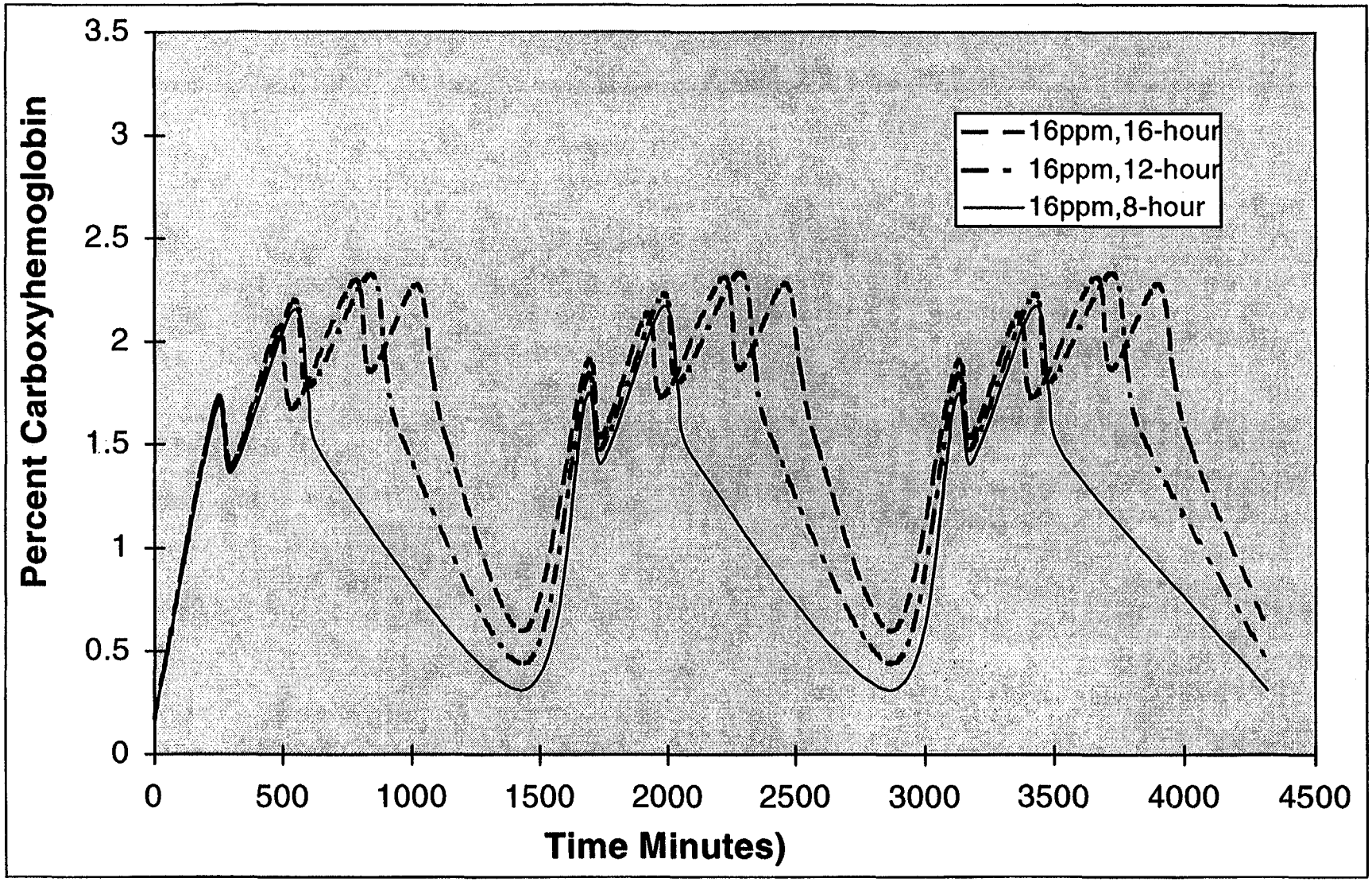

Figure 5-31. Simulated carboxyhemoglobin concentrations. Assumptions: moderate physical activity, non-smoker, male, 200 pounds, 16.4 ppm CO/8-hr workshift TWA, 4 ppm average CO during non-work hours.

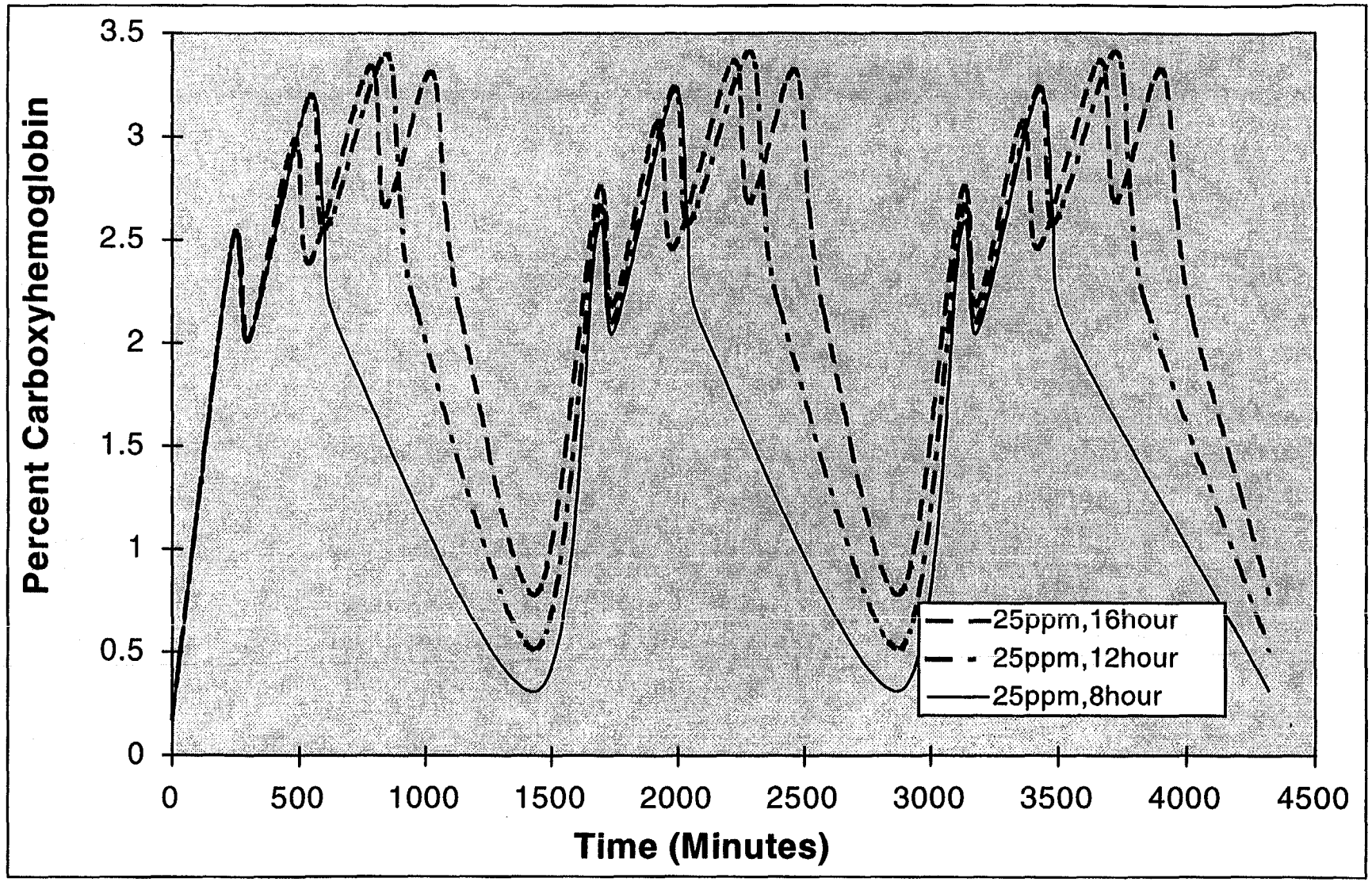

Figure 5-32. Simulated carboxyhemoglobin concentrations. Assumptions: moderate physical activity, non-smoker, male, 200 pounds, 25 ppm CO/8-hr workshift TWA, 4 ppm average CO during non-work hours.

Chapter 6: Summary, Conclusions, and Recommendations for Future Research

Summary

Carbon monoxide exposure is a serious public health problem from the perspectives of both morbidity and mortality. Based on national mortality records the lifetime risk of dying from accidental CO poisoning is about 10^{-4}. The American Association of Poison Control Centers reported 19,000 unintentional CO poisoning incidents in 1995, placing it among the most common causes of poisoning and the number one cause of environmental poisoning.

CO exposures can occur in every microenvironment where combustion gases are present. Exposure in residential and occupational environments are of particular concern. Estimates from the U.S. Department of Health Services' NHANES II, and U.S. EPA's Washington, DC and Denver studies, the only true population-based CO exposure studies that have been conducted to date, suggest that approximately 10% of the U.S. population is exposed above the National Ambient Air Quality Standard.

Costly, miniature, accurate real-time CO monitors, using electrochemical sensors and integrated datalogging systems, which can measure personal exposures over periods of hours to days were used in projects such as the U.S. EPA's Washington, DC and Denver study. Instantaneous and time averaging direct reading CO detector tubes using small sampling pumps are available to measure personal CO exposures. Time-averaging, direct reading diffusion tubes and badges are available for personal CO measurements. Finally a number of methods are available for measuring or estimating CO biologically via blood carboxyhemoglobin (COHb) concentrations either directly from blood samples or calculated from expired alveolar breath samples of CO exposed individuals. Although these methods can be used to provide CO exposure measurements, due to many factors such as unit price and labor costs, size and weight, and poor sensitivity or accuracy, they have been inadequate for use in large-scale population-based exposure assessment projects.

Due a the current lack of CO exposure measurement technology that is inexpensive, yet sensitive and accurate, distributional CO data within U.S. populations are sparse. Similarly, the human health consequences of chronic CO exposure, especially those related to heart disease and reproduction, are poorly understood due to the current cost of collecting sensitive epidemiological data.

Development of new passive CO monitoring technologies

An occupational CO dosimeter and an indoor air quality CO passive sampler were developed to meet the need for an inexpensive, yet accurate and sensitive measurement technology for population-based CO exposure assessment. The primary goal pursued in this work was to develop and validate an occupational dosimeter capable of measuring time weighted average (TWA) CO concentrations ranging from 10 to 800 parts-per-million-hours (ppm-h), i.e., 8-hour workshift TWA CO concentrations of 1 to 100 ppm. It was desired that the device should have an accuracy of ±20% and a precision of ±10 ppm-h at

exposures above 40 ppm-h. A secondary goal was to develop a device with similar accuracy and a precision of ±1 ppm-week, for indoor air quality studies. This device was also to have an operational range of 1 to 100 ppm, but was configured to provide a TWA over one week.

Both devices operate on the principle of gas diffusion sampling and are encased within a standard plastic spectrophotometric cuvette. The difference between the two devices is simply the geometry (cross-sectional area) of the gas diffusion tube. The CO sensor is a solid, translucent porous silica disk with a palladium and molybdenum based coating. The sensor, which responds to CO exposure with an increase in absorbance of 700 nm light energy is mounted within the cuvette, at the end of the gas diffusion tube, and is positioned such that its absorbance can be measured by simply placing it into a spectrophotometer.

From a practical standpoint, the work presented in the last chapters reflects major progress towards the development of a CO passive monitoring technology capable of inexpensive collection of quantitative CO exposure data. The success of the first prototype (PS1) proved that the QGI sensor technology was suitable for use in a diffusion sampler. However, the PS1 was unsuited as a tool for population-based exposure assessment. With the innovations used to develop the PS2 design the passive sampler became a useful device. The primary improvement was that the PS2 response could be directly measured without disassembly. This change made the sampler analysis easy and inexpensive. The PS2 was small enough to wear in the breathing zone as a personal monitor, and due to its size and easy analysis was practical for use in indoor air quality and exposure studies. The small size also made the PS2 ideal for adaptation as an occupational dosimeter. Safety was an important consideration for the passive sampler since it was being designed to be used in population-based studies. A device that could be handled by small children must be tamperproof. The unitized construction of the PS2 ensured that small or sharp parts would not be disseminated into homes or workplaces.

The laboratory studies of the PS2 performance presented in Chapter 4 indicated that the PS2 performance exceeded that of PS1. The MD15 sensor development done with QGI led to improvement in inter- and intra-batch variability, and a marked reduction of the rate of the reverse reaction in the sensor chemistry. The material selection experiments identified appropriate products for the construction of the PS2. The epoxy sealant used to assemble the PS2 significantly reduced ambient CO leakage into the samplers in storage, and more importantly, leakage during sampling.

Laboratory testing of the PS1 indicated that the desired accuracy of ±20% was achievable. The average RSD (precision) across the range of experimental exposures was ±8.5%. At the lowest exposure level (1.2 ppm-week) the RSD was less than 14%. Preliminary field testing of the PS2 showed that it behaved as well as the PS1. The measured results were in good agreement with the standard (bag sampler) method, and the PS2 measurements had a precision better than the goal of ±20%. The effects of exposure to very high RH were evident in the laboratory humidity experiments. The porous polyethylene sensor holder used in the PS2 was insufficiently porous to enable the silica gel to condition the sensor at humidities near saturation. This led to the next generation (PS4/D2) of sensor holders.

The first "occupational dosimeter," prototype PS3/D1, was a PS2 with a larger diffusion tube diameter. The behavior of this device was identical to the PS2, with a sampling rate a

factor of 13 higher. The response slope, $\rho = 0.0027$ A-ppm^{-1}hr^{-1}, of this batch of dosimeters was observed consistently in all of the batches of occupational dosimeters built since.

Following on the success of the PS2/PS3/D1, the sampler was re-designed and tested in a small batch as model PS4/D2, the first true occupational dosimeter. With small changes and using mass production techniques, a large batch of new components were manufactured for model D3 (not substantially different from D2) enabled the dosimeters to be efficiently mass-produced. Experiments showed that the humidity effects were solved by the re-design of the sensor holder. Statistical analyses indicated that there may be a small effect at 100% RH, however this may be an artifact of small sample size and should be confirmed with further tests. The D2 was found to operate well below the desired accuracy of ±20% with the exception of the unexplained variability at 90% RH. The bias of the device was low, ranging from 0 to a maximum of 10%. The bias was not affected by high humidity.

A large batch of PS5/D3 dosimeters were constructed and given the name "LOCD." Their response to CO at 10°C, 20°C, and 30°C were tested. The response at 20°C and 30°C were not statistically different. However, two interesting effects were noticed at the 10°C exposure levels. The first effect was that although the QGI sensors in the dosimeters reacted normally with CO, they did not display their full response (change in absorbance) until they had warmed to room temperature (the Pd-Mo reaction was the rate-limiting step at 10°C). The second observation was that the temperature-suppression of the Pd-Mo reactions at 10°C suppressed the ongoing oxidation of Mo_{blue} to Mo(VI) that occurs at 20°C. Due to this suppression, the effective response of a sensor exposed to CO at 10°C, for which the Pd-Mo reaction was allowed to complete at a 20°C was $\rho = 0.0034$ A-ppm^{-1}hr^{-1}, about 26% higher than expected when the device is exposed to CO at 20°C.

LOCD were exposed to a wide range of potential gaseous interferents, both organic and inorganic, in a series of interferent screening tests. Although fifteen different molecular species were tested, representing a fairly large range of the types of gas-phase pollutants commonly found in occupational and residential environments, it was by no means an exhaustive study. The potentially interfering inorganic gases that were tested included carbon dioxide, and nitrogenous gases (nitrous oxide, nitric oxide, and ammonia). Organic compounds that were tested include alcohols (ethanol and isopropanol), aromatic hydrocarbons (toluene), alkanes (butane, methane, heptane), alkenes (ethylene), halogenated alkanes (trichloroethane), ketones (acetone), and esters (ethyl acetate). In addition a commercial acrylic cement containing a mixture of organic solvents (including methylene chloride and methyl ethyl ketone) was tested.

These tests were demanding in terms of the high interferent concentrations. With two exceptions the dosimeters did not show a significant or practical effect from the exposures. The two exceptions were nitric oxide (a strong negative bias, exposed to NO but not CO, although no effect was seen when exposed to both CO + NO at the same time) and ethylene (strong positive bias, both with and without CO). Missing from the set of screening experiments were exposures to NO_2, aldehydes, and ETS. These tests, and tests of the effects of NO and ethylene at lower, more typical concentrations should be conducted.

LOCDs were used in a set of experiments to determine the dosimeter's CO mass sampling rates. These experiments were conducted because the mass balance of the QGI sensor reaction cannot be derived theoretically. The empirical mass conversion rate was found to

be 4.5 x 10^{-2} $\mu g\text{-}hr^{-1}ppm^{-1}$. This corresponds to a volumetric sampling rate of 39.0 $cm^3\text{-}hr^{-1}$. This rate was consistent (within 2%) with the theoretical sampling rate for a diffusion sampler of the LOCD's configuration, based on Fick's law.

An industrial hygiene CO exposure assessment study using the LBNL/QGI Occupational Carbon Monoxide Dosimeter

An assessment of worker CO exposures and indoor CO concentrations was conducted at the Moscone Convention Center (MCC) in San Francisco, CA during three days of the setup for the Mac World trade show in January, 1997. In this survey the LOCD was used in three modes: they were used to measure personal CO exposures on workers who were also monitored using conventional CO passive samplers; they were used to sample in parallel with real-time CO monitors that were placed on a number of workers; and they were used to measure time-averaged fixed-site CO concentrations in parallel with air samples collected in gas-tight bags and analyzed using an accurate calibrated infrared analyzer.

The underground exhibition halls with three large interior loading docks in the MCC pose challenges to providing adequate ventilation. This problem is exacerbated by the operation of diesel trucks at the loading dock and up to forty propane-powered forklifts used for movement of materials throughout the building.

Fifteen fixed-site 8-hour average CO measurements were made in various location within the MCC over the three study days, using bag samplers and concurrent triplicate LOCDs. Two of the bag samplers failed so that only 13 pairs of data were available for comparison of LOCD to bag sampler data. The level of agreement between the bag samples, analyzed using an infrared CO analyzer, and the average of the 3 LOCD was within 2 ppm and all but one were within 1 ppm. The highest fixed-site CO measurements were all at the docks where 8-hour averages of bag sampler data were as high as 13 ppm. The lowest workday CO averages were observed in the North and South Halls where most of the installer/decorators worked. The average LOCD data were well correlated with the bag sample data, with essentially no bias: the slope of the fitted regression line was 1.01 (95% confidence interval 0.92 to 1.1). The response was also very linear within the range of measurements ($R^2 = 0.97$).

The average absolute difference between all individual LOCD measurements and the bag samplers was 1.2 ± 1.0 ppm. The average absolute difference between the average of three LOCD measurements and their corresponding bag samplers was 0.7 ± 0.4 ppm. Finally the average of all thirteen pairs of the fixed-site LOCD and bag samples were extremely similar, being 4.8 ± 3.8 ppm and 4.8 ±3.5 ppm, respectively.

The LOCD was used to measure 154 workers' 8-hour TWA CO exposures over the three study days. The geometric mean (GM) of all 154 exposures was 7 ppm (GSD = 1.6), 8% were above 12.5 ppm (0.5 x PEL). Only one worker had an 8-hour TWA exposure (34 ppm) in excess of the Cal/OSHA TWA personal exposure limit of 25 ppm. Volunteer participants in the exposure study, including attendants (33), dock foremen (12), general foremen (7), forklift operators (17), dock workers (5), installer/decorators (49), supervisors (11), and others (20), were selected non-randomly from the available pool of workers. Forklift operators had the highest average and maximum measured TWA exposures with GM (GSD) of 9 (1.6) ppm (maximum = 34 ppm). Attendants and installer/decorators had

the lowest exposures with GMs of 6 (1.6) and 7 (1.4), respectively. Workers at the loading docks experienced the highest exposures: 34% of workers at one of the docks (Green Dock) had TWAs of more than 16.7 ppm (0.75 x PEL).

Real-time monitors with dataloggers were used to measure waist-high CO levels on a subset (30) of the workers. An LOCD was attached to each of these monitors for purposes of comparison. Unfortunately, the real-time monitoring data that were collected appeared to be flawed, possibly due to a negative bias in their calibration. However, it was possible to compare the waist-level and breathing zone LOCD data: the TWA CO levels at the breathing zone tended to be several ppm higher in most cases. On average, the 8-hour TWA lapel measurements were 8.5 ± 4.5 ppm versus 6.3 ± 3.5 at waist height.

The breathing zone LOCD and Dräger diffusion tube measurements were compared. In 135 of the 154 instances where workers were monitored using the LOCD, they also wore a Dräger CO diffusion tube. A regression analysis showed that the correlation between the Dräger data and the LOCD data was quite poor. A regression line for all 135 data points had a slope of 0.63 (R^2 = 0.37). A regression of the Dräger data below 6.3 ppm, the effective limit of detection for the device, and the corresponding LOCD data had an even poorer correlation (R^2 = 0.44) and a slope of 0.61. When only the paired data with Dräger Tube TWA values of 10 ppm or more were considered the slope was 0.80 (R^2 = 0.58). The average absolute value of the difference between the Dräger and the LOCD was 3.1 ± 2.5 ppm. This can be compared to the similar statistic for the LOCD comparison to the bag samplers presented above which showed that the average difference between bag samples and individual LOCD measurements was 1.2±1.0 ppm.

A physiologically-based pharmacokinetic (PBPK) model was used to investigate the potential body burden of the CO exposures of the MCC workers and how CO exposure during extended workshifts might effect the workers. The American Conference of Governmental Industrial Hygienists recommends a Biological Exposure Index (BEI) of 3.5% COHb to protect workers' health. The PBPK model was used to predict the COHb levels of the MCC workers given their measured CO level, the duration of their workshifts, and the number of consecutive days that they worked. Many of the MCC workers signed on for 12 or 16 hour workshifts. It was found that the dominating effect on ultimate COHb levels was the TWA CO exposure, not the length of work shift or the number of days of consecutive work. Peak COHb levels reached roughly 1.5% at 10 ppm workshift exposures and 4 ppm off-shift exposures. The COHb level peaked at about 2.5% when the workshift exposures were raised to 16.4 ppm. Finally, COHb levels approached 3.5% when 25 ppm exposures were simulated. Exposures to 25 ppm appeared to be required to approach 3.5% COHb, regardless of the duration of the workshift. This is consistent with the rule-of-thumb suggestion for extended workshift adjustments to PELs for substances with biological half-lifes less than 3-hours (CO half-life is about 1.5 h) recommended in the literature. Based on the PBPK modeling it did not appear that it would be necessary to adjust the Cal/OSHA PEL of 25 ppm for extended workshifts.

Conclusions

A review of the literature indicates that CO exposure in the U.S. is a serious public health problem. The literature also indicates that the currently available types of personal and indoor air quality CO monitoring instrumentation are insufficiently accurate and/or prohibitively expensive to be effective for use in assessing the distribution of CO exposures in the U.S. Additionally, for the same reasons, the current state of CO personal monitors restricts the ability to conduct population-based (epidemiological) research into the health effects of chronic CO exposure that would be sensitive enough to observe possible health effects.

Based upon the need for an inexpensive technology capable of providing sensitive, accurate, and precise CO exposure measurements for population-based CO exposure assessment studies, a new type of occupational CO dosimeter and an indoor air quality CO passive sampler was investigated here. The stated goal was to develop an occupational CO dosimeter accurate to ±20% with a precision of ±10 ppm-h for 8-hour TWA samples, and an indoor air quality passive sampler accurate to ±20% with a precision of ±200 ppm-h for one-week TWA samples.

These devices were both successfully designed and tested in the laboratory and the field. Laboratory testing proved that the devices could operate with precision much better than ± 20%, usually below 10%. Bias of the devices was equally low ranging from 0-10%. The calculated accuracy of the LOCD ranged from 5-16%. Exposures at very high relative humidity may have lead to calculated accuracy up to ±27%, however this must be confirmed with future experiments.

Screening with high concentrations of a wide range of classes of organic and inorganic gasses indicated that the LOCD is resistant to many potential interferents. The exceptions were that the device is not selective against ethylene (positive interferent with and without CO) or nitric oxide (when CO is not present).

The LOCD was tested in the range of 10°C through 30°C, and a temperature effect was found at 10°C. This finding indicates that the device requires a temperature correction in order to accurately assess CO exposures at temperatures lower than 20°C. This finding requires further investigation.

Both devices were successfully tested in preliminary field tests. The indoor air quality CO passive samplers PS1 and PS2 were tested in field settings, including residential settings and parking garages, where they performed within its design criteria. The LOCDs were tested in both small residential settings where they were exposed for several days, and in a large scale industrial hygiene exposure assessment survey where they were used to measure 8-hour workshift TWA CO exposures. Their performance was excellent in all of the field tests. They not only yielded accurate data as compared to concurrent bag sampler measurements, but they were simple to use and analyze, and they behaved reliably.

In conclusion, the results of this work are that the new technology using the QGI palladium-molybdenum based MD15 sensors, configured into the passive diffusion sampler, has been proven to be a valuable device for measurement of CO exposures. In particular, the LOCD is a simple, reliable and accurate method for occupational exposure assessment.

Future Research Needs

Although considerable ground has been covered in the development and testing of the passive sampler/occupational dosimeter, more work is necessary to validate the devices fully. More field studies, under rigorous conditions, should be conducted to further test and validate both the occupational and residential versions of the device. Further testing of the device for interferents including NO_2, aldehydes, and ETS is necessary. Temperature effects tests should be conducted at a broader range of temperatures (i.e., 10°C - 40°C). The effects of high humidity should be further investigated in order to rule out the possible small effect observed in the LOCD at high RH. In addition, the NIOSH (Cassinelli, 1986) validation protocol for passive samplers should be applied to testing these samplers. The portable reader for the dosimeter should also be developed.

NIOSH validation for the LOCD

NIOSH has developed a protocol for validation of passive samplers for use in industrial hygiene measurements (Cassinelli, 1986). The protocol describes a rigorous testing regimen including nine phases. Characteristics of these phases are (1) analytical recovery, (2) sampling rate and capacity, (3) reverse diffusion, (4) storage stability, (5) factor effects, (6) temperature effects, (7) accuracy and precision, (8) shelf life, and (9) behavior in the field. Phase 5, or factor effects, is a fractional factorial experimental design which is intended to test interaction between the following factors: analyte concentration, exposure time, face velocity, relative humidity, interferents, and monitor orientation.

It should be noted that although the work presented here did not attempt to explicitly follow the NIOSH protocol in a separate series of tests, many phases of the protocol have been addressed in this study. With the exception of the factor effects experiments, the investigations discussed in Chapter 4 touched all of these phases. Nonetheless, it would be appropriate to test the LOCD using the NIOSH protocol in a set of experiments conducted for that purpose alone.

Issues of potential concern for the validation of the CO passive sampler and dosimeter are the effects of relative humidity and other interferents, especially NO and ethylene, which have been observed to interfere with the samplers' performance at high concentrations. The effects of ETS, aldehydes, and NO_2 should also be studied at this time.

Develop a portable reader for dosimeter

A simple and inexpensive portable spectrometer optimized for a 700nm wavelength should be developed. The advantages of a portable reader is that samplers could be analyzed immediately at the place of measurement. Such a device will be an important part of a commercialized occupational dosimeter. It will enable industrial hygienists to conduct ongoing worker exposure surveillance necessary for high CO-risk occupational environments.

The full spectral capabilities of a commercial spectrophotometer are unnecessary for analyzing the response of the passive samplers. The use of commercially available, narrow-band, solid-state, light sources such as high-energy 700nm light emitting diodes or laser diodes, paired with a photo-diode or photo-diode array (for more sensitivity), and the

necessary temperature compensation circuitry has the potential to be a very sensitive measurement device. Such a reader, dedicated to analysis of the samplers should be considerably less expensive than a full spectrum laboratory spectrometer.

References

Cassinelli, M. E., Hull, D. H., Crable, J. V., and Teass, A. W. (1986). "Protocol for the evaluation of passive monitors." In *Diffusive sampling: an alternative approach to workplace air monitoring*, The proceedings of an international symposium held in Luxembourg, 22-26 September, 1986, Berlin, Brown, and Saunders, eds., Royal Society of Chemistry, London, UK, Luxembourg, 190-202.